Understanding sit-to-stand through experimentation and constraint-based modelling

Mitchell, Ross Harvey

Award date:
2004

Awarding institution:
University of Bath

UNDERSTANDING SIT-TO-STAND THROUGH EXPERIMENTATION AND CONSTRAINT-BASED MODELLING

Submitted by

ROSS HARVEY MITCHELL

for the degree of PhD

of the University of Bath

2004

Signature of Author: .....

R. H. Mitchell

ProQuest LLC
789 East Eisenhower Parkway
P.O. Box 1346
Ann Arbor, MI 48106-1346

ABSTRACT

Understanding sit-to-stand through experimentation and modelling
R. H. Mitchell, University of Bath, 2004

Industrial workstation design has included little concern for matching operator ability with the tasks concerned, which was in part responsible for user injury. Consequently, an improved ergonomic design input was required. An investigation was conducted to understand the whole body movement kinematic characteristics of sit-to-stand (STS) to create an design aid in the form of a computational human movement model.

Critical actions that occurred throughout STS were established to provide a generalised motion characterisation, and the constraints which influenced STS movement patterns were obtained from this. The influence of three factors: *rise duration, initial seated posture* and *seat height* were experimentally investigated on spatiotemporal characteristics to form a series of regression equations. This provided a means of predicting whole body mass centre (CM) trajectory for STS movements over a range of conditions.

Movement constraints and predicted CM trajectory were used to drive a manikin model that was based on experimental data of a single subject. When validated against this subject, root mean square difference between model and experimental lower limb joint angle displacement data was just 4.2°. Knee and ankle joint rotations successfully achieved accuracy levels to remain within established ranges of natural variability. The model was further validated against two additional subjects representing different body types. The average joint angle displacement predictions fell within 5.7° and it was concluded that the model could represent a range of able-bodied subjects.

With the generalised rise scheme, the study radically progressed the understanding of CM spatiotemporal characteristics throughout STS, particularly with reference to the stability strategies chosen to overcome varying rise demands. This was the first human movement investigation to apply a factorial experimental design, a novel approach resulting in a comprehensive presentation of main and interaction effects occurring in STS responses. A kinetic energy motion definition was developed to bound STS, providing real improvement over traditional methods. Subsequently, the study has offered a number of useful methodologies and results that can be used alongside the manikin model by clinicians, engineers, and human movement scientists.

PUBLICATIONS

Published conference proceedings:

Mitchell, R.H., Salo, A.I.T. and Medland, A.J. (2003). Determining mass centre trajectory variations for application to human modelling. *Proceedings of IASTED International Conference on Biomechanics, Rhodes,* pp. 147-152.

ACKNOWLEDGEMENTS

For their valued contribution to this thesis and the associated work, I would like to thank the following:

My supervisors: Dr Aki Salo for initially offering me the opportunity to study for the degree, for his commitment to the project and for the genuine guidance that he offered; and Professor Tony Medland for his creative input and enthusiasm for the academic process of inquiry.

Dr Glen Mullineux for providing computational programme writing assistance.

The Technical University of Delft for the use of their Anthropometric Design Assessment Program System.

The subjects for their time, patience and effort during data collection sessions.

The EPSRC for financial support.

Andreas Wallbaum for his technical aid during data collection sessions.

The Sport and Exercise Science research group for creating a challenging yet genuinely pleasant research atmosphere in which to work and develop scientific integrity.

My postgraduate friends, particularly Marianne, Ross, Dani and Ian for really providing excellent, fun and enjoyable surroundings for both study and play.

Becky for the love and support that she gave over many years; and Louise for helping me to regain the energy to finish the thesis off.

My family: Lauren, Craig, and Nan for showing big love; and to Mum and Dad for the free and encouraging environment that they provided whilst I was growing up, leaving me able to accomplish anything I wanted.

TABLE OF CONTENTS

LIST OF FIGURES

Chapter Two

Chapter Four

Chapter Five

Chapter Six

Chapter Seven

LIST OF TABLES

Chapter Four

Chapter Five

Chapter Six

Appendix C

Appendix G

Appendix H

NOMENCLATURE

ADAPS	- Anthropometric design assessment program system
BS	- Base of support provided by the feet
BALANCE	- Whole body mass centre comes over rear of BS
$BALANCE_{TIME}$	- Time of BALANCE
$BALANCE_{HOR\ VEL}$	- Whole body mass centre horizontal velocity at BALANCE
CAD	- Computer aided design
CM	- Whole body mass centre
$CM\text{-}BS_{HOR\ DISP}$	- Horizontal displacement between CM and rear of BS
CNS	- Central nervous system
CP	- Centre of Pressure
CT	- Computerised axial tomography
EMG	- Electromyography
END	- Termination of STS movement
$END_{HOR\ DISP}$	- $CM\text{-}BS_{HOR\ DISP}$ at END
$END_{VER\ DISP}$	- CM vertical displacement from ONSET to END
$END_{HOR\ VEL}$	- CM horizontal velocity at END
$END_{VER\ VEL}$	- CM vertical velocity at END
GRF	- Ground reaction force
HAT	- Head, arms and torso
isp	- Initial seated posture factor, measured in mm
ISP	- Scaled initial seated posture factor
KE	- Kinetic energy
MRI	- Magnetic resonance imaging
ONSET	- Initiation of STS movement
$ONSET_{HOR\ VEL}$	- CM horizontal velocity at ONSET
$ONSET_{VER\ VEL}$	- CM vertical velocity at ONSET
rd	- Rise duration factor, measured in s
RD	- Scaled rise duration factor
RMSD	- Root mean square difference
SOC	- Seat-off completion

SOC_{TIME}	- Time of SOC
$SOC_{HOR\ DISP}$	- CM-$BS_{HOR\ DISP}$ at SOC
SOO	- Seat-off onset
SOO_{TIME}	- Time of SOO
$SOO_{HOR\ DISP}$	- CM-$BS_{HOR\ DISP}$ at SOO
$SOO_{VER\ DISP}$	- CM vertical displacement from ONSET to SOO
$SOO_{VER\ VEL}$	- CM vertical velocity at SOO
sh	- Seat height factor, measured in °
SH	- Scaled seat height factor
STS	- Sit-to-stand
VVMAX	- Occurrence CM maximum vertical velocity
$VVMAX_{TIME}$	- Time of VVMAX
$VVMAX_{VER\ VEL}$	- CM velocity at VVMAX

CHAPTER 1: INTRODUCTION

1.1 RESEARCH OVERVIEW

Within the UK, the manufacturing industry expenditure due to non-fatal injury amounts to the equivalent of 4-8% of each company's gross trading profits (Health and Safety Executive, 2002). In the past, industrial workstation designs have included little concern for matching the abilities of the operator with the task concerned, which was in part responsible for a sizeable proportion of the injuries that occurred (Das and Sengupta, 1996). As such, a new emphasis must be placed upon workstation design where harmful postures and imposed stresses on the user are minimised.

Natural human motions can be defined as a restricted set of body and limb movements that meet the requirements of load carrying, normal posture positions and social conditions etc. Within the environment of a manufacturing workstation, many separately identifiable motions are used by the operators. One of the most common motions that occurs is that of a person moving from a sitting position to a standing position, as it acts as a pre-cursive movement allowing many other activities to occur (Janssen et al., 2002). Sit-to-stand (STS) studies have considered the influence of a variety of factors on movement responses. For instance, rise duration was seen to affect movement patterns by altering the path of the whole body mass centre (Pai and Rogers, 1990). Foot position influenced the degree to which the upper body was required to flex forward to achieve a stable position before whole body upward movement (Vander-Linden et al., 1994, Papa and Cappozzo, 2000).

Development of computer based engineering techniques has allowed designers to create products and machines virtually. However, interactions of a human operator with the machines are difficult to quantify (Molenbroek and Medland, 2000). Further, regulations governing packaging machinery require a design to be proved inherently safe for the human operator before they are put into commercial use (van Ekelenburg et al., 1995).

Human model packages are available to aid the design of industrial man-machine environments (Porter et al., 1997). Still, the ability of these packages to accurately and conveniently replicate human motions under a variety of situations is limited. A research programme has been established at the Technical University of Delft into human modelling. This programme of research draws upon many years of experience at Delft of ergonomics and the collection of anthropomorphic data. The information has been incorporated into a constraint modeller, created at the University of Bath, and allows human posture and movement pattern approximations to be created in response to a set of task objectives.

The constraint-based human manikin can represent a changeable skeletal representation of a man. Using mathematical search techniques to find solutions to mathematically formulated problems, human posture can be created if the physical problems of that posture are posed in the right mathematical sense. A study of the STS action and, the understanding of it, will form part of the process necessary to create a human movement model for that task, providing a valuable aid for the design of safer operator environments for many industrial tasks.

1.2 ORGANISATION OF CHAPTERS

The chapters of the thesis are organised as follows:

1.2.1 CHAPTER 2: REVIEW OF LITERATURE

A review of relevant literature is provided in Chapter 2. This covers a description of the movement of sit-to-stand and how changes in certain factors can affect parameters of interest. A section is also provided on movement subdivision techniques employed by other authors. Issues associated with ergonomic design are presented and current ergonomic human models introduced. Techniques of human segmental mass centre data estimation are given.

1.2.2 CHAPTER 3: RESEARCH PURPOSE AND QUESTIONS

This short chapter outlines two main purposes of the research. These are supported by several research questions that were used to guide the investigation, and these are also presented.

1.2.3 CHAPTER 4: DEVELOPMENT OF METHODOLOGIES

Methodologies used for the main experimental study were developed and are discussed in the fourth chapter. This included description of the appropriate experimental set-up and discovery of appropriate movement descriptors. Further, definitions of movement *events* were developed and described in terms of 16 individual spatiotemporal movement responses. Finally, a series of movement hypotheses are presented for testing in the main studies.

1.2.4 CHAPTER 5: METHODOLOGY

Methods used in the main studies are presented in Chapter 5. Three factors for investigation; *rise duration, initial seated posture,* and *seat height* are introduced. A factorial experimental design is established along with statistical techniques used for the creation of regression equations. The use of an ergonomic human model is shown in terms of its set-up and input requirements to produce predicted movement. A series of model validation techniques are also provided.

1.2.5 CHAPTER 6: RESULTS

Chapter 6 presents the various results of the studies. These include experimental results and a series of main and interaction effects, obtained statistically for STS responses. Model results are presented in terms of absolute and relative root mean square difference (RMSD) from known experimental results for lumbar, hip, knee and ankle joint data.

1.2.6 CHAPTER 7: DISCUSSION

Obtained results are discussed in Chapter 7. The success of the experimental design is considered and the effects from the statistical study judged for the spatiotemporal responses. Validity of the initially proposed movement hypotheses is examined. The difference between predicted movement patterns of the manikin model and chosen experimental trials is evaluated in terms of the variability that would be expected to occur naturally within certain experimental conditions.

1.2.7 CHAPTER 8: CONCLUSIONS

Conclusions are presented in the final chapter. These are made with regard to the adopted initial research purposes and the approach. The application of the model to populations outside of the tested subjects is considered. Usefulness of the model to ergonomists in the context of a design aid for industry is given. Finally, future research directions have been suggested.

CHAPTER 2: REVIEW OF LITERATURE

This review of literature is presented in five distinct parts. The first of these provides a description of the whole sit-to-stand (STS) movement as suggested by previous authors. The second section details previous experiments that show how characteristics of STS vary due to changes in influencing factors. The third section demonstrates how previous authors have subdivided the STS movement in order to improve understanding of the motion. Moving away from the specifics of STS, the next section considers design methods for human movement in the context of industrial environments, followed by an overview of current approaches to ergonomic human models in a commercial and academic context. Finally, there is a presentation of the methods available to determine subject-specific segmental mass centre parameters.

2.1 SIT-TO-STAND DESCRIPTION

The first section of this review demonstrates the general scheme of the rising from onset of movement, through seat-off, and to the end of movement. It explains what happens to a normal subject under normal conditions. For clarity, this rising scheme has been sub-sectioned into: initiation, forward movement, transition, upward movement, and termination.

2.1.1 INITIATION

Muscle activation

Initiation of movement starts with muscle activation. Millington et al. (1992) noted that there was a lack of information covering the trunk musculature activation and presented mean onset times of muscle activity detected by surface electromyography (EMG). The Erector Spinae was repeatedly the first muscle to be activated, followed shortly after by muscles of the Quadriceps group. However, detection of this activation came approximately 14% into the defined STS cycle (Millington et al., 1992) i.e. activation was detected sometime after movement was seen. The authors suggested

that initiation could have occurred at many locations including the head and the upper body, and that it could be difficult to identify the movement initiation muscles as they may lie deep within the body.

Muscle activation was also considered in a study by Khemlani et al. (1999). The Tibialis Anterior was seen to be the muscle that was consistently activated first and frequently before the author's definition of movement onset. Whilst the Erector Spinae was not measured (as in Millington et al. (1992)), onset of Quadriceps muscles was recorded and occurred at a comparable time to Millington et al. (1992). Khemlani et al. (1999) suggested that the early onset of the Tibialis Anterior muscle reflects its contribution in stabilising the foot. However, some studies have shown that at the onset of movement a reduction in reaction force at the foot occurs (Hirschfeld et al., 1999). Therefore, the onset of Tibialis Anterior activity could be a consequence of this. Thus, it remains unknown if the Tibialis Anterior is the initiating muscle or activated as a consequence of other muscles or muscle groups.

Ground reaction forces

Despite a lack of detailed knowledge of which muscle initiates movement, there is an apparent change in ground reaction forces (GRFs) at the feet and the buttocks (Shepherd and Gentile, 1994). Hirschfeld et al. (1999) used four force plates to describe reaction force trends under the buttocks and feet. The study showed that reaction forces at the buttocks increased approximately 90 ms before kinematic analysis detected CM movement. These GRFs applied beneath the buttocks were in a vertical and posterior direction, and followed by a decrease in the force applied beneath the feet. The decrease in the force applied by the feet occurred at approximately the same time as change in kinematic whole body mass centre (CM) data were detected. Hirschfeld et al. (1999) suggested that the changes in the ground reaction forces were due to muscles flexing at the hip, although no further evidence was provided for this. The study also reported that increased loading and backward directed force beneath the buttocks initiated the STS task and generated the propulsive impulse. Pai and Rogers (1990) also recognised that STS required a propulsive impulse in the horizontal direction at the beginning of movement to initiate forward motion. However, the authors did not suggest where or how this would be generated.

In a study which used one force plate under both the seat and the feet (unlike the study by Hirschfeld et al. (1999) where four force plates were used), centre of pressure (CP) was seen to initially move back several centimetres before moving forward (Kralj et al., 1990). These results were supported by the work of Hirschfeld et al. (1999). The movement of the CP was said to be due to the need to generate forward momentum (Kralj et al., 1990). Whilst the description was limited, the authors claimed that the seated subject had no means of executing horizontal force other than by generating trunk mass forward velocity. In reality, it is the posterior forces apparent at the buttocks and feet (as recorded by Hirschfeld et al., 1999) that allowed trunk mass forward velocity to occur.

2.1.2 FORWARD MOVEMENT

Trunk flexion

After the propulsive impulse, movement occurred to bring the whole body mass centre (CM) towards the final base of support provided by the feet (BS), characterised by flexion in the trunk and pelvis (Millington et al., 1992). Many authors have noted this characteristic flexion along the length of the trunk or at the pelvis, although some have suggested the that the initial body segment movement could not be identified due to subject differences (Nuzik et al., 1986). Schenkman et al. (1990) considered torso bend as two segments pivoted at the top of the pelvis. The majority of subjects showed the upper segment flex on top of the lower segment (by an average of 16°). A small number of subjects showed the lower and upper segments move together, i.e. flexion was only recorded at the hip. Hirschfeld et al. (1999) described forward movement in the head and upper trunk occurring significantly earlier than flexion at the pelvis or the hip, due to the flexion that occurred along the trunk.

Generation of upper body momentum

When the upper-body was rotated, it was accelerated forward to a peak velocity, and momentum in the upper body was generated (Kralj et al., 1990). It was demonstrated that the upper body (defined by the head arms and torso (HAT)) provided the major

contribution to CM horizontal momentum, as well as allowing the adjustment of CM position at seat-off (Pai and Rogers, 1990; Riley et al., 1991). It further was speculated that control of CM horizontal velocity may represent an invariant feature of the STS task (Pai and Rogers, 1990; Riley et al., 1991). The tight regulation of CM horizontal momentum was considered to be a stabilising factor for controlling balance in STS, as an increase in speed could represent a progressively greater potential disturbance to stability. Pai and Rogers (1990) proposed that a simplifying strategy could have been adopted by the neuromuscular control system, reducing the number of separate independent aspects of movement that must be controlled. However, even if this strategy was implemented it was stated that rising still required considerable co-ordination of multiple redundant degrees of freedom (Reisman et al., 2002).

Upper body braking

At the required CM peak horizontal velocity, braking occurred at the trunk and hip extensor muscles (Kralj et al., 1990; Pai and Rogers, 1990), slowing the forward movement and preparing the body for initiation of upward movement. This was associated with a frictional force at the feet (Pai and Rogers, 1990). The same frictional force was also noted by Hirschfeld et al. (1999) taking place approximately 260 ms before the thighs left the chair. The braking period always started before the onset of seat-off which coincided with the time of CM peak horizontal velocity (Pai and Rogers, 1990; Riley et al., 1991). Thus, having generated the propulsive impulse at the beginning of the movement, a braking impulse was required to bring horizontal movement of the body to a stop (or forward falling would occur). The magnitude and timing of the propulsive and braking forces in the horizontal direction were critically related to balance control. Riley et al. (1991) suggested that this braking phase was linked with limits of pelvic and hip ranges and may be used to transfer momentum from the upper body to the lower body. However, differences in the hip range of movement implemented in STS have occurred due to changes in a variety of conditions (Wheeler et al., 1985; Papa and Cappozzo, 2000). This suggested that seat-off does not always occur at the limits of pelvic or hip flexion, and that the braking phase may not be linked to these limits.

2.1.3 TRANSITION

The period of rise around the transition from forward movement to upward movement was considered the most challenging and complex part of the movement (Schultz et al., 1992). Several aspects of rise were occurring at the same time around this phase and there were many constraints on balance control, co-ordination of propulsive forces, and organisation of degrees of freedom.

Initiation of seat-off

The transition from forward movement to upward movement was first recognised by the initiation of seat-off. At this phase the body began a period whereby almost full body weight was present at the seat, to a period where this was transferred fully to the feet (Millington et al., 1992). By the time seat-off occurred the majority of forward movement was completed (Pai and Rogers, 1990), and the greatest joint torque values would also have been achieved (Ikeda et al., 1991; Kotake et al., 1993).

Stability strategies

Whole body mass centre (CM) positioning during seat-off was crucial to the success of rise and two stability strategies have been suggested (Berger et al., 1988). The first of these was to position the CM over and within the BS (provided by the feet) before and during seat-off such that static stability was achieved. This approach was observed in elderly subjects (Papa and Cappozzo 2000; Vander-Linden et al., 1994). The second option enabled rise to occur under conditions of increased dynamic stability i.e. the CM was outside the BS at seat-off. In this situation upper body momentum was generated from the forward movement whilst the body was still supported by the chair and then used to effectively carry the body through the dynamic portion of the sequence (Berger et al., 1988). With dynamic strategies the CM was thought to have positive forward velocity at seat-off, whereas with static strategies the CM was thought to have zero velocity at seat-off (Schenkman et al., 1990). Unfortunately, no data were presented to confirm this. In a study using young adults rising at natural to fast pace, Riley et al. (1991) considered stability and found the distance between the vertical

projection of the CM to be 70 mm posterior to the CP immediately after seat-off. The CP was reported to be beneath the ankles at this time. In this example, further calculation would show the vertical projection of the CM to be 30-40 mm behind of the BS at the time seat-off occurred, thus not satisfying conditions of static stability. Movements where a greater emphasis was placed on dynamic stability strategies required less apparent effort as upper body forward momentum facilitated lower limb extension when raising the body to standing position (Shepherd and Gentile, 1994). However, the subject needed to be capable of controlling forward CM momentum after seat-off through adequate strength and co-ordination of appropriate musculature (Schenkman et al., 1990). It was proposed by Riley et al. (1991) that it was possible for both strategies to be employed at the same time, i.e. one where the CM was in a statically stable position at seat-off whilst still possessing some forward velocity. Schenkman et al. (1996) suggested that the choice of strategy may be based on knee musculature. This was because with a stabilisation strategy the torque required to be generated at the knee was less, although upward movement was generated solely by the knee musculature and not with the aid of upper body momentum.

In a paper using elderly subjects, Hughes et al. (1994) suggested that three rise strategies could occur around seat-off. These were termed: momentum transfer, stabilisation, and combined strategies. Momentum transfer required fine postural control and the movement was generally shorter in duration. Stabilisation strategy required greater knee musculature to extend the knee and may include sliding forwards on the chair or translating the feet back. Torque at the knee was reduced in this condition, although the study also noted that it would have to be generated solely by knee musculature. Thus, stabilisation strategies sacrificed efficiency in order to gain success and facilitate control. A combined strategy was characterised by initial repositioning of the BS, whilst still requiring momentum to allow a dynamic period of rise around seat-off.

Millington et al. (1992) showed that because of lower limb soft tissue, contact remained between the thighs and the chair as seat-off was initiated through knee extension. Hirschfeld et al. (1999) explained that the definition of seat-off as described by Schenkman et al. (1990, 1996) (also used by Riley et al. (1991)), occurred at the instance when the vertical force vector beneath the feet began to increase i.e. whilst the thighs were still in contact with the seat. This happened approximately 250 ms before the full

seat-off time as shown in Hirschfeld et al. (1999). This drew into question the nature of the strategies as described by Schenkman et al. (1990) and Riley et al. (1991), as it appeared the suggested stability strategies were based on an incorrect definition of seat-off. In the study by Hirschfeld et al. (1999), the CM was seen to be above the CP by the time full seat-off occurred.

Movement control

In a paper by Brunt et al. (2002) measurement of the Tibialis Anterior was considered, as it was in the EMG studies reviewed earlier. The study suggested that the role of the muscle at this phase of the movement was to provide dorsiflexion torque at the ankle and in doing so, maintain a CP position beneath the feet. Without the Tibialis Anterior activity the CP would move forwards to the front of the foot as the CM moved forwards. Thus the role of the Tibialis Anterior in STS could have been to maintain the CP just anterior to the malleoli and in doing so, stabilise the ankle and maintain heel contact.

Carr (1992) highlighted that the CM must be controlled within the limits imposed by the need to balance the massive upper body as it rotated about the hip and was transported over the fixed foot from one base of support to another. It was around this transition part of the movement that Schenkman et al. (1990) recorded maximum ankle and hip flexion and head extension. Head extension was seen to be related to the degree of trunk flexion if the subject was making an attempt to remain looking forward. Stevens et al. (1989) discussed the importance of maintaining head control during the movement, although the study did not suggest that the subject would always strive to look forward. Nuzic et al. (1986) showed that subjects naturally allowed their neck to go through a period of extension and then flexion, perhaps allowing the eye gaze to continue looking forward, or to reduce joint moments in the neck. In that study, the time of peak neck extension occurred within 5% of peak hip flexion. Maximum hip and knee torque were seen around this portion of the movement, as the legs became fully load bearing (Millington et al., 1992; Kotake et al., 1993; Hirschfeld et al., 1999). Kerr et al. (1997) suggested that forward trunk lean continued for an average of 0.3 s after the initiation of vertical movement. This continuation of trunk lean was also noted by Kotake et al. (1993).

2.1.4 UPWARD MOVEMENT

During the upward phase, the spread of segmental activation was seen to move from the head to the pelvis in the upper body (Nuzik et al., 1986). In the lower limbs joint extension order was knee, hip and then ankle (Carr, 1992; Shepherd and Gentile, 1994; Khemlani et al., 1999).

Movement control

Upward propulsion continued after the buttocks left the chair, controlled by concentric activity of Quadriceps muscles at the knee, and eccentric activity of Biceps Femoris at knee and Gluteus Maximus at the hip (Millington et al., 1992). The support base lessened to the area of the feet, and along with CM displacement, the central nervous system (CNS) was challenged to control whole body movement and equilibrium at the same time. In a study by Yu et al. (2000), the completion of this seemingly simple task was said to require complex co-ordination of the CNS and neuromuscular system. Further, it was proposed that the extension phase was more complex than the flexion phase (Pai and Rogers, 1990) posing serious challenges to the success of STS (Hirschfeld et al., 1999).

Upward movement generation

In the vertical direction the thigh segment was seen to be the main generator of CM vertical momentum (Pai and Rogers, 1991). The results of Pai and Rogers (1991) were refuted somewhat in the work of Riley et al. (1991) who suggested that the upper body must rise at least as fast as the thighs, whilst also having the property of being more massive. This would imply that the upper body had more momentum. However, Riley et al. (1991) were mistaken in their judgement. This was because Pai and Rogers (1991) were commenting on which segment generated the momentum, not which segment contributed most to total CM momentum. Carr and Gentile (1994) suggested that arm movement can also contribute to the vertical propulsion required to accelerate the body into a standing position.

2.1.5 TERMINATION

An essential requirement for standing was that movement of CM was controlled within the limits imposed by the BS of the feet. In one of the earliest STS studies Yoshida et al. (1983) showed the CP to be comfortably within the central region of the BS for able subjects at the end of the rise movement. Pai and Rogers (1990) agreed with this showing the CM to finish at 50 ± 10% of the BS length. Few studies have considered the stabilisation phase at the end of rising because of the difficulties in distinguishing it from the end of rise and the start of standing. Kralj et al. (1990) considered the boundary between rising and stabilisation to be defined by a threshold of knee extension, although the authors did not give any reason for the choice other than it was appropriate. In research conducted by Kerr et al. (1994, 1997), STS was studied as a cycle which also included stand-to-sit, with a quiet phase separating the two movements of standing-up and sitting-down. However, the paper did not adequately describe the difference between the end of rise and the start of this quite phase.

2.1.6 SECTION SUMMARY

A scheme for the complete STS movement as found in previous studies has been presented. It was shown that the initiating muscle(s) have yet to be fully identified. Characteristic flexion along the length of the trunk was used to generate momentum in the upper body before seat-off occurred. During the transition from forward to upward movement different stability strategies were chosen depending on subject type and conditions of rise. A high degree of co-ordination was required as the support base reduced to the area of the feet, and complex stability demands were imposed as the subject rose to a standing position whilst maintaining equilibrium.

2.2 FACTORS AFFECTING SIT-TO-STAND CHARACTERISTICS

The section above described the general organisation of the STS movement. The following presents the effect certain variables have on tested characteristics of STS. This section is sub-divided into groups of affecting variables, namely: age and functional inability, initial body posture, rise duration, chair issues, and arm use.

2.2.1 AGE & FUNCTIONAL INABILITY

Many of the works published in the area of STS were aimed at understanding how and why certain subject groups have difficulty in rising, as this can influence the quality of life of those subject groups. As such, various levels of functional inability have been studied by authors. The effect of age was most frequently tested, grouping a number of commonly occurring functional inability types into one category (e.g. Wheeler et al., 1985; Schultz et al., 1992; Hughes et al., 1996). Other authors have been more specific in their choice of defined and tested factor, e.g. the study by Galli et al. (2000) that considered obesity.

Postural stability strategies

Older subjects were seen to use a rise strategy that placed a greater emphasis on postural stability (Wheeler et al., 1985; Papa and Cappozzo, 2000), particularly around the time of seat-off where stability was most threatened (Schultz et al., 1992). This was achieved by placing the CM closer to the BS as the buttocks left the seat (Wheeler et al., 1985; Papa and Cappozzo, 2000). Schultz et al. (1992) showed that at seat-off, young subjects placed their CP location 1.5 cm posterior to the ankle joint, whilst the elderly placed their CP location 1.9 cm anterior to the ankle joint. The latter strategy was typically implemented by placing the feet more under the body before rise was initiated (Wheeler et al., 1985; Alexander et al., 1996), or by increasing the amount of flexion in the trunk at seat-off (Wheeler et al., 1985; Schultz et al., 1992; Hughes et al., 1996; Lundin et al., 1999; Papa and Cappozzo, 2000). One study (Papa and Cappozzo, 2000) showed the elderly to place their feet in a more forward position than the young.

This was counter to the previous argument and attributed to possible Arthrosis in the knee or ankle in the tested subjects.

Muscle weakness strategies

A further strategy used by the elderly enabled the reduction of joint torque to compensate for muscle weakness (Wheeler et al., 1985). This may have been implemented simultaneously with the previously discussed postural stability strategies, because greater trunk flexion also reduced joint torque at the knee (Schultz et al., 1992). Additionally, a larger trunk flexion angle increased the length of the trunk/hip extensor muscles, subsequently increasing their force generating capacity (Lundin et al., 1999). Further to this, bringing the BS backwards at the start of the movement, as used as a postural stability strategy, lessens the required trunk flexion and reduces torque at the hip. Wheeler et al. (1985) showed that elderly subjects used a greater percentage of maximum musculature activity (in the Vastus Lateralis). When taking into account the increased trunk flexion seen in the elderly (i.e. the body moves through a greater distance (Papa and Cappozzo, 2000)) and that older subjects are generally heavier, it was perhaps not surprising that they were shown to have worked harder. However, the Wheeler et al. (1985) study did not show the maximum values of musculature activity for the subject groups. Thus, it may have been that absolute values of musculature activity between old and young subjects were similar. The study showed no difference in movement duration time between subject groups.

Some authors have suggested that maximum trunk flexion angle was not determined by knee or trunk-hip extensor strength (Lundin et al., 1999). Schultz et al. (1992) showed that with the exception of the very frail, joint torque requirements were within the maximum levels available to the subjects as demonstrated by other authors. Thus, ability to generate joint torque may not be a major factor in limiting the success of lift off from a chair. However, it was suggested that as rise conditions become more challenging, torque-generating requirements may become more important. For example, the old were disproportionately challenged by decreasing seat height, increased seat tilt/recline, and perhaps by a more compliant surface (Alexander et al., 1996). It was shown that knee joint extensor strength was a limiting factor in rise in functionally impaired adults (Hughes et al., 1996), and at higher rise speeds elderly

groups were unable to perform the movement in the same duration as younger subjects (Papa and Cappozzo, 2000).

Movement co-ordination

Whilst no differences were reported in trunk flexion velocity between young and old subject groups (Schenkman et al., 1996), it was found that smooth co-ordination of movement towards the end of rise was compromised in the elderly group. This information highlighted the increased importance placed on stability by the elderly, which may be affected when rising at higher speeds.

Other authors also found co-ordination of movement to be compromised in the elderly (Papa and Cappozzo, 2000). After seat-off, young subjects tended to rotate the trunk forward and elongate the body at the same time, whereas the elderly tended to make these movements separately. Riley et al. (1997) also noted that young adults were able to rise using a constant and specific strategy in comparison to the elderly. In contrast to the findings of Schenkman et al. (1996), Papa and Cappozzo (2000) found that at seat-off elderly subjects had higher trunk flexion velocity than the young, generating greater upper body momentum. It was said that this reduced the global muscular effort required to rotate body forward and gain stability. A similar strategy was noted by Su et al. (1998) in a study of total knee arthroplasty patients, where increased upper body momentum was used to compensate for the reduced ability to generate torque at the knee.

Rise duration

Rise duration was seen to be both similar between old and young in some studies (Wheeler et al., 1985; Ikeda et al., 1991; Papa and Cappozzo, 2000), whilst different between old and young in other studies (Yoshida et al., 1983; Alexander et al., 1996). Such a contradiction in this basic measurement may well indicate that the simple use of age as an influencing factor was insufficient when attempting to understand STS characteristics, and that more specific variables should be considered in future studies.

Body morphology

The functional limitations imposed by body morphology were studied by Galli et al. (2000) and Lou et al. (2001). In these studies a general decrease in trunk flexion was recorded due to increasing abdomen size. In pregnant subjects (Lou et al., 2001) this point was linked to the physical limitations imposed by the subject's body shape. As the term of the pregnancy increased, maximum trunk flexion angle decreased which was accompanied by an associated decrease in hip joint torque and increase in knee joint torque. Rise duration also increased under these conditions.

In obese subjects, limited trunk flexion was initially used as a strategy to alleviate back discomfort (Galli et al., 2000). This resulted in higher moments at the knee which would often be problematic in subjects suffering from Osteoarthritis of the knee (Gonarthritis). After ten trials had been performed (i.e. the subject had become fatigued), an increase in trunk flexion was recorded, apparently to decrease knee moments whilst at the sacrifice of lower back pain. Thus, the study suggested that changing rise strategies could be used to counteract fatigue. Obesity in the UK is on the increase (British Nutrition Foundation, 1999; Department of Health, 2003), so more insightful studies into this area would be useful.

Rise ability

Riley et al. (1997) described mechanisms of failed STS activities in terms of the magnitude and timing of momentum generation and dissipation, knee extensor torque, and GRFs. Whilst a primary cause of failure could not be inferred, failed rises were generally less energetic than successful rises and attributed to muscle weakness, balance control and co-ordination impairment. Two modes of failure were proposed: 'sit-back', where there was insufficiently generated momentum, and 'step', where there was excessively generated momentum. However, it was found that 'step' failures, whilst sufficiently energetic to permit rising, were due to poor momentum control, not excessive momentum generation. This was highlighted by the fact that most steps were in a lateral or backward direction, not forward. The reasons for the lack of forward step failure were not tackled in the paper.

In a study by Alexander et al. (2001), biomechanical analysis of STS performance was carried out, under varying task demands, to determine whether a 12 week strength training program may improve chair-rise success. The authors found that subjects unable to rise in some conditions generally generated less momentum, supporting the findings of Riley et al. (1997). Whilst the training group in the study by Alexander et al. (2001) did demonstrate some changes in STS mechanisms, there was no difference recorded in ability to perform successful rise. It was concluded that longer term training schedules may be more successful in producing rise success in impaired subjects. Lord et al. (2002) suggested that pain (over and above other physiological and psychological factors) had the greatest effect on measures of rise success in the elderly.

2.2.2 INITIAL BODY POSTURE

The second factor to be considered in terms of its effect on the STS movement was initial body posture. This referred to the position or arrangement of the body and its limbs at the start of the movement. Aspects of initial body posture have been studied by several authors, as they were thought to have an influence on the execution of the movement (Stevens et al., 1989).

Influences of foot position on movement parameters

Much of the reported work focused on the location of the feet in comparison to the CM (Fleckenstein et al., 1988; Stevens et al., 1989; Vander-Linden et al., 1994; Khemlani et al., 1999; Papa and Cappozzo, 1999, 2000). Foot location represented the position of the final base of support (in the standing position) and was closely related to how far the CM had to be moved forward before being elevated during standing up. The influence that foot position had on trunk flexion was discussed in Section 2.2.1 (age and functional inability) and will not be repeated here.

Changing the foot position from a 'foot-forward' position to a 'foot-backward' position influenced several STS responses. Authors commented on the increase in ankle and knee joint excursion (Vander-Linden et al., 1994), reduction in head displacement and velocity (Stevens et al., 1989; Vander-Linden et al., 1994) and reduction in trunk

velocity (Khemlani et al., 1999; Papa and Cappozzo, 1999, 2000). Normalised time of seat-off occurred earlier (Vander-Linden et al., 1994), as did the time at which CM maximum vertical velocity occurred (Vander-Linden et al., 1994; Papa and Cappozzo, 2000). Maximum ankle dorsiflexion occurred later when the feet were in the more posterior position (Vander-Linden et al., 1994). At seat-off, joint torques were seen to decrease at the hip and increase at the knee (Fleckenstein et al., 1988). This was suggested in the context of lower levels of muscle activity in the Upper Trapezius and Erector Spinae due to decreased trunk flexion and greater hamstrings and quadriceps activity. In a discussion of the work of Fleckenstein et al. (1988) by Munro et al. (1998), it was suggested that reductions in joint moments and loading forces were associated with less damage to the joint structures, although the nature of that damage was not mentioned further.

As the foot position changed from a foot-forward position to a foot-backward position, a decrease in movement time was noted (Fleckenstein et al., 1988; Khemlani et al., 1999). This was particularly associated with changes in the extension phase of the movement (Khemlani et al., 1999). Pai and Rogers (1990) showed that this vertical/extension phase of the movement was more variable than other parts of the movement. Conversely, other authors suggested that overall duration did not change with different foot positions (Vander-Linden et al., 1994; Papa and Cappozzo, 2000).

Despite modification of movement strategy, key variables such as GRF timings remained the same and thus may be ankle angle (foot position) invariant (Vander-Linden et al., 1994). Stevens et al. (1989) showed that whilst a reduction was noted in the initial negative trace of the antero-posterior force on the feet no difference was recorded in the maximum vertical force on the feet. In addition to this, the movement was also proposed to be 'smoother' (i.e. incorporating less trunk flexion) when the feet were in the more posterior position (Stevens et al., 1989). The sequence of muscle onset in the flexion phase remained the same between foot positions however, the timing of muscle or joint extension onsets were effected, demonstrating the stable yet flexible nature of critical STS actions in this phase (Khemlani et al., 1999).

Influences of upper body position on movement parameters

Shepherd and Gentile (1994) investigated the movement of the upper body as it was thought to facilitate strategies in the lower body. Rise was initiated from various starting trunk angles. By limiting trunk flexion, transfer of energy was minimised and it was suggested that this may possibly affect extension order. It was demonstrated that the more flexed the initial trunk position, the closer in time extension started at the knee and hip. The overall support moment remained consistent despite variability at individual joints. When rise was initiated from a fully flexed trunk, joint extension onset order was hip, knee and then ankle. In this situation, STS was compared with the movement of jumping up, especially when the CM was over the BS. More muscular effort was required when the forward rotation of the upper body was fully flexed. The presented findings indicated that the momentum in the upper body aids extension in the lower limbs so that the major burst of muscle activity would be brief and propulsive. Shepherd and Gentile (1994) commented that with more initial flexion, joint extension at the hip, knee and ankle occurred earlier in cycle and closer together. However, this would be expected as the flexion phase of the movement was effectively missing.

2.2.3 RISE DURATION

This section considers rise duration, i.e. that being the elapsed time between the start and end of STS. Two aspects of rise duration are presented. The first demonstrates variables that may influence rise duration, excluding influences of age and functional inability and initial body posture as these have been previously discussed. The second shows how changing rise duration affects STS characteristics.

Movement definition

Measures of rise duration were directly related to how the start and end of the STS was defined. In published studies, many definitions have been implemented and no common technique existed. This made comparison across studies extremely difficult. When stated in the literature, data types for the start definition have included:

horizontal shoulder velocity (Khemlani et al., 1999), initial horizontal head movement (Vander-Linden et al., 1994), torso flexion onset (Kotake et al., 1993) or CM horizontal velocity (Pai and Rogers, 1990; Yu et al., 2000). There have also been a number of methods used to define rise end: hip horizontal velocity (Shepherd and Gentile, 1994; Khemlani et al., 1999), CM horizontal velocity (Pai and Rogers, 1990), torso flexion termination (Kotake et al., 1993), and CM vertical velocity (Yu et al., 2000). Along with these data types, in general, threshold values were also presented in the literature. One of the most obvious differences was that some authors included the final stabilisation period in their definition (Kralj et al., 1990), whilst others did not (Wheeler et al., 1985; Nuzik et al., 1986; Pai and Rogers, 1990; Schenkman et al., 1990; Kotake et al., 1993; Kerr et al., 1997; Papa and Cappozzo, 2000). A number of studies have commented specifically on rise duration whilst neglecting to mention how start and end were defined (Alexander et al., 2001; Lou et al., 2001), making informed judgements very difficult.

Movement parameter influences on rise duration

The range of average rise duration in studies of normal subjects at self-paced speed varied from 1.3 s to 2.5 s (Wheeler et al., 1985; Nuzik et al., 1986; Pai and Rogers, 1990; Schenkman et al., 1990; Kotake et al., 1993; Kerr et al., 1997; Papa and Cappozzo, 2000). However, the value could be as low as 0.8 s for subjects rising as fast as possible (Kotake et al., 1993) or as high as 5.2 s in paraplegic subjects (Bahrami et al., 2000).

Lord et al. (2002) considered STS rise duration in older subjects, suggesting it was associated with good vision, lower limb propreoception, tactile sensitivity, simple foot reaction time, postural sway, body weight, reported pain, vitality, and anxiety. Joint strength (knee extension/flexion and ankle dorsiflexion) was found to be most important in explaining variance in rise duration, although there was little supporting evidence to quantify this. Schenkman et al. (1990) also considered joint strength as an important influence on STS rise duration. Body height was not thought to influence rise duration (Lord et al., 2002).

Influences of rise duration on movement parameters

Vander-Linden et al. (1994) showed that peak vertical force at the feet was greater under faster conditions, although other movement strategies were demonstrated to remain invariant. Three studies (Kotake et al., 1993; Papa and Cappozzo, 1999; Mitchell et al., 2003) found that the onset of seat-off and the completion of seat-off occurred later in the cycle in faster movements. However, Pai and Rogers (1990) suggested that there was no change in normalised time of full seat-off as a result of a change in rise speed.

The influence of rise duration on CM trajectory was approached by Pai and Rogers (1990). The authors argued that as speed increased, the upward portion of the movement (i.e. the vertical part of the path travelled by the CM) occurred earlier. Because there were less pronounced forward and upward phases, the total distance travelled by the CM was shorter as a more direct path was traversed between the start and end positions. The authors showed that the majority of a reduction in rise duration would be achieved in the vertical part of the movement, with the duration of the horizontal part of the movement being more tightly controlled. In a later study, the same authors suggested that the variable nature of the vertical movement was predominantly controlled by movement of the thigh segment (Pai and Rogers, 1991). This prompted the suggestion that control of CM in the horizontal direction may be an invariant feature of STS, and differences in task constraints were satisfied by other variant degrees of freedom. Papa and Cappozzo (2000) claimed that timing of maximum vertical velocity occurred later in the normalised rise cycle due to an increase in speed, while Pai and Rogers (1990) found it to happen earlier. Whole body mass centre (CM) peak linear velocity changed from 0.60 $m \cdot s^{-1}$ to 0.98 $m \cdot s^{-1}$ as rise speed went from natural to fast pace (Papa and Cappozzo, 1999), with a similar increase noted by Pai and Rogers (1990).

Kotake et al. (1993) analysed the effects of rise duration on angle data and in general noted no difference in joint angle patterns. However, it was suggested that in slow rise, the hip joints were in flexion for a longer period after the hips left the chair, causing the torso to incline to a greater extent. Papa and Cappozzo (1999) recorded trunk angle with regard to the horizontal axis and found increased trunk flexion from slower rise conditions.

2.2.4 SEAT DESIGN

Seat height

A decrease in seat height lowered the initial CM of the subject making rise mechanically more difficult (Burdett et al., 1985; Alexander et al., 1996; Schenkman et al., 1996). Schenkman et al. (1996) studied relationships between seat height and rise, and found that initial trunk flexion velocity increased with a reduction in seat height. It was suggested that the increased momentum recorded in the upper body as seat height decreased aided rise during the seat-off phase. Trunk flexion and extension angular velocities increased, as well as hip and knee extension angular velocities. In this study (Schenkman et al., 1996) rise duration was constrained so increases in joint angular velocities could be expected as the body had further to move in the same time. When knee extension velocity was normalised for displacement, trends disappeared. It was suggested that the use of upper-body momentum in STS may be used as a mechanism to compensate for decreased seat height and increased lift-off difficulty, not as a mechanism for increasing the overall speed (Schenkman et al., 1996). In an earlier study of chair rise strategies, Hughes et al. (1994) showed that in the elderly STS became less successful with decreasing seat height. In patients recovering from total knee arthroplasty, Su et al. (1998) recorded an increase in CM horizontal displacement as seat height decreased. This reduced the associated increase in knee joint torque in the subjects.

Lou et al. (2001) considered STS over different periods of pregnancy. In the second and third trimester periods of pregnancy, rise duration increased with decreasing seat height. Maximum trunk flexion angle increased with decreasing seat height which also increased hip joint torque. This might be expected considering the greater degree of initial hip flexion seen in rise from a lower chair compared to rise from a higher chair. Further, the increased hip flexion may reflect the conditions of greater required stability expected of rising from a lower chair. Hip and knee moments were reported to increase with decreasing seat height. Alexander et al. (2001) noted that lowering the seat height generally increased rise time, anterior CP placement over total rise duration, and maximum CM horizontal and vertical velocity. Additionally, hip flexion and hip and knee torque were shown to increase in a similar manner as described in Lou et al. (2001).

Other seat design factors

Alexander et al. (1996) studied the affect of several aspects of seat design on rise. A number of seating conditions were tested including seat height, arm rests, surface compliance, seat tilt and backrest recline. These represented a variety of seating situations. The degree of rise difficulty increased with decreasing height, seat tilt, backrest recline and the addition of foam to the seat. In such situations it was suggested that the elderly suffered more from these challenges. A compromise between this degree of challenge and comfort was highlighted. A higher seat can be used to reduce the required muscle strength however, if the seat becomes too high, circulation in the legs can be compromised.

In an early study by Burdett et al. (1985), STS characteristics from two chairs of different heights were reported. One chair was a specially designed Artherapedic chair, with the other being a more standard armchair. Joint torque was used as a measure of ease of rise. The results showed that rising from the higher Artherapedic chair reduced the total range of movement and the required joint torque of the lower extremities.

In a study of elderly patients, Munro et al. (1998) investigated movement patterns from two seat heights of a chair which incorporated an ejection mechanism to aid rise in the elderly. A higher seat height and use of the ejector mechanism were found to facilitate rising in elderly rheumatic patients. Rising from a higher seat resulted in a greater normalised time to seat-off. Also noted were greater trunk angles at seat-off, increased ankle angular displacements and decreased reaction forces. Whilst some differences were shown between ejector conditions (i.e. its use or non-use) in CM horizontal velocity measures, the seat height did not affect level or time of CM peak horizontal velocity. This was in line with the previous reviewed strategies of tightly controlled CM horizontal velocity as suggested by Pai and Rogers (1990).

2.2.5 ARM USE

Seat armrests

The placement of armrests did not affect total duration of STS (Alexander et al., 1996). Wheeler et al. (1986) noted that both old and young subjects would instinctively opt to use armrests if available. In the elderly, this relationship was in part linked to the greater muscle force required to move the generally greater body mass of the tested subjects in the elderly group. However, for both subject groups a strategy of using arms where possible seemed to be an appropriate way of distributing the force required to rise throughout the body.

Arm movement support strategies to aid STS

Several authors have commented on the use of the arms to aid rising. In particular, in situations where the subjects' feet were in a relatively anterior position, arms were used to generate increased CM horizontal and vertical momentum (Stevens et al., 1989), or CM horizontal location at seat-off (Fleckenstein et al., 1988; Schultz et al., 1992). Such strategies might be used where seat design does not allow a more posterior positioning of the feet. The arms may also be related to the strategies proposed by Berger et al. (1988) concerning CM position. For subjects less able to rise effectively (e.g. the elderly), Chan et al. (1999) recommended the application of hand force to aid postural stability. Burdett et al. (1985), Butler et al. (1991) and Schultz (1992) all suggested that hip and knee torque could be reduced by using a similar strategy as that suggested by Chan et al. (1999). However, this was at the cost of increased shoulder joint torque. Butler et al. (1991) further suggested that pushing down on the knees with the arms in the early phases of rise could compensate for weak extensor muscles in hips.

In a study by Carr (1992) the role of arm movement in STS by aiding translation and propulsion to the whole body was investigated. STS was tested under three arm-position conditions: a preferred condition had the subject's hands on the knees, a restricted condition had the subjects holding a light box, a pointing condition had the subjects point towards a stationary target. The CM was demonstrated as being above

or in front of the heel marker at full seat-off in all conditions, similar to Schultz et al. (1992). Whole body mass centre (CM) vertical and horizontal momentum was greatest when subjects were pointing. Subjects moved forward slower and the CM rose more steeply in the arms restricted condition, possibly reflecting a safety mechanism used to counteract the subjects' fear of falling forward. There were also greater variations recorded in ankle joint angle displacement in the restricted arm condition suggesting that restricting the arm can increase the demands on the postural system. The use of the arm was demonstrated to augment the total support moment (Shepherd and Gentile, 1994). This could suggest that rising with the arms folded across the chest may produce an unnatural movement and draws into question those studies in which subjects have risen with these or similar arm restrictions.

2.2.6 FACTOR COMBINATIONS

The experimental approach in many of the STS studies was generally concerned with single factor experiments. Where multiple factors were presented, typically only main effects on output measures were discussed. Consequently, a greater understanding of the nature of a response may have been missed because some human related studies have shown output measures to be affected by interaction between factors (e.g. Babski-Reeves and Crumpton-Young, 2003; Goble et al., 2003). In recent STS studies, the reporting of interaction effects has begun to occur. Alexander et al. (2001) considered the effect of five factors on a variety of STS responses. Although the experimental design was not able to offer full screening of all factors, interaction effects between *seat height & subject group* and *seat height & hand use* were noted, particularly with reference to CM vertical momentum. Munro et al. (1998) found interactions between *chair height & seat type* on trunk bend and vertical impulse in elderly rheumatic patients. With the exception of these STS studies, more thorough investigation of how responses of STS change due to combinations of factors could greatly improve the understanding of the underlying co-ordination of the STS movement.

2.2.7 SECTION SUMMARY

Several factors were shown to affect characteristics of STS. Elderly subjects used strategies to overcome postural stability difficulties and muscle weaknesses. The use of age as a factor was regarded as a possible hindrance to the greater understanding of true influencing factors in the elderly. Initial body posture was shown to be approximated by foot position, which played a large role in the degree of CM horizontal displacement required to bring the body to a position of equilibrium over the feet. The difficulties of comparison between reported rise duration times was due to the numerous start and end definitions used by authors. Rise duration was shown to vary between 0.8 s and 5.2 s, dependent upon subject type and rise condition. A reduction in seat height made rise mechanically more difficult, which was overcome by increased trunk flexion and extension angular velocities. The use of arms had an important influence on STS characteristics. It was suggested that studies that allow rise to occur whilst subjects placed their arms folded across their chests may produce unnatural rise patterns in those subjects.

2.3 MOVEMENT SUBDIVISION

2.3.1 OVERVIEW

Dividing movement into phases has been considered a useful tool for understanding the nature of a movement. It has been used successfully in the past, for example in gait analysis (Novacheck, 1998). Several STS studies have classified rising into discreet phases. These are discussed below and presented diagrammatically in Figure 2.1. In the figure, 0% of movement cycle represents the start of movement and 100% represents when full standing has occurred. Studies that included a stabilisation phase within the movement definition show that stabilisation period occurring outside of this 100%.

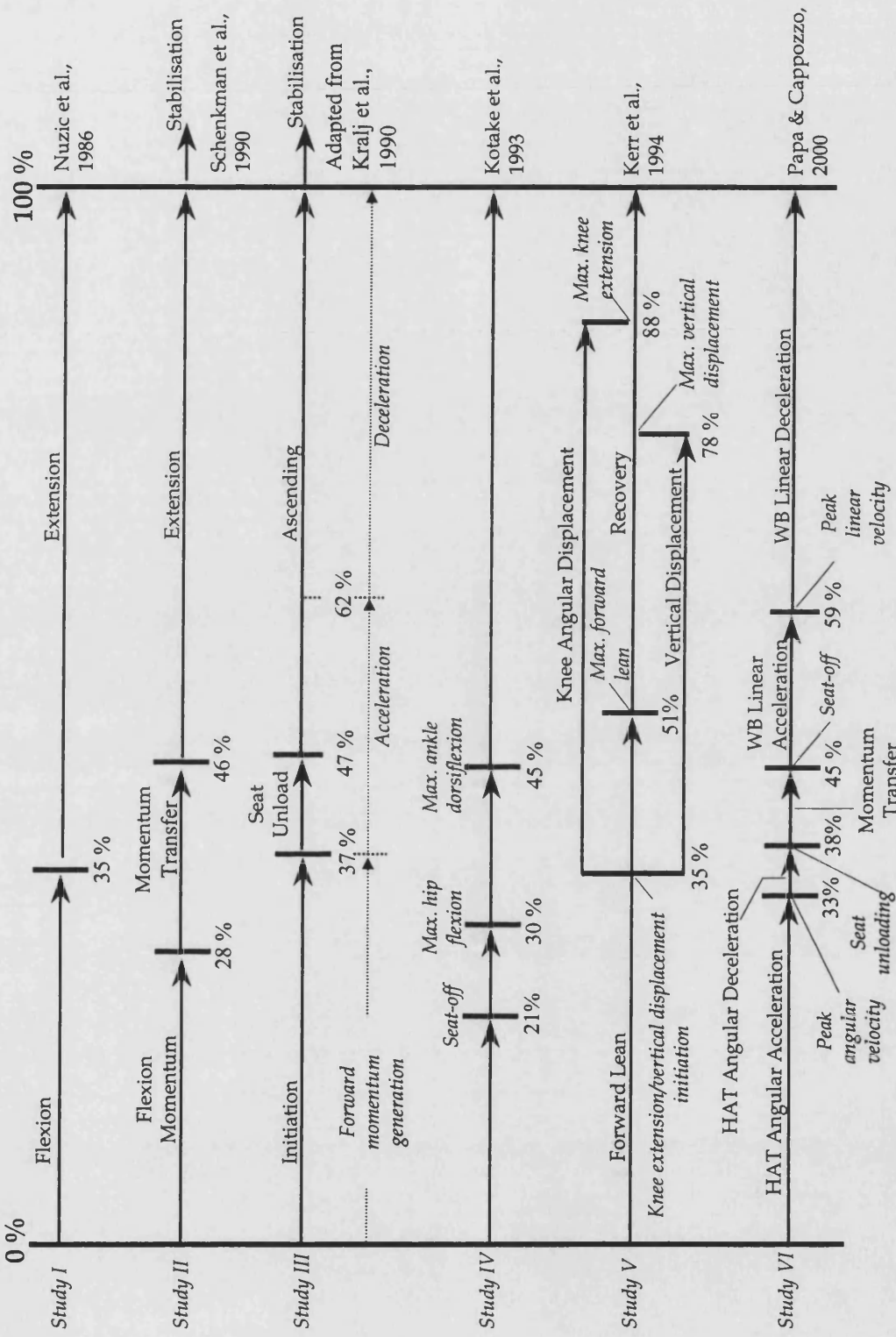

Figure 2.1. Compilation of previous studies that expressed STS movement as sub-divided phases. Note: Two studies showed that a stabilisation phase was included in some form in the original study. However, the stabilisation phase has been adapted in this figure as shown by the arrows outside of the 100% duration time.

Frequently, subdivision of movement has been made to provide baseline data from which further studies could consider the affects of variables or, as an aid to monitor rehabilitation of patients etc. However, problems have arisen because in general authors have suggested divisions based on their own requirements. As such, no single adequate definition of sub-movement has been consistently implemented by authors, which restricts full interpretation of results. A scheme proposed by Schenkman et al. (1990) was perhaps the most commonly used by other authors (Ikeda et al., 1991; Riley et al., 1991; Vander-Linden et al., 1994; Su et al., 1998; Lou et al., 2001). However, it was somewhat limited by the ambiguous definitions used to constrain the phases. Due to the fact that definitions of the start and end of STS differ between studies, direct comparison between studies should be treated with appropriate caution. The individual studies are discussed as follows.

Study I by Nuzic et al., 1986

One of the first studies to divide the STS movement was conducted by Nuzic et al. (1986) (Figure 2.1). Two discrete phases defined *flexion* (on average encompassing the first 35% of the movement), and then *extension* which completed the motion. The transition of these phases was marked by the time at which the neck moved from a period of extension to a period of flexion. This stands as one of the main limitations of the study, as the time of neck extension/flexion was somewhat dependent on where the subject was looking, and this was not controlled within the study. The knee was also seen to start a period of extension at around the same time (35%), which would coincide with the initiation of seat-off. However, the occurrence of seat-off was not explicitly mentioned. It was shown that during the flexion phase, the head slowly tilted in an anterior direction and the change in knee angle remained close to zero. Further, the trunk continued to flex for a short time into the extension phase. This study represented a good first attempt to split the movement to aid the description of STS. However, weak definitions used to define the start and end of the movement, added to the simple approach used to describe a complex movement, meant that the study had limited influence on current understanding of STS. A study carried out by Butler et al. (1991) acknowledged the above phase definition and used it to study STS in some patients suffering neuromuscular diseases.

Study II by Schenkman et al., 1990

Perhaps the best known subdivision of movement comes from the work of Schenkman et al. (1990), who categorised rising into four phases: Flexion-Momentum, Momentum-Transfer, Extension, and Stabilisation (Figure 2.1). The work was approached from a physiotherapy point of view, and was based around the idea that momentum was first generated in the upper body and then used to aid the initiation of vertical movement. Specifically, the Flexion-Momentum phase, beginning at movement initiation and ending just prior to seat-off, was used to generate momentum in the upper body through trunk flexion. The Momentum-Transfer phase, starting from seat-off and ending when the ankles reached maximum dorsiflexion, used the generated momentum to aid the whole body through a period where stability demands were high. The study used maximum dorsiflexion of the ankles to mark the end of this phase because it approximated the time at which maximum horizontal displacement was achieved. However, if rise was started from a foot position where the ankles were very dorsi-flexed, as in Vander-linden et al. (1994), then the maximum dorsiflexion could have occurred at the start of rise. The Extension phase continued until the hips stopped extending. Knee and neck extensions also came to an end during this phase. The final phase, Stabilisation, continued until stable postural sway was achieved. Because the end of this phase was difficult to define, it was not included in the analysis of the movement. In Figure 2.1, the normalised time scale ends at the termination of the Extension phase.

Study III by Kralj et al., 1990

Kralj et al. (1990) created a standardised sit-stand-sit cycle (part shown in Figure 2.1) equivalent to the gait cycle as reviewed by Novacheck (1998). The aim was to describe and propose definitions and terminology for STS in normal subjects. The defined phases included one encompassing Stabilisation which was presented outside of the normalised cycle in Figure 2.1. Because the Stabilisation phase was included in the definition of STS by the authors, the timing values within the figure were adjusted. The remaining sections allowed rise to be divided into three phases, the first being Initiation bounded by the start of movement and the beginning of seat-off. The second phase was termed Seat-Unloading with the authors being the first to classify seat-off as

a phase and not as a discreet event. The final phase was titled Ascending, which ended with full extension of the knee. Alongside these, activities of momentum generation, and body acceleration and deceleration were analysed. The average time to rise across all subjects (to include stabilisation) was 3.33 s (range 2.58-5.12 s). It was suggested that it was necessary to identify events in terms of the normalised cycle. This was to enable STS to be compared across a range of movement speeds. However, the authors did not take into account the fact that these normalised event times may change as movement speeds varied, as shown by other authors e.g. Pai and Rogers (1990) or Papa and Cappozzo (1999).

Study IV by Kotake et al., 1993

The study by Kotake et al. (1993) sub-divided rise into four phases (Figure 2.1) based on joint angle turning points, with the authors showing an appreciation that some joint rotations crossed the boundaries of the phases. However, the completion of the seat-off event occurred earlier in the cycle than in all other studies (20.9% as opposed to around 35%). Thus, some doubts could be raised as to the validity of the data. It was difficult to assess the study further because no solid definitions were presented for the subdivisions.

Study V by Kerr et al., 1994

Kerr et al. (1994) noted that well-defined terminology or definitions had not been clearly established for the sit-stand-sit cycle movement as it had been for the biomechanics of gait. The authors believed that a formal definition was required before the problems with rising could be fully understood. The temporal overlap of forward lean and vertical displacement was documented and described in terms of discrete phases that at times coincided with each other (Figure 2.1). Seven events were used to form the description of STS via the overlapping phases of Forward Lean, Knee Angular Displacement, Vertical Displacement and Recovery of Trunk. The study also suggested that a reversed cycle could be applied to the motion of stand-to-sit. Whilst not specifically documented, it was possible to calculate the normalised times for these events from other data in the paper. These are shown in Figure 2.1. The work was later

repeated for a larger subject sample in Kerr et al. (1997). Despite the valid purpose of the paper, the ambiguous description of events and movements meant that it was unable to be applied widely across STS studies, as had been its intention.

Study VI by Papa and Cappozzo, 2000

Recently, Papa and Cappozzo (2000) offered a five-phase rise model (Figure 2.1). Phase 1 marked a period of angular acceleration of the head, arms and torso (HAT) segment. This was followed by phase 2, where the HAT went through a period of angular deceleration. Phase 3 defined seat unloading and was titled Momentum Transfer, similar to Schenkman et al. (1990). The penultimate phase established a period of body linear acceleration in the vertical direction, and finally, there was a period of body linear deceleration, to finish in a standing position. The normalised times presented in Figure 2.1 were for a young subject rising at natural pace. However, Papa and Cappozzo (2000) recognised that these normalised times could change due to rise duration and subject type.

2.3.2 SECTION SUMMARY

The subdivisions of the movement as found in six individual studies were presented. These varied in complexity from the simple two-phase movement described by Nuzic et al. (1986) to the five-phase movement described by Papa and Cappozzo (2000). Normalised times were presented such the rise schemes could be applied to movements of differing rise duration. However, there was a general lack of appreciation with regard to the change in these normalised times due to changes in rise duration. Definition of rise events were frequently based on some threshold or peak value of a parameter, and not necessarily on critical actions which must occur for rise to be successful.

2.4 DESIGN FOR HUMAN MOVEMENT IN INDUSTRIAL ENVIRONMENTS

2.4.1 INTRODUCTION

The UK manufacturing sector employs around 3.46 million people (Sly, 2004). In recent years, the costs due to non-fatal injury in industrial environments accounted for large amounts of expenditure. It was estimated that the equivalent of around 4-8% of each company's gross trading profit (£143-£297 per employee) was spent per year for costs associated with non-fatal injury (Health and Safety Executive, 2002).

Within the environment of a manufacturing workstation (e.g. at a conveyor belt), many separately identifiable motions were used by operators. These might include: reaching (e.g. for a component or to add an ingredient to a food product), pushing or pulling (e.g. a product as it comes to an operator from a conveyor), lifting (e.g. a part from a component bin to workstation height or, to fill a hopper), body translation or twist (e.g. from one part of the workstation to another). In addition to these, one of the most common motions that occurred was that of a person moving from a sitting position to a standing position, as it acted as a pre-cursive movement allowing many other activities to occur (Magnan et al., 1996).

2.4.2 DEVELOPMENT OF APPROACHES TO ERGONOMIC DESIGN

Historically, products and workstations were built on an individual basis where measurements of individual users were used to form a design. As small series of products began to be built, anthropometric design was based on general 'rules-of-thumb'. However, when production outputs became larger, an alternative approach was required. Thus, systems were required to give estimates of body dimensions or movement patterns over a range of populations (Molenbroek, 1994).

It has been suggested that the majority of products or workstations were designed for healthy, young males. Thus, a disadvantage was often placed on handicapped, female, young, or elderly users (Molenbroek, 1994). Further, it was shown that in young subject groups in western countries, design standards quickly became outdated as body dimensions altered between generations (Molenbroek, 2003), and it seemed likely

that the same may be true for other subject groups. Thus, the requirement for frequent and correct ergonomic assessment of product and workplace design was evident.

2.4.3 CONSEQUENCES OF POOR ERGONOMIC DESIGN

Various theories, principles and methods have been generated through ergonomics research with a view to the improvement of workstation design (Eastman Kodak Company, 1983; Das and Sengupta, 1996; Department of Trade and Industry, 1998; Huijboom et al., 1999). In the past, many of the design approaches to workstations have failed to be fully anthropocentric (i.e. human-centred) (Venema and Hannaford, 2001). As such, the design of industrial workstations were primarily concerned with the improvement of equipment performance, and limited thought was given to matching task requirements with the functional abilities of the operator. This has resulted in generations of inadequately designed workstations due to the relatively minimal significance placed upon anthropometric measurement and user movement patterns. This has reduced worker productivity and added to unnecessary injury in the workplace (Das and Sengupta, 1996; Solman, 2002). Typically, the injuries associated with processing operations include sprains, strains, and to a lesser extent, body part contact with rollers and blades (Health and Safety Executive, 2002). For example, inadequate posture caused from operating a workstation of flawed design could increase static muscle effort. This may result in acute localised muscle fatigue or painful affliction of the musculoskeletal system such as cumulative trauma disorder. This can decrease performance and increase operator related health hazards (Das and Sengupta, 1996). To address the issues of operator health and safety, some design recommendations have previously been made with regard to STS environments (Eastman Kodak Company, 1983). However, these recommendations only suggested the use of a seat or stool. They did not address deeper issues such as placing an emphasis upon workstation design where harmful postures and imposed stresses on the user were minimised (Das & Sengupta, 1996).

2.4.4 CURRENT ERGONOMIC ISSUES

In recent years society has become more conscious about the health and safety aspects of machinery design, specifically in the context human-machine interactions. Indeed, the importance of an ergonomics input is now recognised as essential by many industries (Porter et al., 1999). Whilst the interaction between human operator and machine is still considered difficult to assess through current computational techniques (Molenbroek and Medland, 2000), the ergonomics field is constantly developing. New computer technology and products provide increased opportunity for bringing ergonomic information in a more useable form to design engineers (Liu et al., 1997). Additionally, with these advancements the aims of ergonomic intervention also change (Solman, 2002). In workstation design, the current challenge is for designers to achieve solutions that will optimally fit the diverse anthropometry of the targeted operator population, to satisfy task demands, and to accommodate the physical size and layout of the workstation components (Das and Sengupta, 1995, 1996).

The anthropocentric approach to design brings with it difficulties in terms of understanding and modelling human movement. This was with particular reference to the infinite number of posture possibilities that can occur due to excessive degrees of freedom of the human body (Zhang et al., 1998). Further, size variations across human populations complicates anthropocentric design analysis, creating conflict between the need to avoid custom design for each operator and the desire to accommodate a large number of people (Venema and Hannaford, 2001).

2.4.5 LEGISLATION CONSIDERATIONS

An important issue in the field of design for human movement is the legislation that applies to it, which has to be considered throughout the design process (Molenbroek and Medland, 2000). Safety regulations have now accelerated to a point where many societies have extensive legal statutes governing the circumstances under which a product may be used or sold (Green, 2000). For the design of machines, international regulations have reached a stage where the machines are required to be demonstrated as being inherently safe for use by operators before being put into commercial use (van Ekelenburg et al., 1995). Additionally, usability assessments in accordance with

ISO 9241 were required to be performed (Solman, 2002). These included three indicators of deficient interaction: effectiveness, efficiency and satisfaction.

2.4.6 DEMAND FOR ERGONOMICS

Today, the design of machines with regard to the human-machine interface can be crucial to the performance of a human-machine system (Solman, 2002). The success of the interface critically influences the effort required by an operator and consequently there are associated health and safety issues (Green, 2000). Thus, whilst this can make the process of product development complex and lengthy, there is a primary demand to optimise the human-machine relationship through techniques of user-centred design. Consequently, the increasing complexity of modern systems and social, economic and legislative pressure for good design have led the demand for the ergonomics input to be available as early in the design phase as possible (Porter et al., 1999).

2.4.7 SECTION SUMMARY

The average cost to industry due to non-fatal industry was estimated between 4-8% of each company's gross trading profit. Whilst the influence of poor workstation layout on injury rate was described, the positive impacts associated with correct ergonomic design were highlighted. The nature of engineering design is fast moving, modern systems are becoming increasingly complex, and social and economic pressures are high. Consequently, requirements were placed on ergonomic contributions to be available as early as possible in the design process. Further, studies showed that the changing nature of body types should be used as a driver for more frequent ergonomic intervention. Finally, it was shown that legislation was required to demonstrate product/workstation design to be inherently safe before being used by human operators.

2.5 APPROACHES TO ERGONOMIC HUMAN MODELLING

2.5.1 INTRODUCTION

Models can be used to increase our understanding of the world around us or to predict outcomes of untested conditions - they attempt to conceptualise reality (Nigg and Herzog, 1999). In the context of product design, ergonomic models based on biomechanical principles may be used in the design of workstations to increase productivity or to reduce the possibility of operator injury.

2.5.2 COMPUTER AIDED ERGONOMICS

In recent times, ergonomic packages have become increasingly popular within the commercial sector, allowing the limitations and capacities of human subjects to be explored without fear of injury or inconvenience. This ergonomic input has been supported with the development of computer aided design (CAD) packages that are capable of simulating the designed environment. CAD packages are commonly used by engineers as they provide more flexibility than traditional, non-computer systems. However, whilst common within the manufacturing industry, many CAD systems ignore the most important component of the human-machine system being designed, i.e. the humans themselves (Porter et al., 1999).

Ergonomic analysis was commonly concerned with spatial accommodation, posture, reaching abilities, clearance and interference of the body segments, field of vision, strength of operator, and biomechanical stresses (Das and Sengupta, 1995). Typically, information for body size, strength, segment masses and inertial properties from established databases may be used, and assessments carried out through manual drafting, stick figure modelling, drawing board manikins, or analytical modelling (Das and Sengupta, 1995). Green (2000) argued that traditional ergonomic techniques had served well in terms of applying boundary condition data, whilst current ergonomic inputs were required to give a greater understanding of human-machine relationships. It was suggested that four levels of anthropometric model could be used: Anthropometric tables, 2D modelling systems, 3D modelling systems and real test subjects (Molenbroek, 1994; Molenbroek and Medland, 2000). However, Venema and

Hannaford (2001) commented that the most useful of these were based on 3D modelling systems because of the three dimensional nature of workstation designs.

2.5.3 COMPUTER AIDED HUMAN MODELS

Computer-aided graphical human modelling programmes have been emerging since the 1960s (Das and Sengupta, 1995). These have experienced continued development. Currently, a number of manikin models exist based upon articulated human representation that can be manipulated and positioned within a workspace to resolve design issues. Several research teams have developed man-modelling CAD systems and these now include a number of advanced 3D manikins (Faraway et al., 1999; Porter et al., 1999). Requirements for 3D models include: the generation of groups of manikins, positioning the model in a workspace design, allowing the model to move or make a movement pattern, and assessment of contact between the manikin and the environment or machine (Molenbroek and Medland, 2000). Models have met with varying degrees of success, although essentially they are design tools that enabled the evaluations of postural comfort, assessments of clearances, reach and vision etc. (Porter et al., 1999).

Selection factors of a modelling system may include: the computer modelling environment, ease of manikin manipulation and interpretation, flexibility of the model to represent postures and actions, or degree of realistic appearance. Selection should also be guided by the evaluation required, cost, and the availability of computer hardware and software (Das and Sengupta, 1995).

Commercial packages

There are numerous versions of ergonomic man-models being used within industry today. These include: AnyBody, ANTHROPOS, BMDHMS, Boeman, BUFORD, CYBERMAN, COMBIMAN, CREW CHIEF, Jack, RAMSIS, and SAMMIE, amongst others. Graphical representation of AnyBody and SAMMIE models are presented in Figure 2.2. Such systems were used particularly in aeronautic and automotive industries (Das and Sengupta, 1995; Porter et al., 1999; Venema and Hannaford, 2001).

All of these human models are commercially available and provide a convenient means to analyse fit to workstation components. However, they do differ in programming techniques, operating characteristics, and capability (Das and Sengupta, 1995). Most of those mentioned were well able to re-create realistic 3D environments, with man-models capable of adjustment to a wide variety body-size percentiles. In an overview given by Molenbroek and Medland (2000) it was suggested that Jack provided high-level presentation and animation, RAMSIS was suited to evaluating problems of sitting in cars and workspaces, ANTHROPOS satisfied the lower end of the market and BMDHMS was able to evaluate cockpit and shuttle environments.

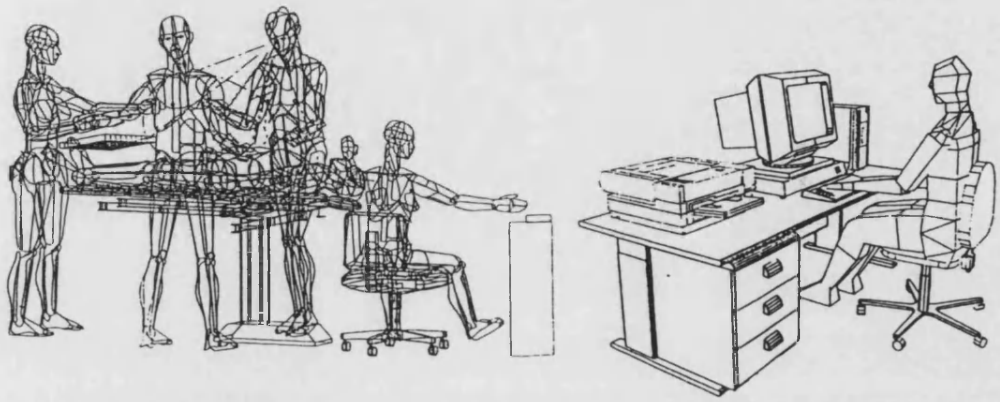

Figure 2.2. Graphical representation of AnyBody (left) and SAMMIE (right) models (Porter et al., 1999).

The packages normally included joint range of movement data to prevent the human model from assuming unnatural postures. This was achieved through application of constraints to joints, representing comfortable limits of working. Additionally, the user could select type of person, body size, gender, percentiles etc., or separate body segment sizes. Variation of these parameters could be used to allow multidimensional workstation design (Porter et al., 1999). Because anthropometry files were generally embedded into the manikin models, this relieved the user from having to search the published literature (Das and Sengupta, 1995).

The disadvantage to the systems was that each posture had to be individually created by the separate positioning of segments. Thus, the user required some knowledge of what positions could be expected in certain situations, making manipulation of body posture time intensive. It was shown that the programmes could not solve workstation problems by themselves, and were only able to act as an alternative to wooden or other

models (Das and Sengupta, 1995). As such, the success of the design depended highly on the designers' judgement and ability to incorporate sound ergonomic principles into the design. Frequently, there was little analysis other than to check whether the limbs were at an acceptable attitude. Thus, the designer was left to carry out a visual check to determine whether such actions and postures were acceptable in real life. However, methods of setting the posture were limited by the fact that it is often difficult to predict the actual position that people would adopt in some circumstances (Zhang and Chaffin, 2000).

It has been proposed that future developments could include dynamic strength modelling and improved methods of man-model control. Additionally, collision avoidance in association with virtual reality and dynamic human movement for use with animated visualisations is also a possibility. Other developments include more complex constraint modelling (e.g. the ability to define multiple constraints such as sitting in an automobile cockpit, fixing the foot to pedal and the buttocks to the seat, whilst forcing the knees and ankles to remain within a comfort tolerance as the seat is moved) (Porter et al., 1999).

The reported studies generally commented on the development state of the models as they were around the early to mid-1990s. As such, and in the context of the current rapid increase in ergonomic technology (Solman, 2002), the description of these models in the published literature is somewhat dated (Das and Sengupta, 1995).

Predictive ergonomic human models

Predictive computerised models can have considerable practical value for designers, reducing product development time and costs etc. However, the development of models that realistically predict how people normally move and interact with systems presents a challenge in the field of ergonomics (Zhang and Chaffin, 2000). Primarily, this challenge comes from the kinematic redundancy associated with the body's many degrees of freedom. Whilst it was appreciated that humans adopt strategies to resolve this, quantitative representation of such strategies was difficult.

Recently, work has been conducted into the prediction of human motion for application to ergonomic models. HUMOSIM have simulated motions such as reaching (Zhang and Chaffin, 1999) and lifting (Zhang et al., 2000) using computational manikins. These investigations predicted motion by first recording experimental data many times. In the case of HUMOSIM, there were in excess of several thousand trials recorded for each motion (Faraway et al., 1999; Faraway, personal communication, 4th October 2001). Subjects were recorded and their segmental joint centres digitised whilst performing tasks. From this, averaged data were achieved for joint angular displacements and graphical functions were created to mimic the averaged data. Other inputs to the model included the start and end conditions i.e. starting posture and target position.

HUMOSIM body motion was described in terms of joint angle data as opposed to joint co-ordinates (Faraway et al., 1999). This was considered to be desirable because angle data were less variant to changes in body size. Posture could be also specified more compactly in terms of angles than co-ordinates. However, problems could occur when predicting motion of different subjects under different constraints. This was because the system did not guarantee that the reconstructed posture would be correct, for example putting the hand on a target. Two reasons were identified for the error. Firstly, the prediction models were not perfect so there would be some error in the angle prediction, and secondly, body segment length was not an explicit component of such models and so this variation resulted in joint co-ordinate error. Rectification techniques were demonstrated to account for this and used with a degree of success (Faraway et al., 1999). However, it was unclear at this stage as to how realistic motions were for anything other than those where the original data were collected.

The constraint modelling software SWORDS has been set up as a tool to investigate a range of research orientated issues. It was developed at the University of Bath and has been successfully used in the packaging industry to solve complex design problems where there were many degrees of freedom (Bowler et al., 2000; Medland, 2000; Hicks et al., 2002). The constraint resolution environment operated on the principle of applying direct search techniques to seek states that satisfied sets of chosen objectives. The objectives were cast as constraints that needed to be true if the design objective was to be met. The search was conducted by declaring a number of free design parameters that were manipulated during the process to seek a true overall state.

Constraints could be constructed from mathematical relationships, logical expressions and geometrical conditions which could in turn be combined to create a set of rules that must be true if a specified problem was to be solved. In the context of human modelling, the rules can be expressed to form constraints on a created manikin model during a desired action with articulation governed by connectivity constraints at each joint (Molenbroek and Medland, 2000). Thus, critical actions that must occur for a movement type to be successful could be described as a series of task objectives (constraints), and manikin movement could be created between successive critical actions.

The SWORDS system is now being used within a research programme in conjunction with the Anthropometric Design Assessment Program System (ADAPS) modelling language, developed at the Technical University of Delft. ADAPS was initiated in 1979, and draws upon many years of experience at Delft of ergonomics and the collection of anthropomorphic data. An example of the ADAPS model is illustrated in Figure 2.3.

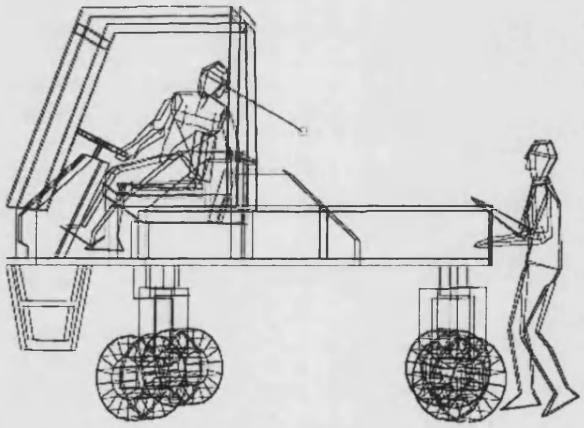

Figure 2.3. Example of ADAPS model for ergonomic assessment.

The ADAPS 3D digital human model allowed designers to visualise a human within a work environment on a computer screen. Flexibility in the manipulation of the model e.g. to create chosen percentiles, alter joint range of movement, or direct lines of sight, were key features of the system. To aid model manipulation, it incorporated reach and displacement algorithms for easy manipulation of the human model (Hoekstra, 1996). However, it remained a graphically simple yet powerful tool for interactive design, visualisation and evaluation of human workspaces. Presently, the system runs under the DOS-window in WINDOWS-NT. Recent improvements to the model have included the introduction of a range of manikin models of small children and the

development of field of view representations. Current developments include automatic manikin model generation from 3D anthropometric surface scans.

The combined operating system in SWORDS allowed realistic human postures to be created as a direct result of constraints applied to the anthropometric human model (manikin). The manikin can be displayed as a stick skeletal model, wire frame or simple solid geometric model. It can be placed into natural postures undertaken by a human when carrying out common operative tasks, for example, to assess the ability of an operator to fit into a given space (Williams and Medland, 2001). The advantage of such a model is that large numbers of subjects do not initially have to be studied and realistic postures can be created despite a changing environment or starting position (Medland, 2000). Stability assessment of a given posture can also be analysed by determining the CM position in relation to the base of support provided by the feet or other body part in contact with the ground. Thus, the designer has the potential to simultaneously evaluate and modify a machine design to suit an operator.

For current human-machine assessments, the need for a manikin to seek configurations and postures to meet operational demands and ergonomic conditions was highlighted by Molenbroek and Medland (2000). Whilst other systems such as SAMMIE or Jack can provide manikin animations, these have to be pre-defined each time a design modification is made which can be time consuming. This was not the case for the SWORDS manikin that achieved movement strategies based on proposed movement rules (Williams and Medland, 2001).

Two authors (Green, 2000; Solman, 2002) have highlighted that an ergonomic background would be required by persons using specific ergonomic framework and methods. Consequently, the other strength in the *SWORDS* modelling system was that an end user would need little knowledge of the movement characteristics (i.e. the desired posture or movement pattern) of the particular pre-defined motion that they required for their own simulations.

2.5.4 SECTION SUMMARY

The use of models as an approach to ergonomic design was discussed, and four levels of anthropometric model were proposed: anthropometric tables, 2D modelling systems, 3D modelling systems, and real test subjects. Computer aided 3D modelling systems were discussed, and a number of commercial packages were considered in the context of their individual strengths. However, a common limitation across these models was their inability to predict movement patterns implying that new postures had to be created on an individual basis, possibly by a skilled operator. Two predictive modelling packages were described. Firstly, HUMOSIM was capable of reaching and lifting movement patterns based on graphical functions applied to joint angular displacements. Whilst end conditions were used as an input to the HUMOSIM model, no constraint was provided to ensure that this occurred, apparently limiting the predictive ability and application of the model. Secondly, the constraint modelling software, SWORDS, was described in conjunction with an established 3D human model, ADAPS, as a proposed means of human movement simulation. It was suggested that critical actions occurring within movement patterns could be described as a series of constraints which could be used as an input to the model.

2.6 DETERMINATION OF BODY SEGMENT MASS PARAMETERS

Knowledge of human body segment inertia parameters are fundamental to biomechanical analysis (Jensen, 1976) such that forces, joint torque and whole body mass centre location can be calculated. However, determination of reliable subject-specific inertia data is notoriously difficult and various techniques of segmental inertia parameter estimation have been proposed. Of the many methods that have been developed, three stood out as being the most frequently used within biomechanics literature. These were: cadaver, mathematical model, and medical imaging techniques, which will be discussed individually below.

2.6.1 CADAVER METHODS

Several studies have presented ratios and regression equations of inertia data based on cadavers and that could be applied to subjects to determine segmental mass properties (Dempster, 1955; Clauser et al., 1969; Chandler et al., 1975). These techniques existed on the assumption that segments were rigid links, were of uniform density and had a fixed segmental CM location. Such methods were advantageous for studies where larger numbers of subjects were used because of the ability to quickly obtain the subject segmental mass properties.

One restriction of cadaver studies was the limited sample sizes from which the inertia data and consequent ratios were obtained. For example, Dempster (1955) based inertia ratios on just eight cadavers, and Clauser et al. (1969) 14. Jensen and Wilson, (1988) suggested that the limited sample size used in these studies could introduce sampling biases into the regression equations that were used to predict segment inertias. Furthermore, the data were often based on subjects that differed in terms of race, age and body size to the sample being tested. This was of concern as Cappozzo and Berme (1990) recommended that if regression techniques were to be used, the subjects under investigation should be of similar body configuration and the same gender as the sample population from which the equations were derived. In an earlier study, Jensen (1976) commented that the knowledge of the size and mass distribution of the subjects was essential to biomechanical analysis. Hence, cadaver methods for segmental mass property estimation were further limited because the body morphology of individual subjects could not be generally accounted for by these techniques.

2.6.2 MATHEMATICAL INERTIA MODEL METHODS

For mathematical inertia model methods, subject body segments were approximated by geometric solids and combined with the density values obtained from cadaver studies. The size and shape of each geometric solid was described by anthropometric measurements that were taken directly from individual subjects. From the measurements segmental mass, mass centre position and principle moments of inertia for each geometric solid were obtained.

At its simplest, the approach assumes that each segment is a single homogenous solid such as an elliptical cylinder or circular cone (Cappozzo and Berme, 1990). An example was presented in Hanavan (1964, as described in Cappozzo and Berme, 1990), where 25 anthropometric measurements were collected to represent simple solids for 15 body segments. However, this approach failed to take account of any shape fluctuations that occurred along the length of each segment. Consequently, variation in segment morphology was considered by dividing the geometric solids into smaller sub-sections. Jensen (1978) subdivided each of 16 body segments into elliptical discs of 20 mm width by digitising photographic records of subjects. A total of 408 measurements were required to define the complete geometric model. Jensen (1978) showed that by using the segment densities of Dempster (1955) body mass could be predicted to within 2%.

A more accurate model was presented by Hatze (1980) that was able to predict body mass to 0.5%. The study proposed a 17 segment model based on 242 anthropometric measurements. The method accounted for varying densities and made no assumption about segment symmetries. Whilst the technique achieved a high degree of accuracy, the excessive time required to obtain the large number of measurements made the model impractical for studies with large numbers of subjects.

An alternative model (Matsui, 1958, described in Hay, 1973) divided each solid into two parts representing bone volume and muscle volume, and different density values were attributed to male and female subjects. In light of a lack of human information available at the time, bone and muscle densities were taken from rabbits. For male subjects, bone and muscle density values of 1418 $kg \cdot m^3$ and 1076 $kg \cdot m^3$, respectively were used. These were adjusted to 1265 $kg \cdot m^3$ and 1041 $kg \cdot m^3$, respectively, for females. In a later study, Clarys and Marfell-Jones (1986) reported bone and muscle density values for the limbs to be 1219 $kg \cdot m^3$ and 1045 $kg \cdot m^3$, respectively, derived from an average of three male and three female cadavers. Because the description of Matsui's (1958) study in Hay (1973) did not include the shape of the geometric solids used, it was difficult to ascertain what affect using rabbit based density values would have had on CM location. However, results were reported to compare favourably with other human CM data available at the time of the original study.

Yeadon (1990) used 95 anthropometric measurements to define a series of truncated cone, semi-ellipsoid, and stadium solids that were capable of predicting whole body

mass within 3% whilst accounting for the differences between male and female body shape. Fewer segmental subdivisions were used than that incorporated into the Jensen (1978) or Hatze (1980) models which limited the number of anthropometric measurements required. Consequently, the Yeadon (1990) model provided a useful compromise between anthropometric measurement time and the ability of the model to predict segment inertia parameters.

The uniform density assumption for given cross sections was considered a limitation of most mathematical inertia model methods (Ackland et al., 1988). Hatze (1980) suggested that the uniform density assumption could introduce errors into the computed values of body segment parameters of between 4-7%. However, it was further suggested that the largest source of error in mathematical models may not come from the assumption of uniform density but from incorrect volume estimates (Ackland et al., 1988).

2.6.3 MEDICAL IMAGING METHODS

Several medical imaging techniques have been developed for the estimation of segment inertia parameters. These imaging techniques sliced body segments at regular intervals along the axes such that the volume, density, and mass of each segment interval could be determined. Zatsiorsky and Seluyanov (1983) used 100 subjects in a gamma-mass scanning study to produce regression equations based on body weight and stature. Computerised axial tomography (CT) was described in a study by Ackland et al. (1988). The investigation reported that the CT technique was capable of estimating the density of a cadaver leg to within 5% of the directly measured density value. However, in recent times such gamma-mass and CT scanning techniques have become less favoured due to subject exposure to the potentially harmful radioactive waves.

Magnetic resonance imaging (MRI) techniques were described by Mungiole and Martin, (1986, 1990). These methods were not dangerous and appeared valid, particularly when investigating soft tissue densities (Mungiole and Martin, 1990). However, it was suggested that the limited availability and high cost of MRI facilities added to the time consuming nature of the analysis did not make the method

particularly feasible (Mungiole and Martin, 1986). Whilst the availability of MRI facilities is now more widespread, the time required for analysis remains a limitation.

2.6.4 SECTION SUMMARY

Cadaver-based, mathematical model, and medical imaging techniques are the three most commonly used techniques to find subject specific inertia data. Cadaver studies are limited by the number and nature of the sample subjects on which the ratios were based. Mathematical models can provide data that is more specific to individual subjects. The model provided by Matsui (1958) allowed different data sets to be created for male and female subjects. The model given in Yeadon (1990) could also account for differences between male and female body shape whilst able to provide a compromise between accuracy and measurement time. Gamma mass and CT scanning techniques were potentially dangerous to subjects, whereas MRI techniques, whilst accurate and safe, were limited by facility access and processing issues.

2.7 SUMMARY

STS was described through the sub-sections; initiation, forward movement, transition, upward movement, and termination. Factors that affected characteristics of STS were discussed. In particular, age and functional inability, initial body posture, rise duration, chair issues, and arm use were highlighted as factors that play important roles in STS movement patterns. Studies that have previously sub-divided the movement were presented. It was shown that the definitions used to bound phases were often based on some data threshold and not necessarily critical sub-movements within the STS scheme. Issues related to the design for human movement within industrial environments were detailed and a range of approaches to ergonomic human modelling were introduced. The chapter concluded with a discussion of the most common techniques used to provide subject specific inertia data.

CHAPTER 3: RESEARCH PURPOSE AND QUESTIONS

The research had two purposes:

To understand the movement constraints which bound and influence STS movement patterns,

and

to obtain a greater comprehension of spatiotemporal characteristics of the STS movement.

Specifically, the following questions were posed in order to drive the investigation:

What kinematic description of the STS can be used to conveniently express a specific posture at any point throughout the movement?

Numerous kinematic descriptors have been used to depict instances of STS movement patterns (e.g. Fleckenstein et al., 1988; Kerr et al., 1994; Hirschfeld et al., 1999). However, few studies have provided an adequate description for the total movement. A total movement descriptor could be useful to ergonomists or biomechanists when considering postures and hence movement patterns throughout STS.

Are certain definitions that are used to identify the start and the end of STS better able to consistently identify the movement than others, and if so why?

Many different techniques have been used to identify the start and end of the STS movement (e.g. Kotake et al., 1993; Vander-Linden et al., 1994; Khemlani et al., 1999). Because the chosen definitions directly influence the parameter times that have been reported in the studies, comparison between studies using different definitions should be approached with caution. Further, it may be found that some definitions inconsistently identify the start and end of STS due to the movement variation that occurs between subjects and trials. Recognition of the most consistent definitions, or

the creation of improved definitions, may allow more confident identification of movement characteristics in future studies.

What levels of variability exist within STS movement patterns, and how should these be considered in order to understand the underlying mechanisms?

Variability is inherent in all human performance (Bates et al., 1992). By appreciating how much variability exists within STS movement patterns between different subjects and rise conditions, the required degree of experimental control can be set. Further, quantitative assessment of subject variability could be used to assess the required level of accuracy of a predictive human model.

What critical actions exist within the STS movement and why do these affect the movement patterns?

Sit-to-stand has been subdivided with a variety of phase definitions in order to improve the understanding of the movement (e.g. Nuzik et al., 1986; Kralj et al., 1990; Schenkman et al., 1990). Phase definition has predominantly been based on changes in kinetic and kinematic data, and does not necessarily represent critical actions within the motion. Phase definition based on critical actions that must occur for rise to be successful could provide a more generalised characterisation that is applicable across all STS conditions. By understanding why the movement changes at these events, it may be possible to identify the constraints which bound the movement.

Do changes within rise factors affect the occurrence of the kinematic descriptors of STS, and if so why?

Previous studies have shown effects of many influencing factors on measures of STS (e.g. Pai and Rogers, 1991; Arborelius et al., 1992; Galli et al., 2000). Some factors have a greater influence on STS characteristics than others or are more likely to experience a change within the workplace environment. Knowledge of how and why important rise

factors affect STS movement characteristics would be useful to ergonomists in regard to the design of STS orientated workstations.

To what extent can a human model predict STS movement patterns across a range of rise conditions?

A manikin model, which uses as its inputs the identified movement constraints and knowledge of how kinematic descriptors change due to the influence of rise factors, could be used to predict movement patterns across a range of conditions. An assessment of how well STS movement patterns can be predicted may indicate that the model could be used by ergonomists when designing STS orientated workstations.

CHAPTER 4: DEVELOPMENT OF METHODOLOGIES

A development programme was established in order to understand STS issues, create movement hypotheses, and appreciate the transfer of information from experimental data collection to an ergonomic man-model. The programme is documented in this chapter, sectioned into four areas representing the breadth and complexity of the work, and demonstrating the manner in which it was approached. The first section details a pilot study. Next, a section on the development of data processing methods is presented, followed by a description of important issues that were raised from the pilot study. Finally, movement theories to be tested in a larger study are developed.

4.1 PILOT STUDY DESCRIPTION

4.1.1 AIM

The aim of the study was to attain and analyse data to aid the understanding of STS such that movement hypotheses could be proposed for testing in a larger study. Additionally, a further aim was to achieve a comprehension of the complexities of the task and to investigate how experimental data were best transferred into an ergonomic human model.

4.1.2 METHOD

A two-dimensional video data collection session was conducted to attain CM spatiotemporal data and joint angle data during STS. Five subjects gave informed consent: 1 female and 4 males (mean $\pm$ standard deviation: age 23.6 ± 1.1 years, mass 72.8 ± 9.3 kg, height 1.75 ± 0.06 m). The participants were healthy, active and reported no musculo-skeletal impairment.

Reflective markers were adhered to the subject to indicate 12 body landmarks from which body segments were defined. The positions of the markers were found using palpative techniques. The location of the markers have been illustrated in Figure 4.1,

the associated segments have been shown in Table 4.1. Subjects were dressed in clothing that allowed markers (with exception of skull vertex marker) to be attached directly to the body. A rubber swimming cap was worn to allow the skull vertex marker to be attached effectively to the skull.

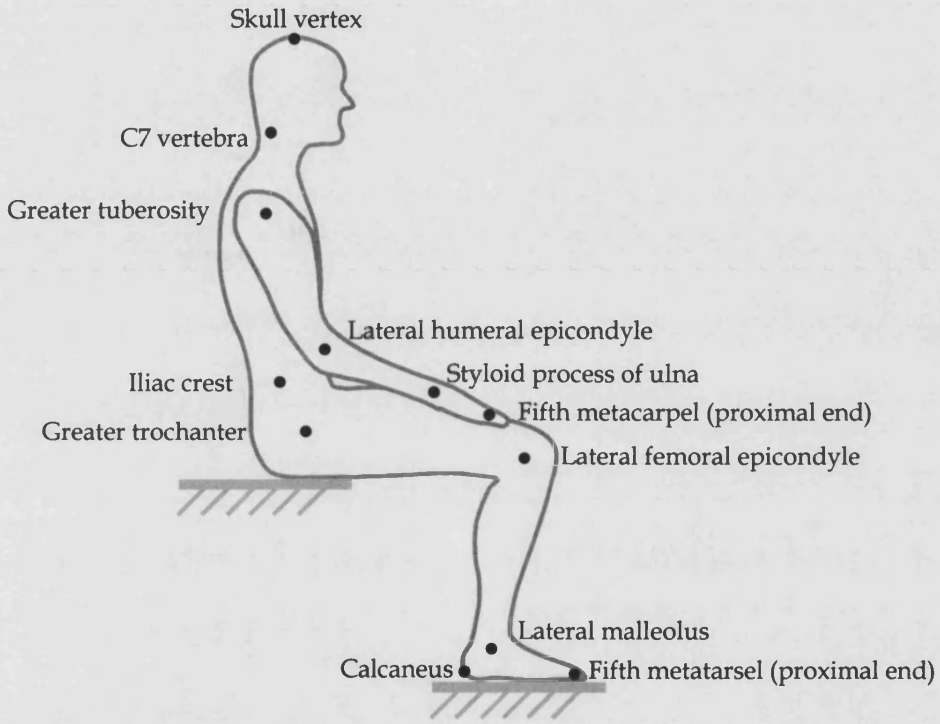

Figure 4.1. Locations of reflective markers attached to the subject.

Table 4.1. Body segment definition. Proximal and distal ends defined from hip joint.

Segment name	Marker position	
	Proximal end	Distal end
Head	C7 vertebra	Skull vertex
Neck	Greater tuberosity	C7 vertebra
Trunk	Greater trochanter	Greater tuberosity
Chest	Iliac crest	Greater tuberosity
Pelvis	Greater trochanter	Iliac crest
Thigh	Greater trochanter	Lateral femoral epicondyle
Shank	Lateral femoral epicondyle	Lateral malleolus
Top Foot	Lateral malleolus	Fifth metatarsal head
Back Foot	Lateral malleolus	Calcaneus
Sole	Calcaneus	Fifth metatarsal head
Upper Arm	Greater tuberosity	Lateral humeral epicondyle
Forearm	Lateral humeral epicondyle	Styloid process of the radius
Hand	Styloid process of the radius	Fifth metacarpel

Individual subjects were seated on an adjustable stool that was set at a height of 90% of the floor to knee height of that particular subject. No backrest was used. A digital video camera recorder (DCR-TRV 900E, Sony Corporation) was positioned such that the centre of the lens was at the approximate height of the subject's hip when standing. The camera was set perpendicular to the proposed plane of subject motion, with the centre of the camera tripod placed approximately 8.3 m away from the plane of motion (Figure 4.2). The camera operated at 50 Hz with a shutter speed of 1/425 s, and with an 'open' iris. A darkened background was used behind the test area and an 800 W spotlight (Varibeam 800, AC Lighting Ltd) was applied to illuminate the subject and obtain appropriate reflection from the markers. The camera was connected to a large monitor, such that the captured image could be more readily seen and focused.

A calibration plane frame (1.98 m x 0.98 m) was placed parallel to the plane of motion, in line with the proposed location of the subject's right extremities (closest to camera). The majority of the markers remained in this plane throughout the movement (Figure 4.2). The calibration frame was videotaped after which the subject performed the

experimental trials. The subjects' hands were placed on the knees although the subjects were asked to apply no additional hand-force to aid rising. The arms were placed in this orientation such that they would be less likely to hinder the view of any of the markers during the motion, and to reduce movement pattern modifications associated with a restricted arm position (Carr and Gentile, 1994). No other aspect of the starting posture was controlled.

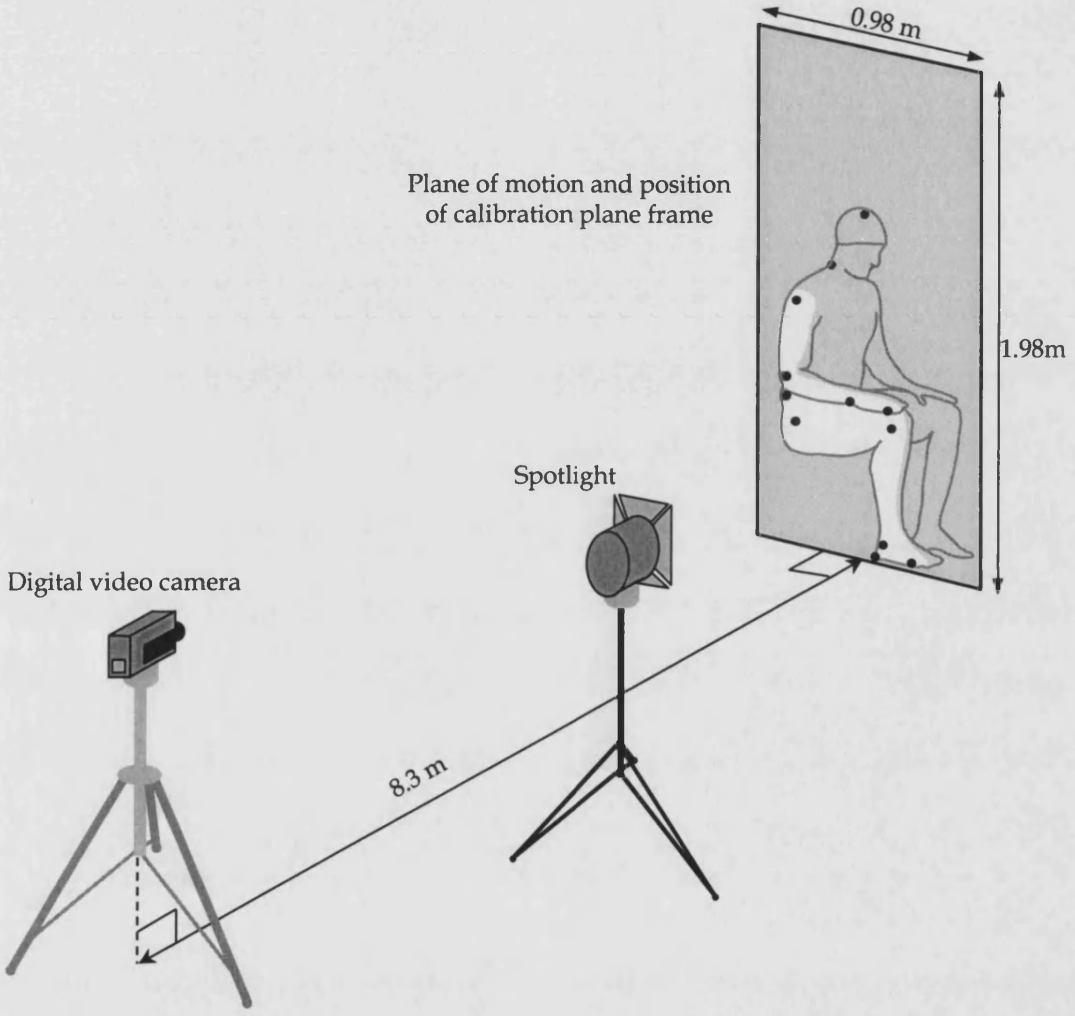

Figure 4.2. Basic experimental set-up (not to scale).

A manual data board was used to document subject and trial information. The subjects were allowed to familiarise themselves with the activity and environment by rising approximately five times prior to data collection. Standing-up and sitting-down data were collected. The commands of "Ready, stand ····· and sit ····· and stand..." were repeated to initiate the standing-up and sitting-down movements. The subjects were asked to move under three different pace conditions: slow, natural, and fast. The actual speed of rise used to satisfy this instruction was chosen subjectively by the

participants. The sit-stand-sit cycle was repeated ten times. Adequate time was given to rest between trials to minimise effects of fatigue.

4.1.3 MOTION ANALYSIS

Video data were digitised using Peak Motus software (Peak Performance Technologies Inc.). The four corners of the calibration frame were manually digitised and an affine scaling routine was used to calibrate camera and digitiser. In this study, the reflective markers placed on the body were tracked automatically. This was achieved by the software identifying areas of contrast in the video data i.e. the contrast between the bright white of the reflective marker and the dark of the background. The centre of the identified marker area was calculated from information based on the perimeter of the area of contrast. This centroid position was exported as a series of co-ordinates as the marker changed position throughout the motion. Within Peak Motus, a spatial model was defined such that CM position and joint angle data could be achieved (Figure 4.3). Body segments were defined between the digitised marker co-ordinates, and angle data were analysed for the C7 vertebra, neck/shoulder, lumbar, hip, knee, ankle, elbow and wrist joints. Additionally, the segmental inertia data of Matsui (1958), as described in Hay (1973) (Table 4.2) were applied to the generated body segments. This allowed calculation of CM displacement and its derivatives throughout the movement. The data of Matsui (1958, cited in Hay, 1973) was chosen over other authors for several reasons: two sets of data were presented for male and female subjects, data were derived from both bone and muscle densities not a combined estimate of the two, and the defined segments adequately aligned with a computer-based manikin model (used in a later part of this study).

The 3rd, 6th, and 9th trial within each pace condition, for each subject, were digitised in the motion analysis software, representing the motion across the duration of the experiment. This created a total of 45 separate STS trials across the 5 subjects and 3 pace conditions. It was unknown at that stage what definitions of the start and end of rise would be appropriate for the STS movement. Therefore, in each trial at least eight additional fields of data before the first visible forward movement and after the last visible upward movement, were included. This adequately ensured that complete rise motion data were captured. Within the digitising software data were smoothed with a

generalised cross-validated quintic spline (Woltring, 1986). Velocity data were attained from differentiated displacement data. Joint angle displacement and velocity, and digitised body landmark and calculated CM co-ordinate and velocity data were exported to an Excel spreadsheet where further handling and analysis took place.

Table 4.2. Inertia data of Matsui (1958, cited in Hay, 1973).

Segment	Segment mass (% of total body mass)		CM location (% of segment length from proximal end)	
	Male	Female	Male	Female
Head	4.4	3.7	37	37
Neck	3.3	2.6	50	50
Trunk	47.7	48.5	52	52
Arm	5.4	5.2	46	46
Forearm	3.0	2.6	41	42
Hand	1.8	1.2	50	50
Thigh	19.8	22.4	42	42
Shank	10.8	10.8	41	42
Foot	3.8	3.0	50	50

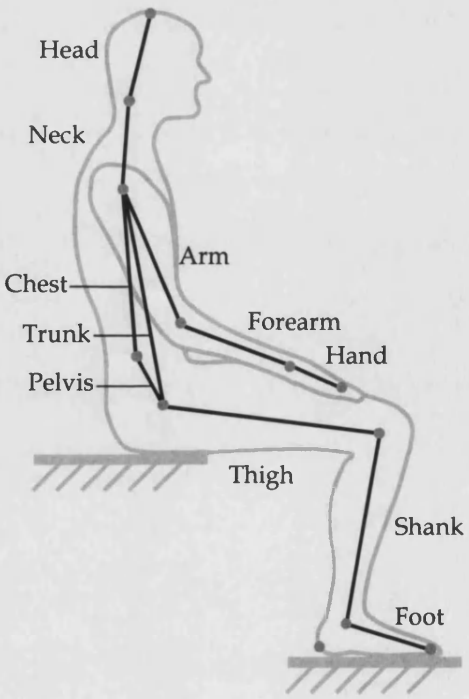

Figure 4.3. Spatial model.

4.2 DATA PROCESSING

4.2.1 START AND END DEFINITION

Definition of the start and end of STS was required such that analysis considered just the part of movement of interest. Previous researchers have used a variety of definitions, as described in Section 2.2.3. Each of the methods (Section 2.2.3) was tested against each of the subjects in the pilot study to find the most appropriate start/end definition. However, the techniques generated inconsistent results across the range of subjects and trials. Consequently, the methods sometimes appeared to cut the movement noticeably short, or include movement that was not part of STS. For example, an unrelated postural adjustment at the start of movement, or a prolonged period of stabilisation at the end of movement may have been included. These assessments were made with the aid of the video data. In addition to this, a large degree of variation was seen in the initiating body segment movement between subjects, as was similarly noted by Nuzik et al. (1986). Therefore, it was inappropriate to use a specific marker (i.e. shoulder or head marker) to define the start of movement. Movement of the CM was selected as a whole body description. Because the energy of a system is a measure of that system's ability to do work, kinetic energy (KE) was considered to be an appropriate means of identifying when the human was working to create the movement of STS. Further, KE was used because it is generally defined as the mechanical energy that a body has by virtue of its motion. Additionally, the v^2 term in the equation describing KE (Equation 4.1) meant that differences between small values (i.e. close to zero) and larger values (i.e. greater than 1) were exaggerated. This allowed easier detection of the STS duration. A threshold of CM linear KE was chosen.

$$Kinetic\ Energy,\ KE = \frac{1}{2} \cdot m \cdot v^2 \qquad [4.1]$$

where m was the subject mass and v was the resultant CM linear velocity.

Initially a threshold value of 0.05 Joules was chosen to mark the start and end of rise. Figure 4.4 shows typical KE trends for one subject performing STS under one pace condition. It can be seen by the variability in energy trends that the inappropriate choice of threshold meant that start and end of movement was not marked reliably. A

period of testing showed a relative threshold to be more appropriate. The final values used were 0.5% of CM peak linear kinetic energy for the start of movement, and 1.2% of CM peak linear kinetic energy for the end of movement. Figure 4.5 shows the same kinetic energy data as in Figure 4.4 with these new thresholds applied. Interestingly, the greater value required for the end definition may reflect the increased movement required to balance the CM over the smaller base of support provided by the feet than balancing over the chair at the start of the movement. Using a relative threshold value over an absolute value implied that the definition was subject specific, allowing more appropriate comparison across subjects of different masses.

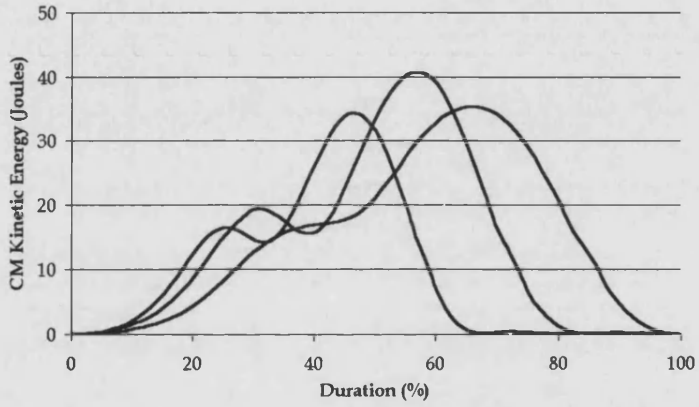

Figure 4.4. CM linear kinetic energy with 0.05 J start and end threshold for three natural pace STS trials from one subject.

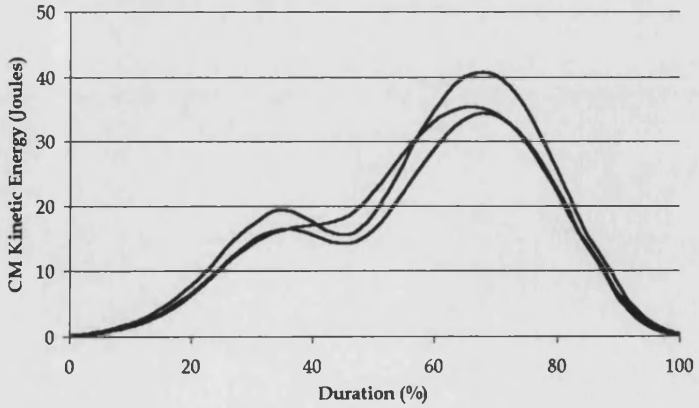

Figure 4.5. CM linear kinetic energy with 0.5% (of peak) start threshold and 1.2% (of peak) end threshold for the same subject and trials as demonstrated in Figure 4.4.

Having defined the start and end of rise, the total rise time for each trial was calculated. Rise duration for the five subjects and three pace conditions are presented in Table 4.3. A temporal overlap between pace conditions can be seen.

Table 4.3. Rise duration ranges for digitised trials over different pace conditions.

Pace condition	Rise duration range across 5 subjects (s)
Fast	0.88 - 1.54
Natural	1.20 - 2.04
Slow	1.44 - 2.76

4.2.2 DATA ANALYSIS

Data collected from the motion analysis system was used for the following:

- To investigate trends between different STS conditions.
- To propose the occurrence of important *events* that occur throughout the movement.
- To aid the formulation of STS movement hypotheses.
- To test transfer of information from motion analysis system to an ergonomic human model.

Joint angle data were used to consider instances of changes in movement patterns. Thus, joint angle displacement onset, peak value, and termination were found to initially identify movement characteristics throughout rise. Definitions of these instances are presented Table 4.4. Thresholds of joint angular velocity were used to mark the onset joint angular displacement. Thus, slope data were used to approximate turning points in angle-displacement data. The occurrence of seat-off was included (Table 4.4) as it was thought to be important in understanding the stability strategies employed in STS. Definition thresholds were set to consistently mark the angle data across the range of trials. This was checked visually against the video data to ensure that the definitions appeared appropriate. Joint angle definitions were described in Appendix A.

Table 4.4. Data definitions employed to describe STS characteristics.

Data	Onset	Peak	Termination
• Neck joint angular displacement	Field closest to $10^{o} \cdot s^{-1}$	Field of maximum extension	Field closest to $-10^{o} \cdot s^{-1}$
• Hip joint angular displacement	Field closest to $10^{o} \cdot s^{-1}$	Field of maximum flexion	Field closest to $-10^{o} \cdot s^{-1}$
• Knee joint angular displacement	Field closest to $10^{o} \cdot s^{-1}$	-	Field closest to $10^{o} \cdot s^{-1}$
• Ankle joint angular displacement	Field closest to $2^{o} \cdot s^{-1}$	Field of maximum dorsiflexion	Field closest to $-2^{o} \cdot s^{-1}$
• Seat-off	First field of positive and continuous hip vertical displacement.	-	First field where Gluteus Maximus was visually clear of seat

Trends in joint angle data were noted between subjects and conditions. It became clear that it was inappropriate for key STS *events* to be proposed from characteristics of the joint angle data, as suggested by Kotake et al. (1993). Whilst the joint angle data reflected the posture of the body throughout STS, it did not provide information regarding the reasons for the posture, thus, it did not represent critical actions of STS. Additionally, considering every angle at each joint was a cumbersome way to describe the motion. Thus, a new description was generated.

The trajectory of the CM was an appropriate description of the motion because it reflected the contribution of all parts of the body to the whole motion, eliminating the need to consider a list of other trends e.g. joint angle time data. Thus, CM positions were used to approximate a series of postures representing the whole of the movement. This was possible because the constrained nature of STS (e.g. feet on the floor, head looking forward, hands on knees etc.) implied that individual body segment motions could not move to cancel one another out in terms of CM

displacement. Further, to understand STS it was necessary to attain the instances of critical actions that occurred throughout STS and that would affect the nature of the CM trajectory.

CM trajectory was split into its horizontal and vertical components. Figure 4.6 shows horizontal and vertical trajectory profiles for one pilot subject. Along with CM displacement, horizontal and vertical components of CM velocity were also considered. Figure 4.7 shows the CM velocity trends associated with the displacement data presented in Figure 4.6. The timings and values of the peak CM velocities were studied because they represented points of inflexion on the corresponding trajectory curves. All pilot subjects demonstrated clear and repeatable velocity patterns, characteristically showing two 'bell' shaped curves with the horizontal maximum velocity always occurring before the vertical.

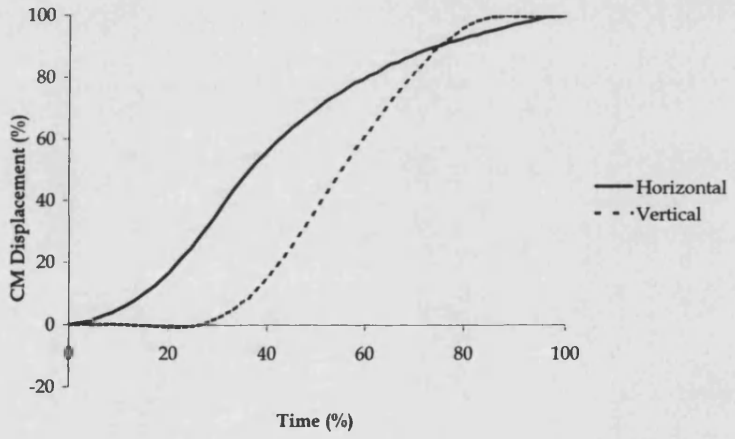

Figure 4.6. CM trajectory profile of one pilot subject rising under natural pace conditions, representative of all pilot subjects.

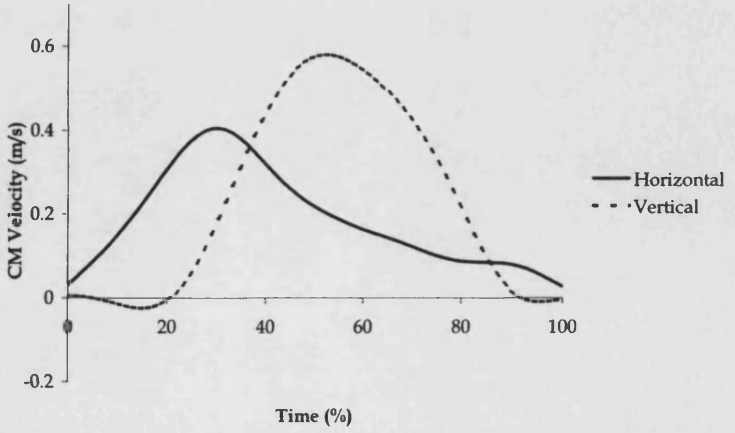

Figure 4.7. CM velocity profile of one pilot subject rising under natural pace conditions, representative of all pilot subjects.

4.2.3 MOVEMENT EVENTS

Critical actions occur at stages in the motion to allow the movement to be completed successfully. In the context of this work, the proposed critical actions of STS were termed *events*, and these needed to be established. An *event* allowed the spatial pattern of the movement to change, and was independent of rise condition. The occurrence of each *event* influenced the final CM motion and consequently the posture of the subjects throughout STS. In addition to the *event* question posed in Chapter 3, answers to the following questions were sought:

- In what order and at what time did *events* occur?
- In what position was the CM at the *events*?
- What factors most influenced the *events*, and why?

After a period of study, and by considering at which points the trends changed in CM trajectory and velocity information, the *events* as shown in Table 4.5 were proposed. The objective of each *event*, i.e. its justification as a critical action, are also presented.

Table 4.5. Proposed *events*, representing critical STS actions, based on CM trajectory and velocity information.

Event	Abbreviation	Objective
Onset of movement	ONSET	Initiate STS.
Onset of seat-off phase	SOO	Initiate vertical body displacements.
CM comes over base of support provided by feet	BALANCE	Achieve stability required for full standing.
Completion of seat-off phase	SOC	Lose body contact with seat such that rapid vertical movement can occur.
CM maximum vertical velocity	VVMAX	Achieve vertical velocity required to complete STS in chosen rise duration.
End of movement	END	Terminate STS.

The events were considered in terms of the spatial and temporal occurrence of the CM. All event timings were normalised to 100% of movement duration as defined by the

period between ONSET and END. Horizontally, the CM position was measured in relation to the rear of the BS. Vertically, the CM position was measured in relation to the CM starting height (Figure 4.8). The responses recorded for each *event* are shown in Table 4.6. Thus, data were collected for CM horizontal velocity at ONSET ($ONSET_{HOR\ VEL}$), CM horizontal displacement at SOO ($SOO_{HOR\ DISP}$), and time occurrence of BALANCE ($BALANCE_{TIME}$), etc.

Table 4.6. Summary of tested responses.

Event	Time	Horizontal Responses		Vertical Responses	
		Displacement	Velocity	Displacement	Velocity
ONSET			✓		✓
SOO	✓	✓		✓	✓
BALANCE	✓		✓		
SOC	✓	✓			
VVMAX	✓				✓
END		✓	✓	✓	✓

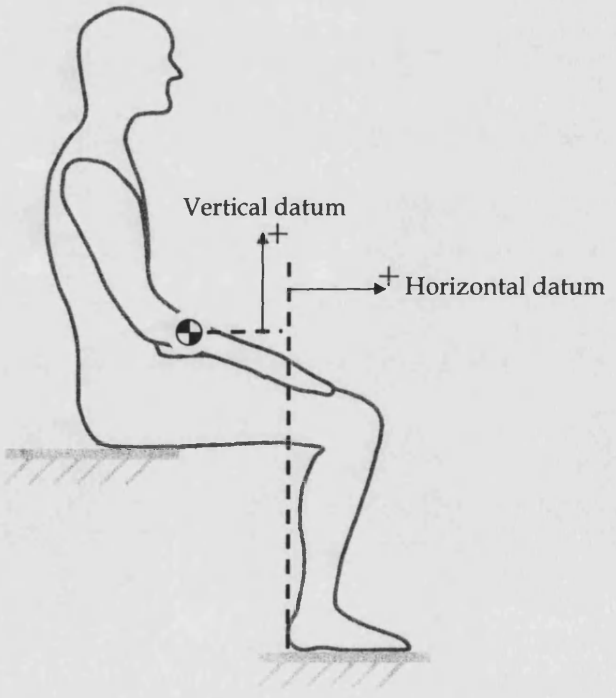

Figure 4.8. Horizontal and vertical datum used for CM displacement.

Collection of these responses allowed points on the corresponding trajectory curves to be known, which were used with curve fitting techniques to create total trajectories. Figures 4.9 and 4.10 show the responses applied to raw data horizontal and vertical trajectories, respectively. In these figures, velocity responses are shown with tangential lines.

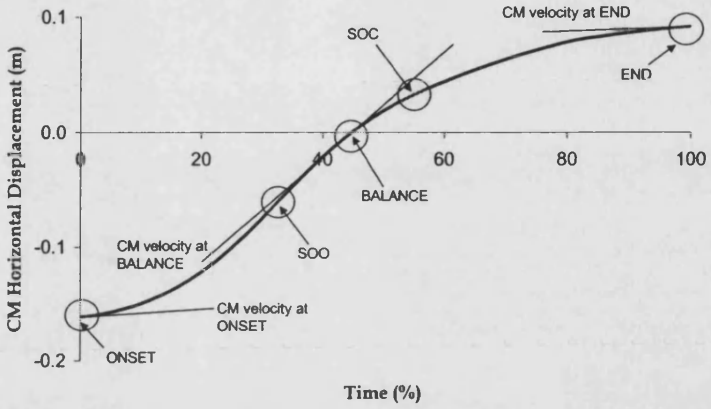

Figure 4.9. Horizontal trajectory responses.

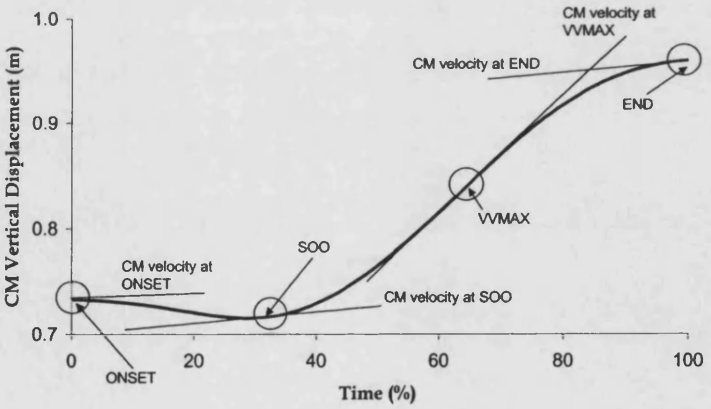

Figure 4.10. Vertical trajectory responses.

4.3 CONSIDERATION OF METHODS

Having conducted the pilot study, important issues associated with the approach to movement understanding were considered. Such findings could then be implemented in a developed, future experimental study. These are discussed below.

4.3.1 VARIABILITY IN DATA

Large variations in data were seen within and between subjects, evident in all of the data types collected. This was of particular concern because it made it difficult to identify common characteristics in the movement. Although joint angle flexion-extension trends remained the same throughout STS, the duration, time of peak data, and the magnitude to which the values occurred changed considerably. Figures 4.11 and 4.12 show the variability that was evident in hip and neck joint angle data, respectively. The figures represented all five subjects performing three trials of STS at natural pace.

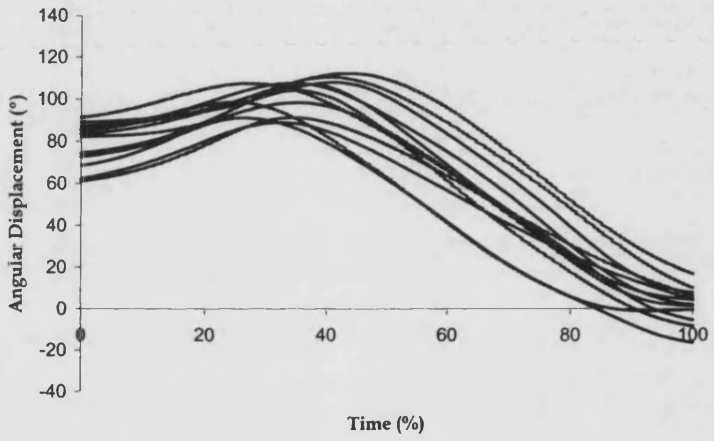

Figure 4.11. Hip joint angular displacement data for all subjects at natural pace.

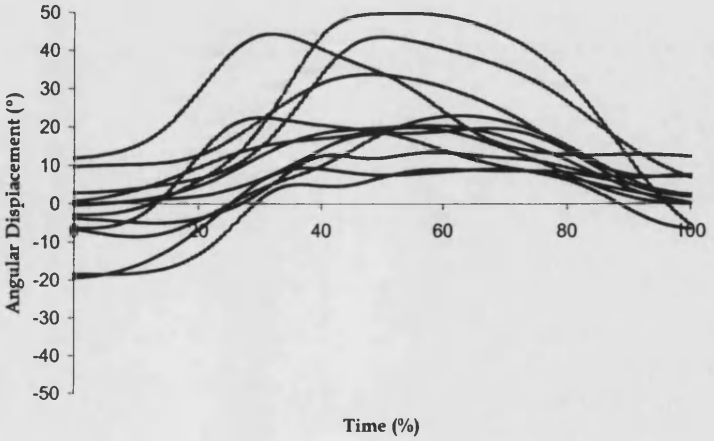

Figure 4.12. Neck joint angular displacement data for all subjects at natural pace.

It was apparent that variability was greatest in those joints that were closer to the top of the body and less associated with the action of STS. For example, the neck angle played a less crucial role in the execution of STS than the knee, as may be expected. It was thought that much of this variability was due to the lack of control of starting position and pace under which the subjects rose, as this has been found by many authors to play an important role in movement patterns. To account for this, subject control in terms of starting position and rise duration was more rigorous for the main experimental study. A certain amount of variability was expected in the movement, and this was considered further in Section 5.4.1.

4.3.2 EXPERIMENTAL SET-UP

On the whole the experimental set-up was deemed successful. However, problems did occur with the Iliac crest marker that represented the lumbar joint between the pelvis and the trunk. This frequently became obscured from the camera view during the movement. To account for this, consideration was given to the appropriateness of the Iliac crest marker for use in the main experimental study, as described in Appendix C.

4.4 DEVELOPMENT OF MOVEMENT THEORY

Hypotheses were formed to act as a guide for the main studies. They were proposed with regard to the stated *events*, in light of the review of literature and with observations made from the pilot study. Specifically, the hypotheses considered the individual components of the *events* i.e. in terms of the time, or horizontal and vertical displacement and velocity (Table 4.6).

Three factors were chosen for investigation because they had been shown to have measurable effects on STS movement patterns by previous authors (e.g. Fleckenstein et al., 1988; Pai and Rogers, 1990; Schenkman et al., 1996; Khemlani et al., 1999; Papa and Cappozzo, 2000). Additionally, STS realistically occurs under a range of these factors within domestic and industrial environments. The investigated factors were:

- *rise duration*
- *initial seated posture,* and
- *seat height.*

The following three sections discuss each rise factor individually, demonstrating particular hypotheses associated with that factor in the context of the stated *events,* specifically SOO, BALANCE, SOC and VVMAX. Hypothesis statements are presented in italic font.

4.4.1 RISE DURATION

A decrease in *rise duration* was achieved predominantly by an increase in CM vertical velocity, whilst CM horizontal velocity remained relatively constant (Pai and Rogers, 1990, Riley et al., 1991). These findings highly influence many of the *rise duration* hypotheses. Several authors discussed the nature of stability strategies, where it was suggested that faster movement may be more dynamic in nature (Schenkman et al., 1990; Riley et al., 1991; Hughes et al., 1994). It was further suggested that momentum in the upper body may have allowed the implementation of dynamic stability strategies (Berger et al., 1988). Understanding this transition period of rise (from seat-off onset to seat-off completion), where subjects move from one base of support to another, was important in the context of describing these strategies. Whilst horizontal movements in STS were less variant than vertical movements due to changes in *rise duration,* it was unclear as to whether changes in *rise duration* really did influence stability strategies as suggested by previous authors. It may be reasonable to suggest that STS of lower *rise duration* may allow an increased emphasis to be placed on dynamic stability at seat-off onset (SOO). Thus it was hypothesised:

CM horizontal displacement at SOO ($SOO_{HOR\ DISP}$) decreases as rise duration decreases.

Note: Figure 4.8 defined the positive and negative directions for horizontal displacement. Horizontally, the datum was relative to the rear of the base of support and not a fixed point on the ground. Similar consideration should be given to all displacement orientated hypotheses.

It was thought that the normalised duration between SOO and BALANCE, the time at which static stability was achieved, would increase due to the emphasis placed on dynamic stability strategies in faster movements. Thus:

Normalised duration between the time of seat-off onset (SOO_{TIME}) and the time of BALANCE ($BALANCE_{TIME}$) increases as rise duration decreases.

The event of BALANCE approximated the time of transition between the respective horizontal and vertical components of the movement. The actual duration of the vertical part of rise decreases more than the horizontal part due to a decrease in total rise duration (Pai and Rogers, 1990). This means that in the normalised cycle $BALANCE_{TIME}$ would occur later. Thus:

$BALANCE_{TIME}$ occurs later as rise duration decreases.

The seat-off phase (SOO - SOC) lasts a finite time at a particular *rise duration*. It was hypothesised that as *rise duration* decreases, duration between SOO_{TIME} and $BALANCE_{TIME}$ increases. Therefore, under the same conditions, the duration between $BALANCE_{TIME}$ and the time of seat-off completion (SOC_{TIME}) must decrease:

Normalised duration between $BALANCE_{TIME}$ and SOC_{TIME} decreases as rise duration decreases.

Further, because of the increased emphasis placed on dynamic stability strategies:

CM horizontal displacement at SOC ($SOC_{HOR\ DISP}$) decreases as rise duration decreases.

Some authors showed the timing of maximum vertical velocity to occur later in the normalised rise cycle due to a decrease in *rise duration* (Papa and Cappozzo, 2000), whilst other authors showed it to occur earlier (Pai and Rogers, 1990). Figure 4.13 shows simplified horizontal and vertical CM velocity profiles, occurring over a *rise duration* of 2 s. Figure 4.14 shows the same profiles over a rise duration of 1.5 s, assuming that the majority of the change is achieved through changes in vertical velocity (Pai and Rogers, 1990).

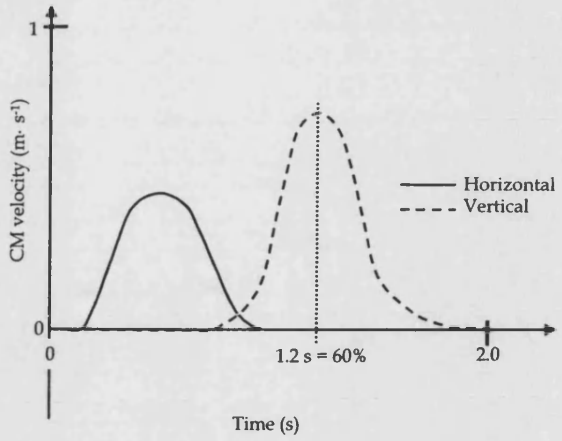

Figure 4.13. Hypothetical CM velocity profile for 2.0 s duration rise.

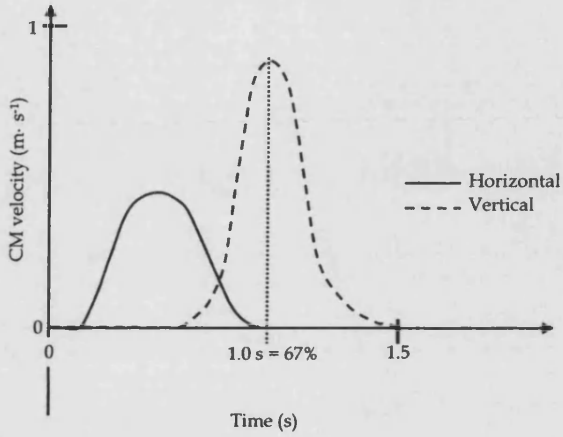

Figure 4.14. Hypothetical CM velocity profile for 1.5 s duration rise.

The vertical profile was effectively shortened in duration, whilst the horizontal profile remained approximately similar. An assumption was made that faster movements are achieved through the attainment of higher peak velocities and not just higher average velocities. Consequently, in normalised terms a vertical velocity profile of shorter duration made $VVMAX_{TIME}$ occur later. Thus:

$VVMAX_{TIME}$ occurs later as rise duration decreases.

The objective of VVMAX was to achieve rise within the required pace, and therefore VVMAX would increase to complete the same displacement within a shorter time. Thus:

CM peak vertical velocity ($VVMAX_{VER\ VEL}$) increases as rise duration decreases.

4.4.2 INITIAL SEATED POSTURE

In general the further the feet were away from the CM, the more the trunk flexed during the initial part of the movement to bring the CM towards the BS (Wheeler et al., 1985; Alexander et al., 1996). However, limits of trunk flexion or duration constraints may imply that the CM was not coincident with BS at seat-off. Consequently, as the feet are placed further forward greater emphasis is placed on dynamic stability strategies during STS. Thus:

$SOO_{HOR\ DISP}$ decreases as initial foot-forward position increases, and

normalised duration between SOO_{TIME} and $BALANCE_{TIME}$ increases as initial foot-forward position increases.

Foot position directly affected the horizontal distance that the CM was required to move through to reach the BS. This greater horizontal distance may take longer to achieve, due to the invariant nature of horizontal movement strategies. This will have the effect of making $BALANCE_{TIME}$ occur later as the feet are moved further forward, thus:

$BALANCE_{TIME}$ occurs later as initial foot-forward position increases.

The increased demands placed on dynamic stability strategies due to the increased foot forward position yields the hypotheses:

$SOC_{HOR\ DISP}$ decreases as initial foot-forward position increases, and

normalised duration between $BALANCE_{TIME}$ and SOC_{TIME} decreases as initial foot-forward position increases.

No hypotheses were presented for the *event* VVMAX with regard to *initial seated posture,* as neither literature nor pilot study highlighted any noticeable trends.

4.4.3 SEAT HEIGHT

Schenkman et al. (1996) reported an increase in CM total horizontal displacement due to an decrease in chair height, compromising the synergism of the movement. This was reported to be because of the greater emphasis placed on postural stability in rise from lower chairs.

$SOO_{HOR\ DISP}$ increases as chair height decreases, and

normalised duration between SOO_{TIME} and $BALANCE_{TIME}$ decreases as chair height decreases.

At its simplest, *seat height* effects the vertical distance that the CM has to rise to achieve full standing height. Because of the additional time spent in the vertical part of the movement, BALANCE (which approximates the transition between the horizontal and vertical components of the movement) may occur earlier in rise from lower chairs. Thus:

$BALANCE_{TIME}$ occurs earlier as chair height decreases.

Because of the increased emphasis placed on postural stability when rising from lower chairs (Schenkman et al., 1996):

$SOC_{HOR\ DISP}$ increases as chair height decreases, and

normalised duration between $BALANCE_{TIME}$ and SOC_{TIME} increases as chair height decreases.

Seat height plays a direct role in the vertical displacement required to rise and consequently, a greater velocity is required to complete a greater displacement in the same time. Thus:

CM peak vertical velocity ($VVMAX_{VER\ VEL}$) increases as chair height decreases.

By considering the velocity profiles as demonstrated in Figure 4.13, it was thought that there was no reason for the time of VVMAX to change to allow rise to occur in the chosen duration. Thus:

$VVMAX_{TIME}$ does not change as chair height decreases.

4.4.4 FACTOR COMBINATIONS

It was difficult to quantify the effects of combinations of factors on *event* timings and objective levels. However, it seemed reasonable to believe that combinations of factors that produced similar results e.g. short rise duration and an initial foot-forward position, may have a reinforcing effect, or indeed an interaction effect. Additionally, the influence of some factors may well cancel each other out when present in certain combinations. Therefore, the ability to test for this in the main experimental study was thought to be a useful development from the pilot study.

4.5 SUMMARY

A pilot study was conducted to investigate movement characteristics of STS, and as a means of comprehending the complexities of the experimental approach. A two-dimensional video data session was conducted to attain movement characteristics of five subjects. Reflective markers were attached to the subjects to represent segmental joint centres and video data were automatically digitised in Peak Motus software (Peak Performance Technologies Inc.). The inertia data of Matsui (1958, cited in Hay, 1973), was applied to created body segments to attain CM position data.

Movement definitions were developed to allow the start and end of STS to be identified. Definitions of STS characteristics in terms of joint angular displacement were proposed, but shown to be inadequate descriptors. Whole body mass centre trajectory was chosen as an appropriate method to describe STS movement patterns. Six *events* were proposed and it was shown that these affected the CM trajectory and consequently the posture of the subject throughout STS.

A series of movement hypotheses were created based on findings presented in the literature review and observations from the pilot study. The hypotheses described how the occurrence of the proposed *events* changed due to the influences of three factors: *rise duration, initial seated posture,* and *seat height.* The possibility of factor interactions affecting the *events* was raised. Whilst no interaction hypotheses were presented, it was suggested that an experimental approach that was capable of testing for interaction may aid the understanding of STS movement patterns.

CHAPTER 5: METHODOLOGY

This chapter details the methods that were used for the main investigation. It has been divided into four distinct study areas: experimental analysis, statistical analysis, manikin modelling and validation. The first section describes the experimental design and methods employed within a laboratory-based experimental study. The statistical analysis study gives a detailed description of the manner by which the data from the experiment were handled to create a series of regression equations. These equations were used for the prediction of STS movement characteristics. The next section overviews the use of a computer-based manikin model to predict STS movement patterns. The final section establishes the techniques that were used to validate the manikin model. Figure 5.1 gives an overview block diagram that shows how the separate parts of the combined methodology relate.

5.1 EXPERIMENTAL ANALYSIS STUDY

A two-dimensional video data collection session was conducted on planned rise treatments to attain spatiotemporal data on subject CM during STS. The information was gathered to ascertain the main and interaction effects within identified STS responses, to be used with factor-response regression equations. These equations would later be used as a means of predicting STS movement patterns.

5.1.1 EXPERIMENTAL DESIGN

In Section 4.3.1, variability was noted within the movement patterns and was attributed partly to the lack of control of the factors. This issue was addressed by a more rigorous approach to experimental design and the setting of the factor levels as described below.

The investigated factors were *rise duration, initial seated posture* and *seat height.* All factors were investigated at two levels. An experimental design region was represented

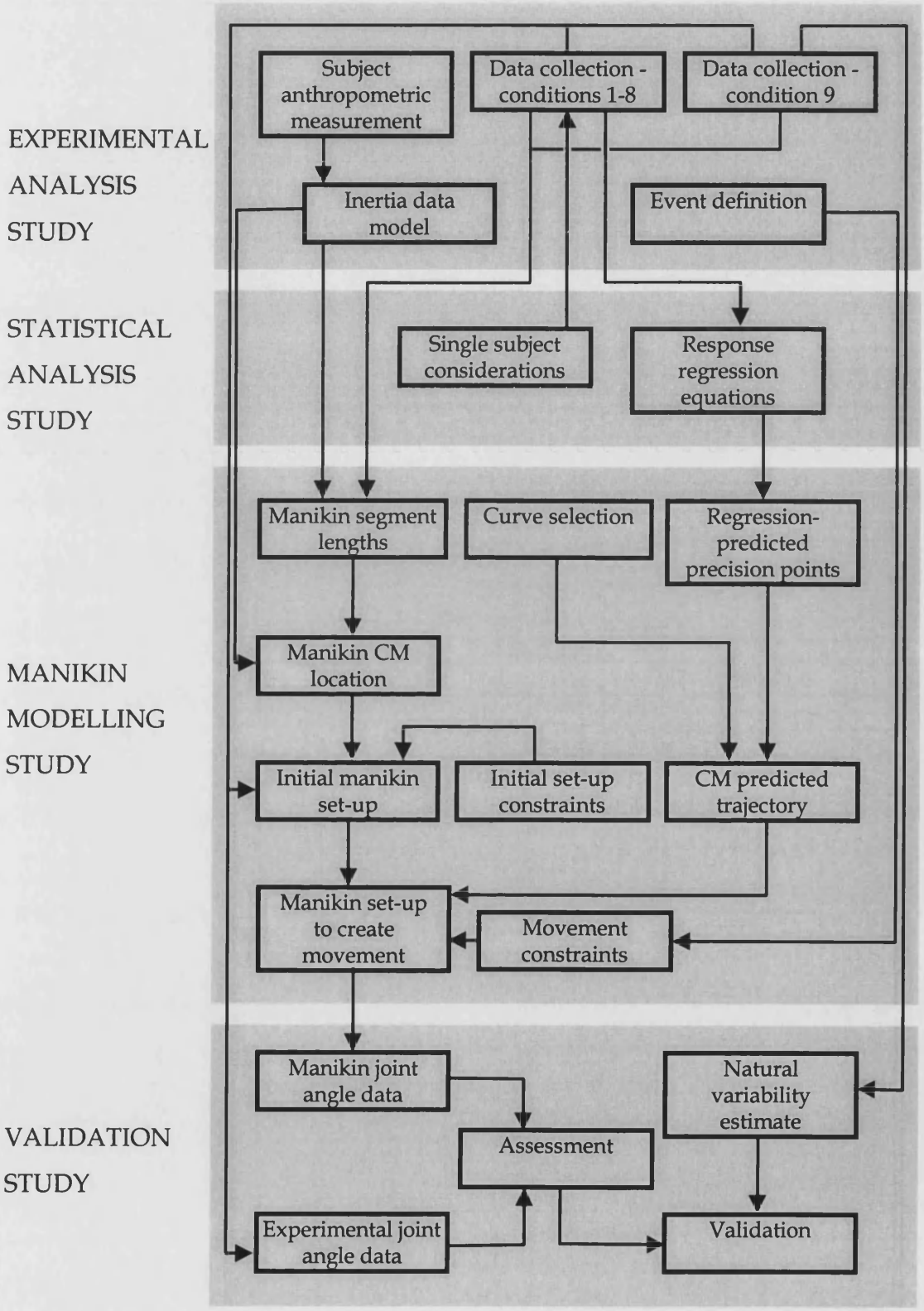

Figure 5.1. Methodology overview block diagram.

in terms of the three factors (Figure 5.2), where the direction of the arrows corresponded to a move from a low level to a high level (Table 5.1). Eight data points were collected that represented each of the factor/level treatments. Additionally, three repeated centre-points were collected, allowing estimation of the associated measurement variation in each of the treatments. Factor levels were set to represent extremes of conditions that might be expected to occur in real situations (Table 5.1). In Appendix B a general discussion is presented on the use of factorial experimental designs when investigating more than one factor at a time.

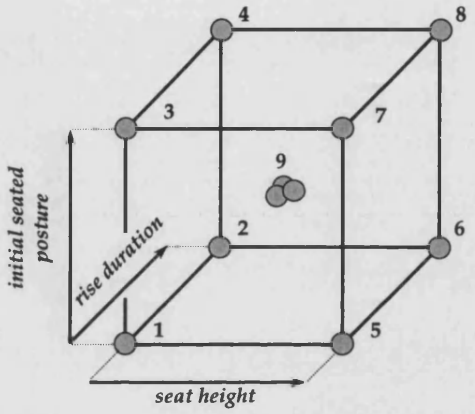

Figure 5.2. 2^3 experimental design region (with additional centre-points) for the factors *rise duration*, *initial seated posture* and *seat height*. Note: Directions of the arrows correspond to a move from low level to high level.

Table 5.1. Pre-set factor levels.

	low level	centre level	high level
rise duration	0.8 s	1.4 s	2.0 s
initial seated posture	6°	12°	18°
seat height	-10°	10°	30°

Note: *Initial seated posture* was a measure of the displacement between the CM and the BS, but was set by the angle of the shank from the vertical. *Seat height* was a measure of the height of the chair, but was set by the angle of the thigh from the horizontal.

Rise duration was defined as the time taken between the start and end of the movement (Section 4.2.1). Subjects rose to spoken commands prompted by audio 'beeps'. As the start and end of movement could not be calculated until a later data processing stage, it was unknown whether the subject had completed the movement in the required

duration. Thus, to take into account the variability that naturally occurred in a subject's execution of a movement, ten trials were performed in each condition. The six most representative trials (closest to the chosen duration) were selected from these ten. Six trials were used on calculated recommendations taken from work produced by Bates et al. (1992) concerning trial size for studies in the presence of human variability (refer to Section 5.2.1). Thus, the total number of treatments used for the complete analysis was 66, as there were 11 conditions (i.e. eight corner-points plus three repeated centre-points) repeated 6 times each.

Initial seated posture was defined by the horizontal distance between the calculated whole body mass centre (CM) and the rear of the support base provided by the feet (BS). This was controlled via foot position that was set by the angle formed between the shank and the vertical axis (relative to the floor). The subject was also asked to start each trial from an upright sitting posture, ensuring that the CM position due to the upper body in the start position was similar between trials. A backrest was used to aid this. Subjects were not allowed to move their feet throughout the movement.

The final factor, *seat height*, indicated the height of the chair and was set by the angle formed between the thigh segment and the horizontal axis (relative to the floor). In an effort to keep the subject comfortable and motivated during the data collection session, *seat height* levels were set before the anthropometric measurements and the attachment of the reflective markers to the body.

5.1.2 SUBJECT INFORMATION

Two male subjects and one female subject gave informed consent for the study. The participants were healthy, active and reported no musculo-skeletal impairment. Anthropometric measurements were performed on the subjects for the creation of body segmental mass and mass location data (Yeadon, 1990). Reflective markers were adhered to the subjects to define 10 body landmarks, as described in Sections 4.1.2 and 5.1.4. One male participant (age 22 years, mass 82.05 kg, height 1.75 m), referred to in the remainder of this section, was labelled subject A for the investigation. In terms of height, subject A represented a 50th percentile UK male adult (Department of Trade and Industry, 1998). The two remaining subjects are described further in section 5.4.3.

5.1.3 EXPERIMENTAL SET-UP

The experimental study was a replica of that previously described (Section 4.1.2) with the following exceptions. The iliac crest marker was removed because of its tendency to be obstructed by the arms during movement. This was replaced by a 'virtual point' that was created within the Peak Motus software (Peak Performance Technologies Inc.). The position of this virtual point was calculated from the digitised locations of the shoulder, hip and knee. For a detailed description of the methods employed to create this point, refer to Appendix C. Additionally, the use of the C7 vertebra marker was omitted. This was because preliminary tests showed that within the movement of STS, the approximation of the head and neck as a single segment had practically no effect on the movement of the CM. This more simple approximation to the human body was considered favourable as it meant that the manikin model would be able to search for solutions by using fewer degrees of freedom. However, the manikin model did contain individual head and neck segments. Thus, segment mass data were still collected for the individual segments although it was assumed that the head and neck segments did not bend in relation to one another throughout the movement. Similarly, the manikin model also contained a three segment spine model (pelvis, lumbar and upper torso). Mass data were collected for these three segments although it was assumed that the lumbar and upper torso did not bend in relation to one another such that the spine description matched that shown in Appendix C. The position of the reflective markers associated with the fingers and toes were also changed slightly (for original definition refer to Section 4.1.2) to align with the use of inertia data that were different to the set used in the pilot study. The new positions put the markers at the distal ends of the fingers and toes.

A further spotlight (Varibeam 800, AC Lighting Ltd) was used to illuminate the test area. This was required because a change in the laboratory environment, specifically the use of darker wall paint, meant that a single spotlight did not produce enough reflection from the body markers. Additionally, the subject was asked to look forward with line of sight fixed on a target approximately 8 m away and at a height of 1.60 m. Adequate time was given to rest between trials to minimise the effects of fatigue.

5.1.4 DATA PROCESSING

The techniques of data processing were the same as those described in Section 4.2 with the following exceptions. Yeadon's (1990) mathematical inertia model was used with anthropometric data obtained from subject A to determine subject-specific inertia parameters. This approach was superior to the previously implemented Matsui (1958, cited in Hay, 1973) model (section 4.1.3) due to an improved reliability in the generated data whilst maintaining the ability to account for differences between male and female body shapes. For subject A, these parameters were calculated using the density values of Dempster (1955), which gave lower model error (in terms of total body mass, 1.4%) than other density data sets (Clauser et al., 1969; Chandler et al., 1975). Density values were scaled to achieve the original mass of subject A. Inertia data were applied to body segments generated between the digitised co-ordinates to allow calculation of CM position and velocity throughout the movement. The generated inertia data are presented in Table 5.2. Additionally, data were collected on two further subjects, referred to in section 5.4.3.

Table 5.2. Inertia data for subject A, generated from Yeadon's (1990) mathematical inertia model for a human body, based on the scaled density values from Dempster (1955).

Segment	Segment mass (% of total body mass)	CM location (% of segment length from proximal end)
Head	4.72	44.64
Neck	3.50	45.39
Pelvis	17.51	46.76
Lumbar	12.54	51.67
Chest	11.17	47.80
Arm	5.78	42.51
Forearm	3.30	42.79
Hand	0.97	39.90
Thigh	27.30	41.72
Shank	10.83	44.20
Foot	2.38	37.79

Co-ordinate and velocity data of the digitised body landmarks and calculated CM were exported from Peak Motus to an Excel spreadsheet where further data handling and analysis took place. The responses for use in the statistical analysis study (Section 5.2.2) were based on the established *events* occurring throughout the movement (Section 4.2.3). These were identified by a series of Excel macro filters with the exception of the event of seat-off completion (SOC) which was identified manually from the video data. Table 5.3 demonstrates the definitions used to identify the *events* within the Excel macros. The definitions were chosen to allow consistent comparison across trials and conditions, taking account of natural resting oscillations that occurred in the data.

Table 5.3. Definitions of identified *events* of rise.

Name	Event	Definition
ONSET	Onset of movement	First field where CM kinetic energy > 0.5% CM peak kinetic energy
SOO	Onset of seat-off phase	First field of continuous and upward displacement of hip marker
BALANCE	CM comes over BS	First field where CM horizontal position ≥ horizontal position of heel marker
SOC	Completion of seat-off phase	First field in video data where there is no visual body/seat contact
VVMAX	CM maximum vertical velocity	Field of CM maximum vertical velocity
END	End of movement	First field where CM kinetic energy < 1.2% CM peak kinetic energy

5.1.5 SECTION SUMMARY

An improved two-dimensional video data collection session study was described for use with a single subject. An experimental design region was proposed in terms of the three factors *rise duration, initial seated posture* and *seat height*. Yeadon's (1990) mathematical inertia model was used to determine the subject-specific inertia data for the single subject. Finally, a series of *event* definitions were presented.

5.2 STATISTICAL ANALYSIS STUDY

This section is divided into two parts. The first of these describes the statistical methods that were employed to account for the implications of using single subject studies. The second part overviews the techniques that were used in order to apply regression models to the digitised video data.

5.2.1 CONSIDERATIONS FOR SINGLE SUBJECT STUDIES

To eliminate issues of inter-subject variability (Section 4.3.1) a single subject investigation was used. This allowed response changes to be observed due solely to factors. However, due to the natural variability seen in human movement, single-subject investigations should be carefully considered to allow acceptable statistical power in order to identify meaningful differences in performance (Bates et al., 1992). To support this, STS performance variability and effect size were used to calculate the appropriate number of trials required to show statistical power of 90% (Bates et al., 1992). Subject variability and effect size data for a range of responses were collected from the previously described pilot study and were used to estimate the trial size for the current study.

Using the model statistics approach as described in Bates et al. (1992), the weighted mean standard deviation and mean difference of two sample conditions were calculated. The effect size was determined (Equation 5.1) which was cross-referenced with a series of values to suggest the required number of trials to produce the chosen statistical power in the presence of the estimated variation (Bates et al., 1992).

$$Effect\ Size = \frac{MEAN_{DIFFERENCE}}{SD_{WEIGHTED\ MEAN}} \qquad [5.1]$$

The required trial size for each response was six or less in all but one case. This was the response of CM horizontal position at the onset of seat-off ($SOO_{HOR\ DISP}$) which yielded a required trial size of nine. However, it was decided that fewer trials would be chosen in preference to a higher significance level at that one response. Thus, each treatment in

the design would be repeated six times. This meant that the total number of analysed trials would be 66 (as described in Section 5.1.1).

5.2.2 CREATION OF REGRESSION EQUATIONS

Statistical analysis of the data collected from the 66 trials was used to produce appropriate regression equations that described responses in terms of the factors *rise duration* (*rd*), *initial seated posture* (*isp*) and *seat height* (*sh*). A multiple linear regression of the form below (Equation 5.2) was applied.

$$Y = \gamma_0 + \gamma_1 RD + \gamma_2 ISP + \gamma_3 SH + \gamma_4 RD * ISP + \gamma_5 RD * SH + \gamma_6 ISP * SH + \gamma_7 RD * ISP * SH + \varepsilon \quad [5.2]$$

where Y was the response, the values $\gamma_0 \ldots \gamma_7$ were the regressed coefficients and ε was the residual error not explained by the model. The factors *rd*, *isp* and *sh* were scaled and centred to produce the respective regressed factor variables *RD*, *ISP*, and *SH* where 'low' levels = -1 and 'high' levels =1. Of the regression coefficients:

γ_0 =	the constant. This would be the value of the response if all factors were set at their centre-levels.
$\gamma_1 - \gamma_3$ =	the main effects. This gave the strength of each factors' effect on the response.
$\gamma_4 - \gamma_7$ =	the interaction effects. This gave the strength of combinations of factors' effect on the response.

The multiple linear regressions were used to compute the coefficients of the model by minimising the sum of squares of the residuals. Thus, values were found for the main and interaction effects, and considerations given to those that were significant in relation to associated errors.

All responses were treated independently. Thus, different main and interaction effects were used to form a separate model for each response. Whilst responses generated by the same underlying system could be correlated, treating them in this manner allowed each model to include response-specific terms. From the initial model the normal

distribution was assessed and outliers were evaluated and removed if appropriate. Outliers were classified as data points that lay outside of 4 standard deviations of the normal distribution, as assessed by residual plots. Non-significant terms ($p>0.05$) were deleted using backwards elimination. The quality of the new model was assessed based on several measures that were available to the statistical package, MODDE 5.0 (UMETRICS AB). These measures included: assessments of goodness of fit and predictive power (R^2 and Q^2), ANOVA tables to consider statistical significance of the regressions and whether there was any lack of fit in the model, and histograms to check for normal distribution.

Hierarchy of terms was maintained so the constant term (Y_0) was never deleted and lower order terms (e.g. *RD*) were only deleted if there were no significant higher order terms containing that term (e.g. *RD*ISP*) in the model. As a result some regressions included non-significant lower order terms such that significant higher order terms were included. In these cases, the value of a higher order effect was required to be at least twice the associated standard error for that same higher order effect to be kept in the model.

Finally, in the few cases where responses were not normally distributed, the Box-Cox method (Draper and Smith, 1998) was used to recommend appropriate power transformations to improve the quality of the model. Within the statistical package, transformations between -2 and 2 were considered in terms of their ability to create a simple model with approximately constant model error variance and approximately normal model error distribution. The transformation that best satisfied these constraints was suggested. Figure 5.3 shows a skewed response distribution obtained from the experimental data. A power transformation of -0.25 was recommended to allow statistical analysis to take place on a normally distributed response (Figure 5.4). In such a case, coefficients in the Results chapter (Section 6.2) were shown in their transformed state. Consequently, the transformed effects (Tables 6.9 and 6.10) had to be re-transformed before they could be directly interpreted. Re-transformation occurs by taking the value of the response and raising it to the power of one over the original transformation, i.e. -4 for the case shown in Figure 5.4.

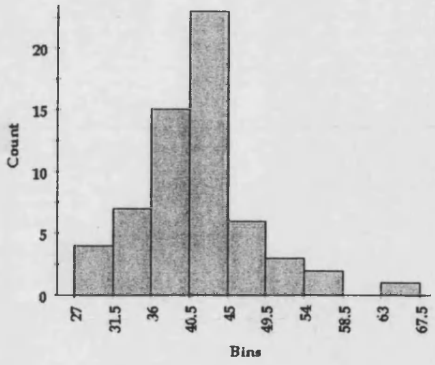

Figure 5.3. Skewed response distribution.

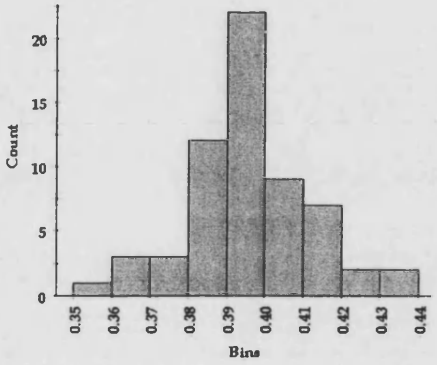

Figure 5.4. Normal, transformed response distribution.

5.2.3 SECTION SUMMARY

The statistical techniques used in the study were introduced. The work of Bates et al. (1992) was used to calculate the appropriate number of trials required to account for variability in human movement. Regression analysis techniques were described as a means of finding main and interaction effects in the responses of interest. The statistical procedures that were performed, e.g. power transformations, were demonstrated.

5.3 MANIKIN MODELLING STUDY

The use of *events* as a useful description of STS was to be tested through the modelling of STS movement strategies for a range of conditions. A computer-based manikin, created from a description of the human body held in ADAPS (Technical University of Delft), was created within a constraint modelling software environment (Appendix D). A series of related programmes were written in the RASOR modelling language that described the manikin in terms of its skeletal representation and the application of movement-type constraints. An overview of the complete modelling programme scheme can be found in Appendix E. The following sections describe how the manikin was set up within the user environment to create motion.

5.3.1 INITIAL MANIKIN SET-UP

The initial inputs to the manikin model were the starting position, in terms of the *initial seated posture* and *seat height* factor levels. Thus, the objective was to achieve a seated position from which rise could occur (Figure 5.5). Manikin representation was based on a skeleton with segment lengths and joint limits that were held in an ADAPS data file. The information held in these data files was obtained from anthropometric measurement and experimental data. Additionally, the skeleton was surrounded by a wire-frame representation for the body exterior.

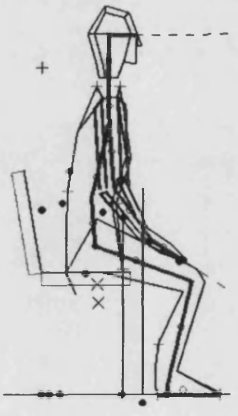

Figure 5.5. Manikin in sitting position replicating a centre-point condition experimental trial.

Note: the experimental set-up included the use of a backrest in order to standardise upper body position. However, because body contact with the backrest was minimal,

no constraints were associated with its use. Consequently, the backrest was not required to be included within the manikin model.

A main, manually called programme was executed, opening a graphics window in which the manikin was displayed. Manikin representation sub-programmes were automatically called from within the main programme (Appendix E). Figure 5.6 shows the complete design environment of SWORDS, to include the graphics window, command line and menu buttons. The manikin's starting posture and orientation (Figure 5.6) were based on pre-set values held within a sub-programme. These values represented model-space orientations (each of which was related to a particular manikin body segment). Following this, the manikin was set up to replicate the starting position of any one of 11 evaluation trials that were tested and used in later stages of the investigation to evaluate the final model.

Note: The 11 evaluation trials were taken from the 66 experimental trials. One trial was chosen randomly from each of the eight corner-point conditions, and three trials were chosen randomly from the centre-point condition. Three trials were used to represent the centre-point as there were three times as many data points collected in that condition. Further, the centre-point condition most likely represented average rise factor levels and consequently, cross-condition mean validation results were biased towards the most likely rise condition due to the additional tests taking place in that condition. Thus, the evaluation trials represented the entire experimental region. The same 11 trials were used at various stages throughout the investigation.

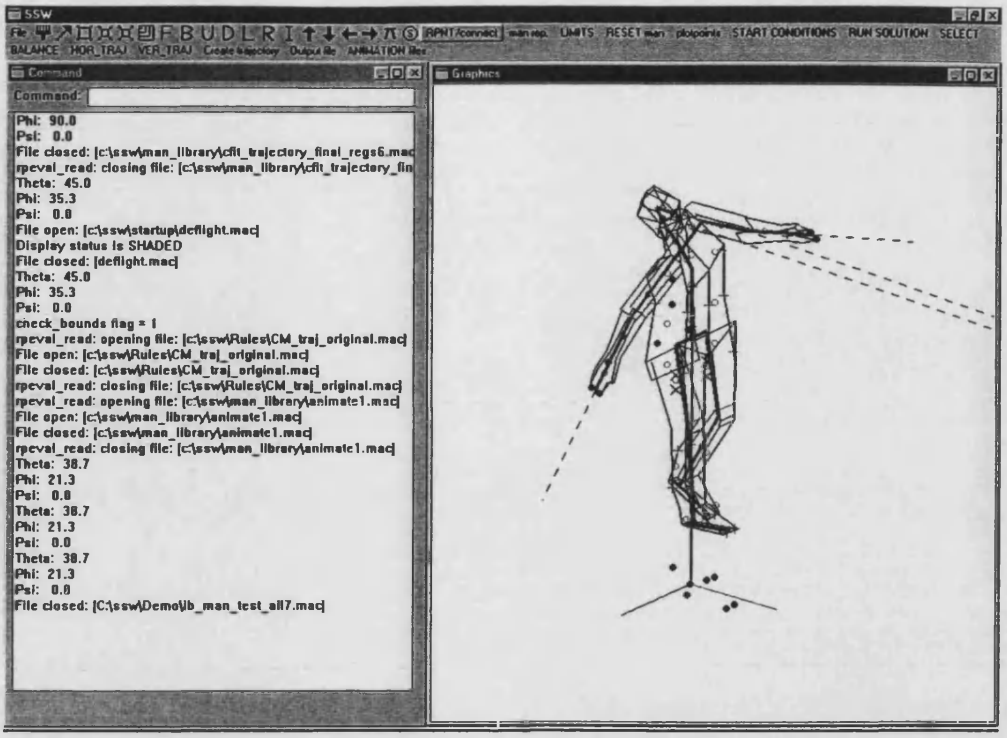

Figure 5.6. Manikin starting posture shown within the SWORDS graphics window. Note: also shown is the entire constraint modeller software environment including menus, command line and response and graphics windows.

The manikin was configured into an approximate sitting position (Figure 5.7), achieved with a further series of pre-set model-space orientations. The view of the manikin was changed such that it was observed from its right side, i.e. the same as that used in the experimental study (Figure 5.8). At that stage there was no seat representation and the feet were not in contact with the ground.

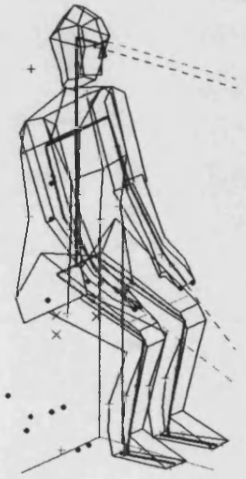

Figure 5.7. Manikin in approximate sitting posture.

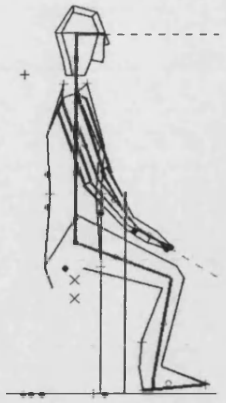

Figure 5.8. Manikin orientation changed to the same viewpoint as experimental trials.

A wire-frame seat object was imported into the manikin environment (Figure 5.9). The height of the seat was chosen on a trial-by-trial basis, such that identical initial body postures to particular evaluation trials could be created. The ability to choose any seat height (in addition to those representing evaluation trials) also existed. A position marker (line segment) was loaded into the environment and used as a means of setting the foot position. This line segment lay in the same plane as the ground and perpendicular to the plane of motion (Figure 5.10). Its location was set such that the foot positions represented the original body orientations (specifically, knee and ankle angles) of the chosen evaluation trials. The seat and the foot marker were created from a sub-programme that defined the location and orientation of line segments.

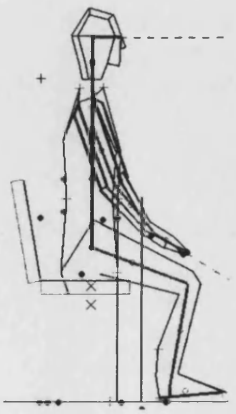

Figure 5.9. Manikin shown with imported seat object.

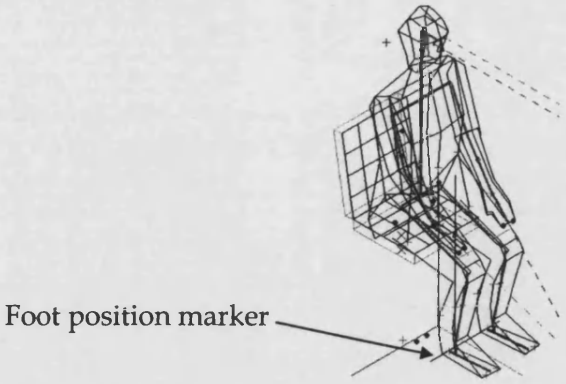

Figure 5.10. Manikin foot position marker.

A collection of constraints were then applied by using the techniques as described in Appendix D. These represented:

- body contact with chair
- foot contact with floor
- heel contact with position marker (line segment)
- eye ray contact with target
- hand contact with knee and thigh

Consequently, direct search techniques (Appendix D) were used to attain a manikin posture that satisfied each of these constraints by automatically manipulating a chosen set of free variables. The declared free variables were:

- Neck joint – transverse axis rotation
- Lumbar joint – transverse axis rotation
- Hip joint – transverse axis rotation
- Knee joint – transverse axis rotation
- Ankle joint – transverse axis rotation
- Shoulder joint – transverse axis rotation
- Shoulder joint – longitudinal axis rotation
- Elbow joint – transverse axis rotation
- Elbow joint – longitudinal axis rotation
- Wrist joint – transverse axis rotation
- Wrist joint – frontal axis rotation

- Manikin origin - transverse axis rotation
- Manikin origin - horizontal translation
- Manikin origin - vertical translation

Note: with the exception of the manikin origin and the neck and lumbar joints, freed variables were applied to both left and right sides of the manikin. The manikin origin was a point located near the base of the spine of the manikin and needed to be freed to allow whole body translations to occur.

Additionally, specific hip and lumbar joint angle data were applied to the manikin. These angles were read directly into the model-spaces and were not formed through the use of constraints. This was done to achieve specific starting positions representing experimental trials, specifically with reference to the posture of the trunk. This was a required step for appropriate validation techniques to be carried out (refer to Sections 5.4.2 and 6.4.3). This process was only necessary to test movement from a very specific starting posture. If required, the user could choose to position the manikin into any arbitrary seated posture to investigate the nature of STS movement patterns from other starting conditions. The achieved constraint-based manikin posture was demonstrated in Figure 5.5. Additionally, Figure 5.11 shows a wide-angle view of the manikin to demonstrate the placement of the eye ray on a target. This target was set in the same position as that used in the experimental set-up.

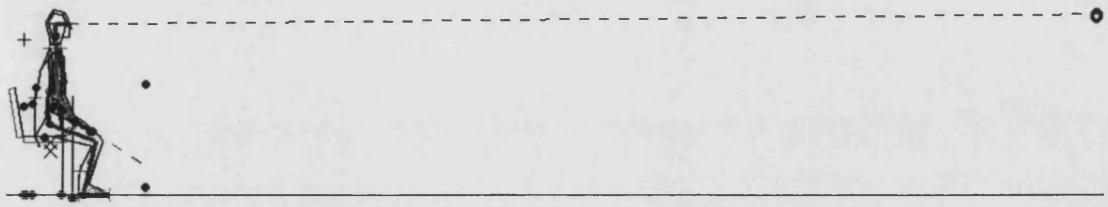

Figure 5.11. Manikin environment including visual target.

Thus, constraint equations and freed variables were used to create a manikin starting posture. The same approach was used to simulate movement throughout STS by applying constraints that were applicable to movement between the proposed critical actions i.e. the *events*. The following section describes how this was implemented.

5.3.2 IMPLEMENTATION OF REGRESSION EQUATIONS

Regression equations were created from experimental data and a series of statistical procedures, as previously described. Sixteen regression equations were used to represent the occurrence of the CM at the *events* of rise as demonstrated in Section 4.2.3. These regression equations were written directly into the 'curve fit' sub-programme (as illustrated in Appendix E) and used to plot 'precision points' in the appropriate curve domain. These procedures are described in greater detail in the following section. The regression equations were written in terms of the three factors *rise duration, initial seated posture,* and *seat height* (see also Section 6.2.2). The factor levels were obtained via a series of menu buttons within the SWORDS operating window. For example, by choosing a certain seat height, the corresponding factor level (calculated by scaling the low and high value in Table 5.1 to -1 and 1, respectively) would be read directly into each of the regression equations that included the term *seat height.* Consequently, as the user chooses different settings of *seat height, initial seated posture* or *rise duration,* the values of the regression equations changed which in turn altered the position of the precision points within the curve domains.

5.3.3 CURVE FITTING TECHNIQUES

Free-form curves are used widely in computer-aided design systems (McGarva and Mullineux, 1995), and are commonly implemented in terms of either Bézier or B-spline formulations (Bézier, 1972). Appendix F gives an introduction to the use of Bézier curves. Typically, the B-spline form is defined in terms of a number of control points and a sequence of scalar knots producing an open form of the curve with distinct start and end points. McGarva and Mullineux (1995) argued that it was advantageous to change this form and deal with the differences between successive knots rather than the knots themselves. This allowed open and closed curves to be handled within the same implementation, and was the form of curve execution used within SWORDS. Further, it was suggested that the curve was defined not in terms of its control points, but rather 'precision points'. These were points through which the curve must pass and were a more intuitive method by which to define the curve. This adjustment to the traditional method of describing a Bézier curve or B-Spline was achieved by an internal, least squares fitting procedure.

The precision points were created within the curve domain by the values obtained from the regression equations, and these were then joined smoothly using appropriate curves from the graphics mode of the system. The precision points represent *events* as shown in Figures 4.9 and 4.10. User-defined curve functions within the RASOR modelling language were used to set up the curve in SWORDS. The functions represented the curve degree, curve type (e.g. cartesian or polar, 2D or 3D), and a matrix of scalar values representing the differences between successive knots and components of control points.

Curve degree and number of control points were decided upon. More control points permit greater control over the curve to fit to the data, and the smoothness of the curve can be increased or decreased by the degree of the curve to suit the desired application. However, these steps should be carefully considered because curve-fitting techniques can sometimes give unexpected or unwanted results, typically in the form of curve oscillations between precision points (Twyman, 1999). For this application, these two variables (curve degree and number of control points) were chosen by conducting a curve selection test (as presented in Sections 5.3.5 and 6.3.2). Additionally, the spacing of 'knot values' was considered. The knot values control the parametric flow along the curve and where the control points occur. Equally spaced 'knot values' generated reproducible, controlled curves between conditions with little compromise in error values. More specifically spaced 'knot values' (matching a particular set of curve data) could be used to obtain superior curves for single rise conditions. However, these would be extremely difficult to generalise for all the curve conditions required to represent the experimental region.

Levels of each of the factors (chosen by the user via SWORDS menu buttons) were read into the regression equations. Values were generated and used to create precision points within the curve domains. This was done for both horizontal and vertical components of CM trajectory, both of which were plotted against normalised time. It was noted that certain factor combinations could lead to the regression equations predicting the *events* out of order, leading to poor predicted trajectories. This was particularly the case for the three *events* SOO, BALANCE and SOC that occurred in quick succession around seat-off in the horizontal displacement time domain. The incorrect *event* order was due to the responses being treated as independent to each other (i.e. each regression equation could include different main and interaction effects,

as described in Section 5.2.2). The issues associated with *events* being predicted out of order are demonstrated as follows:

If the *events* of SOO, BALANCE and SOC occurred in the following time domain order:

$$SOO_{TIME} < BALANCE_{TIME} < SOC_{TIME},$$

then observations from experimental data suggested that they also occurred in the same order in the displacement domain, i.e.

$$SOO_{HOR\ DISP} < BALANCE_{HOR\ DISP} < SOC_{HOR\ DISP}$$

This is illustrated in Figure 5.12 with a typical section of CM horizontal trajectory (note that $BALANCE_{HOR\ DISP}$ is by definition zero). However, if predicted *events* occurred in the same order temporally, but in the wrong order spatially, i.e.

$$BALANCE_{HOR\ DISP} < SOO_{HOR\ DISP} < SOC_{HOR\ DISP},$$

as illustrated in Figure 5.13, then the fitted curve must oscillate to pass through the precision points. This trend was never observed in the experimental data. A series of checks was thus put in place to ensure that the precision points were not plotted in some inappropriate order. Simple 'if' statements, written within the RASOR modelling language were used in order to identify and locate the precision points that would lead to oscillating trajectories. Once out of order *events* were detected, a further regression equation representing CM horizontal velocity at BALANCE was implemented to improve the prediction. The trajectory slope obtained from this regression equation was used to extrapolate forwards and backwards (over a small portion of the activity) to improve the prediction of events occurring in that area. The addition of these procedures ensured that all predicted trajectories followed recognised trajectory patterns.

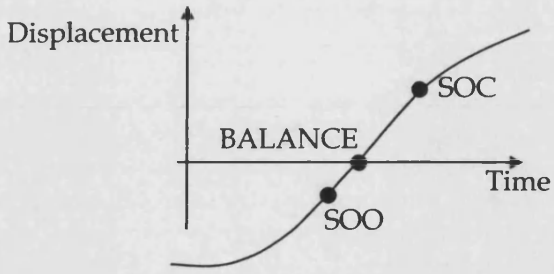

Figure 5.12. Curve fitted to continuous *events*.

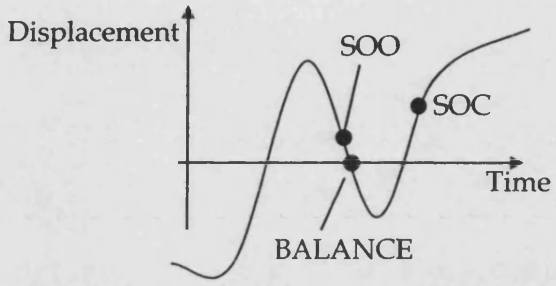

Figure 5.13. Curve fitted to non-continuous *events*.

Precision points were plotted within the curve domain and the appropriate curve type was applied. In the cases where regression equations represented velocity data (e.g. at the event VVMAX), the curve was forced to fit a particular slope, not a co-ordinate. This was a noted ability of the SWORDS system which could fit simultaneously to values of co-ordinates and velocity, or if required acceleration and jerk. Figures 5.14 and 5.15 give examples of fitted curves in the horizontal and vertical displacement time domains.

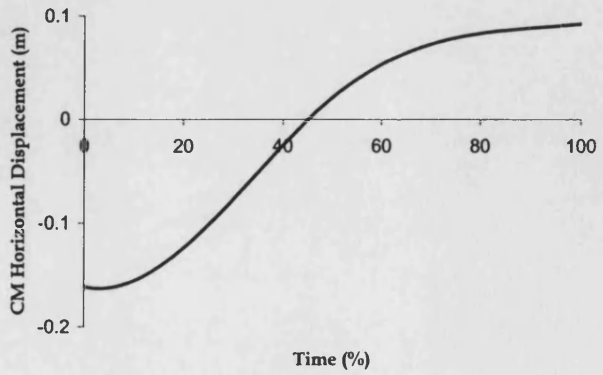

Figure 5.14. Fitted horizontal displacement time trajectory.

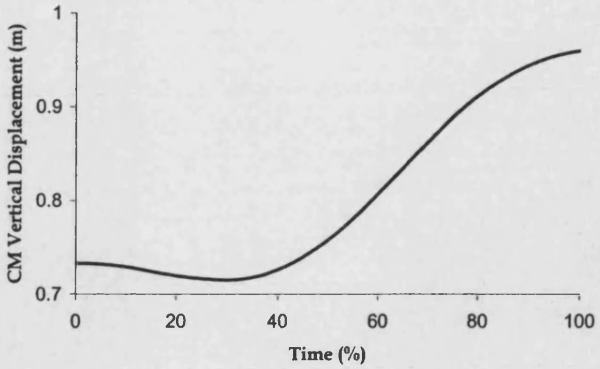

Figure 5.15. Fitted vertical displacement time trajectory.

Each curve was evaluated in terms of its horizontal and vertical components at time steps equivalent to 0.02 s. For each pair of fitted curves the vertical components from the graphs were extracted and plotted against each other to represent the CM trajectory (See Results: Figure 6.6). This created a point in space for the CM for each 0.02 s time step which represented the total predicted manikin CM trajectory. Consequently, faster movements contained fewer points to make the total trajectory. The model was set up this way for two reasons. Firstly, when re-playing a simulation (as an animated file, used by an end-user to check movement patterns), an appreciation of the movement speed would be gained. Secondly, root mean square difference (RMSD) (used to evaluate the model) could be made directly between the experimental and model data, i.e. data did not have to be re-sampled.

5.3.4 REGRESSION EQUATIONS EVALUATION

A selection of the regression equations were used to predict experimental response data (Table 6.11). These represented those regressions that played the greatest influence on the final shape of the fitted curve. Thus, responses which had a small range of values around zero (e.g. CM vertical velocity at ONSET ($ONSET_{VER\ VEL}$), CM vertical displacement at SOO ($SOO_{VER\ DISP}$), and CM vertical velocity at END ($END_{VER\ VEL}$)) were excluded. Six trials were chosen at random from the collected 'centre-point' data to test the predictive ability of the regressions. These data points were chosen as an independent test as they were not used to form the original regressions.

5.3.5 CURVE FITTING SELECTION

This activity assessed the ability of different curves to fit to experimental data points. It was used to determine the most appropriate curve degree and number of control points to be employed when producing the curves. A series of curves of different degree and number of control points were fitted to the experimental data points in an attempt to recreate horizontal and vertical displacement time trajectories of each of the 11 evaluation trials. Each of these curves was split into the same number of data points as the particular experimental trials. The co-ordinates of the fitted and experimental data were exported to an Excel spreadsheet and a root mean square difference (RMSD) was calculated. Relative RMSD in terms of the total horizontal and vertical displacement, for second to fifth degree curves, and for seven to 16 control points were calculated. Mean values across 11 evaluation trials (representing the experimental region) were produced (Tables 6.12 and 6.13) from which an optimal curve was chosen. The optimal curve was that combination of curve degree and control points that created the minimum global RMSD across all 11 evaluation trials. Random curve type combinations were tested outside of the chosen ranges in an effort to check that local error minima were not being found within the defined curve degree and control point ranges.

5.3.6 EVALUATION OF CURVES FITTED TO REGRESSION-PREDICTED PRECISION POINTS

The purpose of this evaluation was to allow the assessment of the error caused in the predicted trajectory due to the regression models. Factor levels were extracted from 11 evaluation trials in an attempt to recreate experimental precision points. Root mean square difference (RMSD) was again used to calculate the difference between the experimental data and the curves fitted to the predicted precision points. Regression model error in the trajectories was defined as the total RMSD between predicted and real data, minus the curve fitting RMSD (as demonstrated in section 6.3.3). This is illustrated in Equation 5.3.

$$Error_{REGRESSION} = Error_{TOTAL} - Error_{CURVE} \qquad [5.3]$$

5.3.7 MANIKIN SET-UP TO CREATE MOTION

With the curve fitting techniques applied to the horizontal and vertical displacement time trajectories, CM trajectory was predicted based on the chosen conditions of rise. The trajectory was positioned into the manikin environment and aligned such that the first trajectory co-ordinate was placed in the same location as the manikin's CM in the starting position (Figure 5.16).

Figure 5.16. Manikin shown with predicted trajectory.

Constraints were applied in order to create manikin movement patterns. Appendix H demonstrates how each movement constraint could be weighted in order to change the influence that it had on the generated movement patterns. The constraints can be broadly divided into two types: those that are constant throughout the movement, and those that are changeable. Of the constraints demonstrated in Section 5.3.1,

- foot contact with floor
- heel contact with position marker (line segment), and
- eye ray contact with target

remained present throughout the movement, reflecting subject performance throughout the experiment. Additionally, there was a further constraint that was considered constant. This was:

- manikin CM contact along predicted CM trajectory

This constrained the manikin to place its CM along each of the consecutive trajectory points for each 0.02 s time step. This was the dominant constraint that drove the manikin to move from a sitting to a standing position.

Other constraints were present in one part of the motion but not in another. These could also change in terms of the degree of influence that they had on the STS patterns over certain periods of the movement. In this way, the weighting applied to a constraint could change from being high in one part of the movement, to low or zero sometime later. They included:

- body contact with seat
- hand contact with knee and thigh

The constraint of 'body contact with seat' was applied up until the onset of seat off event, i.e. when the hip marker started to move vertically. During this phase, variables that allowed the movement to occur e.g. transverse rotation of the hip, lumbar, neck and shoulder joints, were freed. After the event of SOO, the 'body contact with the seat' constraint reduced in its influence to allow the body to pull away from the seat slightly whilst still remaining close to it. This represented the seat-off phase reported from the experimental data. The influence of this constraint was reduced to zero after the event SOC.

The other constraint to change was 'hand contact with knee and thigh'. This remained constant up until VVMAX, approximating the movement patterns in the experimental trials. After this time the influence of the constraint was reduced which meant that there was less of a requirement for the manikin to keep the hand on the knees. This was required because the physical configuration of the body meant that the manikin (or experimental subject) could not stand up fully if hand/knee contact was maintained. Consequently, as the manikin rose after VVMAX the hands slid up the thighs such that they remained in contact with the legs but not the knees, reflecting what occurred in the experimental trials.

5.3.8 SECTION SUMMARY

A manikin model was set-up to predict STS movement patterns. Steps were presented to illustrate how to configure the manikin into a starting position using applied constraints and freed variables. Regression equations were coded into a curve fitting routine in order to predict CM trajectory, and 'if' statements were incorporated to adjust predicted event orders that caused CM horizontal trajectory oscillation. Curves were fitted to experimental data in order to select the appropriate curve degree and number of control points for the horizontal and vertical trajectories. These selected curve types were then fitted to regression-predicted precision points, and techniques to assess the errors due to the regression and the fitted curve were demonstrated. The implementation of the predicted trajectories, along with the use of further constraints and freed variables to produce manikin movement were described.

5.4 VALIDATION STUDY

Validation tests were conducted to assess the manikin model, allowing a confidence measure to be made in its ability to predict STS movement patterns. The validations compared experimental data against predicted data. Eleven evaluation trials were used to represent the original experimental region (as described in Section 5.3.1). However, before the validation tests occurred an assessment was made of the variability that would be expected to occur in the STS movement patterns.

5.4.1 NATURAL VARIABILITY IN STS MOVEMENT PATTERNS

A series of tests were made to consider joint angle displacements in the presence of the natural variability that occurred in human movement. This measure of variability in the experimental data became the required level of accuracy for the model i.e. the error between manikin predicted movement and experimental movement patterns were not required to decrease below this level of accuracy. All centre-point data (i.e. the repeated trials of condition nine, Figure 5.2) were used for this evaluation as these were the trials that were most likely to represent the condition under which rise would

occur. The centre-point condition also included a greater number of trials (three times as many) as corner-point conditions, giving an improved estimate of the variation.

Joint angle displacement time trends were collected. Because each trial did not include the same number of samples, each data point could not be compared directly. To account for this, a non-smoothing, interpolating spline (Wood and Jennings, 1979), implemented through a FORTRAN code, was fitted through each trend. These were re-sampled to 101 samples and exported to an Excel spreadsheet. Across all trends, maximum and minimum data points were found for each one sample time step, providing a range in data for each one sample time step (Figure 5.17). This value was halved to give the difference between a median trial and the maximum or minimum trial. In turn, these values were averaged to give a value of variability over the total duration, or over individual phases (i.e. sections of movement bounded by the *events* START, SOO, BALANCE, SOC, VVMAX, and END).

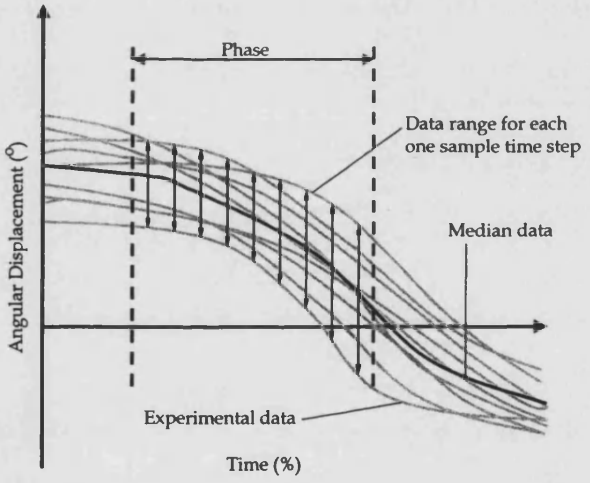

Figure 5.17. Technique used to provide estimate for movement variability.

5.4.2 VALIDATION OF MANIKIN MODEL AGAINST SUBJECT A

This first manikin model examination investigated the total predicted movement patterns that were created from applying the predicted trajectory and movement constraints. Data comparison occurred in terms of joint angle displacement time histories at the ankle, knee, hip, and lumbar joints. These data sets were chosen

because they represented joints that played the most important role in the execution of STS (Pai and Rogers, 1991). RMSD between the experimental and the predicted joint angle displacement time histories over the duration of rise were obtained (Tables 6.19-6.29). This occurred at each 0.02 s time step. An average value was calculated for all of the 11 evaluation trials. This test did not represent a totally independent test for the model as eight (the corner-points of the experimental region) of the 11 evaluation trials also supplied data that were used to create the regression models.

5.4.3 VALIDATION OF MANIKIN MODEL AGAINST SUBJECTS B AND C

The second manikin test gave a comparison of the model performance against two additional subjects, both of whom gave informed consent for the study and were healthy, active and reported no musculo-skeletal impairment. The participants were called subjects B and C, and represented samples of the population that were different to subject A (section 5.1.2). In terms of height, subject B represented a 95th percentile UK male adult, subject C represented > 50th percentile UK female adult (female 50th percentile was 1.62 m). In terms of mass, subject C represented < 50th percentile UK female adult (50th percentile was 66.70 kg) (Department of Trade and Industry, 1998). Consequently, an assessment of the applicability of the total manikin model to wider populations was obtained. A description of the anthropometric data of two subjects, along with the associated inertia data sets (as attained by the methods described in Section 5.1.4) can be seen in Table 5.4. Subjects B and C were allowed to rise in a less controlled manner than subject A. For example, foot position and *rise duration* were chosen in a more subjective manner. However, the rise conditions of the subjects were guided such that each experimental condition was approximately tested. Figure 5.18 illustrates the assignment of the two subjects to the experimental conditions. The same restrictions as the original experiment i.e. upright initial sitting posture, hands on knees, eyes on distant target etc., remained. The experimental set-up and data processing techniques were the same as those described in Section 5.1.3 and 5.1.4, respectively. Assessment techniques were conducted in the same manner as described in Section 5.4.2. Within the SWORDS modelling system, programmes that represented subject-specific data e.g. segment length, segment mass centre position etc., were changed to reflect subjects B and C.

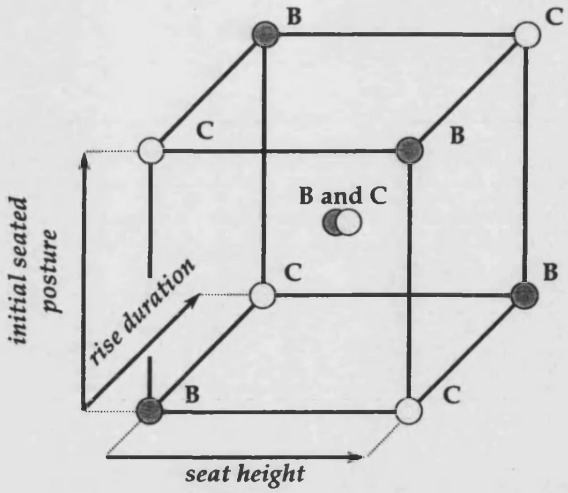

Figure 5.18. Assignment of rise conditions for subjects B and C.

Table 5.4. Inertia data for subjects B and C, generated from Yeadon's (1990) mathematical inertia model for a human body, based on the scaled density values from Dempster (1955).

	Subject B		Subject C	
Gender	Male		Female	
Age (years)	28		24	
Mass (kg)	95.00		54.40	
Height (m)	1.86		1.67	
Segment	Segment mass (% of total body mass)	CM location (% of segment length from proximal end)	Segment mass (% of total body mass)	CM location (% of segment length from proximal end)
Head	3.17	42.22	5.76	45.40
Neck	4.97	42.29	4.51	40.62
Pelvis	14.63	47.03	17.14	44.13
Thorax	14.38	52.54	13.81	54.69
Chest	9.59	47.89	7.35	46.32
Arm	5.57	44.34	5.41	41.68
Forearm	3.16	42.43	3.09	44.51
Hand	1.16	41.44	1.19	40.64
Thigh	28.77	43.36	26.82	42.33
Shank	12.12	43.68	12.22	43.67
Foot	2.48	37.09	2.70	36.64

The inertia data for subjects B and C used density values of Dempster (1955), which gave the lower model error than other density data sets (Clauser et al., 1969; Chandler et al., 1975). In terms of total body mass the error due to the model was 2.1% and 1.9% for subjects B and C, respectively. Density values were scaled to achieve the original mass for subjects B and C.

5.4.4 SECTION SUMMARY

Techniques to establish variability in human data trends were established and identified as the required accuracy level for manikin predicted movement patterns. Eleven evaluation trials were used to represent the experimental design region, and validation methods to assess the model against a range of subjects were presented.

5.5 SUMMARY

This chapter detailed the methodological techniques of the investigation. An experimental design was presented that allowed the effect of three factors: *rise duration, initial seated posture* and *seat height* to be investigated simultaneously. A single subject design was used and a controlled experiment was performed. Aspects of the study differed to those presented in Chapter Four and these were demonstrated and justified. A series of statistical analysis techniques were performed in order to create regression equations from the experimental data. The regression equations were created such that movement characteristics could be predicted over a range of factor combinations.

A computer-based manikin model was introduced and steps were presented to show how the model was set up to perform STS simulations. The implementation of regression equations into the manikin model was then discussed. Curve fitting techniques were presented and it was shown that in some cases the regressions could predict movement *events* out of order, causing oscillatory curves to be fitted. Some rectification techniques were presented to account for these inconsistencies. The implementation of predicted CM trajectory into the manikin model was shown, along with the appropriate movement constraints required to produce STS motion in the manikin. In the final section model validation techniques were demonstrated.

CHAPTER 6: RESULTS

The following chapter illustrates the results that were obtained from the different studies. Data obtained from the experiment are presented and subsequently used with regression techniques to form a series of predictive movement expressions. Manikin movement is illustrated by a sequence of figures, and predicted joint angle displacement data are tested against original experimental data.

6.1 EXPERIMENTAL ANALYSIS STUDY

This section presents the results from the experimental study as described in Section 5.1. Because of the large amount of data obtained from the study (16 responses from 66 trials, a total of 1056 data points), this section presents mean and standard deviation response data for each of the nine experimental conditions (Figure 5.2). Table 6.1 shows the actual mean factor levels obtained for each of the experimental conditions. It was noted that despite the efforts of the controlled experiment, the factor levels did not completely represent the initial proposed experimental region. This was particularly the case for the *seat height* factor that appeared to show an approximate 10° offset from the desired levels. Consequently, the test region changed to that shown in Figure 6.1.

Table 6.1. Mean factor levels for individual experimental conditions.

Condition	Factors		
	rise duration (s)	*initial seated posture* (°)	*seat height* (°)
1	0.95 (0.05)	7 (2)	1 (1)
2	1.85 (0.09)	10 (1)	1 (0)
3	1.05 (0.04)	19 (1)	2 (1)
4	1.80 (0.16)	18 (1)	2 (0)
5	1.09 (0.05)	8 (0)	40 (0)
6	1.82 (0.06)	13 (1)	36 (0)
7	0.83 (0.06)	17 (0)	44 (1)
8	1.61 (0.09)	18 (0)	42 (0)
9	1.23 (0.12)	13 (1)	20 (1)

mean (standard deviation)

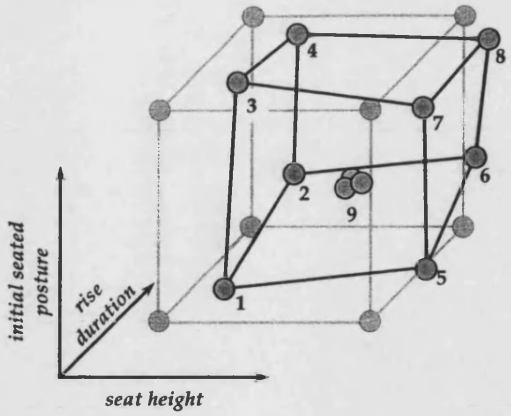

Figure 6.1. Actual experimental design region (dark grey) shown against proposed experimental design region (light grey) for the factors *rise duration, initial seated posture* and *seat height*.

The low and high levels of the factors were changed accordingly such that the correct scaling (i.e. between -1 and 1, see Section 5.2.2) could occur to produce the regressed factor variables. This produced a test region in terms of mean high and low values (Table 6.2) as shown in Figure 6.2.

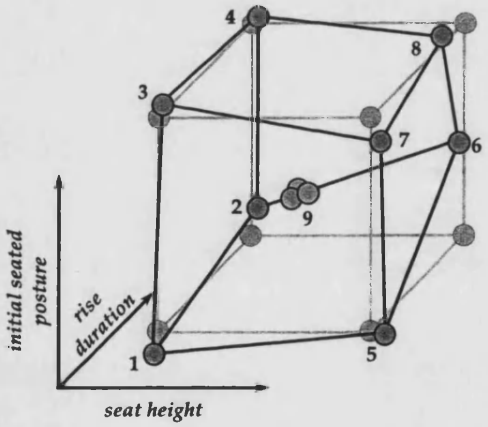

Figure 6.2. Actual scaled experimental design region (dark grey) shown against the proposed scaled experimental design region (light grey) for the factors *rise duration, initial seated posture* and *seat height*. Factors are scaled to -1 and 1.

Table 6.2. Low and high levels of factors, required for scaling of regressed factor variables.

	low level	centre level	high level
rise duration	0.98 s	1.37 s	1.77 s
initial seated posture	9°	14°	18°
seat height	2°	21°	40°

The values in Table 6.2 were obtained by taking the average of the experimental low and high levels for each of the factors. For example, to attain the low level value of 0.98 s for *rise duration*, the *rise duration* values for conditions 1, 3, 5, and 7 were averaged (see Table 6.1). The centre level values were obtained by averaging all data from the corner-points (i.e. excluding condition nine data). It should be noted that the centre-point condition (condition nine) did not perfectly represent the centre level of the three factors. This did not affect the quality of the regressions, which were based solely on the low and high levels of the factors.

Changes in *seat height* influenced *initial seated posture*, despite the control placed upon ankle angle. As *seat height* rose there was a tendency for the CM to move forward horizontally (as well as vertically) due to the more stance-like configuration of the body segments. Whilst changes in CM horizontal position due to *seat height* were anticipated, data processing showed the displacement to be larger than expected.

The experimental region shown in Figure 6.2 expressed scaled *initial seated posture* in terms of ankle angle. However, when the region was presented in its true unit of measure, i.e. the horizontal displacement between the CM and the rear of the BS (CM-$BS_{HOR\ DISP}$), it appeared as that shown in Figure 6.3.

Tables 6.3-6.6 show the responses obtained from the nine experimental conditions. The presented means and standard deviations in these tables do not include the data points that were eliminated through statistical techniques as described in Section 5.2.2. The number of trials used to create the mean values of condition nine were three times the number of trials used for conditions one to eight. The responses arose from the movement *event* theory as described in Section 4.2.3.

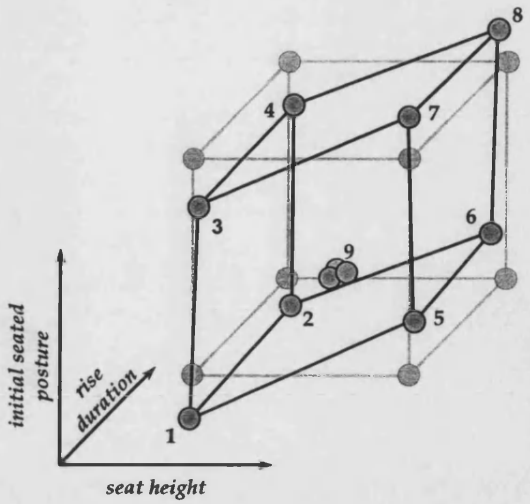

Figure 6.3. Hexahedron-shaped scaled experimental design region (dark grey) expressed in its real unit of measurement for *initial seated posture* (i.e. CM-$BS_{HOR\ DISP}$), against proposed scaled experimental region (light grey).

In Table 6.3, two CM velocity responses are presented for the event ONSET. These values dictated the initial slope of the respective horizontal or vertical displacement time trajectory. The horizontal component of CM velocity tended to be higher than the vertical component. Horizontal CM velocity was also higher in faster rise conditions than in slower rise conditions. Thus, condition one was higher than condition two, condition three was higher than condition four, and so on. The time of onset of seat off (SOO_{TIME}) occurred as early as 18.4%, and as late as 34.3%, of the normalised movement cycle. Mass centre horizontal displacement at SOO ($SOO_{HOR\ DISP}$) was shown in the final column (Table 6.3). It can be seen that at SOO the CM was as close as 0.02 m to the BS (condition four), or as far as 0.11 m from the BS (condition five).

Two further SOO responses are presented in Table 6.4. The vertical displacement data ($SOO_{VER\ DISP}$) represented the amount the CM moves between ONSET and SOO. The vertical velocity data ($SOO_{VER\ VEL}$) represented the slope of the vertical displacement time trajectory at SOO. $BALANCE_{TIME}$ represented the mean time at which the CM comes above the rear of the BS. It can be seen that $BALANCE_{TIME}$ occurred later in the fast rise conditions than in the slower conditions. For example, condition one was later than condition two, condition three was later than condition four, and so on. The data for horizontal velocity at BALANCE were collected as a means of curve adjustment in cases of erroneous response prediction, as discussed in detail in Section 5.3.3.

Table 6.3. Mean ONSET and SOO responses for individual experimental conditions.

Condition	$ONSET_{HOR\ VEL}$ ($m \cdot s^{-1}$)	$ONSET_{VER\ VEL}$ ($m \cdot s^{-1}$)	SOO_{TIME} (%)	$SOO_{HOR\ DISP}$ (m)
1	0.07 (0.01)	0.02 (0.01)	34.3 (1.4)	-0.07 (0.01)
2	0.05 (0.01)	0.01 (0.01)	22.6 (1.7)	-0.08 (0.01)
3	0.06 (0.01)	0.03 (0.01)	30.0 (3.3)	-0.03 (0.01)
4	0.04 (0.01)	0.00 (0.00)	27.2 (2.6)	-0.02 (0.01)
5	0.04 (0.01)	-0.01 (0.01)	18.4 (2.3)	-0.11 (0.01)
6	0.03 (0.01)	0.00 (0.00)	24.3 (2.3)	-0.09 (0.01)
7	0.04 (0.01)	-0.01 (0.01)	26.7 (1.7)	-0.04 (0.01)
8	0.02 (0.00)	-0.01 (0.00)	20.6 (2.6)	-0.03 (0.01)
9	0.04 (0.00)	-0.01 (0.00)	26.4 (2.1)	-0.09 (0.01)

mean (standard deviation)

Table 6.4. Mean SOO and BALANCE responses for individual experimental conditions.

Condition	$SOO_{VER\ DISP}$ (m)	$SOO_{VER\ VEL}$ ($m \cdot s^{-1}$)	$BALANCE_{TIME}$ (%)	$BALANCE_{HOR\ VEL}$ ($m \cdot s^{-1}$)
1	-0.01 (0.00)	0.06 (0.03)	51.8 (3.1)	0.29 (0.06)
2	-0.01 (0.01)	-0.06 (0.04)	31.5 (3.5)	0.37 (0.04)
3	-0.02 (0.00)	0.00 (0.04)	36.9 (2.9)	0.45 (0.05)
4	-0.02 (0.01)	-0.05 (0.01)	28.8 (3.6)	0.46 (0.04)
5	0.00 (0.00)	0.06 (0.02)	46.4 (3.0)	0.31 (0.07)
6	-0.01 (0.01)	-0.01 (0.01)	42.2 (2.7)	0.23 (0.04)
7	0.00 (0.00)	0.06 (0.02)	42.6 (1.5)	0.33 (0.02)
8	0.00 (0.00)	0.02 (0.01)	28.0 (0.7)	0.24 (0.02)
9	-0.02 (0.01)	-0.03 (0.02)	46.1 (2.6)	0.28 (0.05)

mean (standard deviation)

Table 6.5 presents data for the events SOC and VVMAX. The time at which SOC occurred (SOO_{TIME}) was between 30.6% (condition two) and 55.3% (condition seven). At this event, the CM was in the most posterior position in conditions one and five (0.02 m behind the rear of BS), and the most anterior position in conditions four and

eight (0.05 m in front of the rear of BS). The time of CM maximum vertical velocity ($VVMAX_{TIME}$) occurred between 41.5% (condition two) and 65.5% (condition one). $VVMAX_{VER\ VEL}$ showed higher values from lower seat height levels (condition one, two, three, and four) than from higher seat levels.

Table 6.5. Mean SOC and VVMAX responses for individual experimental conditions.

Condition	SOC_{TIME} (%)	$SOC_{HOR\ DISP}$ (m)	$VVMAX_{TIME}$ (%)	$VVMAX_{VER\ VEL}$ ($m \cdot s^{-1}$)
1	45.2 (2.0)	-0.02 (0.01)	65.5 (2.2)	0.90 (0.06)
2	30.6 (2.2)	0.00 (0.01)	41.5 (4.1)	0.40 (0.06)
3	42.1 (2.7)	0.03 (0.01)	61.3 (4.7)	0.77 (0.07)
4	35.3 (3.3)	0.05 (0.01)	46.0 (5.9)	0.45 (0.06)
5	39.1 (2.8)	-0.02 (0.01)	44.8 (6.0)	0.32 (0.02)
6	42.6 (2.5)	0.00 (0.01)	50.9 (6.5)	0.18 (0.02)
7	55.3 (4.7)	0.03 (0.01)	60.7 (3.1)	0.33 (0.02)
8	41.1 (3.7)	0.05 (0.01)	47.6 (3.8)	0.16 (0.02)
9	41.9 (3.0)	-0.01 (0.01)	57.6 (5.1)	0.42 (0.05)

mean (standard deviation)

Table 6.6 corresponds to the data of the final event, END. The vertical displacement data ($END_{VER\ DISP}$) showed the amount of CM vertical displacement from ONSET to END, with noticeable differences between the low, centre and high seat height conditions. The horizontal and vertical velocity data ($END_{HOR\ VEL}$ and $END_{VER\ VEL}$, respectively) reflected the slope of the according horizontal and vertical displacement time graphs at END.

Table 6.6. Mean END responses for individual experimental conditions.

Condition	$END_{HOR\ DISP}$ (m)	$END_{VER\ DISP}$ (m)	$END_{HOR\ VEL}$ ($m \cdot s^{-1}$)	$END_{VER\ VEL}$ ($m \cdot s^{-1}$)
1	0.06 (0.01)	0.34 (0.00)	0.05 (0.02)	0.08 (0.01)
2	0.10 (0.01)	0.34 (0.00)	0.02 (0.01)	0.05 (0.01)
3	0.08 (0.01)	0.34 (0.00)	0.02 (0.02)	0.06 (0.01)
4	0.12 (0.02)	0.34 (0.00)	0.00 (0.02)	0.04 (0.01)
5	0.09 (0.02)	0.13 (0.01)	0.05 (0.00)	-0.01 (0.01)
6	0.10 (0.02)	0.14 (0.01)	0.02 (0.03)	0.02 (0.01)
7	0.09 (0.01)	0.12 (0.01)	0.09 (0.01)	0.03 (0.01)
8	0.13 (0.01)	0.13 (0.00)	-0.01 (0.02)	0.02 (0.01)
9	0.09 (0.01)	0.23 (0.01)	0.04 (0.02)	0.03 (0.01)

mean (standard deviation)

Absolute *event* times are presented in Table 6.7. In each case, the individual event time occurred earlier in the fast rise condition than the slow rise condition. The time shown for END was also a representation of total *rise duration* as shown in Table 6.1. The small standard deviations associated with the data may imply that the occurrences of rise events were highly controlled.

Table 6.7. Mean absolute time of *events* for individual experimental conditions.

Condition	SOO (s)	BALANCE (s)	SOC (s)	VVMAX (s)	END (s)
1	0.33 (0.02)	0.49 (0.04)	0.43 (0.02)	0.62 (0.02)	0.95 (0.05)
2	0.42 (0.02)	0.58 (0.05)	0.56 (0.03)	0.76 (0.05)	1.85 (0.09)
3	0.31 (0.03)	0.39 (0.03)	0.44 (0.03)	0.64 (0.03)	1.05 (0.04)
4	0.49 (0.03)	0.52 (0.05)	0.63 (0.05)	0.88 (0.18)	1.80 (0.16)
5	0.20 (0.03)	0.50 (0.02)	0.42 (0.02)	0.47 (0.06)	1.09 (0.05)
6	0.42 (0.05)	0.77 (0.05)	0.75 (0.07)	0.93 (0.13)	1.82 (0.06)
7	0.23 (0.04)	0.35 (0.04)	0.46 (0.06)	0.50 (0.04)	0.83 (0.06)
8	0.33 (0.03)	0.45 (0.02)	0.66 (0.04)	0.77 (0.08)	1.61 (0.09)
9	0.31 (0.05)	0.57 (0.04)	0.51 (0.06)	0.72 (0.09)	1.23 (0.12)

mean (standard deviation)

6.1.1 SECTION SUMMARY

Mean experimental results were presented for each described response in the nine tested conditions. Changes in the levels of *seat height* were shown to affect levels of *initial seated posture,* causing the original test region to take on hexahedron characteristics. Results were presented for each of the 16 responses and for the absolute times of *events.*

6.2 STATISTICAL ANALYSIS STUDY

This section presents the results obtained from a regression analysis study. It is divided into two sections. The first of these covers the main and interaction effects as obtained from the fitted regressions. The second section presents the regression equations as applied to the manikin model.

6.2.1 MAIN AND INTERACTION EFFECTS

A total of 16 responses (as shown in Tables 6.3-6.6) were modelled through regression equation techniques to obtain main and interaction effects (see Section 5.2.2). Two models included just main effects in the regression. Of the remaining 14 responses with interaction effects, four showed significant three-factor interactions. Table 6.8 gives a summary of the effects within each response. The magnitude of the effects (and associated standard error) are shown in Tables 6.9 and 6.10, demonstrating the expected change in response due to a change in factor or factors from a centre level to a high level (as demonstrated in Table 6.2). By applying the effects (Tables 6.9 and 6.10) back into the form of the regression equation (Equation 5.2) predictive expressions for each response were formed. These expressions are presented in Section 6.2.2.

Table 6.8. Summary of effects in each modelled response.

RESPONSE	MAIN EFFECTS			INTERACTION EFFECTS			
	RD	ISP	*SH*	*RD*ISP*	*RD*SH*	*ISP*SH*	*RD*ISP*SH*
$ONSET_{HOR\ VEL}$	✓	✓	✓		✓		
$ONSET_{VER\ VEL}$	✓	✓	✓	✓	✓		
SOO_{TIME}	✗	✗	✓	✗	✓	✓	✓
$SOO_{HOR\ DISP}$	✓	✓	✓			✓	
$SOO_{VER\ DISP}$		✓	✓			✓	
$SOO_{VER\ VEL}$	✓		✓				
$BALANCE_{TIME}$	✓	✓	✓	✗	✗	✗	✓
$BALANCE_{HOR\ VEL}$	✗	✓	✓		✓	✓	
SOC_{TIME}	✓	✓	✓	✓	✓	✗	✓
$SOC_{HOR\ DISP}$	✓	✓	✓				
$VVMAX_{TIME}$	✓	✗	✓	✗	✓	✗	✓
$VVMAX_{VER\ VEL}$	✓	✓	✓		✓	✓	
$END_{HOR\ DISP}$	✓	✓	✗		✓		
$END_{VER\ DISP}$		✓	✓			✓	
$END_{HOR\ VEL}$	✓	✓	✓	✓			
$END_{VER\ VEL}$	✓	✓	✓	✓	✓	✓	

Note: Significant effects are marked by a ✓. Non-significant effects may exist in a regression if they support a higher-order significant effect, and are marked by a ✗ (Section 5.2.2).

Mass centre horizontal velocity at movement onset ($ONSET_{HOR\ VEL}$)

The response $ONSET_{HOR\ VEL}$ was the first of three responses to require transformation due to a skewed distribution, as described in Section 5.2.2. The coefficients presented in Tables 6.9 are in their transformed state as it is only the result of the regression that could be re-transformed. With the three factors set at their centre levels, re-transformation of the coefficient Y_0 showed $ONSET_{HOR\ VEL}$ to equal 0.04 $m \cdot s^{-1}$ (the result of $0.4433^{\,1/0.25}$). Three significant main effects and one significant interaction effect (*rise duration & seat height*) were found in the response.

Table 6.9. Effect coefficients and associated standard error of eight responses for *events* ONSET, SOO and BALANCE.

RESPONSE	γ_0	*RD*	*ISP*	*SH*	*RD*ISP*	*RD*SH*	*ISP*SH*	*RD*ISP*SH*
$ONSET_{HOR\ VEL}$ *	0.4433 (0.0021)	-0.0230 (0.0022)	-0.0069 (0.0023)	-0.0303 (0.0029)		-0.0058 (0.0022)		
$ONSET_{VER\ VEL}$ ($m \cdot s^{-1}$)	0.00 (0.00)	0.00 (0.00)	0.00 (0.00)	-0.01 (0.00)	-0.01 (0.00)	0.01 (0.00)		
SOO_{TIME} (%)	25.1 (0.4)	**-0.1 (0.4)**	**0.5 (0.4)**	-3.9 (0.4)	**-0.5 (0.4)**	2.1 (0.5)	**0.4 (0.3)**	-2.3 (0.3)
$SOO_{HOR\ DISP}$ (m)	-0.06 (0.00)	0.00 (0.00)	0.03 (0.00)	-0.03 (0.00)			0.00 (0.00)	
$SOO_{VER\ DISP}$ (m)	-0.01 (0.00)		0.00 (0.00)	0.01 (0.00)			0.00 (0.00)	
$SOO_{VER\ VEL}$ ($m \cdot s^{-1}$)	0.00 (0.00)	-0.03 (0.00)		0.02 (0.00)				
$BALANCE_{TIME}$ (%)	39.2 (0.4)	-4.3 (0.5)	-5.8 (0.4)	4.8 (0.5)	**0.4 (0.4)**	**0.6 (0.5)**	**-0.6 (0.4)**	-1.7 (0.3)
$BALANCE_{HOR\ VEL}$ ($m \cdot s^{-1}$)	0.35 (0.01)	**-0.01 (0.01)**	0.04 (0.01)	-0.09 (0.01)		-0.03 (0.01)	-0.03 (0.01)	

Note: Standard errors associated with each response co-efficient are in brackets. Coefficients highlighted in bold are those that are not statistically significant ($p>0.05$), but which are included because there are significant higher order terms in the model including that term. * indicates the response has been transformed by $Y^{0.25}$, thus units are with reference to the transformed coefficients. Decimal places displayed for a transformed response are equivalent to appropriate decimal places in the re-transformed response.

Table 6.10. Effect coefficients and associated standard error of eight responses for *events* SOC, VVMAX and END.

RESPONSE	γ_0	*RD*	*ISP*	*SH*	*RD*ISP*	*RD*SH*	*ISP*SH*	*RD*ISP*SH*
SOC_{TIME} **	0.3967	0.0043	-0.0025	-0.0038	0.0024	-0.0068	**-0.0005**	0.0065
	(0.0011)	(0.0012)	(0.0010)	(0.0013)	(0.0010)	(0.0013)	**(0.0009)**	(0.0009)
$SOC_{HOR\ DISP}$ (m)	0.01 (0.00)	0.01 (0.00)	0.03 (0.00)	-0.02 (0.00)				
$VVMAX_{TIME}$ (%)	53.1 (0.8)	-4.4 (1.0)	**0.4 (0.8)**	-2.4 (1.0)	**-1.5 (0.8)**	4.9 (1.0)	**0.1 (0.7)**	-2.4 (0.7)
$VVMAX_{VER\ VEL}$ **	1.2903 (0.0044)	0.1174 (0.0037)	0.0103 (0.0041)	0.1531 (0.0051)		0.0190 (0.0038)	0.0143 (0.0037)	
$END_{HOR\ DISP}$ (m)	0.09 (0.00)	0.02 (0.00)	0.01 (0.00)	**0.00 (0.00)**			-0.01 (0.00)	
$END_{VER\ DISP}$ (m)	0.23 (0.00)		0.01 (0.00)	-0.11 (0.00)			0.00 (0.00)	
$END_{HOR\ VEL}$ ($m \cdot s^{-1}$)	0.03 (0.00)	- 0.02 (0.00)	-0.01 (0.00)	0.01 (0.00)	-0.01 (0.00)			
$END_{VER\ VEL}$ ($m \cdot s^{-1}$)	0.03 (0.00)	0.00 (0.00)	0.00 (0.00)	-0.03 (0.00)	0.00 (0.00)	0.01 (0.00)	0.01 (0.00)	

Note: Standard errors associated with each response co-efficient are in brackets. Coefficients highlighted in bold are those that are not statistically significant ($p>0.05$), but which are included because there are significant higher order terms in the model including that term. ** indicates the response has been transformed by $Y^{-0.25}$, thus units are with reference to the transformed coefficients. Decimal places displayed for a transformed response are equivalent to appropriate decimal places in the re-transformed response.

Time of seat-off onset (SOO_{TIME})

The predicted response SOO_{TIME} would occur at a normalised time of 25.1% of the total movement when the three factors were set to their respective centre levels (Table 6.9, see coefficient Y_0). It was shown that neither *rise duration* nor *initial seated posture* had a significant main effect on the response (non-significant effects are highlighted in bold in the table). A significant main effect was seen for *seat height* where it was predicted that if *seat height* changed from a centre level (thighs at 21° to horizontal) to a high level (thighs at 40° to horizontal), then the normalised time of SOO would occur 3.9% earlier. *Rise duration & seat height* was a significant two-factor interaction, with an effect of 2.9%. Additionally, SOO_{TIME} was one of four responses that showed a significant three-factor interaction, showing SOO_{TIME} to occur 2.3% earlier if all factors were at their high levels. In such a condition the subject would be rising from a higher chair with the feet tucked more under the body and with the movement duration lasting longer.

Mass centre horizontal displacement at seat-off onset ($SOO_{HOR\ DISP}$)

Rise duration did not influence $SOO_{HOR\ DISP}$ (Table 6.9). A main effect for *initial seated posture* showed that the CM would move 0.03 m forward (closer to the BS) due to an increase from a centre to a high level. A high *seat height* affected the horizontal CM displacement at SOO by -0.03 m. No interaction effects were seen in this response. It should be noted that it was this response ($SOO_{HOR\ DISP}$) that the model statistics approach (Bates et al. (1992), as described in section 5.2.1) suggested would require more than 6 trials per condition to show adequate statistical significance. Therefore, results for $SOO_{HOR\ DISP}$ should be interpreted with a degree of caution.

Time of mass centre reaching final base of support ($BALANCE_{TIME}$)

When rising under centre level conditions, $BALANCE_{TIME}$ was predicted to occur at 39.2% of the movement cycle (Table 6.9, coefficient Y_0). When changing *rise duration* to its high level, $BALANCE_{TIME}$ was predicted to occur earlier (a -4.3% effect). A large influence was seen for *initial seated posture*, with a -5.8% effect between centre and high foot positions. All two-factor interactions were non-significant. However, they were

kept in the regression because of the significant three-factor interaction (-1.7%) that was observed.

Time of seat-off completion (SOC_{TIME})

The response of SOC_{TIME} was the second of three transformed responses. Coefficients were shown in their transformed state (Table 6.10). With the three factors set at their centre levels, re-transformation of the coefficient Y_0 showed SOC occurred at 40.4% of duration (the result of $0.3967^{1/-0.25}$). For this particular response, several of the interaction effects were comparable or larger in size to the main effects. Thus larger differences were seen in the response when more than one factor was changed from its centre level. For example, when all factors were set at their low levels, the re-transformed regression showed a value of 44.4%. However, when changing the pace factor to its high level the response reduced to 32.5%. Of this 11.9% reduction only 3.5% could be attributed to the main effect of *rise duration.*

Time of mass centre maximum vertical velocity ($VVMAX_{TIME}$)

The time of CM maximum vertical velocity was predicted to occur at 53.1% of duration with factors set at centre levels (Table 6.10). This decreased to 48.7% when *rise duration* increased to its high level (due to the -4.4% *rise duration* effect). There was a non-significant effect for *initial seated posture,* and a -2.4% effect for *seat height.* The largest effect in the response $VVMAX_{TIME}$ was the two-factor interaction between *rise duration & seat height* (4.9%).

Mass centre maximum vertical velocity ($VVMAX_{VER\ VEL}$)

The response for $VVMAX_{VER\ VEL}$ was the last to require transformation due to a skewed distribution. The coefficients were presented in their transformed state (Tables 6.10). A large main effect for *rise duration* was seen. The re-transformed response showed the CM vertical velocity to be 0.36 $m \cdot s^{-1}$ ($1.2903^{1/-0.25}$) with all three factors set at their centre levels. This increased to 0.53 $m \cdot s^{-1}$ ($(1.2903\text{-}0.1174)^{1/-0.25}$) for fast rise, if other

factors remained at their centre levels. The seat height played an important role in the $VVMAX_{VER\ VEL}$ response and in the context of this study was a stronger effect than *rise duration* itself. If the seat height were to reduce to its low level whilst other factors remained at the centre levels, $VVMAX_{VER\ VEL}$ was predicted to be 0.60 $m \cdot s^{-1}$ ((1.2903-0.1531) $^{1/-0.25}$).

Mass centre horizontal displacement at movement end ($END_{HOR\ DISP}$)

At END, the CM was 0.09 m anterior to the rear of the BS with all factors set at their centre levels (Table 6.10). Significant main effects were found for *rise duration* (0.02 m) and *initial seated posture* (0.01 m) and a significant interaction effect was found for *initial seated posture & seat height.*

6.2.2 REGRESSION EQUATIONS

The effects that were presented in the previous section were obtained by fitting regressions to the experimental data as described in Section 5.2.2. These same regressions were then used as response predictors as factor levels changed between -1 and 1 (or outside of that range if required). Specifically, they were implemented to create curve domain precision points to which horizontal and vertical displacement time trajectories were fitted within the SWORDS software as outlined in Section 5.3.3.

The regression equations associated with the event ONSET are:

$$ONSET_{HOR\ VEL}(m \cdot s^{-1}) = \begin{pmatrix} 0.4434 - 0.0230 \cdot RD - 0.0069 \cdot ISP \\ -0.0303 \cdot SH - 0.0059 \cdot RD \cdot SH \end{pmatrix}^4 \quad [6.1]$$

$$ONSET_{VER\ VEL}(m \cdot s^{-1}) = 0.00 - 0.01 \cdot SH - 0.01 \cdot RD \cdot ISP + 0.01 \cdot RD \cdot SH \quad [6.2]$$

In Equation 6.1 it can be seen that the terms in brackets are raised to the power 4. This was performed to re-transform the response into real units after the initial transformation to account for skewed distributions. In cases where regressions found a

main or interaction effect in the response equal to zero, the particular term was excluded from the regression expression as it would have no influence on the response. For example, Equation 6.5 showed just the constant term and the *seat height* effect in the expression. However, the regression actually included three effects (Table 6.9), two of which equated to zero.

The regression equations associated with the event SOO are:

$$SOO_{TIME}\,(\%) = 25.1 - 0.1 \cdot RD + 0.5 \cdot ISP - 3.9 \cdot SH - 0.5 \cdot RD \cdot ISP + 2.1 \cdot RD \cdot SH + 0.4 \cdot ISP \cdot SH - 2.3 \cdot RD \cdot ISP \cdot SH \quad [6.3]$$

$$SOO_{HOR\,DISP}\,(m) = -0.06 + 0.03 \cdot ISP - 0.03 \cdot SH \quad [6.4]$$

$$SOO_{VER\,DISP}\,(m) = -0.01 + 0.01 \cdot SH \quad [6.5]$$

$$SOO_{VER\,VEL}\,(m \cdot s^{-1}) = 0.00 - 0.03 \cdot RD + 0.02 \cdot SH \quad [6.6]$$

The regression equations associated with the event BALANCE are:

$$BALANCE_{TIME}\,(\%) = 39.2 - 4.3 \cdot RD - 5.8 \cdot ISP + 4.8 \cdot SH + 0.4 \cdot RD \cdot ISP + 0.7 \cdot RD \cdot SH - 0.6 \cdot ISP \cdot SH - 1.7 \cdot RD \cdot ISP \cdot SH \quad [6.7]$$

$$BALANCE_{HOR\,VEL}\,(m \cdot s^{-1}) = 0.35 - 0.01 \cdot RD + 0.04 \cdot ISP - 0.09 \cdot SH - 0.03 \cdot RD \cdot SH - 0.03 \cdot ISP \cdot SH \quad [6.8]$$

The regression equations associated with the event SOC are:

$$SOC_{TIME}\,(\%) = \left(0.3967 + 0.0043 \cdot RD - 0.0025 \cdot ISP - 0.0038 \cdot SH + 0.0024 \cdot RD \cdot ISP - 0.0068 \cdot RD \cdot SH - 0.0005 \cdot ISP \cdot SH + 0.0065 \cdot RD \cdot ISP \cdot SH\right)^{-4} \quad [6.9]$$

$$SOC_{HOR\,DISP}\,(m) = 0.01 + 0.01 \cdot RD + 0.03 \cdot ISP - 0.02 \cdot SH \quad [6.10]$$

The regression equations associated with the event VVMAX are:

$$\begin{aligned} VVMAX_{TIME}(\%) = 53.1 - 4.4 \cdot RD + 0.4 \cdot ISP - 2.4 \cdot SH - 1.5 \cdot RD \cdot ISP \\ + 4.9 \cdot RD \cdot SH + 0.1 \cdot ISP \cdot SH - 2.4 \cdot RD \cdot ISP \cdot SH \end{aligned} \quad [6.11]$$

$$VVMAX_{VER\ VEL}(m \cdot s^{-1}) = \left(\begin{array}{r} 1.2903 + 0.1174 \cdot RD + 0.0103 \cdot ISP \\ + 0.1531 \cdot SH + 0.0190 \cdot RD \cdot SH \\ + 0.0143 \cdot ISP \cdot SH \end{array} \right)^{-4} \quad [6.12]$$

Note that Equations 6.9 and 6.12 were raised to the power -4, such that re-transformation of the terms occurred.

The regression equations associated with the event END are:

$$END_{HOR\ DISP}(m) = 0.09 + 0.02 \cdot RD + 0.01 \cdot ISP - 0.01 \cdot RD \cdot SH \quad [6.13]$$

$$END_{HOR\ VEL}(m \cdot s^{-1}) = \left(\begin{array}{r} 0.03 - 0.02 \cdot RD - 0.01 \cdot ISP + 0.01 \cdot SH \\ -0.01 \cdot RD \cdot ISP \end{array} \right) \quad [6.14]$$

$$END_{VER\ VEL}(m \cdot s^{-1}) = \left(0.03 - 0.03 \cdot SH + 0.01 \cdot RD \cdot SH + 0.01 \cdot ISP \cdot SH \right) \quad [6.15]$$

Note that no regression was presented for the vertical displacement at END. This will be discussed further in the next chapter.

6.2.3 SECTION SUMMARY

The main and interaction effects for 16 spatiotemporal STS responses were presented. Only two responses demonstrated the existence of just main effects, and four temporal responses included a three-factor interaction effect. The STS responses were expressed as a series of predictive regression equations.

6.3 MANIKIN MODELLING STUDY

6.3.1 REGRESSION EQUATION EVALUATION

Selected regression equations were used to predict centre-point experimental response data (Table 6.11), as described in Section 5.3.4. Due to difficulty in the control of factors, the presented trials did not lie exactly upon the centre levels of the factors that they represented. The associated factor levels used to obtain the predicted response values are shown at the bottom of Table 6.11. Because the centre-points were not used for the creation of the regressions this test represented an independent check of the ability of the regressions to predict response data.

The results presented in Table 6.11 show the predictive abilities of the regressions for the chosen spatiotemporal responses. The maximum difference between experimental and predicted data of a temporal response was 5.9% ($VVMAX_{TIME}$, trial 2, highlighted by the circle), with the root mean square difference (RMSD) across all test trials of temporal responses being 2.7%. For displacement responses, the maximum error was 0.04 m ($END_{HOR\ DISP}$, trial 3, highlighted by the hexagon) with RMSD across all test trials of displacement responses being 0.02 m. The average horizontal displacement of the CM from ONSET to END was 0.25 m in this condition, equating to a relative average error of 8.0% for displacement regressions. For velocity responses, the maximum error was 0.07 $m \cdot s^{-1}$ ($VVMAX_{VER\ VEL}$, trial 5, highlighted by the square), with RMSD across all test trials of velocity responses being 0.03 $m \cdot s^{-1}$. The average vertical velocity of the CM at VVMAX in these conditions was 0.43 $m \cdot s^{-1}$, equating to a relative average error of 7.0% for velocity regressions.

Table 6.11. Experimental (Exp.) against predicted (Pred.) response data and associated factor levels for six randomly chosen trials from the centre-point condition.

RESPONSE		Test trials					
		1	2	3	4	5	6
$ONSET_{HOR\ VEL}$ ($m \cdot s^{-1}$)	Exp.	0.04	0.04	0.04	0.04	0.05	0.04
$ONSET_{HOR\ VEL}$ ($m \cdot s^{-1}$)*	Pred.	0.04	0.04	0.04	0.04	0.05	0.05
SOO_{TIME} (%)	Exp.	27.4	26.4	28.6	23.7	22.2	24.5
SOO_{TIME} (%)	Pred.	24.7	25.1	24.8	24.8	25.0	24.7
$SOO_{HOR\ DISP}$ (m)	Exp.	-0.08	-0.09	-0.09	-0.09	-0.10	-0.10
$SOO_{HOR\ DISP}$ (m)	Pred.	-0.09	-0.08	-0.09	-0.07	-0.08	-0.07
$SOO_{VER\ VEL}$ ($m \cdot s^{-1}$)	Exp.	-0.02	-0.03	-0.02	-0.05	-0.01	-0.01
$SOO_{VER\ VEL}$ ($m \cdot s^{-1}$)	Pred.	-0.01	-0.01	0.01	0.01	0.02	0.02
$BALANCE_{TIME}$ (%)	Exp.	42.5	44.4	46.0	47.5	46.3	49.1
$BALANCE_{TIME}$ (%)	Pred.	43.6	42.5	45.5	43.7	45.3	45.6
SOC_{TIME} (%)	Exp.	39.7	41.7	42.9	39.0	38.9	41.5
SOC_{TIME} (%)**	Pred.	39.3	39.2	39.7	40.7	40.9	40.9
$SOC_{HOR\ DISP}$ (m)	Exp.	-0.01	-0.01	-0.01	-0.02	0.00	0.00
$SOC_{HOR\ DISP}$ (m)	Pred.	-0.02	-0.01	-0.02	-0.01	-0.01	-0.01
$VVMAX_{TIME}$ (%)	Exp.	54.8	58.3	57.1	50.8	57.4	60.4
$VVMAX_{TIME}$ (%)	Pred.	52.1	52.4	53.9	54.8	55.9	55.8
$VVMAX_{VER\ VEL}$ ($m \cdot s^{-1}$)	Exp.	0.36	0.40	0.41	0.48	0.42	0.48
$VVMAX_{VER\ VEL}$ ($m \cdot s^{-1}$)**	Pred.	0.34	0.36	0.42	0.44	0.49	0.50
$END_{HOR\ DISP}$ (m)	Exp.	0.07	0.10	0.11	0.08	0.10	0.07
$END_{HOR\ DISP}$ (m)	Pred.	0.09	0.09	0.07	0.07	0.07	0.07
FACTOR LEVELS							
Rise duration		0.22	0.16	-0.29	-0.49	-0.75	-0.80
Initial seated posture		-0.91	-0.80	-0.89	-0.39	-0.50	-0.49
Seat height		0.02	-0.09	-0.05	0.00	-0.04	0.00

Note: * indicates response has been re-transformed by Y^4, ** indicates response has been re-transformed by Y^{-4}. Highlighted data show maximum error in temporal (circle), displacement (hexagon), and velocity (square) responses.

6.3.2 CURVE FITTING SELECTION

Bézier Curves, as described in Appendix F, were controlled by three parameters: curve degree, number of control points, and knot spacing. For the curves implemented in this work, knot spacing was equidistant, as discussed in Section 5.3.3. However, values for curve degree and number of control points were required to be set. Results of the methodologies described in Section 5.3.5 are presented in Tables 6.12 and 6.13. The results are in terms of the relative RMSD between the experimental trajectories and the trajectories created by fitting curves to the experimentally obtained precision points. RMSD (averaged over the 11 evaluation trials) is presented for a number of curve degree and control point combinations, and for horizontal (Table 6.12) and vertical (Table 6.13) displacement time trajectories.

Table 6.12. RMSD (%) between experimental and fitted horizontal displacement time trajectory across 11 evaluation trials.

Curve Degree	Number of Control Points					
	10	11	12	13	14	15
2	3.3	2.9	3.5	(2.7)	3.1	3.8
3	4.0	3.5	3.5	2.9	3.3	4.5
4	5.0	4.8	4.3	3.1	3.5	6.7
5	-	4.8	4.2	3.7	8.0	-

Note: Minimum value circled.

Table 6.13. RMSD (%) between experimental and fitted vertical displacement time trajectory across 11 evaluation trials.

Curve Degree	Number of Control Points					
	7	8	9	10	11	12
2	5.3	4.8	5.5	6.7	6.6	11.4
3	5.9	(4.7)	5.6	5.8	6.1	17.3
4	7.0	4.7	6.1	7.5	7.0	-
5	8.5	5.2	6.3	-	-	-

Note: Minimum value circled.

This resulted in 13 control points and a second degree curve for the horizontal trajectory, and eight control points and a third degree curve for the vertical trajectory. In the case of the vertical displacement time trajectory, two combinations produced the minimum RMS error value. The third degree curve was chosen in favour of the fourth degree curve (both with eight control points) to reduce the possibility of curve oscillation in untested conditions.

6.3.3 EVALUATION OF CURVES FITTED TO REGRESSION-PREDICTED PRECISION POINTS

Using the curve combination as assessed in Section 6.3.2, an evaluation was made to judge the error introduced to the trajectory due the combinations of the regressions (i.e. the predicted precision points). The methods for this evaluation were described in Section 5.3.6. The values shown in Table 6.14 are in terms of the mean RMSD (for the 11 evaluation trials) between the experimental trajectory and the predicted trajectory. The combined error (curve fitting + regression equation) in the predicted trajectories across all 11 trials was 7.1% and 8.9% in the horizontal and vertical domains, respectively. Examples of experimental and fitted trajectories in the horizontal and vertical displacement time domains are shown in Figures 6.4 and 6.5, respectively. The associated CM trajectory can be found in Figure 6.6.

Table 6.14. Components of error in fitted curves across 11 evaluation trials.

Error Measure	Error Type		
	Curve Fitting	Regression Equation	Total
Horizontal (%)	2.7	4.4	7.1
Horizontal (m)	0.01	0.01	0.02
Vertical (%)	4.7	4.2	8.9
Vertical (m)	0.01	0.01	0.02

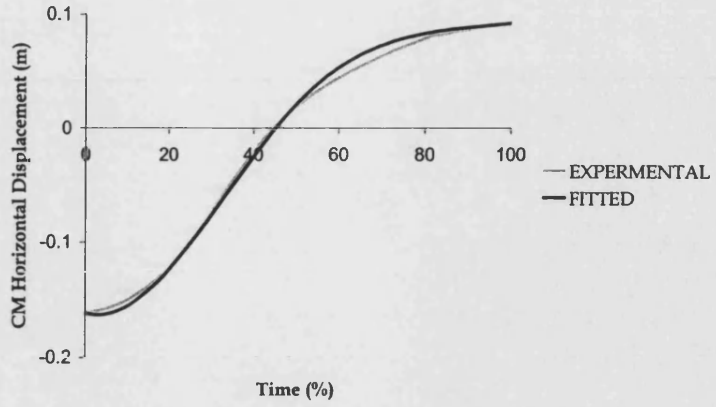

Figure 6.4. Fitted and experimental horizontal displacement time trajectory.

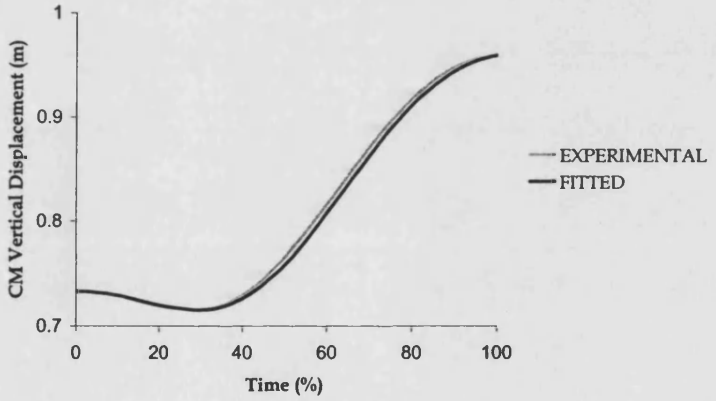

Figure 6.5. Fitted and experimental vertical displacement time trajectory.

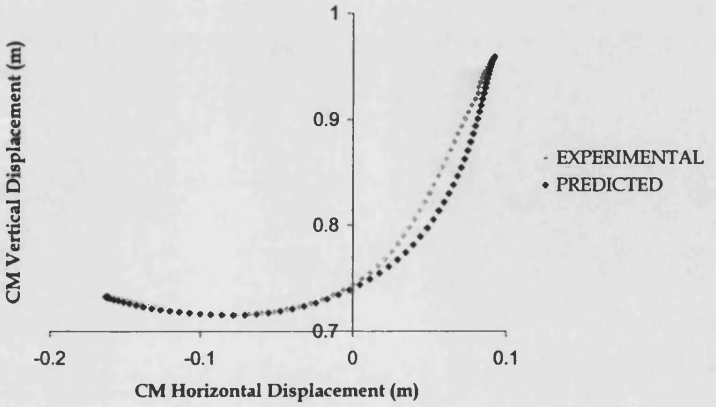

Figure 6.6. Predicted and experimental CM trajectory.

6.3.4 GRAPHICAL REPRESENTATION OF MANIKIN MOVEMENT

This section shows a series of figures representing the manikin movement produced in the SWORDS graphics window as described in Section 5.3.7. Figure 6.7 represents a condition nine (centre-point) rise.

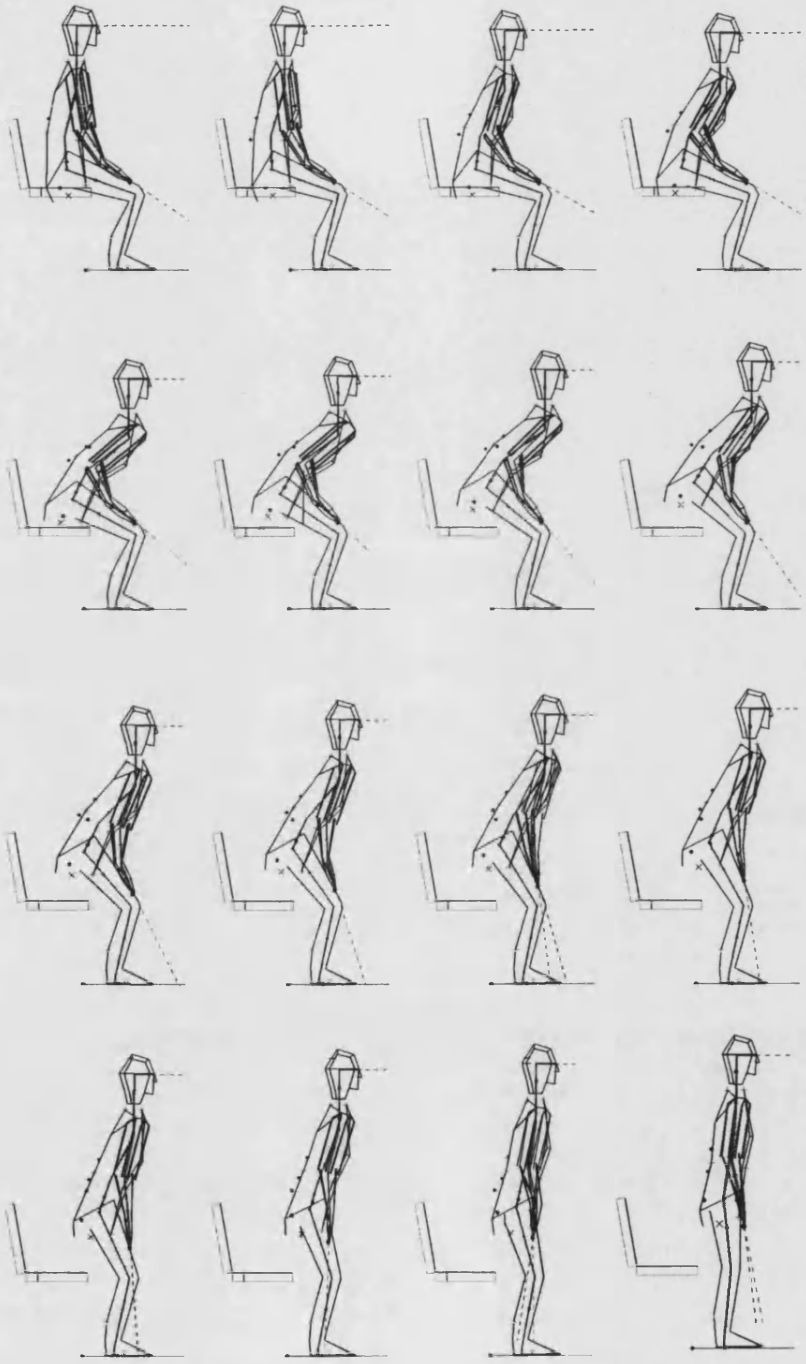

Figure 6.7. Sequence of frames showing manikin movement throughout STS for condition nine (*RD* (0), *ISP* (0), *SH* (0)).

Figure 6.8 represents a condition two rise ((*RD* (1), *ISP* (-1), *SH* (-1)). Additionally, the predicted CM trajectory is shown. Section 5.3.7 described how a constraint to place the CM along this trajectory was used with other constraints to produce STS movement patterns.

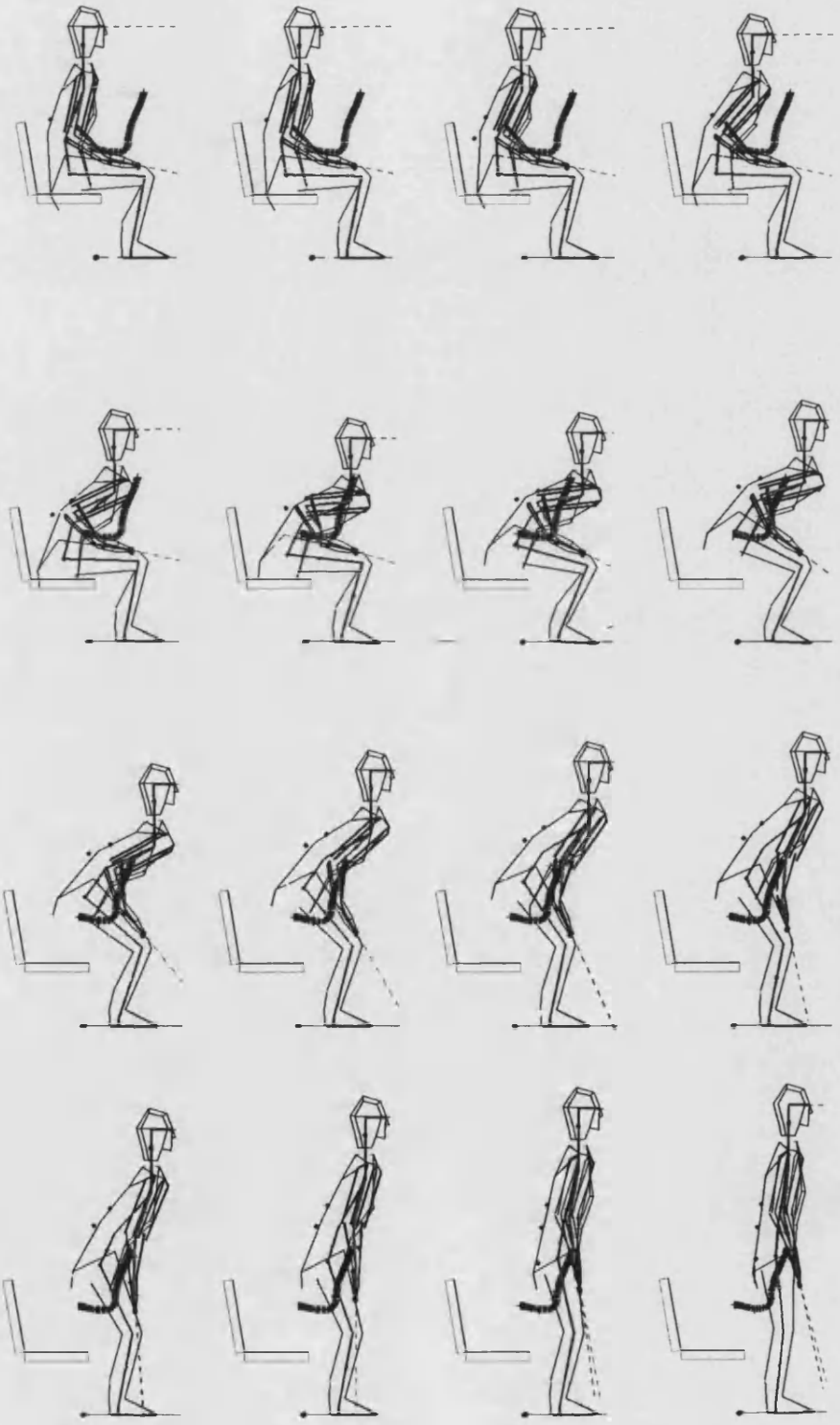

Figure 6.8. Sequence of frames showing manikin movement throughout STS for condition two ((*RD* (1), *ISP* (-1), *SH* (-1)).

Figure 6.9 represents a condition six rise ((*RD* (1), *ISP* (-1), *SH* (1)). The difference in predicted CM trajectory from that demonstrated in Figure 6.8 is evident.

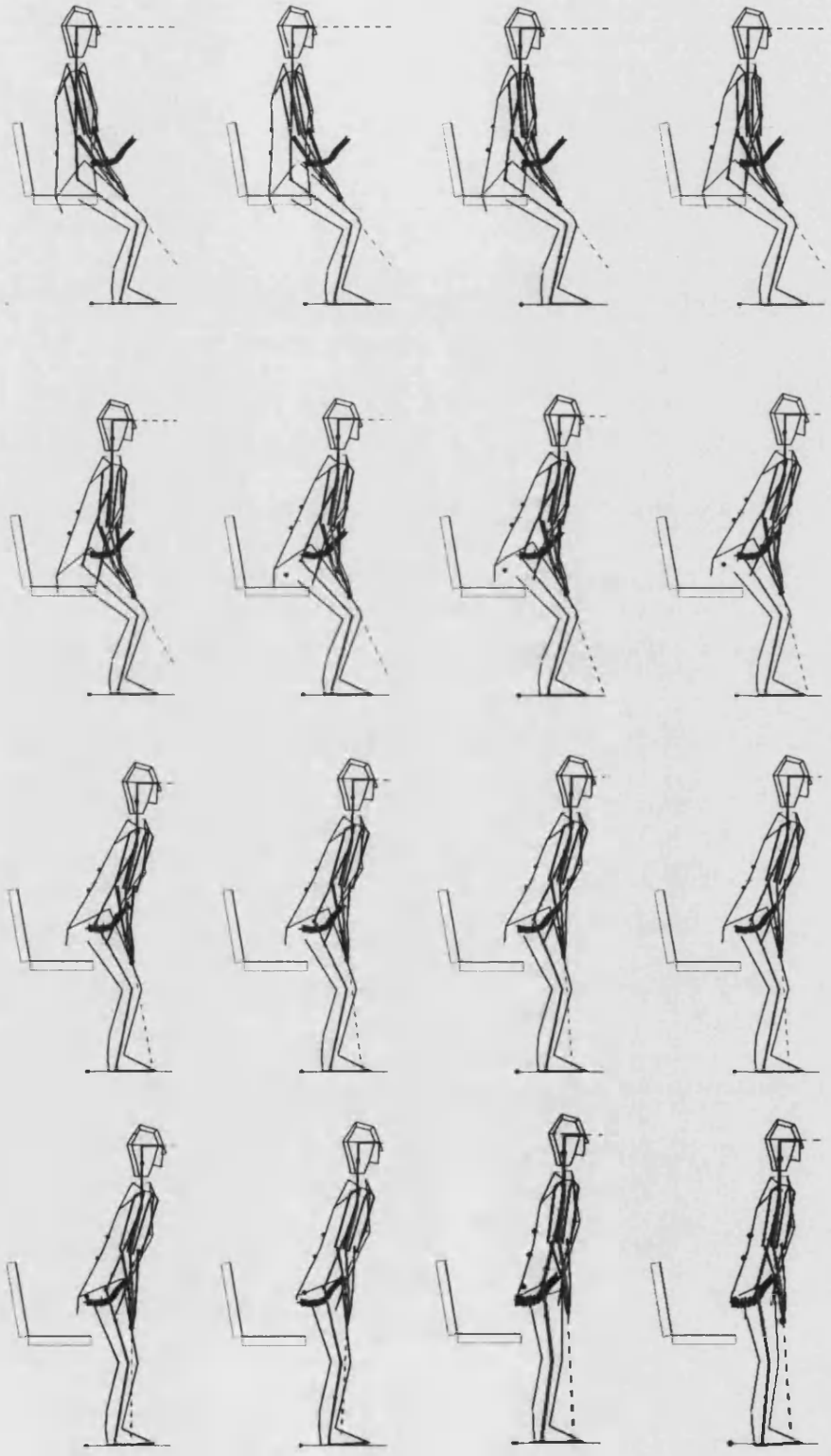

Figure 6.9. Sequence of frames showing manikin movement throughout STS for condition six ((*RD* (1), *ISP* (-1), *SH* (1)).

6.3.5 SECTION SUMMARY

The section presented a series of results and culminated in a graphical demonstration of the movement of the manikin. The regression equations used to find the effects were employed to predict experimental data. It was found that responses were on average accurate to 2.7%, 8.0%, and 7.0% for time, displacement, and velocity measures, respectively. Curves were fitted to experimental data in order to select the most appropriate curve type combination. The selected curves were then applied to the regression-predicted precision points. Predicted CM horizontal and vertical trajectories were accurate to 7.1% and 8.9%, respectively. Manikin movement was shown from three seat heights.

6.4 VALIDATION STUDY

The following section offers an assessment of the natural variability associated with STS movement patterns, followed by a series of validations from which the ability of the manikin to create simulated STS movement could be judged.

6.4.1 NATURAL VARIABILITY IN STS MOVEMENT PATTERNS

A series of tests were made to establish the natural variability that occurred in STS. The methodology for this assessment was described in Section 5.4.1. Centre-point data were used as trials most likely to represent the rise conditions of normal situations. The centre-point condition also included a greater number of trials (three times as many) than corner-point conditions, giving an improved estimate of variation. A presentation was made for each of the joint angles of interest: lumbar, hip, knee and ankle (Figures 6.10-6.13).

The value of variability represented half of the range in data seen over particular phases or the whole movement (Figure 5.17). Table 6.15 shows variability in the lumbar joint over the total STS duration to be 2.2°. In the first phase of movement lumbar joint variability was 1.8°, increasing to 3.7° in phase four. Due to definition of the lumbar joint via a virtual point (Appendix C), about the final 20% showed zero variability. Variation of the hip joint is presented in Table 6.16. Variation was lowest in phase one (2.5°), increasing to its highest value in phase three (5.9°). Similar trends of increasing variability as the movement progressed were also noted for the knee joint (Table 6.17) and the ankle joint (Table 6.18). Values of variability for total movement for the hip, knee and ankle joint were 3.8°, 4.0°, and 2.1°, respectively.

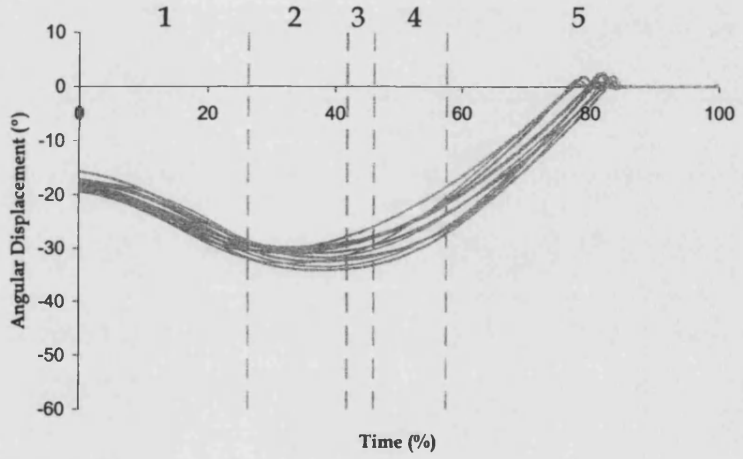

Figure 6.10. Condition nine (centre-point) trials for lumbar joint.

Table 6.15. Variability of condition nine (centre-point) trials for lumbar joint.

	Total	Phase				
	Movement	1	2	3	4	5
Variability (°)	2.2	1.8	1.9	3.0	3.7	2.0

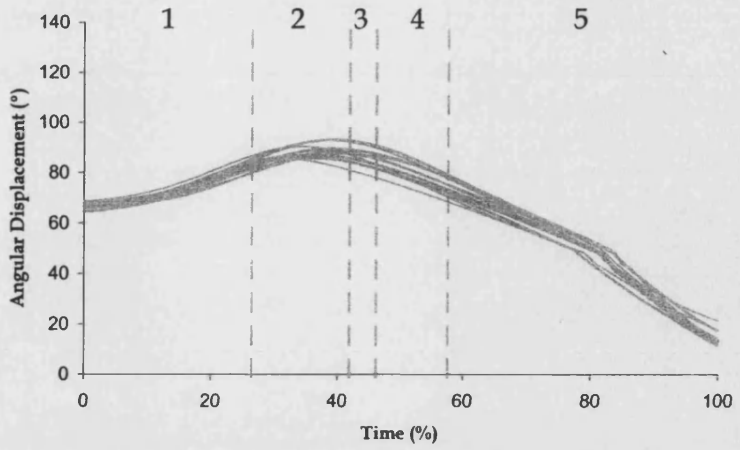

Figure 6.11. Condition nine (centre-point) trials for hip joint.

Table 6.16. Variability of condition nine (centre-point) trials for hip joint.

	Total	Phase				
	Movement	1	2	3	4	5
Variability (°) - centre	3.8	2.5	4.0	5.9	5.4	3.9

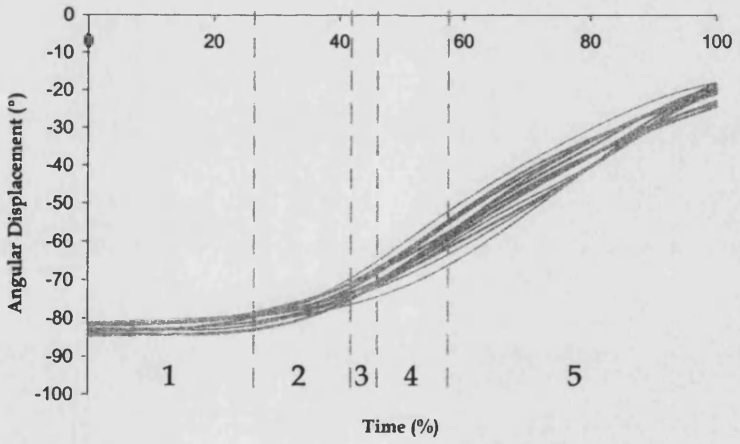

Figure 6.12. Condition nine (centre-point) trials for knee joint.

Table 6.17. Variability of condition nine (centre-point) trials for knee joint.

	Total	Phase				
	Movement	1	2	3	4	5
Variability (°) - centre	4.0	1.9	2.6	4.1	6.2	5.3

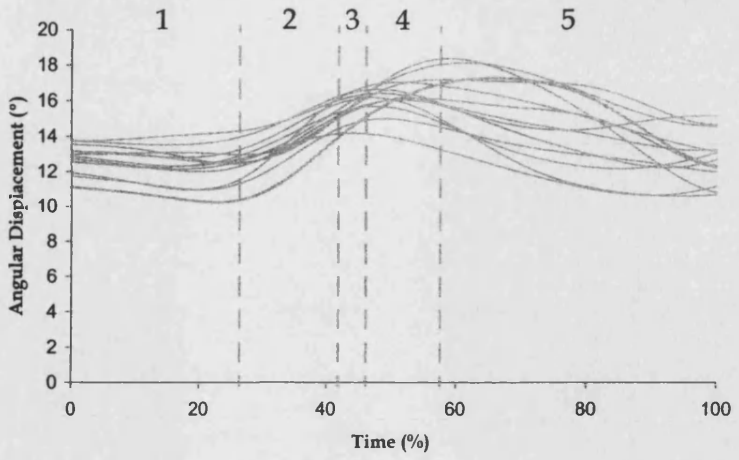

Figure 6.13. Condition nine (centre-point) trials for ankle joint.

Table 6.18. Variability of condition nine (centre-point) trials for ankle joint.

	Total	Phase				
	Movement	1	2	3	4	5
Variability (°) - centre	2.1	1.7	1.6	1.2	2.0	2.7

6.4.2 MANIKIN DYNAMIC JOINT LIMITS

During STS the ankle joint operated very close to its limits of transverse rotation. When the manikin searched for solutions to the imposed constraints, if the ankle joint was near its limit of rotation and the required overall true state (section 2.5.3, *predictive ergonomic human models*) had not been attained, the ankle oscillated back and forth in exploration of a more appropriate solution (Figure 6.14). Because of the influence that ankle joint orientation has on the rest of the body, the oscillations forced the manikin to adopt odd movement patterns to satisfying the imposed constraints (Figure 6.15).

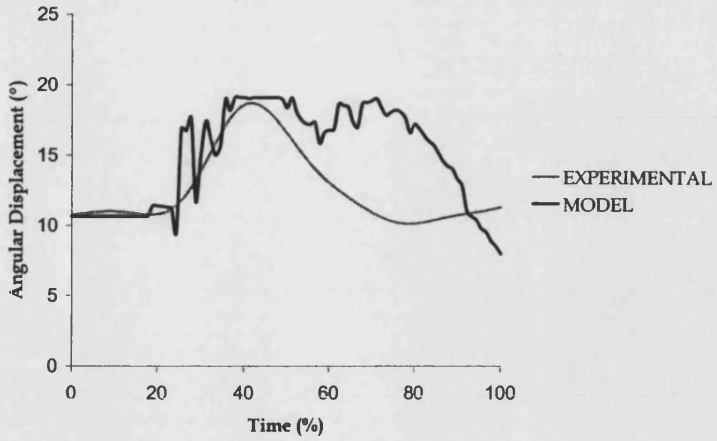

Figure 6.14. Ankle angle experiment (light grey) and model (dark grey) data for condition two (*RD* (1), *ISP* (-1), *SH* (-1)) rise. Note oscillation in model data.

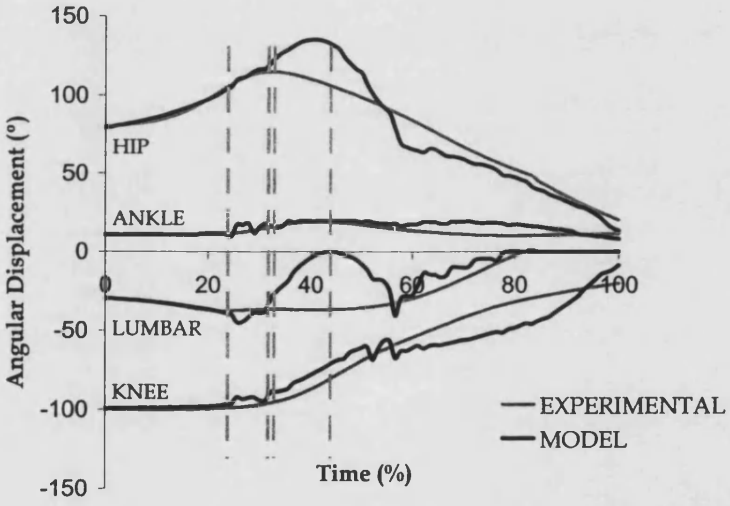

Figure 6.15. Movement patterns created in presence of ankle oscillation.

Consequently, and unlike all other joints, the ankle joint required a certain level of additional control. The control had to be set at the appropriate level to avoid producing movement that was animated. Thus, the following dynamic joint limits were coded:

- No ankle rotation was allowed until SOO.
- If, after SOO, the ankle moved into dorsiflexion, it was not then allowed to plantarflex. This stopped oscillation.
- Maximum ankle dorsiflexion was limited such that it better approximated mean ankle limits of subject A across a range of conditions.

- Ankle motion was reset to allow plantarflexion after VVMAX.
- If, after VVMAX, the ankle moved into plantarflexion, it was not allowed to then dorsiflex. This stopped oscillation.

An example of the affect of this control on the ankle joint can be seen in Figure 6.16. The associated improved movement pattern is presented in Figure 6.18.

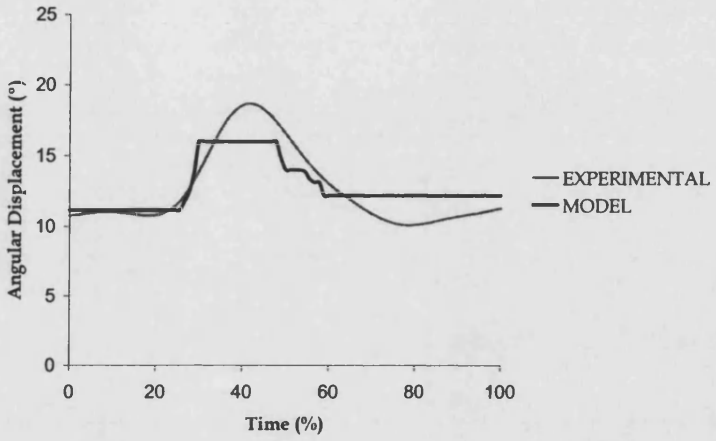

Figure 6.16. Ankle angle experiment (light grey) and model (dark grey) data for condition two (*RD* (1), *ISP* (-1), *SH* (-1)) rise after implementing dynamic joint limits. Note reduced oscillation in model data due to additional control.

6.4.3 VALIDATION OF MANIKIN MODEL AGAINST SUBJECT A

Using the curves evaluated in Sections 6.3.3, combined CM trajectories were created for each of the 11 evaluation trials. These were implemented into the manikin model along with movement constraints (as described in Section 5.3.7) to produce manikin motion. Validation methods were discussed in Section 5.4.2. The results for each validation trial are presented in Figures 6.17-6.27, and Tables 6.19-6.29. Error was assessed over the total duration of movement. For clarity, the particular condition within the experimental region is also presented.

All figures use angle data at the lumbar, hip, knee and ankle joints to assess the model. Additionally, each figure shows a series of dashed vertical lines. These represent the times at which the events were predicted to occur. This was also the time at which

constraint conditions within the SWORDS model changed. The implications of this will be discussed in more depth in the next chapter.

Figure 6.17 represents predicted movement for condition one rise (low *rise duration*, low *initial seated posture*, low *seat height*) in the experimental design region. Hip joint movement of the manikin followed the characteristic flexion and extension trends associated with STS. However, Figures 6.19 and 6.20 show that peak hip flexion was not achieved by the model. Additionally, these figures show rapid changes in hip angle (and similarly at the knee). This occurred at around the time of peak hip flexion as the manikin attempted to solve all movement constraints at this challenging period of rise, and as the influencing constraint sets moved from representing one phase to another (Appendix H).

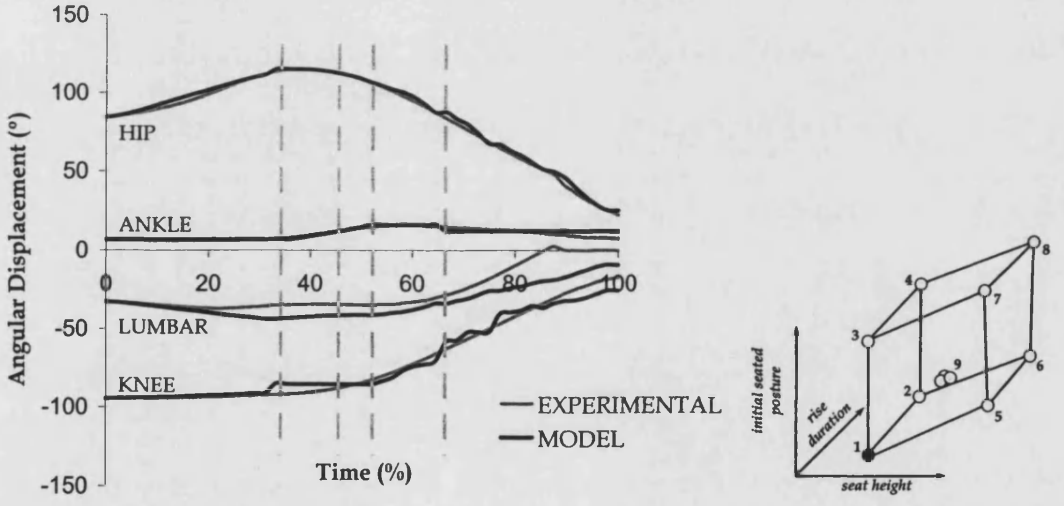

Figure 6.17. Experimental and model data for condition one (*RD* (-1), *ISP* (-1), *SH* (-1)).

Table 6.19. RMSD between experimental and model joint angle data for condition one.

	Hip Angle	Ankle Angle	Lumbar Angle	Knee Angle
RMSD (°)	2.1	1.7	8.7	3.8
RMSD (%)	1.7	9.6	18.3	4.9

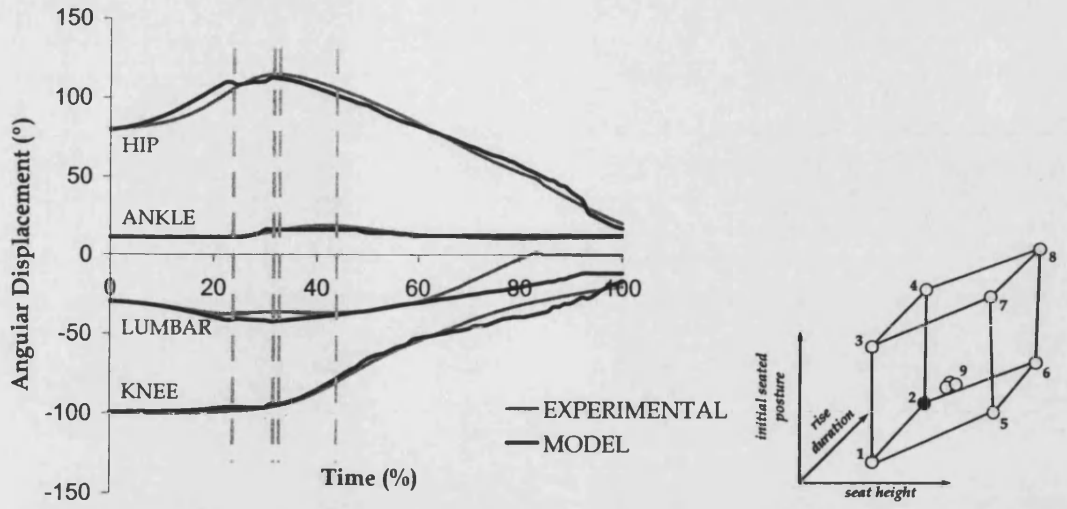

Figure 6.18. Experimental and model data for condition two (*RD* (1), *ISP* (-1), *SH* (-1)).

Table 6.20. RMSD between experimental and model joint angle data for condition two.

	Hip Angle	Ankle Angle	Lumbar Angle	Knee Angle
RMSD (°)	4.1	1.4	8.4	3.5
RMSD (%)	3.2	7.5	16.8	4.3

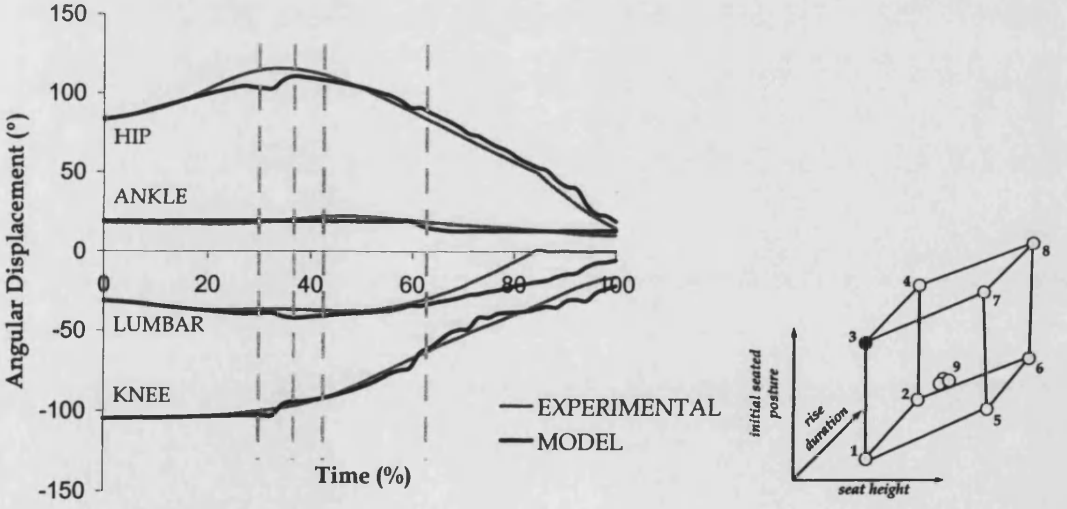

Figure 6.19. Experimental and model data for condition three (*RD*(-1), *ISP*(1), *SH*(-1)).

Table 6.21. RMSD between experimental and model joint angle data for condition three.

	Hip Angle	Ankle Angle	Lumbar Angle	Knee Angle
RMSD (°)	5.0	2.3	7.7	3.6
RMSD (%)	3.7	12.4	16.5	4.1

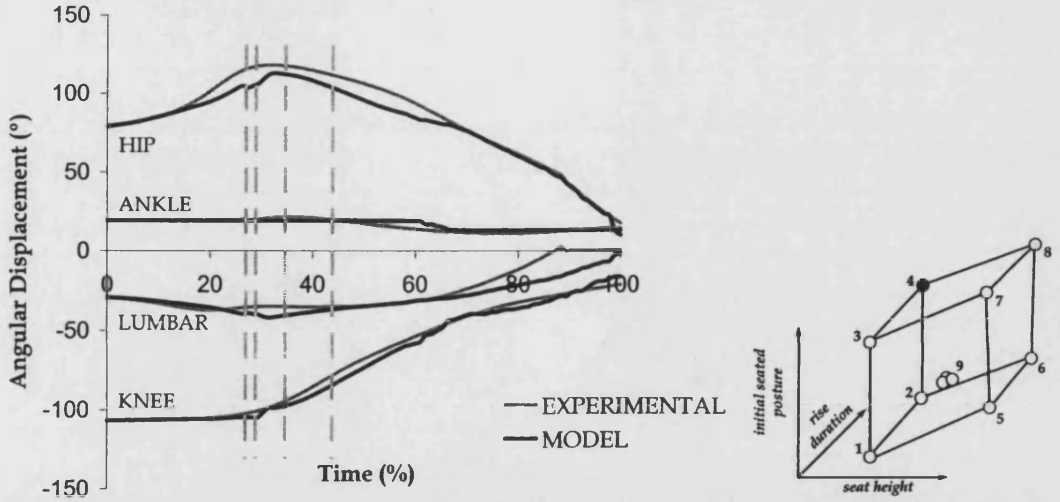

Figure 6.20. Experimental and model data for condition four (*RD*(1), *ISP*(1), *SH*(-1)).

Table 6.22. RMSD between experimental and model joint angle data for condition four.

	Hip Angle	Ankle Angle	Lumbar Angle	Knee Angle
RMSD (°)	6.1	1.9	6.3	3.2
RMSD (%)	4.4	10.8	12.6	3.8

The ankle angle was frequently shown to be the best predictor in terms of absolute RMSD. However, because of the small angular displacement that occurred at the ankle, relative RMSD was large. For example, see Figures 6.21 and 6.22, with the respective data Tables 6.23 and 6.24.

Figures 6.21-6.22 show rise from the high seat height conditions. This tended to reduce the total displacement of the joints making relative RMSD appear larger. Further to this, the high seat height conditions tended to produce a lack of hip extension in the model, particularly in the last 20-40% of the movement.

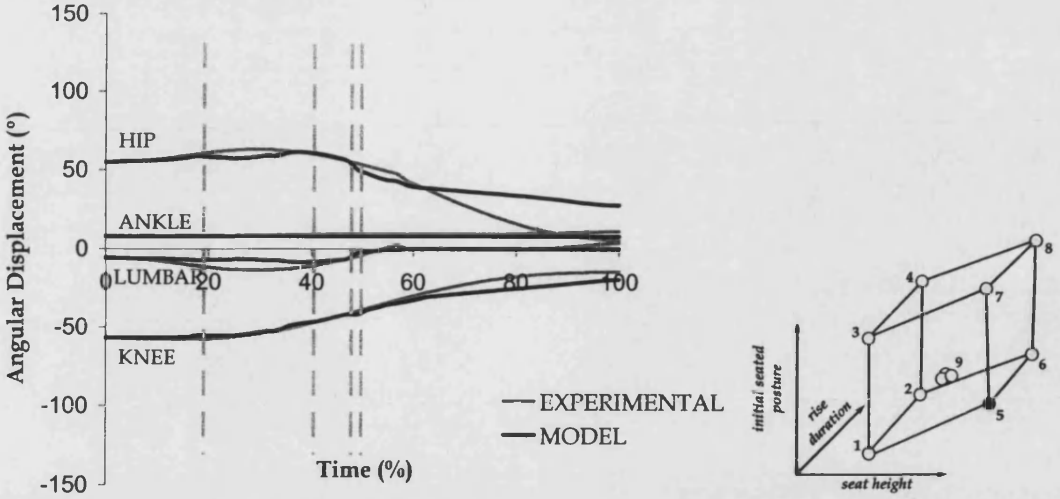

Figure 6.21. Experimental and model data for condition five (*RD*(-1), *ISP*(-1), *SH*(1)).

Table 6.23. RMSD between experimental and model joint angle data for condition five.

	Hip Angle	Ankle Angle	Lumbar Angle	Knee Angle
RMSD (°)	11.0	1.3	3.0	4.1
RMSD (%)	16.5	34.2	9.4	9.4

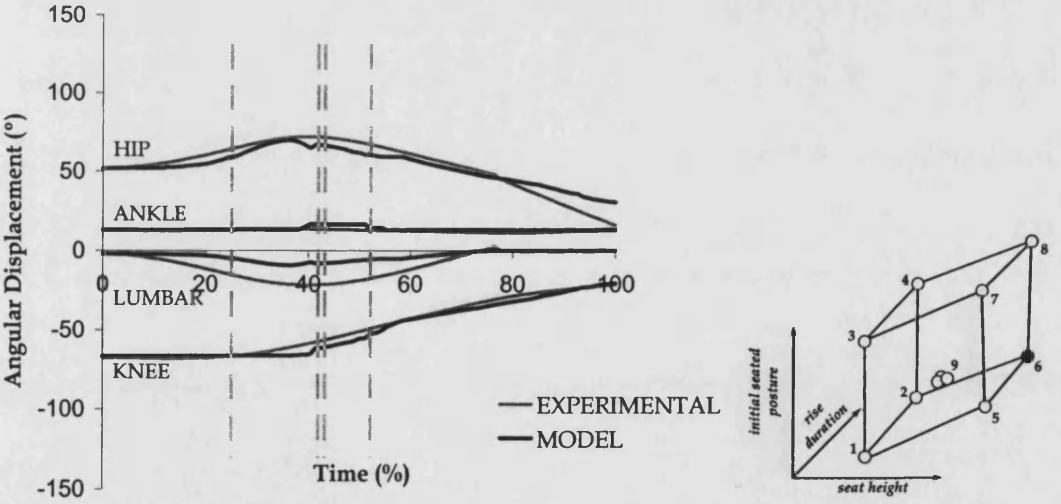

Figure 6.22. Experimental and model data for condition six (*RD*(1), *ISP*(-1), *SH*(1)).

Table 6.24. RMSD between experimental and model joint angle data for condition six.

	Hip Angle	Ankle Angle	Lumbar Angle	Knee Angle
RMSD (°)	5.6	1.4	7.6	2.8
RMSD (%)	7.3	25.6	16.7	6.1

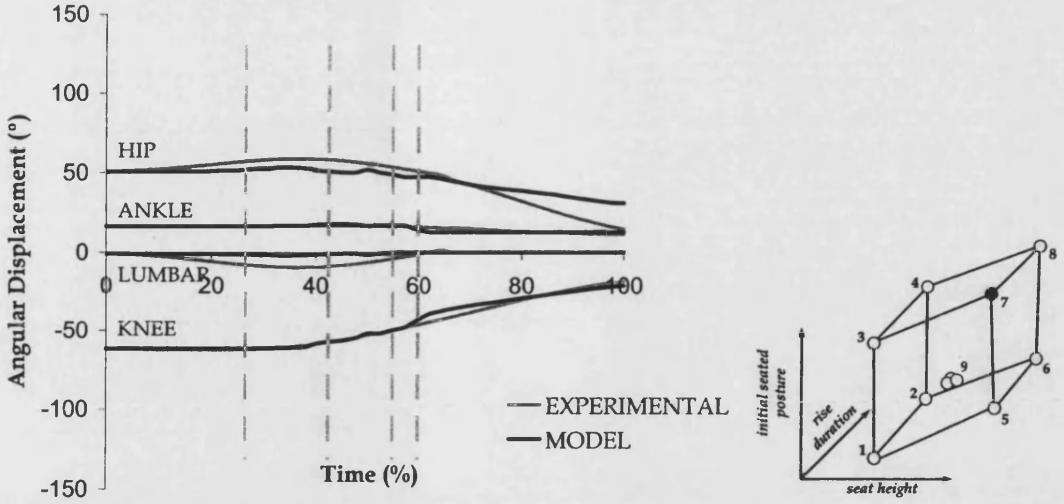

Figure 6.23. Experimental and model data for condition seven (*RD*(-1), *ISP*(1), *SH*(1)).

Table 6.25. RMSD between experimental and model joint angle data for condition seven.

	Hip Angle	Ankle Angle	Lumbar Angle	Knee Angle
RMSD (°)	6.8	1.1	4.1	2.1
RMSD (%)	13.1	19.8	19.4	4.7

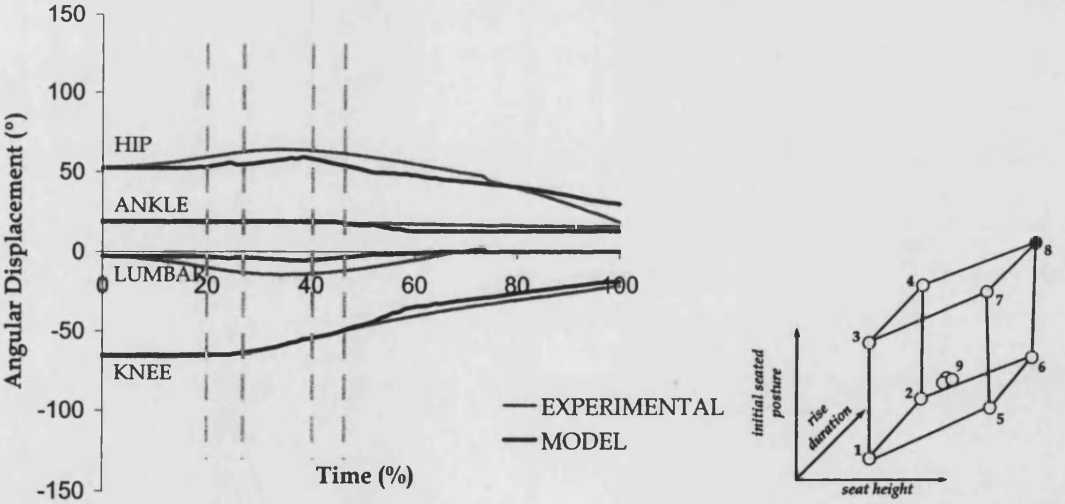

Figure 6.24. Experimental and model data for condition eight (*RD*(1), *ISP*(1), *SH*(1)).

Table 6.26. RMSD between experimental and model joint angle data for condition eight.

	Hip Angle	Ankle Angle	Lumbar Angle	Knee Angle
RMSD (°)	6.0	2.5	5.5	3.1
RMSD (%)	10.5	92.5	17.6	6.9

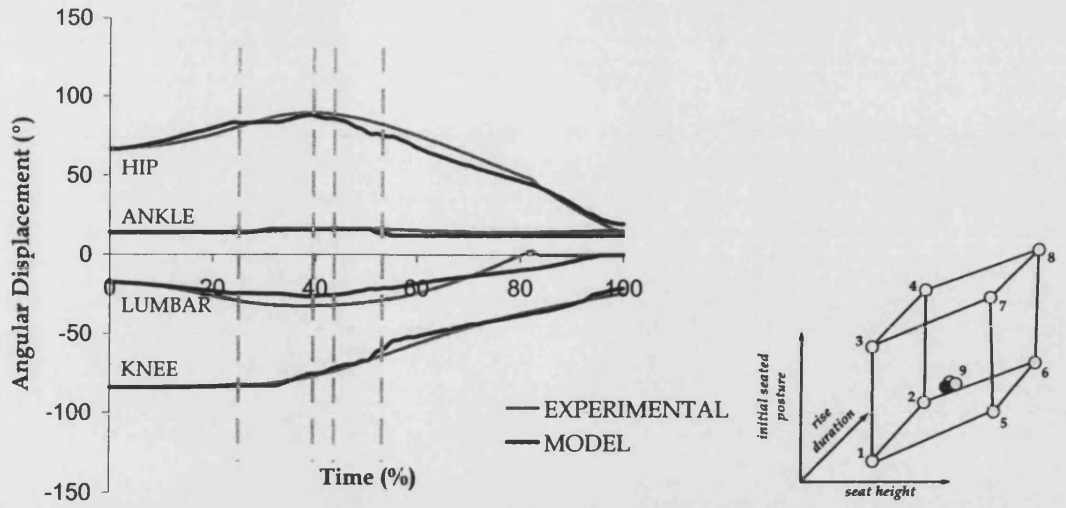

Figure 6.25. Experimental and model data for condition nine (*RD*(0), *ISP*(0), *SH*(0)).

Table 6.27. RMSD between experimental and model joint angle data for condition nine.

	Hip Angle	Ankle Angle	Lumbar Angle	Knee Angle
RMSD (°)	4.5	1.9	5.3	2.2
RMSD (%)	4.6	34.6	10.2	3.7

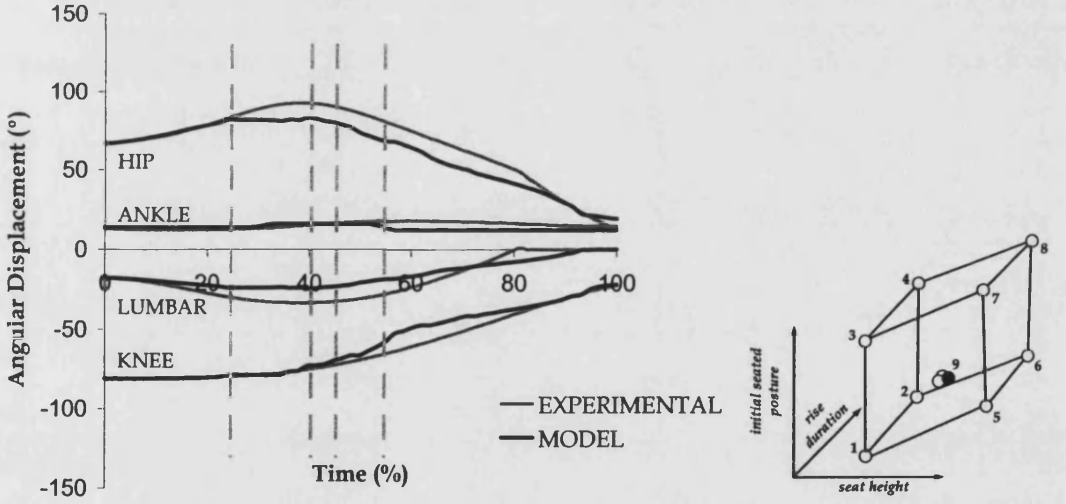

Figure 6.26. Experimental and model data for condition nine, first repetition (*RD*(0), *ISP*(0), *SH*(0)).

Table 6.28. RMSD between experimental and model joint angle data for condition nine, first repetition.

	Hip Angle	Ankle Angle	Lumbar Angle	Knee Angle
RMSD (°)	8.1	3.2	6.2	4.8
RMSD (%)	7.6	32.2	12.1	8.1

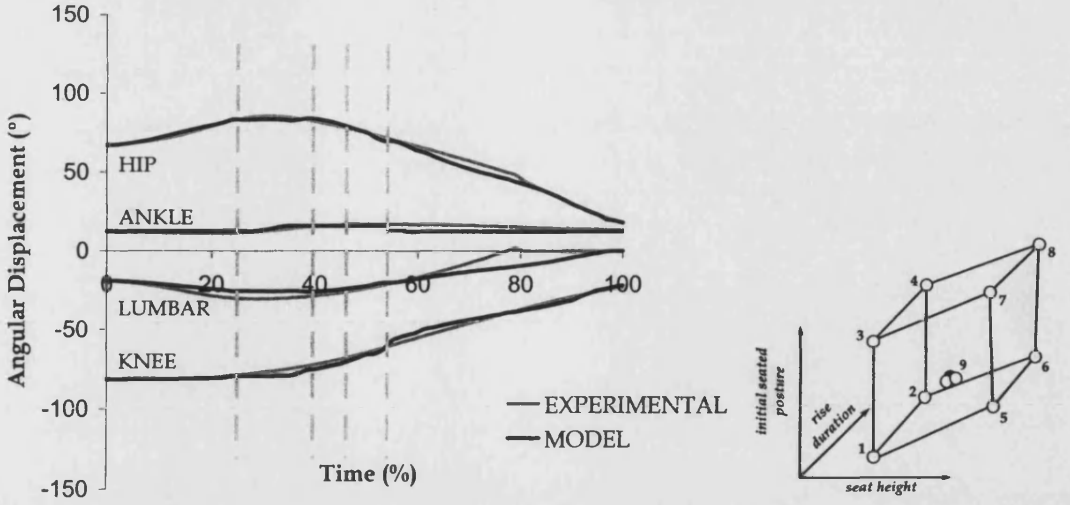

Figure 6.27. Experimental and model data for condition nine, second repetition (*RD*(0), *ISP*(0), *SH*(0)).

Table 6.29. RMSD between experimental and model joint angle data for condition nine, second repetition.

	Hip Angle	Ankle Angle	Lumbar Angle	Knee Angle
RMSD (°)	2.3	2.3	4.5	2.2
RMSD (%)	2.6	21.6	21.6	3.7

As a consequence of the above validations, mean error across all 11 validation conditions and across all evaluated joints (lumbar, hip, knee, and ankle) was 4.2°. This equated to a relative error of 13.5%, although this included the large degree of relative error introduced by the ankle angle. The best and worst cases (in terms of absolute RMSD) of the 11 validation conditions were illustrated by Figures 6.27 and 6.21, respectively.

6.4.4 VALIDATION OF MANIKIN MODEL AGAINST SUBJECTS B AND C

The manikin model was validated against the performances of subjects B and C. For subject B, mean RMSD across the five conditions was 5.7° (relative error was 12.7%). The best and worst of these cases (in terms of absolute RMSD) are presented in Figures 6.28 and 6.29, respectively. For subject C, the mean error across the five conditions was

5.5° (relative error was 13.6%). The best and worst of these cases are presented in Figures 6.30 and 6.31, respectively.

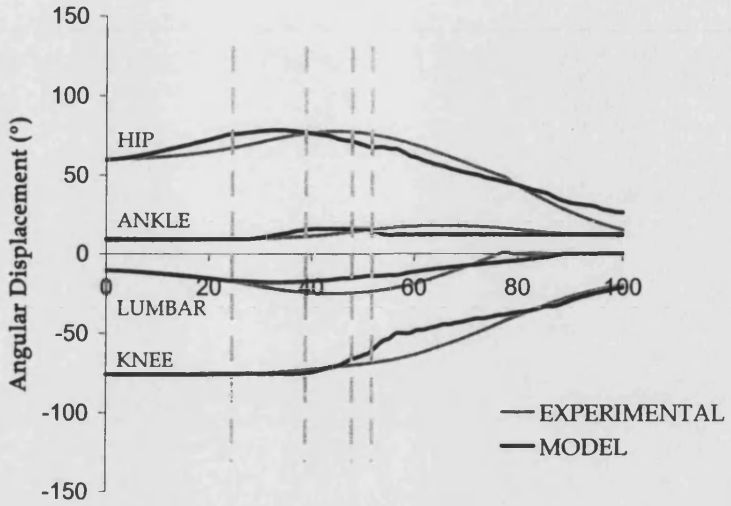

Figure 6.28. Experimental and model data for subject B, approximating centre-point conditions (*RD*(0), *ISP*(0), *SH*(0)), representing trial of minimum error.

Table 6.30. RMSD between experimental and model joint angle data for subject B, representing trial of minimum error.

	Hip Angle	Ankle Angle	Lumbar Angle	Knee Angle
RMS error (°)	6.1	3.0	4.7	6.2
RMS error (%)	7.6	18.4	11.3	10.9

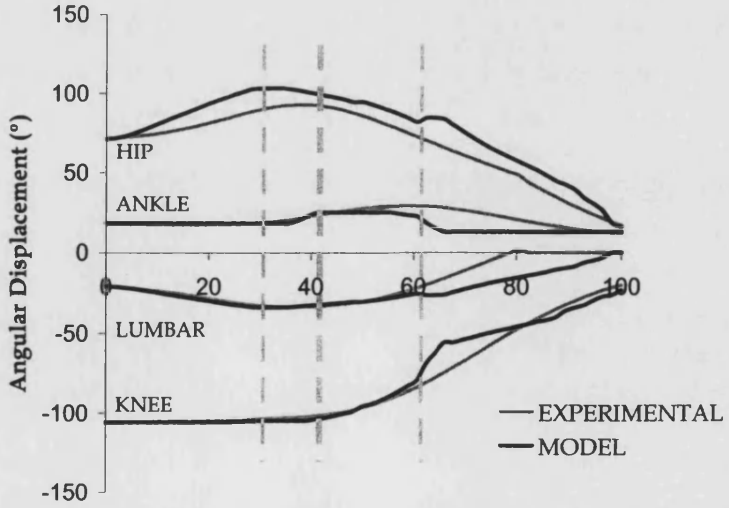

Figure 6.29. Experimental and model data for subject B, approximating condition one (*RD*(-1), *ISP*(-1), *SH*(-1)), representing trial of maximum error.

Table 6.31. RMSD between experimental and model joint angle data for subject B, representing trial of maximum error.

	Hip Angle	Ankle Angle	Lumbar Angle	Knee Angle
RMS error (°)	10.1	5.7	6.9	5.6
RMS error (%)	10.4	19.3	13.9	6.6

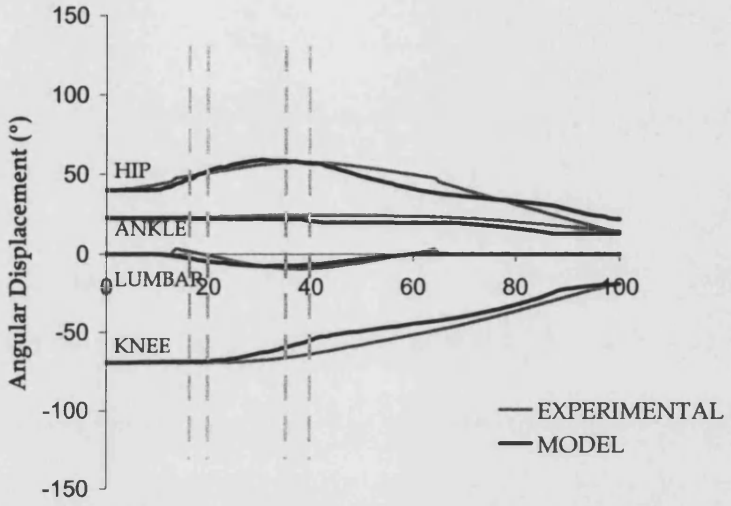

Figure 6.30. Experimental and model data for subject C, approximating condition eight (*RD*(1), *ISP*(1), *SH*(1)), representing trial of minimum error.

Table 6.32. RMSD between experimental and model joint angle data for subject C, representing trial of minimum error.

	Hip Angle	Ankle Angle	Lumbar Angle	Knee Angle
RMS error (°)	4.7	3.2	1.8	5.4
RMS error (%)	7.7	27.2	5.7	10.6

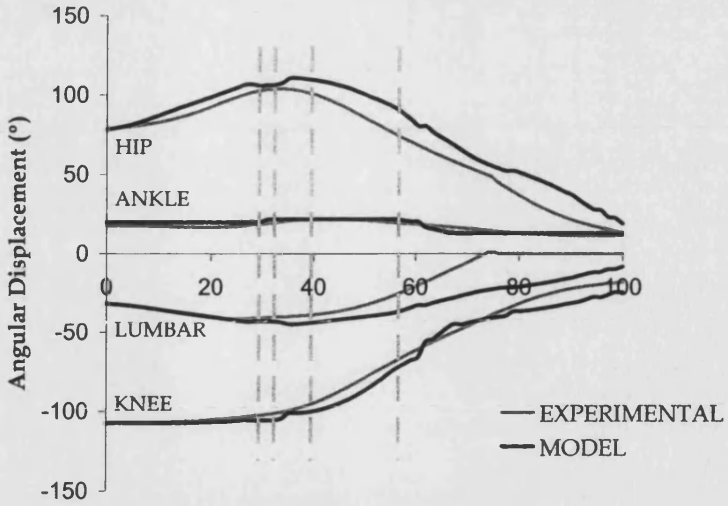

Figure 6.31. Experimental and model data for subject C, approximating condition three (*RD*(-1), *ISP*(1), *SH*(-1)), representing trial of maximum error.

Table 6.33. RMSD between experimental and model joint angle data for subject C, representing trial of maximum error.

	Hip Angle	Ankle Angle	Lumbar Angle	Knee Angle
RMS error (°)	10.4	2.1	11.8	5.1
RMS error (%)	9.0	11.8	22.1	5.7

6.4.5 SECTION SUMMARY

Natural variability in movement patterns was analysed. For the total movement, joint variability ranged between 2.1° and 4.0° for the lumbar, hip, knee, and ankle from centre-point conditions. A developed manikin model showed a mean difference from experimental data of just 4.2°. When the model was evaluated against subjects that were not used to create the regression expressions a successful and comparable difference was found. Table 6.34 summarises all results presented in section 6.4.3 and 6.4.4.

Table 6.34. Summary table of RMSD results for subjects A, B and C.

Subject and condition	Hip Angle	Ankle Angle	Lumbar Angle	Knee Angle
	RMSD (° (%))			
A - condition one	2.1 (1.7)	1.7 (9.6)	8.7 (18.3)	3.8 (4.9)
A - condition two	4.1 (3.2)	1.4 (7.5)	8.4 (16.8)	3.5 (4.3)
A - condition three	5.0 (3.7)	2.3 (12.4)	7.7 (16.5)	3.6 (4.1)
A - condition four	6.1 (4.4)	1.9 (10.8)	6.3 (12.6)	3.2 (3.8)
A - condition five	11.0 (16.5)	1.3 (34.2)	3.0 (9.4)	4.1 (9.4)
A - condition six	5.6 (7.3)	1.4 (25.6)	7.6 (16.7)	2.8 (6.1)
A - condition seven	6.8 (13.1)	1.1 (19.8)	4.1 (19.4)	2.1 (4.7)
A - condition eight	6.0 (10.5)	2.5 (92.5)	5.5 (17.6)	3.1 (6.9)
A - condition nine	4.5 (4.6)	1.9 (34.6)	5.3 (10.2)	2.2 (3.7)
A - condition nine, 1st rep.	8.1 (7.6)	3.2 (32.2)	6.2 (12.1)	4.8 (8.1)
A - condition nine, 2nd rep.	2.3 (2.6)	2.3 (21.6)	4.5 (21.6)	2.2 (3.7)
B – condition nine, minimum error	6.1 (7.6)	3.0 (18.4)	4.7 (11.3)	6.2 (10.9)
B – condition one, maximum error	10.1 (10.4)	5.7 (19.3)	6.9 (13.9)	5.6 (6.6)
C – condition eight, minimum error	4.7 (7.7)	3.2 (27.2)	1.8 (5.7)	5.4 (10.6)
C – condition three, maximum error	10.4 (9.0)	2.1 (11.8)	11.8 (22.1)	5.1 (5.7)

6.5 SUMMARY

The difference between the proposed and the actual experimental regions were noted, from which new high and low levels for factors were formed. Experimental results were presented for 16 responses for each of the nine experimental conditions, and regression equations were fitted. Main and interaction effects were obtained and presented in terms of predictive movement expressions.

The predictive expressions were used to create curve precision points. Fitted curves were assessed before being selected based on minimum RMSD measures across the range of the experimental design region. The selected curves were used to predict CM trajectories that were employed alongside movement constraints in order to simulate STS movement through the SWORDS manikin. This was demonstrated with a sequence of manikin graphics.

The results from the manikin model were validated against a single subject. In particular, it was found that this approach to STS modelling could predict movement at the lumbar, hip, knee, and ankle joints to within 4.2°. The manikin model was then further validated against different subjects where it was found that this approach to human movement modelling was able to predict average joint angle data within 5.7°. This difference should be considered alongside the variability that would be expected to occur in the movement. An estimate for this variation was made and shown to vary between 2.1° and 4.0° for the joints of interest.

CHAPTER 7: DISCUSSION

The following chapter is split into two main areas. The first of these debates the results that arose from the experimental and statistical studies, and how these furthered the understanding of STS. This is followed by a discussion concerning the comprehension obtained from conducting the manikin model tests and how critical movement actions (*events*) could be used for the description of STS.

7.1 UNDERSTANDING SIT-TO-STAND THROUGH EXPERIMENTATION

The discussion of the experimental part of the study is divided into sections covering the consideration of the experimental approach, the experimental and statistical results, and the regression equations.

7.1.1 CONSIDERATION OF EXPERIMENTAL APPROACH

Due to the variation in factor control that inevitably occurs in experimental studies, the actual experimental region differed from the proposed experimental region (Figure 6.3). The differences in terms of each factor are presented below.

Rise duration

Rise duration was anticipated to be hard to set as the occurrence of ONSET and END were not identified until after data collection (Section 4.2.1). However, the low standard deviation values for *rise duration* in each condition (Table 6.1) suggested that the methods employed to control that factor were successful, and that the definitions of ONSET and END were consistent and appropriate. Kotake et al. (1993) suggested that subjects rising at a fast pace could complete the movement in 0.8 s. In the present study, rises from fast conditions (conditions one, three, five, and seven) showed duration's greater than 0.8 s, suggesting that the complete STS movement was unachievable for subject A in this time. In the work by Hirschfeld et al. (1999), reaction forces at the buttocks were seen to increase 90 ms before kinematic analysis detected

CM movement. Thus, it could be that the difference between required and actual rise times was due to this discrepancy between the onset of force application and movement detection via kinematic analysis.

Initial seated posture

In terms of *initial seated posture,* ankle angle in conditions two and six differed greatest from the expected levels (Table 6.1 and Figure 6.1). This was most likely due to subject A sitting a little far forward in the seat, with the feet being brought more underneath the seat. Both of these conditions (two and six) were of longer duration, so it may have been that the subject anticipated the difficulties associated with slow rise by reducing the initial CM-$BS_{HOR\ DISP}$. Stevens et al. (1989) suggested that this would have reduced the demands of rise. Efforts were made (via a backrest) to control subject upper body position while seated. However, combinations of small changes in foot and seated position such as described here would have gone undetected.

When *initial seated posture* was expressed in its true unit of measure (CM-$BS_{HOR\ DISP}$), the experimental region appeared as shown in Figure 6.3. Consequently, the formed regressions should only be applied to factor combinations lying within the new hexahedron-shaped design region. Whilst response points outside this design region could be investigated, these remained untested and the regression expressions may not act in the same manner as the actual responses.

Seat height

Movement of the markers (specifically the hip marker) due to skin displacement produced an artefact in the thigh angle during the experiment. Consequently, the *seat height* factor was shown to have an average 11° offset from proposed levels. Figure 7.1 shows the starting position of a condition one trial. The probable thigh segment line (passing through manually identified hip and knee joint centres) and the thigh segment line created between the hip and knee reflective markers are demonstrated. Kinematic data obtained from the experiment were derived from the co-ordinates acquired from the spatial model based on the position of the reflective markers (Section 4.1.3). Thus,

regression equations and the subsequent manikin model were based on the movement shown by the spatial model created in the digitising software (Peak Motus, Peak Performance Technologies Inc.), and not the movement of the actual subject.

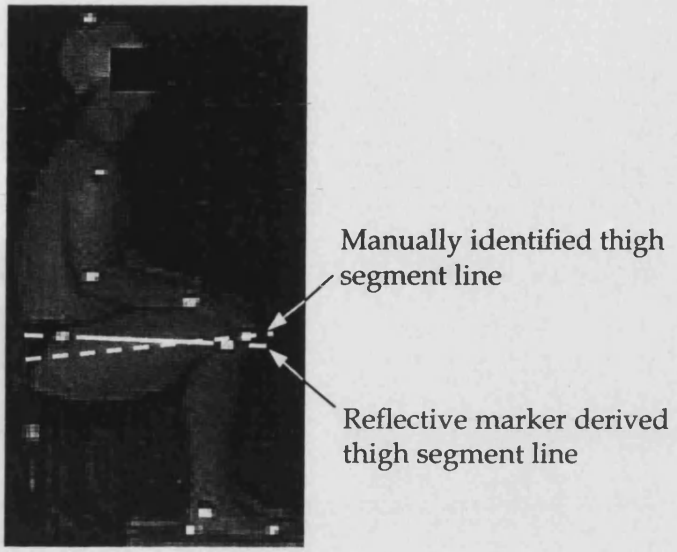

Figure 7.1. Video frame of subject A in a sitting position for a condition one trial (*RD*(-1), *ISP*(-1),*SH*(-1)). Note that the thigh segment line created between hip and knee reflective markers was different to the manually identified thigh segment line.

The reflective marker derived thigh segment appeared at its most offset when the subject was sitting. When standing the line created between the reflective markers was a better approximation to the manually derived thigh segment (Figure 7.2). In the sitting position the 11° offset moved the CM by a maximum of 0.01 m forward and 0.03 m upward. This error reduced throughout the movement as the reflective hip marker became a better approximation of the hip joint centre (i.e. as standing was achieved). These errors impact on how well the regressions and manikin model reflect true human movement. Thus, when the subject was at a particular movement *event* e.g. SOO, the spatial model and regression equations suggested that the CM was as much as 0.01 m further forward and 0.03 m higher than it actually was. Consequently, this had implications on the investigation into the stability strategies used. Effectively, the error in the horizontal dimension could suggest that a greater emphasis was placed on static stability strategies than was actually occurring.

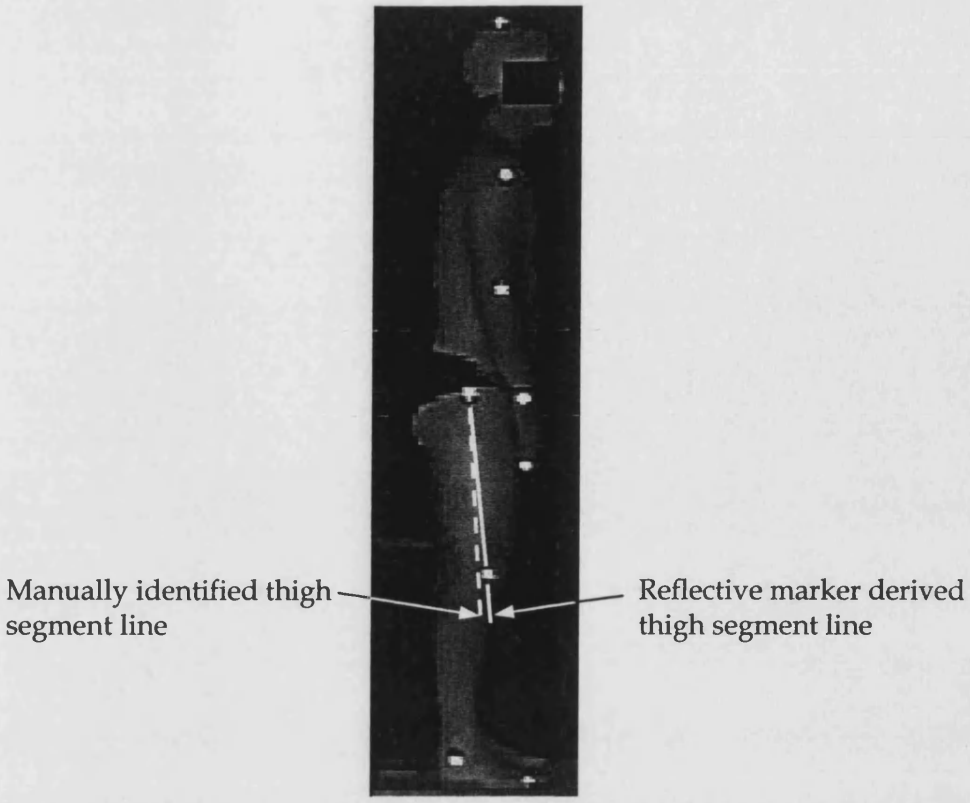

Figure 7.2. Video frame of subject A in a standing position for a condition one trial (*RD*(-1), *ISP*(-1),*SH*(-1)). Note that the thigh segment line created between the hip and knee reflective markers was a closer approximation to the manually identified thigh segment line.

Design orthogonality

An evaluation of the orthogonality of the design region was undertaken within the statistical package (MODDE 5.0, UMETRICS AB). Orthogonality was a measure of the correlation of the model parameters within a response. The statistical package produced a value (termed 'condition number') for each response to indicate the correlation between model parameters. This was a measure of the ratio between the largest and smallest singular values of the X matrix of factor levels. The statistical package proposed that ratios < 3 showed that the model parameters were un-correlated, and > 6 showed that the model parameters were correlated. The range of condition number values for the 16 responses demonstrated throughout Chapter 6 was 1.2 to 3.4 (see also Appendix G). Thus, it was suggested that despite the modification of the experimental design region, the parameters of the model i.e. the effects as demonstrated in Table 6.9 and 6.10, were not correlated.

7.1.2 SPATIOTEMPORAL CHARACTERISTICS OF SIT-TO-STAND

The following discussion regards the results obtained from the experimental and statistical studies, as presented in Sections 6.1 and 6.2. Digitised data and regression obtained effects were considered with findings from previous studies, and with reference to the originally proposed movement hypotheses (see Section 4.4).

Mass centre velocity at movement onset

Horizontal component of CM velocity at ONSET was higher than the vertical component in each condition (Table 6.3). This was expected from the predominantly forward trunk flexion occurring at that time. Additionally, fast rise movements showed higher values than slow movements, as would be expected from the implemented KE definition for ONSET. Rise from low *seat height* conditions (conditions one to four) tended to show positive $ONSET_{VER\ VEL}$ values (Table 6.3), perhaps as a strategy to overcome the more challenging conditions of rise from the lower seat. This was in agreement with the study by Schenkman et al. (1996) that found initial trunk flexion velocity increased with a reduction in chair height.

Time of seat-off onset (SOO_{TIME})

For the response SOO_{TIME}, no significant effects were found for *rise duration* or *initial seated posture* (Table 6.9). Khemlani (1999) reported that a change of foot position had no influence on the onset time of the muscles associated with knee extension (an approximation to the onset of seat-off). However, Vander-Linden et al. (1994) found the opposite with normalised time of seat-off occurring earlier as the feet were brought more under the seat. Table 6.9 showed a significant effect for *seat height* implying that as *seat height* increased SOO_{TIME} occurred earlier. An increase in *seat height* reduced the physical demands of rise (Burdett et al., 1985; Alexander et al., 1996; Schenkman et al., 1996). This reduction in demand could have been exploited by allowing the seat-off phase to occur earlier in the cycle. Within the experimental set-up, an increase in *seat height* decreased $CM\text{-}BS_{HOR\ DISP}$ implying that CM had less far to move forward to achieve a position where seat-off could occur. However, Section 7.1.1 demonstrated

that the design for each response was orthogonal. Thus, the *seat height* effect was considered independent of *initial seated posture*, and so the experimental set-up was not viewed as a reason for the observed effect. With all factors set at their low levels (i.e. *RD* (-1), *ISP* (-1), *SH* (-1)) the regression model would predict SOO_{TIME} to occur at 28.9% of duration. Conversely, with all factors set at their high levels (*RD* (1), *ISP* (1), *SH* (1)) the regression model would predict SOO_{TIME} to occur at 21.3% of duration. This difference is in part attributable to the three-factor interaction effect that was the second largest in the response (-2.3%). These factor settings approximate conditions one and eight, respectively. The associated experimental data can be seen in Table 6.3.

No movement hypotheses were presented for SOO_{TIME}. Rather, the duration between SOO and BALANCE was considered for each factor. These were described in Section 4.4 and summarised in the table below, where the effect on duration (between SOO and BALANCE) was shown as a factor changed from a particular level to another. Duration was proposed to increase as *seat height* increased, and as *rise duration* and *initial seated posture* decreased.

Table 7.1. Summary of hypotheses for duration between SOO and BALANCE.

Factor	Change	Duration
rise duration	decrease	increase
initial seated posture	decrease	increase
seat height	increase	increase

Note: An example of a decrease in a factor level would be for *rise duration* to change from a high to a low level.

The regression models (Equations 6.5 and 6.7) were used to predict the times of both events for a series of conditions in order to evaluate the hypotheses (Table 7.2). The factor settings demonstrated in Table 7.2 considered a change in just one factor e.g. *rise duration* away from central level conditions. Thus, when *rise duration* was set to its high level (1), *initial seated posture* and *seat height* remained at the centre level (0). Each hypothesis was confirmed.

Table 7.2. Predicted SOO and BALANCE *event* times compared against movement hypotheses.

Factor	level	SOO_{TIME} (%)	$BALANCE_{TIME}$ (%)	Duration (%)	Confirmation of hypothesis
• *rise duration*	low	25.2	43.5	18.3	✓
	high	25.0	34.9	9.9	
• *initial seated posture*	low	24.6	45.0	20.4	✓
	high	25.6	33.4	7.8	
• *seat height*	low	29.0	34.4	5.4	✓
	high	21.2	44.0	22.8	

Note: Results were obtained by changing one factor between a low and a high level, whilst keeping the other two factors at their central levels. 'Duration' was a measure of the percentage of total rise duration between SOO and BALANCE.

Mass centre horizontal displacement at seat-off onset ($SOO_{HOR\ DISP}$)

Rise duration did not affect CM horizontal position at SOO ($SOO_{HOR\ DISP}$) (Table 6.9). This was of particular interest because of the relationship between faster movements and increased momentum generated in the upper body. Some authors have suggested that increased momentum in the upper body can allow seat-off to occur under conditions where a greater emphasis was placed on dynamic stability strategies (Schenkman et al., 1990). The result from the present study suggested that this was not the case. Rather, it appeared that whilst dynamic stability strategies were used in STS, these were implemented to overcome postural demands or body inefficiencies, and not as a consequence of faster movements. This was in support of proposals by Pai and Rogers (1990), who suggested that the tight regulation in CM horizontal momentum was a stabilising factor for controlling balance in STS, as an increase in speed could represent a progressively greater potential disturbance to balance control.

A main effect for *initial seated posture* showed that the CM would be 0.03 m closer to the BS (Table 6.9) due to an increase from the centre to the high level in *initial seated posture.* This was comparable to the change in $CM\text{-}BS_{HOR\ DISP}$ due to a change in ankle angle from 13° to 18° (Table 6.1). Thus, SOO occurred when the body had rotated forward a

certain amount and not when the CM was in some position relative to the BS. Kralj et al. (1990) suggested that in rotation the upper body was accelerated up to a peak velocity such that generated momentum could be used to aid seat-off. The main effect for *initial seated posture* also suggested that seat-off onset was dependant on generated upper body momentum.

A high *seat height* affected CM-$BS_{HOR\ DISP}$ at SOO by -0.03 m (Table 6.9), thus rise occurred under conditions where a reduced emphasis was placed on static stability strategies. Schenkman et al. (1996) demonstrated that as seat height increased, the challenge of rise reduced which could allow the change in stability strategy as shown by the main *seat height* effect.

The effects in the SOO_{TIME} response were of interest because of the nature of the stability strategies used in relation to the demands of varying rise conditions. It was found that as the demands of rise increased due to *initial seated posture* a greater emphasis was placed on dynamic stability strategies. However, the opposite was true of *seat height* where reduced demands allowed greater emphasis to be placed on dynamic stability strategies.

Rise hypotheses (Section 4.4) predicted $SOO_{HOR\ DISP}$ to increase due to a decrease in *rise duration* and *initial seated posture*, and an increase in *seat height*. The *rise duration* hypothesis was not valid as explained in the first paragraph of this sub-section. However, the hypotheses for *initial seated posture* and *seat height* were both supported by the main effects of these factors in $SOO_{HOR\ DISP}$.

Time of mass centre reaching final base of support ($BALANCE_{TIME}$)

$BALANCE_{TIME}$ was shown to occur earlier in the movement due to an increase in *rise duration* (Table 6.9). This trend was visible in the experimental data (Table 6.4). The event occurred earlier in the normalised cycle because the majority of the increase in duration was achieved in the later vertical part of rise (Pai and Rogers, 1990), and because the event was presented in normalised time. Thus, the associated movement hypothesis was valid.

In this study a faster movement increased the normalised duration between SOO and BALANCE (Table 7.2). Because $BALANCE_{TIME}$ occurred later in the seat-off phase, this could indicate the greater emphasis placed on dynamic stability strategies over the seat-off phase in faster movements. However, the absolute values between SOO and BALANCE (Table 6.7) remained approximately similar due to changes in *rise duration* i.e. between condition one and two, three and four, and so on. Thus, an increase in *rise duration* does not permit a greater emphasis to be placed on dynamic stability strategies, supporting similar findings for $SOO_{HOR\ DISP}$.

A large effect was seen for *initial seated posture* in $BALANCE_{TIME}$ with a difference of -5.8% between centre and high foot positions (Table 6.9). As CM did not have to move so far forward, BALANCE was achieved earlier in the cycle. This was anticipated in the *initial seated posture* movement hypotheses, and was reflected in the absolute event times presented in Table 6.7 (compare conditions one to three, two to four, and so on).

A 4.8% effect for *seat height* was found for $BALANCE_{TIME}$. If only the factor *seat height* were reduced, the CM would have to cover a greater vertical displacement in the same total duration. To allow this to happen, adjustments were made to the proportion of time spent travelling horizontally and vertically. This was reflected in $BALANCE_{TIME}$, which approximated the time of transition between the two translations. The main effects confirmed the associated hypotheses shown in Section 4.4, which suggested that $BALANCE_{TIME}$ would occur later as rise duration decreased, as initial foot-forward position increased, and as chair height increased.

The regressed factor variables showed a -1.7% three-factor interaction effect on $BALANCE_{TIME}$ when all three factors were at the high level. Whilst this was a small value in comparison to the three main effects, it was important to include the interaction when describing the response. If the interactions were not included the portion of the response they describe would have been taken up by the main effects. This would reduce the quality of the model (as assessed by the statistical methods discussed in Section 5.2.2) and increase the error in the prediction of $BALANCE_{TIME}$.

Mass centre horizontal velocity when mass centre reaches final base of support (BALANCE$_{HOR\ VEL}$)

Schenkman *et al.* (1990) suggested that rise movements characterised by static stability strategies would have zero CM velocity around the time of BALANCE. The present study showed CM horizontal velocity in centre-point conditions to be 0.35 $m \cdot s^{-1}$. Significant main effects were found for *initial seated posture* (0.04 $m \cdot s^{-1}$) and *seat height* (-0.09 $m \cdot s^{-1}$). Thus, as seat height decreased there was an increase in upper body momentum which could have aided rise during the seat-off phase. Conversely, Munro *et al.* (1998) found that seat height did not effect level or time of peak CM horizontal velocity. However, the subject groups used within the study were elderly and suffering from arthritis. Thus, it may have been that these subjects implemented less variant strategies so as not to disturb and increase stability demands.

Time of seat-off completion (SOC$_{TIME}$)

The response SOC$_{TIME}$ (transformed in Table 6.10) contained all seven effects, the strongest of which was the two-factor interaction effect *rise duration & seat height*, and the three-factor interaction. The greatest difference in SOC$_{TIME}$ in the experimental data occurred between condition two (30.6%) (*RD* (1), *ISP* (-1), *SH* (-1)) and condition seven (55.3%) (*RD* (-1), *ISP* (1), *SH* (1)) (Table 6.5). The regression attributed a large portion of this difference in the response to the interaction effects.

Movement hypotheses were not proposed for SOC$_{TIME}$, but rather the duration between BALANCE and SOC. Table 7.3 summarises the hypotheses regarding this duration.

Table 7.3. Summary of hypotheses for duration between BALANCE and SOC.

Factor	Change	Duration
rise duration	increase	increase
initial seated posture	increase	increase
seat height	increase	increase

Note: An example of an increase in a factor level would be for *rise duration* to change from a low to a high level.

The regression models (Equations 6.7 and 6.9) were used to predict $BALANCE_{TIME}$ and SOC_{TIME} for a series of conditions (Table 7.4) in order to evaluate the hypotheses. Factors were set at the same levels as those described and presented in Table 7.2. Interestingly, the times presented in Table 7.4 show rise conditions where SOC occurred before BALANCE, i.e. a full loss of seat contact had occurred before a statically stable posture was achieved. Similar experimental results can be seen in Tables 6.4 and 6.5.

Table 7.4. Predicted BALANCE and SOC *event* times compared against movement hypotheses.

Factor	level	$BALANCE_{TIME}$ (%)	SOC_{TIME} (%)	Duration (%)	Confirmation of hypothesis
•*rise*	low	43.5	42.2	-1.3	✓
duration	high	34.9	38.7	3.8	
•*initial*	low	45.0	39.9	-5.1	✓
seated	high	33.4	40.9	7.5	
posture					
•*seat*	low	34.4	38.9	4.5	✓
height	high	44.0	42.0	-3.0	

Note: Results were obtained by changing one factor between a low and a high level, whilst keeping the other two factors at their central levels. 'Duration' was a measure of the percentage of total rise duration between BALANCE and SOC.

Mass centre horizontal displacement at seat-off completion ($SOC_{HOR\ DISP}$)

Several studies (Carr, 1992; Schultz et al., 1992; Hirschfeld et al., 1999) demonstrated the CM as being above or in front of the heel marker at full seat-off. This was true for most experimental conditions (Table 6.5). However, three conditions (one, five, and nine) showed negative values for $SOC_{HOR\ DISP}$. In condition one, postural demands required the use of a more dynamic stability strategy. Unlike $SOO_{HOR\ DISP}$, *rise duration* did have an effect on $SOC_{HOR\ DISP}$ (Table 6.10), perhaps because it occurred later in the cycle. Two studies (Kotake et al., 1993; Papa and Cappozzo, 1999) suggested that in slow rise the torso inclined to a greater extent. This finding was supported by the main effect for *rise duration*. Thus, faster paced rise allowed the CM to be in a less statically

stable position. In condition five, the higher chair also allowed the use of more dynamic strategies. Similarly, Munro et al. (1998) found decreased trunk flexion from higher chairs. However, Alexander et al. (2001) noted that increasing the chair height generally decreased CM horizontal momentum, which may have suggested a greater emphasis was placed on static stability strategies.

The hypothesis for $SOC_{HOR\ DISP}$ proposed that CM-$BS_{HOR\ DISP}$ increased due to an increase in *rise duration, initial seated posture,* and decreased due to an increase in *seat height.* These were confirmed in the main effects found in the response (Table 6.10), which showed the use of similar stability strategies as commented on for $SOO_{HOR\ DISP}$. There were no interaction effects.

Time of mass centre maximum vertical velocity ($VVMAX_{TIME}$)

The predicted time of CM maximum vertical velocity was comparable to other published studies (Pai and Rogers, 1990; Papa and Cappozzo, 1999, 2000). Pai and Rogers (1990) found $VVMAX_{TIME}$ occurred later in the cycle due to an increase in rise duration (44% when rising in 1.22 s, 52% when rising in 1.55 s). This study found the opposite to occur in the response, where the centre-point value for $VVMAX_{TIME}$ was 53.1%, decreasing to 48.7% for slow paced rise (Table 6.10). However, the results of the current study did support findings by other authors. Papa and Cappozzo (1999, 2000) found whole body maximum linear velocity to decrease in normalised time due to an increase in movement duration (62% when rising in 1.01 s, 59% when rising in 1.56 s). Trends in normalised temporal responses were closely related to definitions of the start and the end of movement. This could account for the conflict between results between this and previous studies.

Another explanation for the difference between the results of the studies was that the two-factor interaction between *rise duration & seat height* yielded the largest effect in the response (4.9%, Table 6.10). In the Pai and Rogers (1990) study interaction effects were not considered and it was difficult to judge their corresponding *seat height* factor level. Therefore, it could be that the large two-factor interaction (*rise duration & seat height*) accounted in part for the reduction seen in $VVMAX_{TIME}$ in faster movements in that study.

Movement theory hypothesised that $VVMAX_{TIME}$ would occur later due to a decrease in *rise duration* (Section 4.4), and this was confirmed. No hypotheses were presented for *initial seated posture,* as theory or literature did not point strongly towards any particular trend. A small and non-significant main effect for this factor was found in the response.

A change in *seat height* was hypothesised to have little influence in $VVMAX_{TIME}$. However, an increase in the factor showed $VVMAX_{TIME}$ to occur earlier (Table 6.10). The reasons for this were not obvious. It could be that the ability to vary vertical movements along with the decreased requirement for CM vertical displacement from the high chair allowed VVMAX to occur earlier. Such a strategy could be incorporated where possible to cause less of a potential disturbance to stability in standing. From a lower chair the potential disturbance may have been sacrificed in order to complete rise in the required duration. An increase in seat height from the centre level to the high level would change the response by -2.4%.

These findings serve well to highlight the increased variability that occurs throughout the movement. Pai and Rogers (1990) illustrated the increased variability in vertical movements over horizontal movements. This appeared to be used as a strategy in rise. Interestingly, the mean standard deviations across all conditions for the absolute event times (Table 6.7) increased throughout the movement (0.03, 0.04, 0.04, 0.08, 0.08) also suggesting that movement variability increased throughout STS.

Mass centre maximum vertical velocity ($VVMAX_{VER\ VEL}$)

$VVMAX_{VER\ VEL}$ showed generally higher values from the lower seat height levels (condition one, two, three, and four) than from higher seat levels, reflecting the need to move a greater distance in the same overall time (Table 6.5). Pai and Rogers (1990) reported on changes to CM vertical linear momentum due to the effect of rise speed where an increase from 44 $kg{\cdot}m{\cdot}s^{-1}$ (when rising in a time of 1.55 s) to 64 $kg{\cdot}m{\cdot}s^{-1}$ (when rising in a time of 1.22 s) was recorded. The mean mass of the subjects was 66.1 kg. Thus, these results were equivalent to mean CM vertical velocities of 0.67 $m{\cdot}s^{-1}$ and 0.97 $m{\cdot}s^{-1}$, respectively. Papa and Cappozzo (1999) presented results for whole body maximal linear velocity. The study showed an increase from 0.60 $m{\cdot}s^{-1}$ (when rising at

1.54 s) to 0.98 $m \cdot s^{-1}$ (when rising at 0.96 s), although this value would have included a small component of horizontal velocity. Thus, these sets of results (Pai and Rogers, 1990; Papa and Cappozzo, 1999) showed a comparable increase due to a change in rise speed. In the present study, regression results suggested CM vertical velocity would be 0.36 $m \cdot s^{-1}$ for centre-point rise increasing to 0.53 $m \cdot s^{-1}$ for fast rise, if other factors were at their centre levels (Table 6.10). Clearly, there was a discrepancy between previously published results and those presented in this study. However, any differences would be closely related to the definitions of start and end. Additionally, the limitation of not knowing the other factor levels (in particular *seat height*) in the other studies makes comparison difficult.

The seat height was seen to play an important role in $VVMAX_{VER\ VEL}$ and in the context of this experiment it yielded a stronger effect than *rise duration* itself (Table 6.10). As seat height reduced the CM was required to move vertically further in the same overall time (due to the *rise duration* constraints). Thus, a higher CM velocity was required to achieve rise successfully. Seat height was 0.43 m in the Pai and Rogers (1990) study and 80% of knee height in the Papa and Cappozzo (1999) study. Both of these were significantly lower than the centre level seat height and more akin to the low level seat height used in this study. When rising from a low seat, $VVMAX_{VER\ VEL}$ was predicted to be 0.60 $m \cdot s^{-1}$ in centre (0) *rise duration* conditions and 0.87 $m \cdot s^{-1}$ in low (-1) *rise duration* conditions. Thus, *seat height* levels potentially made a large contribution to the higher values of CM vertical velocity recorded in the previous studies.

The main effects for *rise duration* and *seat height* followed the hypotheses for the response. It was thought that *initial seated posture* would have no effect. However, whilst small in comparison to other effects, a significant effect was found. As the feet were moved to a more anterior position, $VVMAX_{VER\ VEL}$ increased. It could be that due to the greater trunk flexion associated with this foot position, the CM was required travel further vertically in the same overall duration which may have been satisfied by achieving a higher CM vertical velocity.

Mass centre horizontal displacement at movement end ($END_{HOR\ DISP}$)

Rising from centre-point conditions resulted in the CM finishing 0.09 m anterior to the rear of the BS (Table 6.10). This was comparable to the results of other authors (Yoshida et al., 1983; Pai and Rogers, 1990). Decreasing *rise duration* to its low level moved the CM backward by 0.02 m. Several authors have suggested that a faster movement is more synergistic i.e. the horizontal and vertical components of CM displacement are less distinct (Pai and Rogers, 1990; Papa and Cappozzo, 1999). This was perhaps a reflection of the decreased trunk flexion used in faster movements as suggested by Papa and Cappozzo (1999). Thus, a reduced dominance of CM horizontal displacement at END could account for the effect.

Increasing the *initial seated posture* level moved the CM backward by 0.01 m at END. In this condition the subject started with the feet more underneath them. Thus, less trunk flexion was required at seat-off producing a less forward position at END. An non-significant *seat height* effect was included to support the two-factor interaction *initial seated posture & seat height.*

Mass centre vertical displacement at movement end ($END_{VER\ DISP}$)

$END_{VER\ DISP}$ established whether the CM finished at the same height between trials. *Seat height* was by far the strongest effect in the response and there was a direct correlation between the increased requirement for the CM to rise vertically and the reduction of the initial CM vertical position due to changing *seat height.* Thus, $END_{VER\ DISP}$ was constant (i.e. CM finished at the same height despite rise condition) and this response was ignored from all further modelling.

7.1.3 MOVEMENT SUBDIVISION

Section 2.3 reviewed studies that previously attempted to sub-divide the movement of STS. The majority of the studies failed to recognise that normalised movement phase times could vary due to changes in rise condition, and hence were inappropriately proposed as generalised rise schemes. Figure 7.3 presents the subdivisions used by

previous authors (Figure 2.1) but with the addition of the experimental findings of the current study. The variable nature of movement subdivisions were noted. Further, it was found that in some circumstances movement *events* occurred in changeable order. This was particularly the case with the *events* BALANCE and SOC. The influence of this on the stability strategies is discussed further in the next section.

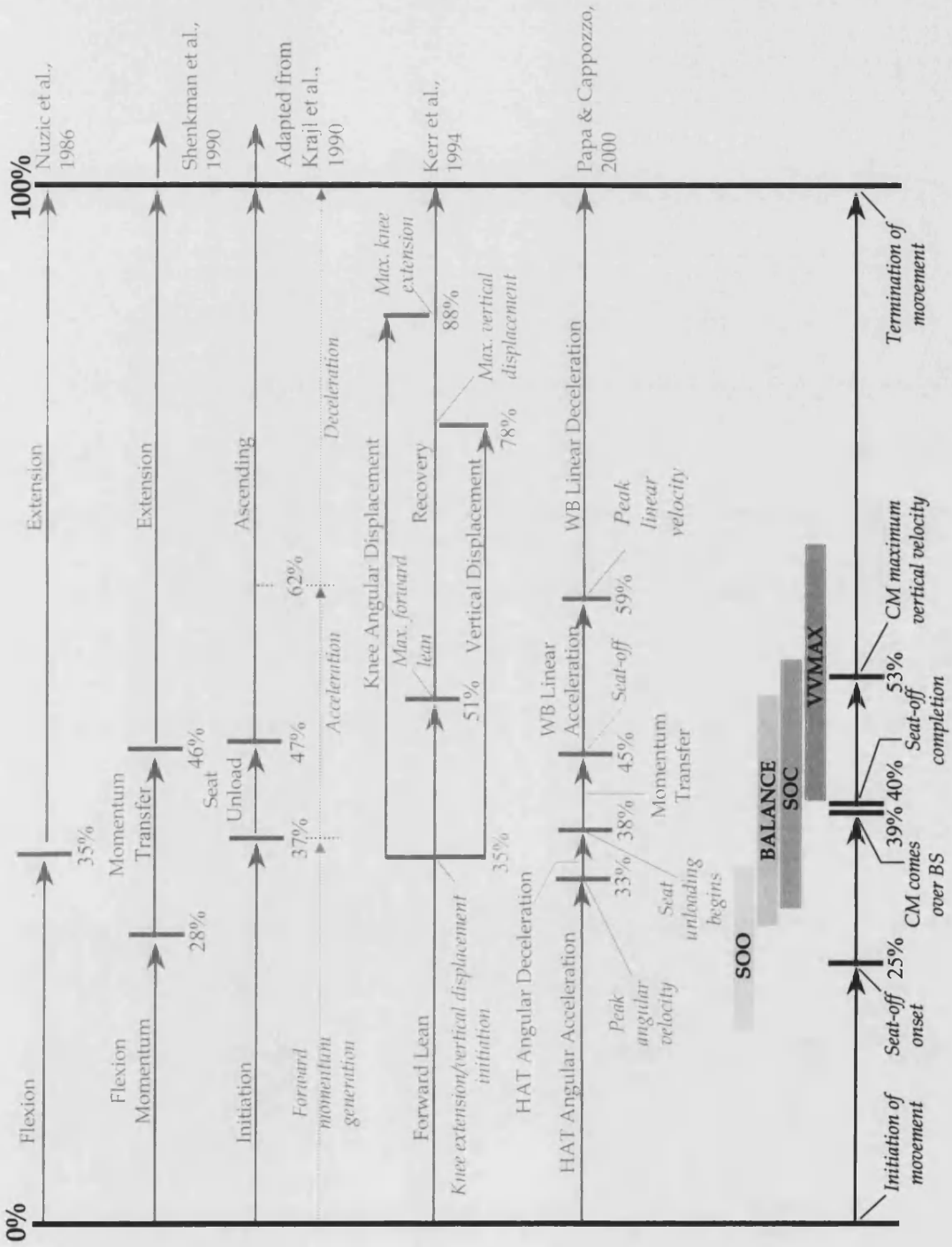

Figure 7.3. Compilation of previous studies that expressed STS movement as sub-divided phases with findings of the current study. Shaded boxes show range of times in which the four events (SOO, BALANCE, SOC, and VVMAX) occurred.

7.1.4 STABILITY STRATEGIES

This section, based upon experimental and statistical results, comments more specifically on the nature of the stability strategies used throughout the seat-off phase. Two stability strategies (dynamic and static) were previously proposed (Berger et al., 1988). Other authors developed this theory by suggesting that a combination of the two could be used (Riley et al., 1991). The current study agreed with this having shown that CM horizontal velocities were present over the seat-off phase, even when the CM was in a statically stable position. However, it was appreciated that whilst both strategies could be used, a greater emphasis could be placed on one or the other depending upon rise conditions. This study established how changes in rise condition affected the stability emphasis.

The majority of responses covered in section 7.1.2 were described with reference to main effects, as was the case with previous authors. Figure 7.4 has been recreated from the results presented in Tables 6.3-6.5. It gives a better representation of stability characteristics in the presence of interaction effects because it considered the experimental data obtained from the corner-points of the experimental design region. Sub-figures (a-h) are presented, each representing a separate experimental corner-point condition. The horizontal axes show normalised time and the vertical axes show the displacement between the CM and the rear of the BS (CM-$BS_{HOR\ DISP}$). Specifically, the *events* SOO, BALANCE, and SOC were considered as these were the most important in the context of describing the chosen stability strategies. The seat-off phase is approximated by grey boxes where the bottom left corner and top right corner represented the events SOO and SOC, respectively. Thus, the CM-$BS_{HOR\ DISP}$ and the duration over which seat-off occurred could be judged. The event of BALANCE is represented by a dashed vertical line. None of the sub-figures show BALANCE to occur before SOO. However, several sub-figures show BALANCE occurring in the latter part of the seat-off phase indicating that an increased emphasis was being placed on dynamic stability strategies. Some conditions (Figures 7.1a, b, and e) show BALANCE was not achieved until body contact was lost with the seat. Consequently, the emphasis placed on stability strategies may be judged in terms of where the seat-off phase occurred in relation to BALANCE.

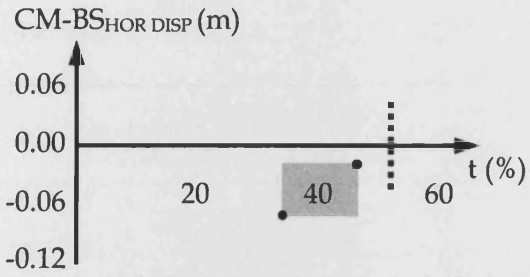

condition one (*RD* (-1), *ISP* (-1), *SH* (-1))

(a)

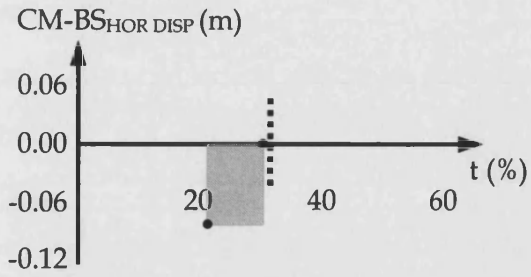

condition two (*RD* (1), *ISP* (-1), *SH* (-1))

(b)

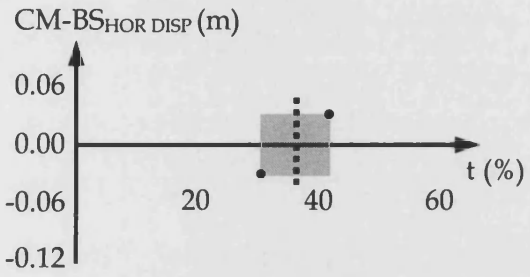

condition three (*RD* (-1), *ISP* (1), *SH* (-1))

(c)

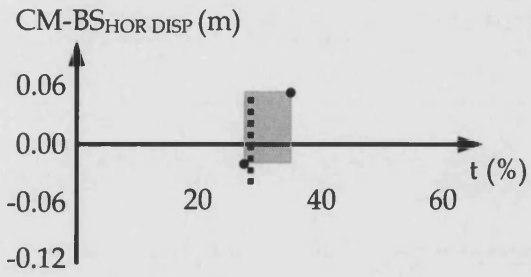

condition four (*RD* (1), *ISP* (1), *SH* (-1))

(d)

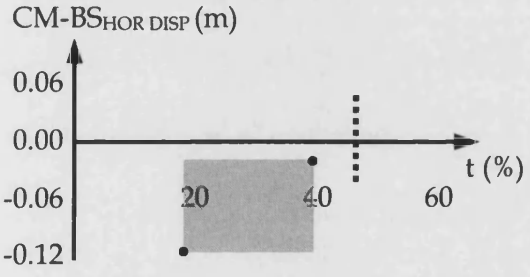

condition five (*RD* (-1), *ISP* (-1), *SH* (1))

(e)

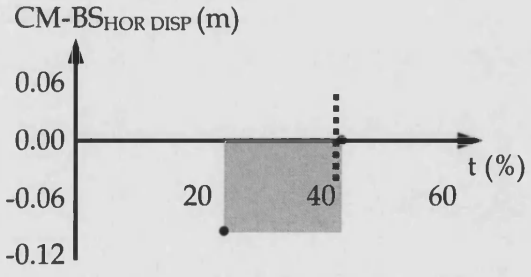

condition six (*RD* (1), *ISP* (-1), *SH* (1))

(f)

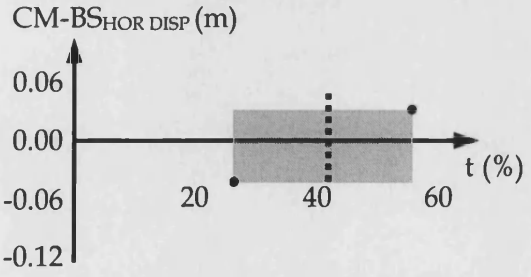

condition seven (*RD* (-1), *ISP* (1), *SH* (1))

(g)

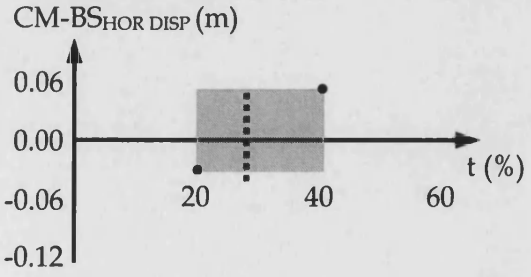

condition eight (*RD* (1), *ISP* (1), *SH* (1))

(h)

Figure 7.4. The occurrence of BALANCE (dashed vertical line) in relation to the seat-off phase (grey box) for the eight corner-point conditions.

Condition one rise (Figure 7.4a) (*RD* (-1), *ISP* (-1), *SH* (-1)) showed a dynamic stability strategy being used throughout seat-off. The postural demands associated with foot position necessitated this to happen. For condition two rise (Figure 7.4b) the pace of rise had changed to slow. Whilst dynamic stability strategies were still used, the emphasis had been reduced with $SOC_{HOR\ DISP}$ equal to 0.00 m. Similar influences were noted over all changes of rise duration (compare Figures 7.4c to 7.4d, 7.4e to 7.4f, 7.4g to 7.4h). In these figures it was shown that the lower *rise duration* did place an emphasis on static stability strategies, with that influence being greater on SOC than SOO.

Differences between *initial seated posture* conditions was notable (compare Figures 7.4a to 7.4c, 7.4b to 7.4d, and so on). A closer foot position allowed the emphasis to be placed on static strategies as $BALANCE_{TIME}$ consistently occurred earlier in the seat-off phase.

There was a small influence on the choice of stability strategy used due to *seat height* (compare Figures 7.4b to 7.4f, 7.4c to 7.4g, and so on). $CM\text{-}BS_{HOR\ DISP}$ for SOO and SOC changed little between these conditions, and $BALANCE_{TIME}$ remained at a similar time relative to the seat-off phase. This appeared contrary to the main effect for seat height as suggested in Table 6.9 and 6.10. However, as Figure 7.4 represented corner-point data, levels for *rise duration* and *initial seated posture* were also changing which may have counteracted the influence of *seat height*. The seat-off phase generally lengthened in the high seat conditions in comparison to the low seat conditions. The reduced vertical displacement requirement for the CM in the high seat conditions allowed a greater time to be taken travelling horizontally and completing the seat-off phase.

7.1.5 SECTION SUMMARY

Previous STS studies have opted to allow subjects to rise with self-paced duration (Fleckenstein et al., 1988; Galli et al., 2000) and self-positioned initial posture (Pai and Rogers, 1990; Bahrami et al., 2000). Whilst rising from a subject's 'comfortable' conditions may well produce the most typical movement patterns, in current industrial environments subjects frequently rise under a wide variety of situations. For the factors *rise duration, initial seated posture* and *seat height* there were strong effects in most of the

responses shown. This in itself could be an argument for the use of controlled factor studies in the future.

Spatiotemporal characteristics of STS were established and the influence of the three factors on them was tested. Some findings were shown to be the same as previous authors whereas others were different, perhaps because previous studies rarely accounted for interaction effects, or because of the reduced factor control under which other studies were conducted. Subdivision of the movement using *events* occurred and it was shown that not only did event timings vary across the range of factors, but that the order was changeable. This was important as previous authors had suggested that non-changeable movement subdivisions could be applied across a range of *rise duration* and *initial seated posture* conditions. A greater insight was given into the choice of stability strategies used throughout the seat-off phase of STS. It was shown that two strategies (dynamic and static) could be used, and that dependent upon rise condition a greater emphasis was placed on one or the other. The nature of this changing emphasis was shown with reference to the shifting order of the *events* SOO, BALANCE, and SOC. Faster movements in general used stability strategies that were more dynamic. However, the level of emphasis placed on the strategy was highly dependent on the levels of other factors present, particularly *initial seated posture.*

7.2 UNDERSTANDING SIT-TO-STAND THROUGH MODELLING

The following discussion concerns the modelling that occurred in the study. It covers a discussion on the use of the regression equations and the resulting CM trajectory that was created from them. A description of the graphical output from the SWORDS constraint modeller window is provided and evaluations of the human model are offered.

7.2.1 REGRESSION EQUATIONS

Regression equations were produced in order to create curve precision points such that CM trajectories could be predicted. Of the 15 responses ($END_{VER\ DISP}$ removed) analysis of variance indicated $SOO_{VER\ VEL}$ to be a poor predictor (Table G.6). This could have

been due to the response being non-linear. However, it was also likely to be related to the fact that the detected responses were on the whole smaller than the associated errors of the motion analysis system. Previous tests had found digitised displacement data to be accurate to 0.006 m for moving reflective markers across the same field of view as that used for the current investigation. In light of this, it was concluded that linear approximations to the chosen spatiotemporal characteristics of STS were appropriate. Statistical tables for each of the responses were produced and were presented in Appendix G.

Generally, the regressions were competent at predicting experimental data when the movement duration, relative foot position and seat height were known. Table 6.11 demonstrated the ability of the regressions to predict experimental data. Using linear approximations for the responses temporal responses were predicted within 2.7%, spatial events were predicted within 8.0%, and velocity responses were predicted within 7.0%. Maximum differences between experimental and predicted figures for the temporal, displacement and velocity data occurred in responses in the latter part of the movement. This could be a further reflection of the increased variability that occurred in movement characteristics in the later phases of STS.

The possibility that factors could interact to affect human movement responses was investigated. It was suggested that where possible interaction effects should be considered in future studies to fully understand changes in a response. Interaction effects have yet to be widely reported in STS literature. However, it was clear that these could play an important role in understanding movement characteristics in the presence of multiple factors, particularly with reference to balance strategies employed during seat-off, as demonstrated in Figure 7.4. Interestingly, the four regressions with 3-factor interactions were all temporal responses, so the inclusion of such interaction effects would be important if the investigated characteristics were of a temporal nature.

7.2.2 PREDICTED MASS CENTRE TRAJECTORY

A 13 control point second degree Bézier curve was fitted to experimentally obtained precision points in the horizontal domain. For the 11 validation conditions a mean RMSD of 2.7% was apparent (Table 6.12) between experimental and model data. In the

vertical domain, an eight control point third degree Bézier curve was fitted. This produced a mean RMSD of 4.7% (Table 6.13) between experimental and model data. As a result of these analyses, it was shown that by using simple techniques, estimates could be made for the most appropriate curve degree/control point combination to use for the two components of trajectory. When conducting the curve analysis, the conditions that produced the minimum error were relatively easy to find as they tended to converge consistently towards a particular combination. When searches were conducted outside of the ranges shown in the Tables 6.12 and 6.13, error values quickly became very large, and the curves were evidently wrong because they tended to oscillate erratically between precision points. Bézier curves were chosen primarily because of their prior coding within the RASOR modelling language and because of their ability to produce smooth 2D curves (Appendix F). The favourable mean RMSD across conditions meant that other curve fitting routines were not investigated.

Bézier curves were fitted to regression predicted precision points. Mean RMSD rose to 7.1% and 8.9% in the horizontal and vertical displacement time trajectories, respectively. Because of error associated with the regressions (Section 6.3.1), certain factor combinations could lead to precision points being predicted in the wrong order, which in turn would lead to oscillation of the trajectory (Section 5.3.3). These were corrected with the regressed response $BALANCE_{HOR\ VEL}$, which was shown to have good fit to the experimental data (Table G.8). Mean RMSD demonstrated in Table 6.14 were produced with this adjustment implemented. The use of one regression to compensate for errors in other regressions (all of which were obtained from the same experimental data) was carefully considered using analysis of variance techniques (Appendix G). Typically, curve oscillation was caused by incorrect predicted order of the *events* SOO, BALANCE, and SOC. Whilst still significant, $SOO_{HOR\ DISP}$ demonstrated a greater lack of fit than other models (Table G.4) which could explain why in some conditions the SOO precision point was predicted before BALANCE, yet with positive $CM\text{-}BS_{HOR\ DISP}$. Thus, the use of another stronger model ($BALANCE_{HOR\ VEL}$, Table G.8) was justified in order to correct $SOO_{HOR\ DISP}$. In the time domain $VVMAX_{TIME}$ showed the greatest error (Table 6.11). However, because of its isolation from other precision points, this error did not cause curve oscillation.

7.2.3 GRAPHICAL REPRESENTATION OF MANIKIN MOVEMENT

Pictorial representations of the manikin built on data held within ADAPS files were demonstrated in Figures 6.7-6.9. Sixteen approximately equi-spaced frames were demonstrated for rise using centre (condition nine), low (condition two) and high (condition six) seat levels. It was shown that the model appeared to represent STS movement patterns. The eye beam remained fixed on the distant target throughout the movement, as well as the hands remaining in contact with the lower thighs. In the latter part of the movement this constraint was relaxed such that the hands could slide up the thighs. The buttocks were seen to move gradually up from the seat. Such movement patterns would be considered useful to the end-user, giving quick assessments of the movement patterns of STS from a range of conditions. Further, such an output could be used to detect collision between manikin and environment, allowing the user to evaluate the movement in relation to the workspace.

7.2.4 NATURAL VARIABILITY IN STS MOVEMENT PATTERNS

Human movement patterns inevitably include a certain amount of natural variability. Section 6.4.1 demonstrated the variability that occurred in joint angle data over a series of trials within the centre-point condition. Variation in angle data at the hip, ankle, lumbar, and knee joints were assessed. Over the complete duration of movement the knee joint showed the greatest variation (4.0°) whilst the ankle joint showed the smallest variation (2.1°). The implications of these results are discussed further in the following sections.

7.2.5 VALIDATION OF MANIKIN MODEL AGAINST SUBJECT A

Within ergonomics, there is a real challenge to develop models that realistically predict how people normally move and interact with systems (Zhang and Chaffin, 2000). Manikin movement was predicted for the 11 evaluation trials. Hip, ankle, lumbar, and knee joint angle data were presented for total STS duration. Mean RMSD over the 11 trials for manikin movement of subject A was just 4.2° (Section 6.4.5). Table 7.5 presents

the mean error in each of the joints within the context of the established natural variability of each joint.

Table 7.5. Actual error in model when taken in context of anticipated movement variability.

	Hip Angle	Ankle Angle	Lumbar Angle	Knee Angle
RMSD between model and validation trials (°)	5.6	1.9	6.1	3.2
Expected human variability (°)	3.8	2.1	2.2	4.0
Actual model error (°)	**1.8**	**< 0.0**	**3.9**	**< 0.0**

Figures 6.17-6.27 showed the difference between the model and the experimental data for the 11 evaluation trials. When taken in context of the expected variability in human movement i.e. the required model accuracy as suggested in Section 5.4.1, the true value of the model is shown. Table 7.5 showed that two joints (ankle and knee) achieved predictions within this required accuracy level. Further, the remaining joints (hip and lumbar) fall within just 4° of the range of expected movement throughout the experimental region. The strengths and weaknesses of the model are further discussed.

Model segment lengths

Manikin segment lengths (within subject) remained fixed throughout STS. These were based on mean values of experimental data across the 11 evaluation trials. Within the spatial model, segment lengths were defined by the distance between appropriate markers, and thus varied throughout STS. This was particularly the case for chest and head/neck segments. In respect of these segments, the chest tended to increase in length in the middle portion of the movement, before decreasing, with the opposite occurring in the head/neck segment. This was primarily due to subject shoulder movement. As a result, the manikin was aiming to achieve CM positions that were based on slightly different spatial model segment lengths. Shoulder movement tended to be greatest when the subject was rising from low *seat height*. Consequently, the discrepancy between manikin and spatial model due to segment lengths was greatest

in these conditions, which may explain why the lumbar joint was shown to over flex around seat-off in these conditions.

Change in rule-sets

In conditions where the manikin is attempting to seek truth states in highly constrained situations (Appendix D), the model may be unable to totally satisfy all imposed constraints. For example, the manikin aimed to achieve postures based on segment lengths that slightly differed to the experimental data (as described above) and CM positions along a predicted trajectory that also included an element of error. Consequently, at instances where a large degree of trunk flexion was required, it was difficult for the manikin to achieve both 'CM on trajectory' whilst maintaining 'buttock contact with chair'.

Appendix H described how the applied constraints changed at the predicted time of *events*. As one constraint-set changed to another, constraints would be relaxed or introduced and accordingly the manikin behaved differently during and after this transition. Hence, in circumstances where the system was highly constrained discontinuities in the movement could be produced as the manikin sought a new truth state. Figure 6.22 showed such an occurrence in the hip and the knee between at the second vertical dashed line. The discontinuity at this point occurred as the manikin changed from one constraint-set representing SOO to SOC, to a second constraint -set representing SOC to BALANCE. The difference in the constraint-sets was that the constraint that bound the buttock to the seat changed from a state of being present to one where the influence of the constraint was reduced to zero (such that the buttock could leave the seat). Consequently, the buttocks tended to translate rapidly (over a short distance) at this point in order to more adequately satisfy all other constraints (specifically, CM position with regard to the predicted trajectory). This caused rapid changes in angular displacement at the hip and the knee (and to a lesser extent, at the lumbar).

Lumbar joint definition

The lumbar joint was set as a virtual point within the spatial-model (Appendix C). Characterised by the marker positions of the shoulder, hip, and knee joint, its description was such that it provided the best representation of torso bend across a range of selected trials. However, this resulted in a reasonably complex definition. When coding this description into SWORDS, it was found that on a practical level, the degree of complexity significantly reduced the solution time to the point where simulations were too time consuming to develop and run. Because of this, a simpler description was used within SWORDS which ultimately was not the same as that used in the spatial model. This approximation produced a constraint that sought to make changes in the lumbar angle that was a factor of 2.5 smaller than changes at the hip angle (i.e. the hip and lumbar bent in unison). Additionally, the spatial model description forced there to be no lumbar bend after the point at which the angle formed between the shoulder, hip, and knee was 140° (Appendix C). This can be seen by the lumbar angle resting at 0° at approximately 60-90% of movement in Figures 6.12 to 6.22. This additional definition was not present in the approximated manikin description which was why manikin joint displacement did not reduce to zero in the same manner as the experimental data. Further, the spatial model definition of lumbar joint remained absolute, whereas the manikin description was constraint-based and as such was subject to compromise in order to minimise global truth-values. The approximation of the lumbar joint as a virtual point was probably the largest source of error in the system as can be seen by the demonstrated errors in Table 7.5.

Ankle angle

Experimental data showed only small changes in absolute angular displacement at the ankle. As such, an error of one or two degrees in the model produced large relative error at the ankle joint (Tables 6.19 to 6.29). Because the ankle was operating close to its limits of range of movement, the optimisation algorithm oscillated the joint when searching for solutions (Figure 6.14). Orientation of the ankle joint had a significant influence on the total body posture (Figure 6.15) and as such oscillatory movements were removed from the ankle joint by imposing dynamic joint limits (Figure 6.16). This radically improved the predicted total body movement patterns.

Variation of fields between trials

The number of fields for each simulation differed. Thus, faster movements contained less individual steps to make the total movement. The model was set up this way for two reasons. When re-playing a simulation (as an animated file, used by an end-user to check movement patterns), an appreciation of the movement speed could be gained. Additionally, RMSD as demonstrated in Section 6.4.3, for example, was attained directly between the experimental and model data. Consequently, some simulations contained too few fields to produce smooth movement. Specifically, Figures 6.17 and 6.19 showed increased fluctuation (over other conditions) in the hip and knee data. Both of these conditions were of fast pace (reducing the number of samples in the predicted CM trajectory), and from the lower seat. This implied that the samples were placed further apart (vertically). Thus, the manikin was repeatedly attempting to solve posture states that were more uncertain for the constraint modeller and which resulted in the increased fluctuation in movement.

Hip flexion and extension

In high seat height conditions the hip angle failed to achieve full flexion around seat-off and full extension at the end of rise (Figures 6.21 to 6.24). The lumbar joint also experienced a lack of flexion at seat-off in these conditions. The lack of flexion (in the hip and lumbar joints) was attributed to the occurrence of a forward translation of the buttocks around seat-off which implied less trunk flexion was required to achieve the constraint of placing the CM along the predicted trajectory. With regard to the extension, a few degrees of extra rotation at the hip did not necessarily play a large role in the height of the CM. This was an inherent limitation of the optimisation systems, where a goal was to optimise a parameter to zero, i.e. to make a series of links become a straight line. In the context of the manikin model the imposed constraints (feet on floor, CM on trajectory etc.) could have been achieved very close to zero and considered as satisfied without the manikin being fully upright. No constraint was provided to specifically produce hip rotation, and as such the manikin was able to solve the constraints using less hip flexion.

Rise from centre-point conditions

The trials that represented the three repetitions of condition nine showed good predictions with low values of error. This result was encouraging because this condition most likely represented the more commonly occurring rise conditions within the range tested. Further to this, because the centre-point data were not used in the creation of the regression equations, these validations represented an independent check against the manikin.

7.2.6 VALIDATION OF MANIKIN MODEL AGAINST SUBJECTS B AND C

Section 6.4.4 presented the results obtained for manikin validation against subjects B and C. This formed an important part of the evaluation as it demonstrated whether or not the regressions that were based on a single subject performance could be applicable to other subjects or a population. Both subjects (B and C) varied considerably in body morphology to subject A (Table 5.2 and Table 5.4). The same conditions were tested with subjects B and C taking alternative corner-points in the experimental region (Figure 5.18). All factor levels for the subjects B and C existed within the experimental design region (Figure 6.3).

Relative RMSD between experimental and model data in the subjects B and C were comparable to subject A. In absolute terms, absolute mean RMSD across all joints and tested conditions were 5.7° and 5.5° for the large (B) and small (C) subjects, respectively. This was in comparison to 4.2° for subject A. Thus, when considering the natural variability that was present in the movement, the additional subjects also predicted movement patterns that were remarkably close to expected ranges.

However, a small amount error was introduced that was probably as a result of the single subject approach. Figures 6.28 and 6.29 showed subject B trials representing minimum and maximum RMSD, respectively. Both figures showed timing of maximum hip flexion to occur approximately 10% earlier in the model data than it did in the experimental data. Additionally, the subject appeared to use a different ankle strategy, where peak dorsiflexion occurred later in the movement cycle. These differences were not found in subject C. Thus, it appeared that subject B employed a

strategy whereby a greater proportion of the time was spent in the initial flexion phase of the movement which shortened the amount of time in extension.

ONSET and END definitions were tested for subjects B and C by considering the KE data and were found to remain appropriate. A weakness of the single-subject approach is that it assumed that movement strategies were solely based upon the factor levels. Consequently, movement strategies employed by subjects B and C may have differed for reasons other than the factor levels. Subject B had a larger degree of dynamic ankle movement available than subjects A and C. The importance of the ankle movement upon total body posture was previously highlighted and this could have led to the different movement patterns. Thus, it might be inappropriate to generalise the single subject regressions to subjects that have significantly different limits of joint range of movement, particularly the ankle joint as STS required the movement to work close to ankle limits. Conversely, the trials of subjects B and C did witness improved hip flexion and extension in high seat conditions. Previous studies have shown different movement strategies between subjects, for example increased trunk flexion at seat-off (Wheeler *et al.*, 1985; Schultz *et al.*, 1992; Hughes *et al.*, 1996; Lundin *et al.*, 1999; Papa and Cappozzo, 2000). However, these cases were predominantly related to differences in age or functional ability. The three subjects used here, whilst of different size, were of similar age and none were functionally impaired.

7.2.7 SECTION SUMMARY

Having achieved this level of understanding, it was suggested the regression equations were able to predict the spatiotemporal characteristics of any point within the experimental design region.

Aspects of the model were evaluated using a number of techniques. The graphical output of the manikin model was considered as a valuable tool for engineers when assessing the interaction of human in industrial environments. Its use as an instrument for human-machine collision was highlighted.

Natural variability in movement patterns was discussed and considered in terms of the differences between the model and the validation trials. It was found that both the

ankle and the knee joint demonstrated successful predicted movement within an expected range, with the hip angle lying just outside of this expected range. The lumbar joint (mean difference of 4° from expected range) was the most inconsistent of joints. This was attributed to virtual point description of that joint.

Modelling of the movement was undertaken to test whether the proposed *events* were the appropriate critical actions with which to describe STS. The high degree of success of the model was a strong indication that this was the case. The model was evaluated against the movement of additional large and small subjects such that subject variation was taken into account. Predicted movement patterns of these subjects were also very successful, indicating that the model could be applied across a range of other subjects.

7.3 SUMMARY

The described spatiotemporal responses showed how the CM moved throughout the duration of rise under the influence if the three factors. From this stability strategies were suggested. It was found that a greater emphasis was placed on dynamic stability strategies as the demands of rise increased due to *initial seated posture,* but decreased due to *seat height.* However, movement of the hip marker in the initial sitting position affected how well the regressions and manikin model reflected true human movement. This resulted in stability strategies possibly appearing to have a greater static emphasis than was actually the case.

The combined aspects of the model were evaluated. The largest source of error in the manikin model was attributed to the lumbar joint definition. All evaluated joints fell within 4° of the expected range. The model was also evaluated against additional subjects and shown to have comparable error value to the initial subject.

It was shown that the framework for understanding movement patterns and pattern variations (based on real movement objectives) could be applied to a constraint-based model. This resulted in a manikin model that could potentially be used to aid the design of man-machine interactions. Thus, by breaking down the understanding of a complex movement into a series of identifiable phases, an effective simulation model was produced.

CHAPTER 8: CONCLUSIONS AND FUTURE WORK

The final chapter presents the conclusions of the study in light of the successful results previously discussed. Comments are made with reference to the study purpose, the implemented approach, application of the model, and future directions for the work.

8.1 APPROPRIATENESS OF STUDY PURPOSE

There were two main purposes for this research. The first of these was to understand the constraints that influence STS movement patterns. By establishing the critical actions that must occur for rise to be successful the movement was sub-divided into phases. This provided a generalised motion characterisation which unlike previous subdivision studies, was applicable across all STS conditions. The critical actions, termed *events*, were points within STS where the movement constraints changed. They included ONSET, SOO, BALANCE, SOC, VVMAX, and END. Consequently, the division of the movement at these events led to the understanding of the constraints that applied to each phase. It was found that the movement constraints could be sectioned into two types: those that remained present throughout the movement, e.g. foot contact with floor or eye ray contact with target; and those that were not present throughout the whole motion, e.g. body contact with seat. The dominant constraint placed the CM along the CM trajectory, providing the main driving input to the manikin.

The movement constraints and their associated influence on STS characteristics that applied to the system were unknown prior to testing. By implementing the constraint modelling approach, it was possible to propose which constraints existed to create STS, where in the movement they applied, and test how their degrees of influence changed the movement characteristics. The success of the manikin model in predicting movement patterns established that the critical actions, and thus the movement constraints, were useful descriptors of the movement.

The second purpose aimed to obtain a greater comprehension of the spatiotemporal characteristics of STS, specifically at the intersection of the movement phases i.e. the

events. Whole body mass centre data were used for the description of spatiotemporal characteristics. Using an experimental approach rise factors were varied in a controlled manner in order to achieve a detailed understanding of CM displacement and velocity trends throughout the movement. These were subsequently modelled using regression expressions. The approach allowed interaction effects to be observed which previously had not been comprehensively considered within STS literature. It was clear that the interaction effects played an important role in understanding movement characteristics in the presence of multiple factors. This was particularly the case when considering the stability strategies chosen by subjects to overcome a variety of rise demands. It was also important for the descriptor of temporal responses, all of which included significant three-factor interaction effects, and which had never been considered in previous studies.

The level of understanding of these trends was aided significantly by the kinetic energy definitions given to the start and end of the movement. As a result, STS could be consistently identified across a range of subjects and conditions. This represented a radical improvement over methods described by previous authors.

The variability that occurred within STS movement patterns was assessed at two points in the investigation. The first assessment found that the variability that existed between subjects as they rose from uncontrolled conditions was large enough for any trends in the data to be obscured. This resulted in the main experimental study using just single subject rising from a series of controlled conditions. The second variability assessment was used to identify the required level of accuracy of the manikin model. Values of variability for total movement for the hip, knee and ankle joint were 3.8°, 4.0°, and 2.1°, respectively.

A predictive manikin model was driven using the movement constraints that were established from the identified critical actions, and the understanding of STS characteristics. The model was initially validated against subject A and showed an average difference from experimental data of just 4.2°. Of the investigated joint rotations, movement at the knee and ankle satisfied the level of accuracy needed to remain within the established ranges of natural variability. Hip and lumbar angle predictions fell just outside of the established natural variability ranges, a result closely linked to the virtual point description of the lumbar joint.

The presented work is useful to clinicians in showing the influence on STS responses due to a variety of naturally occurring factors. This could be extremely helpful when monitoring the progress of patients undergoing clinical intervention. Furthermore, human movement scientists could use the results to determine which factors to investigate if they were proposing to study responses similar to those in the present work.

8.2 APPROPRIATENESS OF STUDY APPROACH

There are often several approaches that can be taken to find solutions to posed questions. This work used a methodology where the influences of factors were tested experimentally to create a series of mathematical expressions that were then imported into a manikin model to predict movement for untested conditions. A series of evaluations established that a high degree of confidence could be placed in the manikin model to predict STS movement over the defined ranges of the factors.

Many previous STS studies allowed subjects to rise with self-paced duration and self-selected initial posture. Whilst it was appreciated that rising from a subject's 'comfortable' conditions may produce typical movement patterns, in industrial environments workers are frequently required to rise from a wide variety of conditions. A controlled experiment was conducted in order to understand the change in movement characteristics across the range of rise conditions. The most frequently tested condition represented factors that were placed at their centre levels. Not only did the validations associated with this condition prove to be among the most successful, this was also most likely to represent the comfortable conditions previously discussed.

Factors were tested at two levels meaning that regression models were inherently linear. This proved to be an adequate description of the response across the range of factors, particularly since the production of non-linear trends would have required three times as many experimental trials. However, caution must be used when testing factor levels outside of the recognised experimental design region.

A modelling approach tested the applicability of the suggested *events* as a useful means of movement description. The findings from the experimental study were used such that combinations of regression equations allowed precision points to be described and used with curve fitting routines. These were employed for the prediction of the CM trajectory and implemented successfully within the manikin model.

Limitations exist in any model. The manikin model limitations were most notably concentrated around the simplified approximation to the human skeleton, specifically the spine that was modelled as two rigid segments pivoted at a virtually described point. This was evidenced by the lumbar joint being the poorest predictor of the movement patterns. Marker movement was shown to introduce an error into the thigh angle of the experimental data which limited the quality of the data that was used to create model movement.

8.3 APPLICATION OF MODEL

8.3.1 THE USE OF THE MODEL TO WIDER POPULATIONS

The model was based on a single subject that represented a 50th percentile UK male adult (in terms of height). Additional subjects, one large and one small, were used that represented different percentiles of the population of UK adults. Thus a 95th percentile male (in terms of height) was tested, and a < 50th percentile female (in terms of mass) was tested. When implemented into the manikin model these additional subjects demonstrated equivalent degrees of accuracy as the initial model. Thus, it was suggested that the model could be confidently applied across a range in able-bodied populations.

It may be inappropriate to employ the model to subjects suffering from musculoskeletal impairments such as reduced limits of joint rotation. For example, Figure 6.8 showed rising occurring from a lower seat height where it was shown that the neck joint attained a large extension angle. This neck angle was achieved by the original subject in order to satisfy the constraint of keeping the eye ray fixed on a distant target. Such a constraint may not be able to be achieved by certain subject groups and hence, the model should be used with caution in these cases, as it should

for all rise conditions where a subject cannot fully satisfy the constraint sets on which the model was based (e.g. the use of arm movements to overcome stability demands around seat-off). It would also be advised that the model not be used to represent subjects with very different body morphologies to those in this study (e.g. obese or pregnant subjects) because of the influence that such factors have on rise characteristics.

The real strength of the manikin model is that its generated movement was based on the critical actions that occurred throughout STS. Because these same constraints are applicable to any subject performing STS, prediction of movement patterns for other subject type should be possible. By implementing alternative subject conditions (e.g. segment lengths or mass distribution) into the ADAPS files and SWORDS programme, the appropriate nature of the rise patterns should be seen. Literature for some subject groups e.g. the elderly or those recovering from total knee arthroplasty showed that a greater emphasis was placed on static stability strategies. To account for this the regression equations could be changed accordingly (direct modification of regression equations within the curve fitting sub-programme of the manikin model) to make the appropriate adjustments to the predicted CM trajectory.

8.3.2 THE USE OF THE MODEL AS A DESIGN AID

The need for an ergonomics input into industrial design has been well established. By producing a movement model that can be altered to represent any human, designers can test the safety, usability and productivity of designs well before they are constructed. An advantage of this system over current ergonomic models is its ability to accurately represent pre-defined movements without the need for some time-consuming operator intervention. This makes the manikin model a particularly attractive tool for engineers that do not have an ergonomics background. The created manikin model was shown to be a reliable method for predicting human movement patterns. As such, it has real potential for being used by engineers to improve industrial workstations with a view to reducing the levels of injury that occur because of poor ergonomic design.

8.4 FUTURE RESEARCH DIRECTIONS

The current investigation provided a thorough understanding of many elements of STS. Specifically, the experimental approach gave insight into CM spatiotemporal characteristics from which stability strategy choice in the context of changing rise demands was described. The modelling approach confirmed the critical actions and associated movement constraints as useful descriptors of the motion whilst giving further insight into other aspects such as the importance of ankle joint limits on the resulting body motion. Interaction effects were well described and provided a good introduction to their existence in STS responses. However, in contrast to the main effects, the fuller reasons of why interactions should exist were not as well established and could benefit from a continued study. Further, the reasons why the temporal responses were the only ones to include three-factor interactions also need to be clarified.

The manikin model was developed to a level where the average differences between experimental and predicted data were very low. However, some discrepancies did occur, particularly in the predicted movement at the lumbar joint. This was primarily linked with the difference in description of the lumbar joint between the manikin and the spatial model which could be more aligned if the sacrifice in simulation time could be excepted. The overall truth-value that was sought by SWORDS was also set at a level such that the simulations could be run in a reasonable time. Theoretically, the model may produce smaller differences between predicted and experimental data should this truth-value be increased, although this would also be at the cost of simulation time. Perhaps the biggest area for model improvement would be in the choice of the constraints 'weighting' that were implemented. The current levels were chosen in a fashion that was based more upon experience and judgement rather than some optimisation routine. Hence, it may be that different weightings would produce a more accurate STS representation and should be investigated.

The model was validated successfully against a range of able-bodied adults. However, the diverse range of subject types (e.g. across age or functional ability) that ergonomists have to design for implies that the current model was limited in its use. It would certainly be important to validate the model against other populations such as the elderly or the obese to consider what changes, if any, are required to be made to the

model. The importance of catering for disabilities in the workplace is an essential topic for ergonomic design. Consequently, using the currently validated model and implementing changes to it to represent disabilities could prove to be a very beneficial line of inquiry.

Three factors were chosen for investigation, based on those that were seen to occur within normal domestic and industrial environments and that had been found to influence other tested parameters of rise. Further factors (e.g. functional limitations, obesity, heavy clothing etc.) could be tested. However, it may not necessarily be advantageous to do so in such a thorough manner as this study. Rather, a more simple appreciation of how the factors of interest affected the emphasis placed on stability strategies may be adequate. This input could even come from the results of previous published studies. The regression equations could then be adjusted (to account for the change in emphasis) and the manikin programme re-run. It would certainly be very interesting to apply the adjusted constraints of disability, clothing or obesity to the model to see if the constraint model attempted to solve the challenges of rise in a manner similar to real subjects. This would give a good indication as to whether any additional movement constraints were required in order to correctly represent movement of any new subject population.

To attain the thorough understanding of the movement characteristics the experiment was conducted in a tightly controlled manner. Consequently, further understanding of the differences that may occur if a subject were to rise in a more relaxed manner, perhaps including the use of armrests, incorporating body twist, or rising whilst carrying some object, may have been eliminated. Clearly it would be useful to incorporate these changes into the model to more completely represent real life situations.

Furthermore, it is equally important to consider other variants of STS e.g. stand-to-sit and sit-to-walk. Additional movements should also be tested, perhaps including reaching and moving motions, or even walking. The framework from this study could be used to propose the critical actions and appropriate movement descriptors. For example, CM trajectory would not be a dominant constraint when describing a reaching movement as the majority of motion takes place in the arm. Perhaps path of the hand may then be chosen as the dominant constraint, with the critical actions of a

reaching motion including the start and end of movement, and maximum reach velocity.

Clearly, ergonomic designers need a wide range of motions available to them to truly estimate the effectiveness of a design that they are assessing. The work that has been demonstrated in this investigation has shown that movement patterns can be successfully predicted across a range of conditions. This information can now be used and built upon to provide a comprehensive ergonomic design aid.

REFERENCES

Ackland, T.R., Henson, P.W. and Bailey, D.A. (1988). The uniform density assumption - Its effect upon the estimation of body segment inertial parameters. *International Journal of Sport Biomechanics,* **4** (2), 146-155.

Alexander, N.B., Gross, M.M., Medell, J.L. and Hofmeyer, M.R. (2001). Effects of functional ability and training on chair-rise biomechanics in older adults. *Journals of Gerontology Series A - Biological Sciences and Medical Sciences,* **56** (9), M538-M547.

Alexander, N.B., Koester, D.J. and Grunawalt, J.A. (1996). Chair design affects how older adults rise from a chair. *Journal of the American Geriatrics Society,* **44** (4), 356-362.

Arborelius, U.P., Wretenberg, P. and Lindberg, F. (1992). The effects of armrests and high seat heights on lower-limb joint load and muscular - Activity during sitting and rising. *Ergonomics,* **35** (11), 1377-1391.

Babski-Reeves, K. and Crumpton-Young, L. (2003). Interaction effects of wrist and forearm posture on the prediction of carpal tunnel syndrome cases within a fish-processing facility. *Human and Ecological Risk Assessment,* **9** (4), 1011-1022.

Bahrami, F., Riener, R., Jabedar-Maralani, P. and Schmidt, G. (2000). Biomechanical analysis of sit-to-stand transfer in healthy and paraplegic subjects. *Clinical Biomechanics,* **15** (2), 123-133.

Bates, B.T., Duffek, J.S. and Davis, H.P. (1992). The effect of trial size on statistical power. *Medicine and Science in Sports and Exercise,* **24** (9), 1059-1068.

Berger, R.A., Riley, P.O., Mann, R.W. and Hodge, W.A. (1988). Total body dynamics in ascending stairs and rising from a chair following total knee arthroplasty. *Proceedings of 34th Annual Meeting, Orthopaedic Research Society, Atlanta, Georgia,* **13**, pp. 542.

Bézier, P. (1972). *Numerical control: Mathematics and applications.* London: John Wiley & Sons.

Bowler, C., Hicks, B.J., Mullineux, G. and Medland, A.J. (2000). Modelling machine systems for competitive design in the packaging industry. *Proceedings of Tools and methods of competitive engineering, Delft, The Netherlands,* pp. 519-527.

British Nutrition Foundation (1999). *Obesity.* Oxford: Blackwell Science.

Brunt, D., Greenberg, B., Wankadia, S., Trimble, M.A. and Shechtman, O. (2002). The effect of foot placement on sit to stand in healthy young subjects and patients with hemiplegia. *Archives of Physical Medicine and Rehabilitation*, **83** (7), 924-929.

Burdett, R.G., Habasevich, R., Pisciotta, J. and Simon, S.R. (1985). Biomechanical comparison of rising from 2 types of chairs. *Physical Therapy*, **65** (8), 1177-1183.

Butler, P.B., Nene, A.V. and Major, R.E. (1991). Biomechanics of transfer from sitting to standing position in some neuromuscular diseases. *Physiotherapy*, **77** (8), 521-525.

Cappozzo, A. and Berme, N. (1990). Subject-specific segmental inertia parameter determination - A survey of current methods. *Biomechanics of human movement: Applications in rehabilitation, sports and ergonomics.* Eds. Berme, N., and Cappozzo, A. Ohio: Bertec Corporation, pp. 179-185.

Carr, J. (1992). Balancing the centre of body mass during standing up. *Physiotherapy Theory and Practice*, **8**, 159-164.

Carr, J.H. and Gentile, A.M. (1994). The effect of arm movement on the biomechanics of standing up. *Human Movement Science*, **13** (2), 175-193.

Chan, D., Laport, D.M. and Sveistrup, H. (1999). Rising from sitting in elderly people, part 2: Strategies to facilitate rising. *British Journal of Occupational Therapy*, **62** (2), 64-68.

Chandler, R.F., Clauser, C.E., McConville, J.T., Reynolds, H.M. and Young, J.W. (1975). *Investigation of inertia properties of the human body.* AMRL-TR-74-137. Wright-Patterson Air Force Base, Ohio.

Clarys, J.P. and Marfell-Jones, M.J. (1986). Anatomical segmentation in humans and the prediction of segmental masses from intra-segmental anthropometry. *Human Biology*, **58** (5), 771-782.

Clauser, C.E., McConville, J.T. and Young, J.W. (1969). Weight, volume, and centre of mass of segments of the human body. AMRL-TR-69-70. Wright-Patterson Air Force Base, Ohio.

Das, B. and Sengupta, A.K. (1995). Computer-aided human modelling programs for workstation design. *Ergonomics*, **38** (9), 1958-1972.

Das, B. and Sengupta, A.K. (1996). Industrial workstation design: A systematic ergonomics approach. *Applied Ergonomics*, **27** (3), 157-163.

DeBeer, J.O., Vandenbroucke, C.V., Massart, D.L. and DeSpiegeleer, B.M. (1996). Half-fraction and full factorial designs versus central composite design for retention modelling in reversed-phase ion-pair liquid chromatography. *Journal of Pharmaceutical and Biomedical Analysis*, **14** (5), 525-541.

Dempster, W.T. (1955). *Space requirements of the seated operator.* WADC TR 55-159, AD-087-892. Wright-Patterson Air Force Base, Ohio.

Department of Health (2003). *Obesity. Annual report of the chief medical officer 2002.* London: Department of Health Publications, pp. 36-45.

Department of Trade and Industry (1998). *ADULTDATA - The handbook of adult anthropometric and strength measurements.* London: Department of Trade and Industry.

Draper, N.R. and Smith, H. (1998). *Applied regression analysis.* Chichester: Wiley.

Eastman Kodak Company (1983). *Ergonomics Design for People at Work.* New York: Lifetime Learning.

Faraway, J.J. (2001). *HUMOSIM.* Personal Communication: 4th October, 2001. Bath.

Faraway, J.J., Zhang, X.D. and Chaffin, D.B. (1999). Rectifying postures reconstructed from joint angles to meet constraints. *Journal of Biomechanics*, **32** (7), 733-736.

Fleckenstein, S.J., Kirby, R.L. and Macleod, D.A. (1988). Effect of limited knee-flexion range on peak hip moments of force while transferring from sitting to standing. *Journal of Biomechanics*, **21** (11), 915-918.

Galli, M., Crivellini, M., Sibella, F., Montesano, A., Bertocco, P. and Parisio, C. (2000). Sit-to-stand movement analysis in obese subjects. *International Journal of Obesity*, **24** (11), 1488-1492.

Goble, D.J., Marino, G.W. and Potvin, J.R. (2003). The influence of horizontal velocity on interlimb symmetry in normal walking. *Human Movement Science*, **22** (3), 271-283.

Green, W.S. (2000). Human factors in competitive product design and engineering. *Proceedings of Tools and Methods of Competitive Engineering, Delft, The Netherlands*, pp. 43-53.

Hatze, H. (1980). A mathematical model for the computational determination of parameter values of anthropometric segments. *Journal of Biomechanics*, **13**, 833-843.

Hay, J.G. (1973). The centre of gravity of the human body. *Kinesiology III.* Washington DC: American Association for Health, Physical Education and Recreation, pp. 20-44.

Health and Safety Executive (2002). The costs to Britain of workplace accidents and work-related ill-health in 1995/96. Internet site: accessed 13th December, 2002. http://www.hse.gov.uk/.

Hicks, B.J., Bowler, C., Medland, A.J. and Mullineux, G. (2002). The role of virtual sequence simulation in the analysis of packaging machines. *Journal of Engineering Design*, **13** (1), 19-32.

Hirschfeld, H., Thorsteinsdottir, M. and Olsson, E. (1999). Coordinated ground forces exerted by buttocks and feet are adequately programmed for weight transfer during sit-to-stand. *Journal of Neurophysiology*, **82** (6), 3021-3029.

Hoekstra, P.N. (1996). "What's Up?" Some aspects of quantifying an anthropometric model's field-of-view in computer aided anthropometric assessment. *International Journal of Industrial Ergonomics*, **17**, 315-321.

Hooke, R. and Jeeves, T.A. (1961). Direct search solution of numerical and statistical problems. *Journal of the Association for Computing Machinery*, **8**, 212-229.

Hughes, M.A., Myers, B.S. and Schenkman, M.L. (1996). The role of strength in rising from a chair in the functionally impaired elderly. *Journal of Biomechanics*, **29** (12), 1509-1513.

Hughes, M.A., Weiner, D.K., Schenkman, M.L., Long, R.M. and Studenski, S.A. (1994). Chair rise strategies in the elderly. *Clinical Biomechanics*, **9** (3), 187-192.

Huijboom, J.M., Molenbroek, J.F.M. and Goosens, R.H.M. (1999). Applying ergonomics to design problems using a computer based tool. *Proceedings of International Conference on Engineering Design, Munich*, pp. 461-464.

Ikeda, E.R., Schenkman, M.L., Riley, P.O. and Hodge, W.A. (1991). Influence of age on dynamics of rising from a chair. *Physical Therapy*, **71** (6), 473-481.

Janssen, W.G.M., Bussmann, H.B.J. and Stam, H.J. (2002). Determinants of the sit-to-stand movement: A review. *Physical Therapy*, **82** (9), 866-879.

Jensen, R.K. (1976). Model for body segment parameters. In *Biomechanics V B*. Ed. Komi, P. V. Baltimore: University Park Press, pp. 380-386.

Jensen, R.K. (1978). Estimation of the biomechanical properties of three body types using a photogrammetric method. *Journal of Biomechanics*, **11**, 349-358.

Jensen, R.K. and Wilson, B.D. (1988). Prediction of segment inertias using curvilinear regression. *Proceedings of Canadian Society of Biomechanics, London, Ontario*, pp. 90-91.

John, J.A. and Quenoullie, M.H. (1977). *Experiments: Design and analysis.* London: Charles Griffin & Company Ltd.

Kerr, K.M., White, J.A., Barr, D.A. and Mollan, R.A.B. (1994). Analysis of the sit-stand-sit movement cycle: development of a measurement system. *Gait & Posture*, **2**, 173-181.

Kerr, K.M., White, J.A., Barr, D.A. and Mollan, R.A.B. (1997). Analysis of the sit-stand-sit movement cycle in normal subjects. *Clinical Biomechanics*, **12** (4), 236-245.

Khemlani, M.M., Carr, J.H. and Crosbie, W.J. (1999). Muscle synergies and joint linkages in sit-to-stand under two initial foot positions. *Clinical Biomechanics*, **14** (4), 236-246.

Kotake, T., Dohi, N., Kajiwara, T., Sumi, N., Koyama, Y. and Miura, T. (1993). An analysis of sit-to-stand movements. *Archives of Physical Medicine and Rehabilitation*, **74** (10), 1095-1099.

Kralj, A., Jaeger, R.J. and Munih, M. (1990). Analysis of standing up and sitting down in humans - Definitions and normative data presentation. *Journal of Biomechanics*, **23** (11), 1123-1138.

Liu, Y.L., Zhang, X.D. and Chaffin, D. (1997). Perception and visualization of human posture information for computer-aided ergonomic analysis. *Ergonomics*, **40** (8), 818-833.

Lord, S.R., Murray, S.M., Chapman, K., Munro, B. and Tiedemann, A. (2002). Sit-to-stand performance depends on sensation, speed, balance, and psychological status in addition to strength in older people. *Journals of Gerontology Series A - Biological Sciences and Medical Sciences*, **57** (8), M539-M543.

Lou, S.Z., Chou, Y.L., Chou, P.H., Lin, C.J., Chen, U.C. and Su, F.C. (2001). Sit-to-stand at different periods of pregnancy. *Clinical Biomechanics*, **16** (3), 194-198.

Loucaides, A., Medland, A.J. and Mullineux, G. (1994). Optimisation techniques in constraint modelling. *Proceedings of Annual Conference on Engineering Design, Plymouth, London*, pp. 50-55.

Lundin, T.M., Jahnigen, D.W. and Grabiner, M.D. (1999). Maximum trunk flexion angle during the sit to stand is not determined by knee or trunk-hip extension strength in healthy older adults. *Journal of Applied Biomechanics*, **15** (3), 233-241.

Magnan, A., McFadyen, B.J. and St-Vincent, G. (1996). Modification of the sit-to-stand task with the addition of gait initiation. *Gait & Posture*, **4**, 232-241.

McGarva, J.R. and Mullineux, G. (1995). The implementation of closed B-spline curves for application to mechanisms. *Computers in Industry*, **27** (3), 287-290.

Medland, A.J. (2000). An interactive approach to design decomposition. *Proceedings of Tools and methods of competitive engineering, Delft, The Netherlands*, pp. 617-626.

Medland, A.J., Mullineux, G., Twyman, B.R. and Rentoul, A.H. (1996). A constraint-based approach to the design and optimisation of mechanism systems. *Proceedings of IUTAM Symposium on Optimization of Mechanical Systems*, pp. 205-212.

Millington, P.J., Myklebust, B.M. and Shambes, G.M. (1992). Biomechanical analysis of the sit-to-stand motion in elderly persons. *Archives of Physical Medicine and Rehabilitation*, **73** (7), 609-617.

Mitchell, R.H., Salo, A.I.T. and Medland, A.J. (2003). Determining mass centre trajectory variations for application to human modelling. *Proceedings of IASTED International Conference on Biomechanics, Rhodes*, pp. 147-152.

Molenbroek, J.F.M. (1994). *Op maat gemaakt. Menselijke maten voor het ontwerpen en beoordelen van gebruiksgoederen*. Delft: Delftse Universitaire Pers.

Molenbroek, J.F.M. (2003). Revision of the design of a standard for the dimension of school furniture. *Ergonomics*, **46** (7), 681-694.

Molenbroek, J.F.M. and Medland, A.J. (2000). The application of constraint processes for the manipulation of human models to address ergonomic design problems. *Proceedings of Tools and Methods of Competitive Engineering, Delft, The Netherlands*, pp. 827-835.

Mullineux, G. (1988). The introduction of constraints into a graphics system. *Engineering with Computers*, **3** (4), 201-205.

Mullineux, G. (1991). A blackboard structure for handling engineering design-data. *Engineering with Computers*, **7** (3), 185-195.

Mullineux, G. (2001). Constraint resolution using optimisation techniques. *Computers & Graphics - UK*, **25** (3), 483-492.

Mungiole, M. and Martin, P.E. (1986). Estimating segmental inertial properties: Magnetic resonance imaging versus existing methods. *Proceedings of North American Congress on Biomechanics, Montreal (Quebec) Canada*, pp. 229-230.

Mungiole, M. and Martin, P.E. (1990). Estimating segment inertial properties - Comparison of magnetic resonance imaging with existing methods. *Journal of Biomechanics*, **23** (10), 1039-1046.

Munro, B.J., Steele, J.R., Bashford, G.M., Ryan, M. and Britten, N. (1998). A kinematic and kinetic analysis of the sit-to-stand transfer using an ejector chair: implications for elderly rheumatoid arthritic patients. *Journal of Biomechanics*, **31** (3), 263-271.

Nigg, B.M. and Herzog, W. (Eds.) (1999). *Biomechanics of the musculo-skeletal system.* Chichester: John Wiley & Sons Ltd.

Novacheck, T.F. (1998). The biomechanics of running. *Gait & Posture,* **7** (1), 77-95.

Nuzik, S., Lamb, R., Vansant, A. and Hirt, S. (1986). Sit-to-stand movement pattern - A kinematic study. *Physical Therapy,* **66** (11), 1708-1713.

Pai, Y.C. and Rogers, M.W. (1990). Control of body-mass transfer as a function of speed of ascent in sit-to-stand. *Medicine and Science in Sports and Exercise,* **22** (3), 378-384.

Pai, Y.C. and Rogers, M.W. (1991). Segmental contributions to total-body momentum in sit-to-stand. *Medicine and Science in Sports and Exercise,* **23** (2), 225-230.

Papa, E. and Cappozzo, A. (1999). A telescopic inverted-pendulum model of the musculo-skeletal system and its use for the analysis of the sit-to-stand motor task. *Journal of Biomechanics,* **32** (11), 1205-1212.

Papa, E. and Cappozzo, A. (2000). Sit-to-stand motor strategies investigated in able-bodied young and elderly subjects. *Journal of Biomechanics,* **33** (9), 1113-1122.

Paterakis, P.G., Korakianiti, E.S., Dallas, P.P. and Rekkas, D.M. (2002). Evaluation and simultaneous optimization of some pellets characteristics using a 3(3) factorial design and the desirability function. *International Journal of Pharmaceutics,* **248** (1-2), 51-60.

Porter, M.J., Freer, M., Case, K. and Bonney, M.C. (1999). Computer aided ergonomics and workspace design. *Engineering Designer,* **25** (2), 4-9.

Reisman, D.S., Scholz, J.P. and Schoner, G. (2002). Coordination underlying the control of whole body momentum during sit-to-stand. *Gait & Posture,* **15** (1), 45-55.

Riley, P.O., Krebs, D.E. and Popat, R.A. (1997). Biomechanical analysis of failed sit-to-stand. *IEEE Transactions on Rehabilitation Engineering,* **5** (4), 353-359.

Riley, P.O., Schenkman, M.L., Mann, R.W. and Hodge, W.A. (1991). Mechanics of a constrained chair-rise. *Journal of Biomechanics,* **24** (1), 77-85.

Robinson, G. (2000). *Practical strategies for experimenting.* Chichester: John Wiley & Sons.

Schenkman, M., Berger, R.A., Riley, P.O., Mann, R.W. and Hodge, W.A. (1990). Whole-body movements during rising to standing from sitting. *Physical Therapy,* **70** (10), 638-648.

Schenkman, M., Riley, P.O. and Pieper, C. (1996). Sit to stand from progressively lower seat heights - Alterations in angular velocity. *Clinical Biomechanics,* **11** (3), 153-158.

Schultz, A.B., Alexander, N.B. and Ashtonmiller, J.A. (1992). Biomechanical analyses of rising from a chair. *Journal of Biomechanics*, **25** (12), 1383-1391.

Shepherd, R.B. and Gentile, A.M. (1994). Sit-to-stand: Functional relationship between upper body and lower limb segments. *Human Movement Science*, **13** (6), 817-840.

Sirkett, D.M., Mullineux, G., Miles, A.W. and Giddens, G.E.D. (2003). Does the minimum energy principle govern wrist kinematics? *Proceedings of IASTED International Conference on Biomechanics, Rhodes*, pp. 241-246.

Sly, F., (Ed.) (2004). National statistics. *Labour Market Trends*, **112** (2), 45-80.

Solman, K.N. (2002). Analysis of interaction quality in human-machine systems: applications for forklifts. *Applied Ergonomics*, **33** (2), 155-166.

Stevens, C., Bojsenmoller, F. and Soames, R.W. (1989). The influence of initial posture on the sit-to-stand movement. *European Journal of Applied Physiology and Occupational Physiology*, **58** (7), 687-692.

Su, F.C., Lai, K.A. and Hong, W.H. (1998). Rising from chair after total knee arthroplasty. *Clinical Biomechanics*, **13** (3), 176-181.

Thomas, M. and Beauchamp, Y. (2003). Statistical investigation of modal parameters of cutting tools in dry turning. *International Journal of Machine Tools & Manufacture*, **43** (11), 1093-1106.

Twyman, B.R. (1999). *An investigation into the use of constraint modelling techniques in the design of packaging machinery motion.* Unpublished PhD Thesis, University of Bath, Bath.

Twyman, B.R., Mullineux, G. and Bowler, C. (1999). Constraints in Motion Design. *Proceedings of International Conference on Engineering Design, Munich, Germany*, pp. 1749-1752.

van Ekelenburg, H.P., Hoogerkamp, P. and Hopmans, L.J. (1995). *A practical guide to the machinery directive.* London: Mechanical Engineering Publications Ltd.

Vander-Linden, D.W., Brunt, D. and McCulloch, M.U. (1994). Variant and invariant characteristics of the sit-to-stand task in healthy elderly adults. *Archives of Physical Medicine and Rehabilitation*, **75** (6), 653-660.

Venema, S.C. and Hannaford, B. (2001). A probabilistic representation of human workspace for use in the design of human interface mechanisms. *IEEE-ASME Transactions on Mechatronics*, **6** (3), 286-294.

Walsch, G.R. (1975). *Methods of optimisation.* London: John Wiley & Sons.

Wheeler, J., Woodward, C., Ucovich, R.L., Perry, J. and Walker, J.M. (1985). Rising from a chair - Influence of age and chair design. *Physical Therapy*, **65** (1), 22-26.

Williams, M.A. and Medland, A.J. (2001). The creation of techniques for the design of machines compatible with human posture. *Proceedings of International Conference on Engineering Design, Glasgow*, pp. 347-354.

Woltring, H.J. (1986). A FORTRAN package for generalised cross-validatory spline smoothing and differentiation. *Advances in Engineering Software*, **8** (2), 104-113.

Wood, G.A. and Jennings, L.S. (1979). On the use of spline functions for data smoothing. *Journal of Biomechanics*, **12**, 477-479.

Yeadon, M.R. (1990). The simulation of aerial movement 2. A mathematical inertia model of the human-body. *Journal of Biomechanics*, **23** (1), 67-74.

Yoshida, K., Iwakura, H. and Inoue, F. (1983). Motion analysis in the movements of standing up from and sitting down on a chair - A comparison of normal and hemiparetic subjects and the differences of sex and age among the normals. *Scandinavian Journal of Rehabilitation Medicine*, **15** (3), 133-140.

Yu, B., Holly-Crichlow, N., Brichta, P., Reeves, G.R., Zablotny, C.M. and Nawoczenski, D.A. (2000). The effects of the lower extremity joint motions on the total body motion in sit-to-stand movement. *Clinical Biomechanics*, **15** (6), 449-455.

Zatsiorsky, V. and Seluyanov, V. (1983). The mass and inertia characteristics of the main segments of the human body. *Proceedings of Eighth International Congress of Biomechanics, Nagoya, Japan*, pp. 1152-1159.

Zhang, X.D. and Chaffin, D. (2000). A three-dimensional dynamic posture prediction model for simulating in-vehicle seated reaching movements: Development and validation. *Ergonomics*, **43** (9), 1314-1330.

Zhang, X.D. and Chaffin, D.B. (1999). The effects of speed variation on joint kinematics during multisegment reaching movements. *Human Movement Science*, **18** (6), 741-757.

Zhang, X.D., Kuo, A.D. and Chaffin, D.B. (1998). Optimization-based differential kinematic modeling exhibits a velocity-control strategy for dynamic posture determination in seated reaching movements. *Journal of Biomechanics*, **31** (11), 1035-1042.

Zhang, X.D., Nussbaum, M.A. and Chaffin, D.B. (2000). Back lift versus leg lift: an index and visualization of dynamic lifting strategies. *Journal of Biomechanics*, **33** (6), 777-782.

APPENDIX A: PEAK-MANIKIN ALIGNMENT

The following table demonstrates how joint angles were defined within the Peak digitising software such that there was correct alignment with the ADAPS orientated manikin model. Only the joint angles that were assessed within this report are presented here. Note that data for knee joint angle displacement, as presented throughout Section 6.4, were the negative of the data that were collected (i.e. each data point was multiplied by -1). This was such that knee joint data could be presented clearly alongside hip, lumbar and ankle joint data in the validation figures.

Table A.1. Joint angle definitions incorporated in Peak digitising software to align with ADAPS orientated manikin model.

Joint angle name	Angle description used within Peak software	Markers used to define angle	Definition of positive rotation
Neck	Anatomical-180 joint angle	Skull vertex, shoulder, lumbar	
Lumbar	Anatomical-180 joint angle	Shoulder, lumbar, hip	
Hip	Anatomical-180 joint angle	Lumbar, hip, knee	
Knee	Anatomical-180 joint angle	Hip, knee, ankle	
Ankle	Anatomical-90 segmental angle	Knee/ankle, toe/ heel	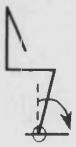

APPENDIX B: FACTORIAL EXPERIMENTAL ANALYSIS

Full-factorial experimental design utilises combinations of the range of values of the chosen variables. When there are not large number of variables of interest, this approach is a practical way of obtaining results. Traditionally, the different variables are known as factors, which are evaluated at different values, known as levels. Output measures are referred to as responses. A particular combination of factors and levels is referred to as a treatment.

Experimental treatments are planned in order to collect the maximum amount of information in as few trials as possible. By using the approach of testing for every combination of factor and level it is possible to obtain a value for the effect of a single factor on the overall response of the system. However, it is also possible to obtain values for interaction effects between factors on a response. This is the main strength of this experimental approach over single-factor approaches and it has been well used in a variety of disciplines (DeBeer et al., 1996; Paterakis et al., 2002; Thomas and Beauchamp, 2003).

Full factorial designs are able to provide mathematical relationships between factors and a response. Multiple linear regressions can be computed to include all main and interaction effects that are greater than an estimated standard error. These allow a response to be predicted continuously across the defined ranges of the factors. Regressions based on factors with just two levels will be linear and may include some error if the response is in fact significantly non-linear. Multi-level factors can be used if non-linear trends in a response are suspected, although this has the disadvantage of increasing the number of trials considerably. For example, an investigation based on three factors at two levels each would require 8 (2^3) trials without repetition whereas, increasing the levels to three per factor would require 27 (3^3) trials, similarly without repetition. Two-level experiments, known as screening designs, are the first stage of an investigation, where the goal is to identify factors that cause substantial effects in a response. Full factorial designs are balanced. Hence, the effect of a factor can be estimated independent of the effects of all other factors. Broader discussions on this and similar designs can be found in texts on experimental theory (John and Quenoullie, 1977; Robinson, 2000).

APPENDIX C: CREATION OF VIRTUAL LUMBAR POINT

Reflective markers were used to approximate segment joint centres. The trunk was modelled as two segments representing the pelvis and upper torso (chest) such that spine flexion information was included into the final model. Due to arm motion throughout STS the joint between the two trunk segments could become obscured from view during part of the movement. To account for this a 'virtual point' representing the location of the joint was created within the digitising software. Its position was such that it best approximated a point as shown in Figure C.1. This was in line with definition provided by Yeadon's (1990) mathematical inertia model.

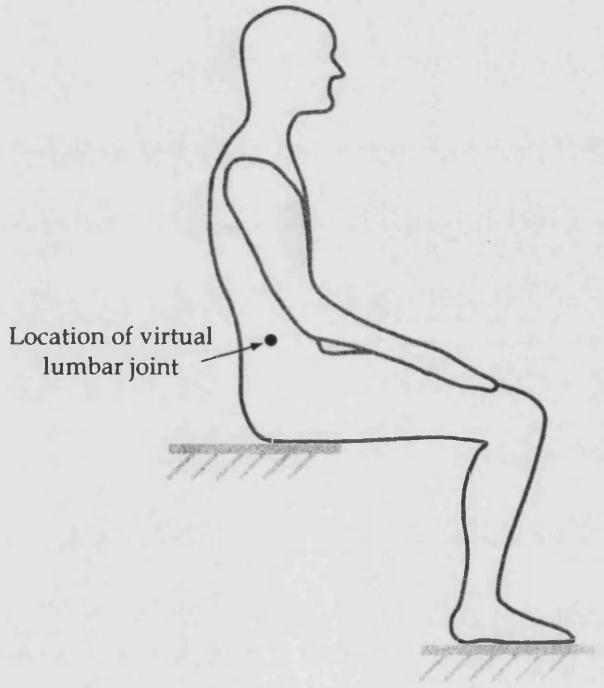

Figure C.1. Location of marker to identify top of pelvis.

Initially, shoulder, hip, knee, and lumbar joint locations were manually digitised. An associated mass centre trajectory for the thigh, pelvis and chest segments was calculated for each of 11 evaluation trials representing the experimental design region. These data were used with RMSD techniques in order to evaluate the virtual lumbar joint descriptions. Movement of the segments appeared as shown in Figure C.2.

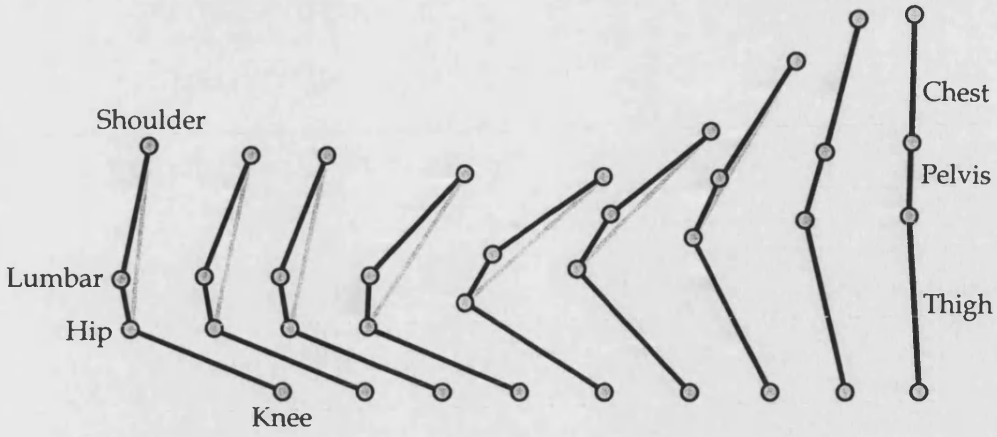

Figure C.2. Patterns of thigh, pelvis and chest segment movement.

During the flexion phase of the movement the rate of change of the angle θ appeared higher than the rate of change of the angle ε (Figure C.3). This was equivalent to the trunk flexion trends described by Hirschfeld at al. (1999). Similarly, during the first part of the extension phase the rate of change of the angle θ appeared higher than the rate of change of the angle ε. After a certain amount of extension θ and ε remained approximately equivalent.

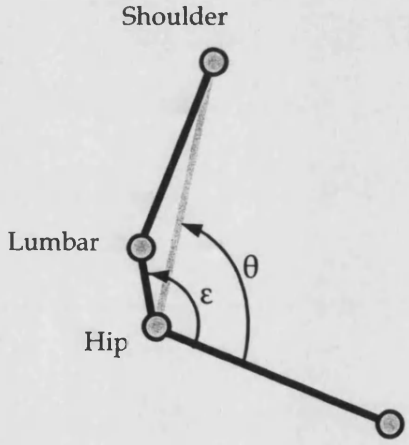

Figure C.3. Angle definitions used to identify movement trends.

A virtual point representing the lumbar joint that would produce trunk flexion/extension patterns as shown in Figure C.2 was created as follows:

An angle β was defined (Figure C.4). This represented the extension angle at which θ and ε would be equal. μ and α were defined representing the angle of the torso (segment between hip and shoulder) and the pelvis, respectively, from the line creating β.

Throughout the movement α changed as a function of μ, termed $rate_{\mu-\alpha}$. For example, if $rate_{\mu-\alpha}$ was 0.5 and μ was 20°, α would be 10°. As μ changed to 30°, α would change to 15°.

β and $rate_{\mu-\alpha}$ were the parameters that were to be optimised in the model. β was changed between 90° and 150°, in 10° intervals. $rate_{\mu-\alpha}$ was changed between $^1/_{1.5}$ and $^1/_5$ in $^1/_{0.5}$ intervals. Whole body mass centre (CM) position throughout the movement was established for each of the 11 evaluation trials with each $\beta/rate_{\mu-\alpha}$ combination. The RMSD in CM horizontal position between trials using a manually digitised lumbar point and trials using the virtual point lumbar joint were calculated. The results are presented in Table C.1.

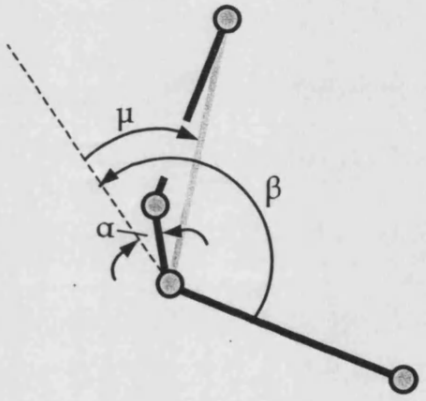

Figure C.4. Angle definitions used for creation of virtual lumbar joint.

Table C.1. RMSD (mm) in CM horizontal displacement time trajectory between trials using a manually digitised lumbar point and trials using the virtual point lumbar joint.

β (°)	$rate_{\mu-\alpha}$						
	$^1/_{2.0}$	$^1/_{2.5}$	$^1/_{3.0}$	$^1/_{3.5}$	$^1/_{4.0}$	$^1/_{4.5}$	$^1/_{5.0}$
100	6	7	8	10	10	12	13
110	5	6	7	8	9	10	10
120	4	5	6	7	7	9	7
130	5	4	5	6	7	7	8
140	5	(3)	4	5	6	7	7
150	6	4	5	5	7	6	7

Note: Minimum value circled.

Consequently, a β angle of 140° and a $rate_{\mu-\alpha}$ of $^1/_{2.5}$ was chosen as the optimal combination to produce the minimum RMSD between manually digitised and virtual point created CM horizontal displacement in the 11 evaluation trials.

APPENDIX D: THE CONSTRAINT MODELLER

The use of computer-based design aids is widespread and covers many aspects of the design process. Such software ability ranges from simple sketching systems to sophisticated finite element packages. Frequently, computer-aided design (CAD) systems contain large databases in which graphical entities such as points, lines or solid objects etc. can be created by the user. However, these systems contain no knowledge of what is described or how the entities relate to one another. Thus, a problem arises if a user wants to specify related geometry e.g. to put the end of a line on a point (Mullineux, 1988).

Other computer-based tools exist specifically for designing mechanisms. One approach is the use of computational atlases of standard mechanism forms and their outputted motion paths. However, in practice existing successful mechanisms were often adapted to achieve a new desired output (Twyman et al., 1999). Consequently, attention is given mainly to the design of the mechanism itself without achieving an optimal motion.

Development of the constraint modelling software used within this study has occurred over a number of years and has been well documented (Mullineux, 1988, 1991; Medland et al., 1996; Mullineux, 2001). The modelling concept arose from studies into engineering design processes, particularly in cases where the design task was open ended or poorly structured, such as those that might occur in mechanism design. When a designer meets a task for the first time, the precise rules which should be applied are ill understood and often only evolve as the design progresses. However, what are frequently apparent are the constraints that bound a subset of feasible designs. For example, these may include limitations on mass, cost, how a component interfaces with other parts of an assembly, or allowable linkage accelerations. Development of the software was driven by a desire to allow these bounding constraints to be manipulated within a software system in terms of design parameters. By doing so, designers can gain a greater insight into the factors that determine how a design will work or fail, or be able to investigate best compromise solutions in cases when the constraints are in conflict.

A number of versions of the constraint modelling software have evolved over the years. The current research version is called SWORDS, providing an interactive software environment in which a designer can specify the design parameters and constraints. Specifically, parameters and constraints are created by way of a user language enabling the designer to model and explore their implications.

The underlying language (RASOR) is unique to the system and has features of BASIC, C and C++. It differs from conventional languages in its ability to define and resolve constraint rules, which are done via user-defined functions (Mullineux, 2001). By implementing the user-defined functions, RASOR can create simple geometric entities (e.g. points, straight line segments, circular arcs, free-form B-spline curves and solids) to handle geometric (mechanism) problems. These entities are available in both two and three dimensions (Medland et al., 1996).

A problem is described in terms of mathematical or logical expressions involving named variables held by the computer that relate to graphical entities. The expressions are required to be 'true' when a solution is found, and this is achieved through optimisation techniques (Mullineux, 1991). A constraint is regarded as true if its expression equates to zero, otherwise the absolute value of the expression is a measure of its falseness. The combined falseness of a number of constraints is what the optimisation procedure attempts to minimise (Mullineux, 1988). The sum of the squares of the constraint values is treated as the function of the variables listed by the user. At the most basic level, these variables are of the same form as one would find in any programming language.

In some cases conflict between constraints may mean that a fully true solution does not exist. Furthermore, the direct search techniques are open to finding false minima positions which may not represent a fully true solution. Additionally, the iterative technique will only attempt to find one solution (there could be several other, or indeed infinite solutions). However, in practise these situations have not been found to present serious drawbacks, as it is usually clear to the user when an inappropriate solution has been found (Medland et al., 1996).

Processing of the function terminates when the truth-value becomes zero (or more precisely, less than a pre-defined limit), or when it is sensed that a minimum value is

achieved (Loucaides et al., 1994). Thus, depending upon the constraints, the system can lead to satisfactory design solutions. In such situations a fully acceptable design would lie within the intersection of all the constraint subsets (Figure D.1a/b). However, in other cases the design issues may have resulted in conflicting requirements and compromises between the constraints can then be investigated (Twyman, 1999). Here, the intersection between constraints remains empty (or non-existent) (Figure D.1c) and the designer may have to decide which constraints can be relaxed without compromising safety or other important design issues. Because of this optimisation approach to constraint modelling, requirements for the software to decide if a problem is over or under constrained are avoided (Mullineux, 2001). Additionally, there is no requirement on the user to form a single objective function. All constraints are treated equal, unless weighted by the designer.

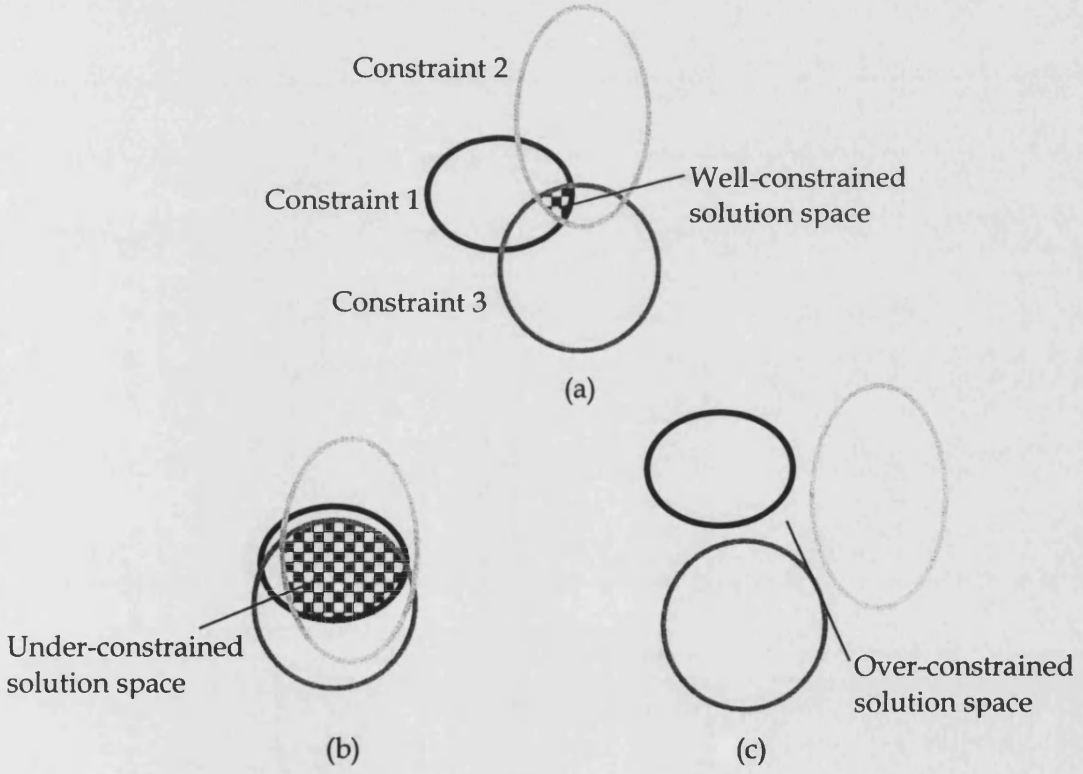

Figure D.1. Solution spaces of a well-constrained system (a) against that of under- (b) and over- (c) constrained systems.

As the computer explores the solution space, the values of the variables can suggest how those variables should be changed to obtain a closer solution to the users constraints. These values are then used for the next iteration and a solution evolves

(Mullineux, 1991). The constraint rules are specified within 'functions' in the user language. Functions also contain the lists of variables that the system is allowed to modify while searching for a solution. Variables can be altered in nine degrees of freedom (three components in each of translation, rotation and scaling).

In the simple example below (Figure D.2) a line (shown on the left of the figure) is described as existing in a known 'model-space' and has two ends, *end 1* and *end 2*. These represent the problem entities. The line exists within a model-space that can be moved around within 'world-space'. If the line were to be moved from its start position a finish position defined by *point 1* and *point 2* two constraints would be required. These would be *'put end 1 onto point 1'* and, *'put end 2 onto point 2'*. For this to occur successfully there has to be a translation of the model-space in the horizontal and vertical directions and rotation about the origin of the model-space. These three degrees of freedom were the variables that would be modified when a search occurred. If the two points were not at a distance apart to allow each end of the line to sit on a point, no fully true solution could be achieved (unless line scaling was introduced as a variable). In such a case the overall truth-value would be minimised to find a solution that best satisfied the imposed constraints.

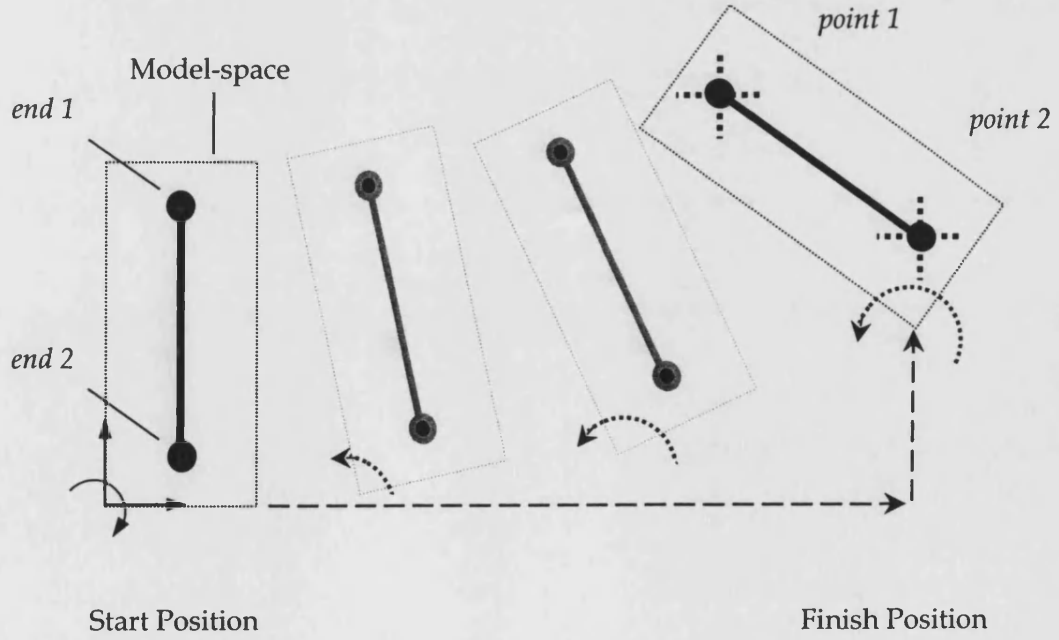

Figure D.2. Constraint modelling example.

The most frequently employed optimisation algorithm in RASOR was based on Powell's method (Walsch, 1975). This method was used to evaluate functions where derivatives were not available (or too time consuming to calculate), or at points along a function where there was no derivative. The combined constraint (objective) function was initially evaluated at the start point of the search (Figure D.3). The objective function was evaluated again as each variable was changed to positions away from the start point. The value of the objective function was used to provide the estimated next step in the direction of that variable. The resultant vector provided the starting position for the next iteration. This allowed a local search in the direction derived from the variables to be made such that the objective function value was reduced. At this stage the individual search directions were updated for the next iteration, and the process repeated (Mullineux, 2001). Once a minima was found the search continues with smaller step lengths until an acceptable truth is established (Figure D.3).

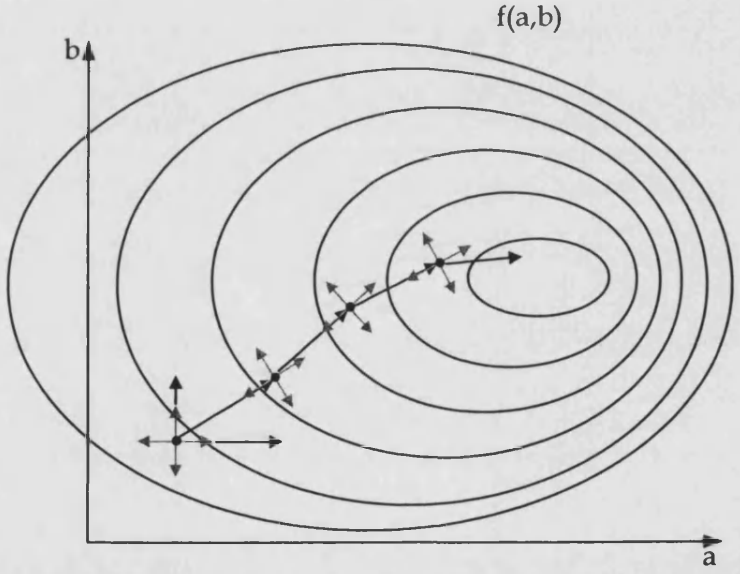

Figure D.3. Contour-type plot showing Powell's search technique to find minimum objective function.

Other techniques have also been investigated. In work regarding minimum energy principles and wrist kinematics, Sirkett et al. (2003) chose to use a Hooke and Jeeve's algorithm (Hooke and Jeeves, 1961) because of its ability to converge to a solution quickly for that particular problem. Genetic algorithms and simulated annealing have also been considered, principally for problems where there were larger numbers of constraints and variables (Loucaides et al., 1994). However, these techniques were not

seen to perform any better than direct search methods, particularly in cases where an accurate solution was required (Mullineux, 2001).

It was noted that while more sophisticated means of finding solutions existed, they can depend upon specific forms of constraint. Conversely, optimisation strategies, particularly those based on direct search techniques, require only the ability to evaluate the imposed constraints. Furthermore, as the speed of computing equipment increases, numerical methods can afford to be simpler and less efficient in speed in favour of approaches that are more robust to the problems posed (Mullineux, 2001).

For the purposes of this study, nine individual sub-programmes and a series of constraint sets were used to support the main programme (see Appendix E). This collection of routines was broadly based around a previous version of SWORDS that allowed a basic manikin model to produce simple posture approximations in response to a set of task objectives. A radical overhaul of these programmes was undertaken by the author and the major changes that occurred are now documented.

The main programme provided commands to set up the graphics window and call sub-programmes. In addition to this it included code to produce a series of menu buttons within the graphics window, providing user control of the manikin system. When activated, each button read certain information to the system, allowing aspects of the manikin environment, rise condition or curve fitting etc. to be implemented. The majority of changes to the main programme were in the form of alterations to the command buttons, and how associated information was directed to and from the sub-programmes. The following list describes the function of the major menu buttons. The associated sub-programmes are highlighted and described in fuller detail after the list.

- Manikin could be placed into an approximate sitting position before simulations were started (sub-programme: *Default*).
- Precision points could be plotted in the horizontal and vertical displacement-time domains representing each of the 11 validation conditions, and curve fitting routines were used to create the predicted CM trajectories (sub-programme: *Curve Fit*).
- Rise conditions in terms of seat height and foot position could be set (sub-programme: *Work Block*).

- Specific manikin seated posture could be created by calling appropriate constraint sets.
- Manikin movement could be created by applying further constraints sets (Appendix H), and the dynamic joint limits (section 6.4.2) could be defined.

Two sub-programmes (*Read Adaps* and *Limits*, Appendix E) were responsible for the spatial representation of the manikin and the degree of joint rotation that could occur between the segments. These were updated to take account of the subjects' dimensions as achieved from anthropometric subject measurement (section 5.1.2) and from data collection (section 5.1.3). Joint range of movement was only updated at the ankle joints due the reasons expressed in section 7.2.5. A further sub-programme (*Body Parameters*) was updated with the segmental inertia data as attained from the Yeadon (1990) inertia model (section 5.1.4 and 5.4.3). Other significant changes to *Body Parameters* enabled calculation of the manikin CM position in the vertical plane as previous assessment could only occur in the horizontal planes.

The programme titled *Default* contained information that could set manikin segments into orientations to form default postures. New information was provided to allow an approximate sitting posture to be rapidly created before simulations were undertaken. Larger changes occurred in *Work Block* (Appendix E) where aspects of the manikin environment were declared. For example, a series of wireframe seats and foot marker positions were produced to represent the different *seat heights* and *initial seated posture* conditions of each of the evaluation trials (section 5.3.1). The visual target that allowed the constraint of placing the manikin eye ray onto a point in the distance was also coded in this programme.

The programme *Curve Fit* was entirely new, and formed a critical component of the entire manikin model. Its main features included:

- Declaration of the degree and number of control points for the horizontal and vertical displacement-time trajectories (section 5.3.3).
- Coding of the regression equations as demonstrated in section 6.2.2 to define the position of precision points in the horizontal and vertical displacement-time domains.

- Application of curve adjustments in the form of 'if' statements (section 5.3.3) to ensure that precision points were plotted in the correct order.
- Plotting of the precision points in the SWORDS graphics window and fitting of the defined Bézier curves to create the horizontal and vertical displacement-time trajectories.
- Evaluation of the two Bézier curves (in terms of their horizontal and vertical components) at 0.02 s interval time steps. The vertical component of each curve was placed in an array and then re-plotted to form the predicted CM trajectory.

Finally, a series of constraint sets (Appendix H) representing different phases of the movement were written. When applied in the correct order manikin movement could take place (section 5.3.7). The correct constraint set to represent different parts of the movement was called from within the main programme.

APPENDIX E: PROGRAMME SCHEMATIC

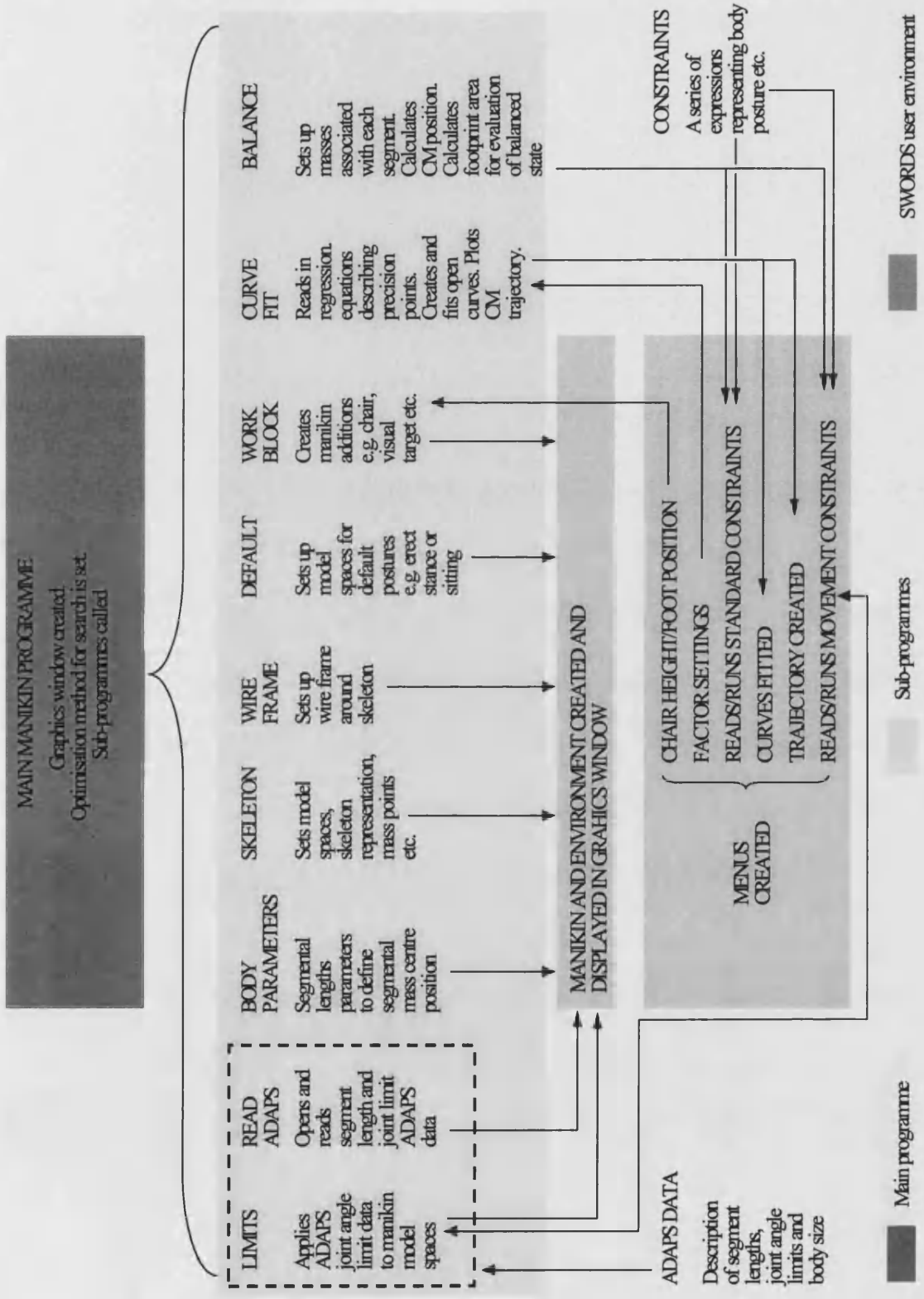

Figure E.1. Programme schematic.

APPENDIX F: BÉZIER CURVES

For computer-aided design (CAD) applications, Bézier curves are one of the most commonly used means of creating smooth 2D curves 3D surfaces (McGarva and Mullineux, 1995). The following (based on the descriptions of Bézier (1972) and other commonly available sources) illustrates how the curves are formed.

If two points, C_o and C_1 were given a position on an xy plane, then a third point, P, could be described in terms of the initial two points. If

$$P = k_0 C_0 + k_1 C_1$$

where k_o and k_1 are any constant, then P can generally lie anywhere in the xy plane. However, if

$$P = (1-t)C_0 + tC_1 \qquad \text{with } 0 \le t \le 1$$

then as t varies, the point P moves along the line between C_0 and C_1 (Figure F.1). Thus, P is defined in terms of the position of the two control points, C_0 and C_1.

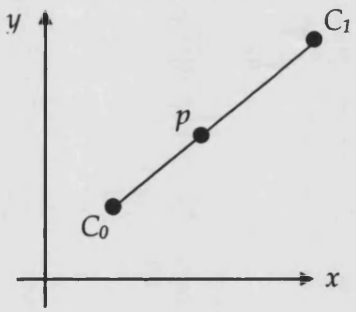

Figure F.1. The defined point, P, moves along the line between C_0 and C_1 as t moves from 0 to 1.

The same theory can be used to find the position of a point along a curve, defined by several control points. Increasing the number of control points increases the control that a user has over a curve. Figure F.2 defines the point, P, and thus the curve, by the control points C_0, C_1 and C_2.

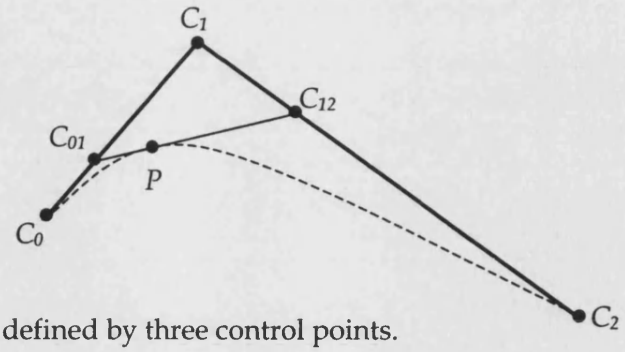

Figure F.2. Curve defined by three control points.

Here,

$$C_{01} = (1-t)C_0 + tC_1$$

$$C_{12} = (1-t)C_1 + tC_2$$

and

$$P = (1-t)C_{01} + tC_{12}$$

By substituting the previously defined equations this expands to

$$\begin{aligned} P &= (1-t)[(1-t)C_0 + tC_1] + t[(1-t)C_1 + tC_2] \\ &= (1-t)^2 C_0 + (1-t)tC_1 + (1-t)tC_1 + t^2 C_2 \\ &= (1-t)^2 C_0 + 2(1-t)tC_1 + t^2 C_2 \end{aligned}$$

This is known as the de Casteljau construction for $0 \le t \le 1$, and it generalises to any control track, such as that seen in Figure F.3.

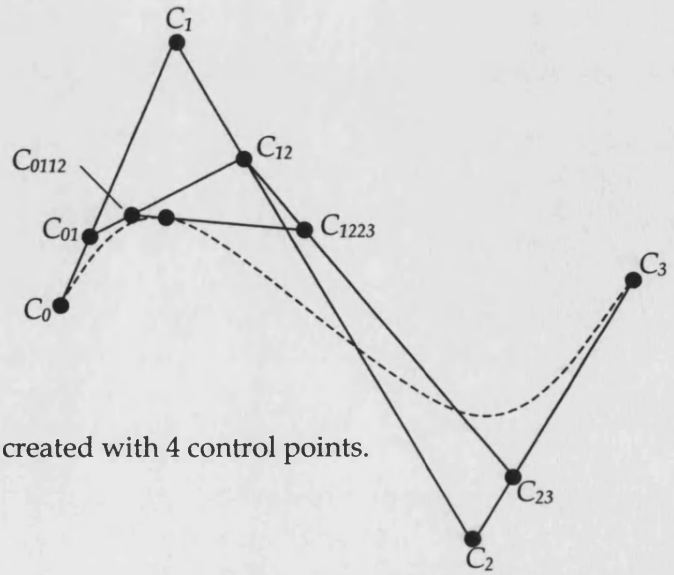

Figure F.3. Curve created with 4 control points.

The resulting curve is known as a Bézier curve. The general equation of which is:

$$P(t) = \sum_{i=0}^{n} C_i B_{i,n}(t)$$

where

$$B_{i,n}(t) = \frac{n!}{i!(n-i)!} t^i (1-t)^{n-i}$$

and is the binomial expansion of

$$[t + (1-t)]^n$$

for a curve with n control points.

Practically, this implies that each control point is multiplied by a weighting which changes as t moves from 0 to 1. The stronger the weighting of a particular control point, the closer P (and hence, the curve) will move towards that control point as t moves from 0 to 1.

In Figure F.3, four control points were used to produce a curve. The appropriate weights (commonly known as Bernstein weights) that would apply to each of the control points would appear similar to those shown in Figure F.4.

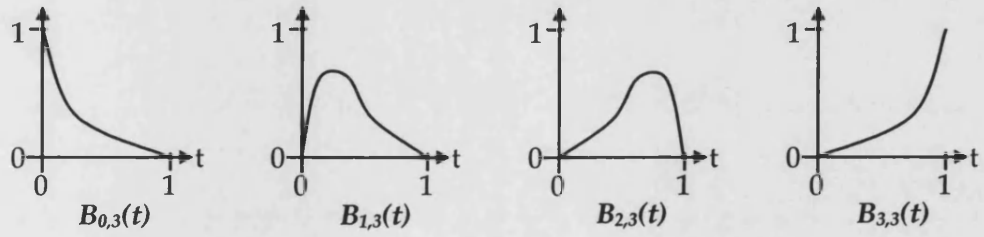

Figure F.4. Bernstein weights for the control points C_0, C_1, C_2 and C_3.

The Bernstein weight functions show how the curve will be influenced by each control point. For example, when $t = 0$, the weight for control point C_0 is 1, and for all the others is 0. Thus, at $t = 0$, P is wholly influenced by C_0, and would lie on top of it, i.e. the curve starts from C_0. As t increases the weight at C_0 diminishes while the weights for the other points rise, so the curve tends towards the other points. The weighting functions are symmetrical, so the curve ends at C_3 in the same manner as it started at C_0. These weighting factors can be expanded for any number of control points.

It is possible to generate a complicated curve with lots of control points generating a high degree polynomial. However, because the whole curve is a single polynomial, if one point is moved then the whole curve changes shape. Frequently, it would be beneficial to change local sections of the curve whilst leaving other areas unchanged. A collection of smoothly joined Bézier curves is called a B-spline. A spline avoids the problems associated with single polynomial functions, whilst still possessing a high degree of continuity.

A spline can be created by choosing values of t at which one curve will end and the next one will start. The previous convention that t goes from 0 to 1 can be abandoned such that the intermediate values can be whole numbers. Figure F.5 shows a spline of smoothly joined Bézier curves.

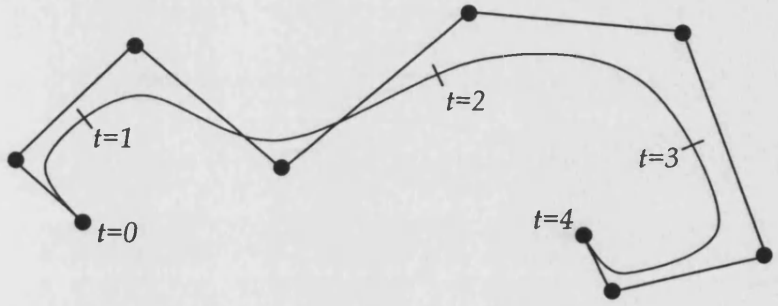

Figure F.5. B-spline formed by smoothly joined Bézier curves.

The equation of the spline of Bézier curves is similar to before, described as:

$$P(t)=\sum_{i=0}^{n} C_i N_{i,k}(t)$$

In this equation the weights, now labelled N, are:

$$N_{i,k}(t)=\frac{t-r_i}{r_{i+k-1}-r_i}N_{i,k-1}(t)+\frac{r_{i+k}-t}{r_{i+k}-r_{i+1}}N_{i+1,k-1}(t)$$

where the value of k is the degree that the joined up Bézier curves will have, the values of r are the values of t at which one Bézier curve will end and the next one will start (0,1,2,3,4 in Figure F.5). These individual values of t are called *knots* and the list of values is called the *knot vector*.

The resulting weighting functions now look like those in Figure F.6. It can be seen that the weights have values of 0 for part of the range of t along the spline. In this range, corresponding point have no influence over the spline for those values of t. Thus, local control over the spline is achieved.

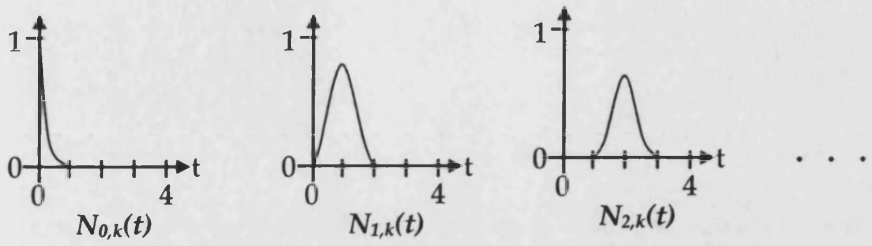

Figure F.6. Bernstein weight functions for control point of a B-spline.

APPENDIX G: REGRESSION MODEL STATISTICAL TABLES

Table G.1 - G.16 show analysis of variance results for of the 16 responses, where:

N =	Number of Runs.
DF =	Degrees of freedom of the residuals.
SS =	Sum of squares
MS =	Mean square
SD =	Standard Deviation
F =	The critical F (the value of the F-distribution over which SD is statistically significant at the 95% confidence level).
Q^2 =	Predictive power of the model (the fraction of variation of the response that can be predicted by the model).
R^2 =	Goodness of fit of model (the fraction of variation of the response explained by the model).
R^2 Adj =	R^2 adjusted for degrees of freedom.
Cond. no. =	Condition number (measure of orthogonality of design).
RSD =	Residuals standard deviation (variation of response not explained by the model).

The analysis of variance (ANOVA) partitioned the total variation of the response (SS, corrected for the mean) into a component due to the regression model and a component due to the residuals. The residual SS was further partitioned into Pure Error and Lack of fit. A goodness of fit test was performed by comparing the MS Lack of Fit to the MS Pure Error.

Significance was excepted at $p<0.05$. Tables G.1 - G.16 all show $p=0.000$ for the regression, indicating statistical significance. Tables G.6 and G.14 show $p<0.05$ for lack of fit of the regression, demonstrating that these models had a significant lack of fit to the experimental data. Table G.6 also demonstrates relatively low Q^2 and R^2 values, further implying the model to be a poor predictor to the response.

Table G.1. ANOVA table for the response $ONSET_{HOR\ VEL}$.

$ONSET_{HOR\ VEL}$*	DF	SS	MS	F	p	SD
Total	61	12.2912	0.201494			
Constant	1	12.1973	12.1973			
Total Corrected	60	0.0938873	0.001565			0.039557
Regression	4	0.0796466	0.019912	78.3003	0.000	0.141109
Residual	56	0.0142407	0.000254			0.015947
Lack of Fit (Model Error)	30	0.00914641	0.000305	1.55603	0.128	0.017461
Pure Error (Replicate Error)	26	0.0050943	0.000196			0.013998
N = 61	Q^2 =	0.819	Cond. no. =	2.2911		
DF = 56	R^2 =	0.848	RSD =	0.0159		
	R^2 Adj. =	0.837				

Note: * indicates response has been transformed by $Y^{0.25}$

Table G.2. ANOVA table for the response $ONSET_{VER\ VEL}$.

$ONSET_{VER\ VEL}$	DF	SS	MS	F	p	SD
Total	60	0.0132	0.00022			
Constant	1	6.00E-05	6.00E-05			
Total Corrected	59	0.01314	0.000223			0.014924
Regression	5	0.008738	0.001748	21.4359	0.000	0.041804
Residual	54	0.004402	8.15E-05			0.009029
Lack of Fit (Model Error)	28	0.002615	9.34E-05	1.35886	0.217	0.009664
Pure Error (Replicate Error)	26	0.001787	6.87E-05			0.008291
N = 60	Q^2 =	0.600	Cond. no. =	2.7895		
DF = 54	R^2 =	0.665	RSD =	0.009		
	R^2 Adj. =	0.634				

Table G.3. ANOVA table for the response SOO_{TIME}.

SOO_{TIME}	DF	SS	MS	F	p	SD
Total	60	40478.1	674.635			
Constant	1	39086.4	39086.4			
Total Corrected	59	1391.67	23.5876			4.85671
Regression	7	1122.92	160.417	31.0393	0.000	12.6656
Residual	52	268.746	5.1682			2.27337
Lack of Fit (Model Error)	25	103.427	4.13706	0.675664	0.836	2.03398
Pure Error (Replicate Error)	27	165.32	6.12295			2.47446
N = 60	Q^2 =	0.747	Cond. no. =	3.0169		
DF = 52	R^2 =	0.807	RSD =	2.2734		
	R^2 Adj. =	0.781				

Table G.4. ANOVA table for the response $SOO_{HOR\ DISP}$.

$SOO_{HOR\ DISP}$	DF	SS	MS	F	p	SD
Total	60	0.3304	0.005507			
Constant	1	0.26136	0.26136			
Total Corrected	59	0.0690402	0.00117			0.034208
Regression	4	0.062007	0.015502	121.224	0.000	0.124506
Residual	55	0.00703324	0.000128			0.011308
Lack of Fit (Model Error)	28	0.00457066	0.000163	1.78975	0.067	0.012777
Pure Error (Replicate Error)	27	0.00246259	9.12E-05			0.00955
N = 60	Q^2 =	0.880	Cond. no. =	2.7339		
DF = 55	R^2 =	0.898	RSD =	0.0113		
	R^2 Adj. =	0.891				

Table G.5. ANOVA table for the response $SOO_{VER\ DISP}$.

$SOO_{VER\ DISP}$	DF	SS	MS	F	p	SD
Total	60	0.0088	0.000147			
Constant	1	0.00486	0.00486			
Total Corrected	59	0.00394	6.68E-05			0.008172
Regression	3	0.00269631	0.000899	40.469	0.000	0.02998
Residual	56	0.00124369	2.22E-05			0.004713
Lack of Fit (Model Error)	30	0.000835612	2.79E-05	1.77465	0.071	0.005278
Pure Error (Replicate Error)	26	0.00040808	1.57E-05			0.003962
N = 60	Q^2 =	0.648	Cond. no. =	2.7176		
DF = 56	R^2 =	0.684	RSD =	0.0047		
	R^2 Adj. =	0.667				

Table G.6. ANOVA table for the response $SOO_{VER\ VEL}$.

$SOO_{VER\ VEL}$	DF	SS	MS	F	p	SD
Total	60	0.1363	0.002272			
Constant	1	0.00204167	0.002042			
Total Corrected	59	0.134258	0.002276			0.047703
Regression	2	0.0691308	0.034565	30.2519	0.000	0.185918
Residual	57	0.0651275	0.001143			0.033802
Lack of Fit (Model Error)	29	0.0434332	0.001498	1.93302	0.042	0.0387
Pure Error (Replicate Error)	28	0.0216943	0.000775			0.027835
N = 60	Q^2 =	0.469	Cond. no. =	1.2318		
DF = 57	R^2 =	0.515	RSD =	0.0338		
	R^2 Adj. =	0.498				

Note that $p<0.05$ for lack of fit of the regression, demonstrating that this model had a significant lack of fit to the experimental data.

Table G.7. ANOVA table for the response $BALANCE_{TIME}$.

$BALANCE_{TIME}$	DF	SS	MS	F	p	SD
Total	62	105233	1697.3			
Constant	1	100968	100968			
Total Corrected	61	4265.01	69.9182			8.36171
Regression	7	3916.33	559.476	86.6466	0.000	23.6532
Residual	54	348.677	6.45698			2.54106
Lack of Fit (Model Error)	26	185.108	7.11953	1.21873	0.304	2.66825
Pure Error (Replicate Error)	28	163.569	5.84176			2.41697
N = 62	Q^2 =	0.894	Cond. no. =	3.2049		
DF = 54	R^2 =	0.918	RSD =	2.5411		
	R^2 Adj. =	0.908				

Table G.8. ANOVA table for the response $BALANCE_{HOR\ VEL}$.

$BALANCE_{HOR\ VEL}$	DF	SS	MS	F	p	SD
Total	62	7.08	0.114194			
Constant	1	6.63352	6.63352			
Total Corrected	61	0.446474	0.007319			0.085553
Regression	5	0.320689	0.064138	28.5543	0.000	0.253254
Residual	56	0.125785	0.002246			0.047394
Lack of Fit (Model Error)	28	0.052436	0.001873	0.714881	0.810	0.043275
Pure Error (Replicate Error)	28	0.0733493	0.00262			0.051182
N = 62	Q^2 =	0.663	Cond. no. =	2.6445		
DF = 56	R^2 =	0.718	RSD =	0.0474		
	R^2 Adj. =	0.693				

Table G.9. ANOVA table for the response SOC_{TIME}.

SOC_{TIME}**	DF	SS	MS	F	p	SD
Total	61	9.57683	0.156997			
Constant	1	9.56178	9.56178			
Total Corrected	60	0.0150499	0.000251			0.015838
Regression	7	0.0126576	0.001808	40.0596	0.000	0.042523
Residual	53	0.00239234	4.51E-05			0.006719
Lack of Fit (Model Error)	26	0.00117597	4.52E-05	1.00398	0.495	0.006725
Pure Error (Replicate Error)	27	0.00121637	4.51E-05			0.006712
N = 61	Q^2 =	0.791	Cond. no. =	3.2191		
DF = 53	R^2 =	0.841	RSD =	0.0067		
	R^2 Adj. =	0.820				

Note: ** indicates response has been transformed by $Y^{-0.25}$

Table G.10. ANOVA table for the response $SOC_{HOR\ DISP}$.

$SOC_{HOR\ DISP}$	DF	SS	MS	F	p	SD
Total	61	0.0534	0.000875			
Constant	1	0.0028918	0.002892			
Total Corrected	60	0.0505082	0.000842			0.029014
Regression	3	0.0453578	0.015119	167.325	0.000	0.12296
Residual	57	0.00515043	9.04E-05			0.009506
Lack of Fit (Model Error)	30	0.00244247	8.14E-05	0.811762	0.712	0.009023
Pure Error (Replicate Error)	27	0.00270796	0.0001			0.010015
N = 61	Q^2 =	0.884	Cond. no. =	2.2157		
DF = 57	R^2 =	0.898	RSD =	0.0095		
	R^2 Adj. =	0.893				

Table G.11. ANOVA table for the response $VVMAX_{TIME}$.

$VVMAX_{TIME}$	DF	SS	MS	F	p	SD
Total	58	173589	2992.92			
Constant	1	169139	169139			
Total Corrected	57	4450.33	78.0759			8.83606
Regression	7	3189.38	455.625	18.0667	0.000	21.3454
Residual	50	1260.95	25.219			5.02185
Lack of Fit (Model Error)	25	783.079	31.3232	1.63868	0.112	5.59671
Pure Error (Replicate Error)	25	477.871	19.1148			4.37205
N = 58	Q^2 =	0.627	Cond. no. =	3.436		
DF = 50	R^2 =	0.717	RSD =	5.0219		
	R^2 Adj. =	0.677				

Table G.12. ANOVA table for the response $VVMAX_{VER\ VEL}$.

$VVMAX_{VER\ VEL}$**	DF	SS	MS	F	p	SD
Total	61	102.26	1.6764			
Constant	1	100.482	100.482			
Total Corrected	60	1.77848	0.029641			0.172167
Regression	5	1.73932	0.347865	488.611	0.000	0.589801
Residual	55	0.0391571	0.000712			0.026682
Lack of Fit (Model Error)	33	0.0211097	0.00064	0.779787	0.747	0.025292
Pure Error (Replicate Error)	22	0.0180474	0.00082			0.028642
N = 61	Q^2 =	0.973	Cond. no. =	2.7173		
DF = 55	R^2 =	0.978	RSD =	0.0267		
	R^2 Adj. =	0.976				

Note: ** indicates response has been transformed by $Y^{-0.25}$

Table G.13. ANOVA table for the response $END_{HOR\ DISP}$.

$END_{HOR\ DISP}$	DF	SS	MS	F	p	SD
Total	62	0.5537	0.008931			
Constant	1	0.525872	0.525872			
Total Corrected	61	0.0278277	0.000456			0.021359
Regression	5	0.0202777	0.004056	30.0807	0.000	0.063683
Residual	56	0.00755004	0.000135			0.011611
Lack of Fit (Model Error)	28	0.00255305	9.12E-05	0.510917	0.960	0.009549
Pure Error (Replicate Error)	28	0.00499699	0.000178			0.013359
N = 62	Q^2 =	0.667	Cond. no. =	2.7868		
DF = 56	R^2 =	0.729	RSD =	0.0116		
	R^2 Adj. =	0.704				

Table G.14. ANOVA table for the response $END_{VER\ DISP}$.

$END_{VER\ DISP}$	DF	SS	MS	F	p	SD
Total	60	3.7662	0.06277			
Constant	1	3.26667	3.26667			
Total Corrected	59	0.499536	0.008467			0.092015
Regression	3	0.498517	0.166172	9132.96	0.000	0.407642
Residual	56	0.00101891	1.82E-05			0.004266
Lack of Fit (Model Error)	29	0.000693951	2.39E-05	1.98824	0.038	0.004892
Pure Error (Replicate Error)	27	0.000324957	1.20E-05			0.003469
N = 60	Q^2 =	0.998	Cond. no. =	2.5272		
DF = 56	R^2 =	0.998	RSD =	0.0043		
	R^2 Adj. =	0.998				

Note that $p<0.05$ for lack of fit of the regression, demonstrating that this model had a significant lack of fit to the experimental data.

Table G.15. ANOVA table for the response $END_{HOR\ VEL}$.

$END_{HOR\ VEL}$	DF	SS	MS	F	p	SD
Total	61	0.1306	0.002141			
Constant	1	0.0682229	0.068223			
Total Corrected	60	0.0623771	0.00104			0.032243
Regression	4	0.0376973	0.009424	21.3844	0.000	0.097079
Residual	56	0.0246798	0.000441			0.020993
Lack of Fit (Model Error)	29	0.0144286	0.000498	1.31044	0.241	0.022306
Pure Error (Replicate Error)	27	0.0102512	0.00038			0.019485
N = 61	Q^2 =	0.533	Cond. no. =	2.2997		
DF = 56	R^2 =	0.604	RSD =	0.021		
	R^2 Adj. =	0.576				

Table G.16. ANOVA table for the response $END_{VER\ VEL}$.

$END_{VER\ VEL}$	DF	SS	MS	F	p	SD
Total	61	0.108	0.00177			
Constant	1	0.072295	0.072295			
Total Corrected	60	0.035705	0.000595			0.024394
Regression	6	0.0303781	0.005063	51.3247	0.000	0.071155
Residual	54	0.00532692	9.86E-05			0.009932
Lack of Fit (Model Error)	27	0.00313846	0.000116	1.4341	0.177	0.010781
Pure Error (Replicate Error)	27	0.00218846	8.11E-05			0.009003
N = 61	Q^2 =	0.809	Cond. no. =	3.1692		
DF = 54	R^2 =	0.851	RSD =	0.0099		
	R^2 Adj. =	0.834				

APPENDIX H: CONSTRAINT SETS

The constraints that were applied to the manikin over part or the complete duration of STS were:

- Feet on floor
- Heel on foot position line marker
- Buttock on seat
- Hip and lumbar joint bend together
- CM along predicted trajectory
- Hand on knees
- Hand on thighs
- Eye ray on target

Each of these could be weighted to a greater or lesser amount to affect the degree of influence that the particular constraint played in achieving the final truth solution. For example, the truth-value for a system containing three constraints is attained by the equation:

$$\textit{Truth-value} = (\textit{Constraint 1})^2 + (\textit{Constraint 2})^2 + (\textit{Constraint 3})^2$$

Consequently, constraints one, two, and three are minimised approximately equally to attain the required truth-value and hence, a design solution.

If constraint one were weighted by a factor of 10 then the truth-value would be achieved by minimising that constraint more than constraints two and three. Hence:

$$\textit{Truth-value} = (10 \cdot \textit{Constraint 1})^2 + (\textit{Constraint 2})^2 + (\textit{Constraint 3})^2$$

For the purposes of this investigation constraint weightings were chosen based upon experience and experimentation with the SWORDS operating system with regard to producing manikin movement.

A constraint set represented the constraints that were present in a particular phase of the movement, e.g. between ONSET and SOO. Alongside this there existed a variable set which defined which manikin variables were freed in order to allow for a truth solution to be achieved.

Figure H.1 represents the constraints that were present throughout a STS trial. For the purpose of this presentation the occurrence of the *events* are shown equidistant in the time domain although the experimental data demonstrated this not to be the case.

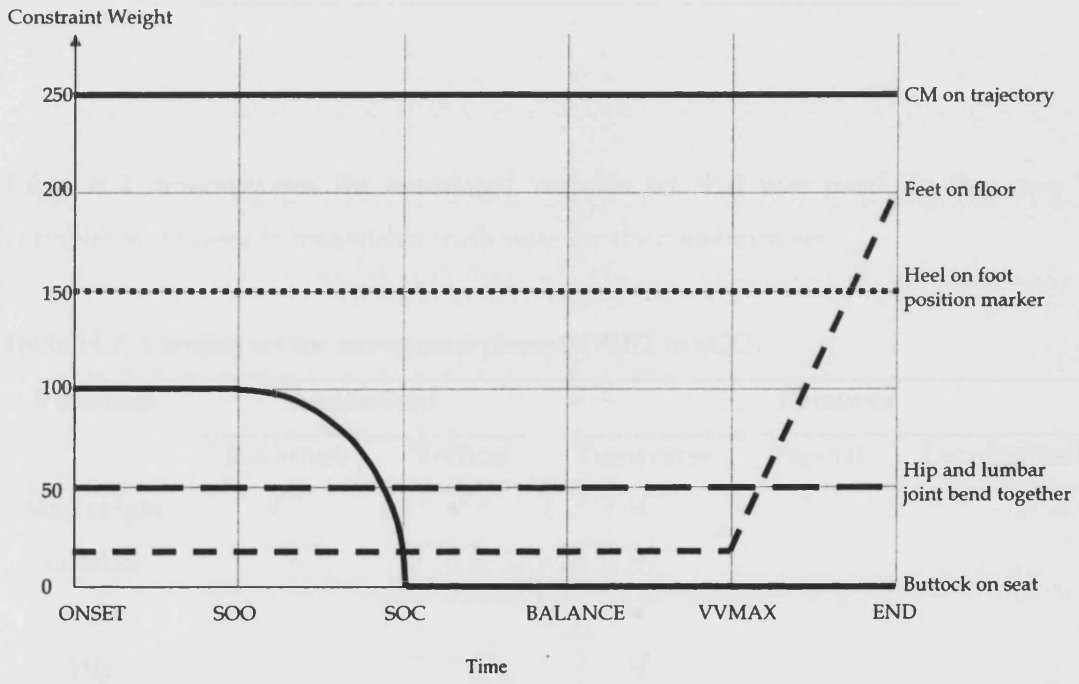

Figure H.1. Constraint weightings throughout a STS trial.

Table H.1 demonstrates the constraint set that was applied in the first phase of movement (ONSET to SOO). Note that the constraints regarding hand contact with the knee and thigh, and eye ray contact with the target, all of which have a weight of one, are not shown in Figure H.1 due to its scale.

Table H.1. Constraint set for movement phase ONSET to SOO.

Constraint	Weighting
CM on trajectory	250
Heel on foot position marker	150
Buttock on seat	100
Hip and lumbar joint bend together	50
Feet on floor	20
Hand on knees	1
Hand on thighs	1
Eye ray on target	1

Table H.2 demonstrates the associated variable set that was used. In this case 12 variables were used to establish a truth state for the constraint set.

Table H.2. Variable set for movement phase ONSET to SOO.

Variables	Translations		Rotations		
	Horizontal	Vertical	Transverse	Frontal	Longitudinal
Man origin	✓	✓	✓		
Lumbar			✓		
Neck			✓		
Hip			✓		
Shoulder			✓		✓
Elbow			✓		✓
Wrist			✓	✓	

Figure H.1 showed that during the second movement phase (SOO to BALANCE) the influence of the constraint 'Buttock on seat' began to reduce in a quadratic fashion. This continued in the third movement phase up until the event SOC, by which time the influence of this constraint had been reduced to zero. To allow this to happen the variable set was altered to include transverse rotation about the knee and ankle joints. This increased the number of variables used to find a solution to 14.

In the final phase of motion (VVMAX to END) the influence of foot contact with floor was increased in a linear fashion from 20 to 200 (Figure H.1). Up until VVMAX there had been no conflicting constraints that would require the foot to be anywhere other than on the floor. However, as the manikin straightened towards the end of movement, the dominant 'CM on trajectory' constraint sometimes compromised foot contact with floor in order to attain the desired overall truth-value. Consequently, the foot contact with floor constraint was increased in this phase in order to maintain realistic movement patterns.

Additionally, in the final phase the influence of the constraint which placed the hand on the knee was reduced to zero (Figure H.2). This occurred such that the hand could slide up the thigh and allowed the hip and lumbar joint to continue to flex.

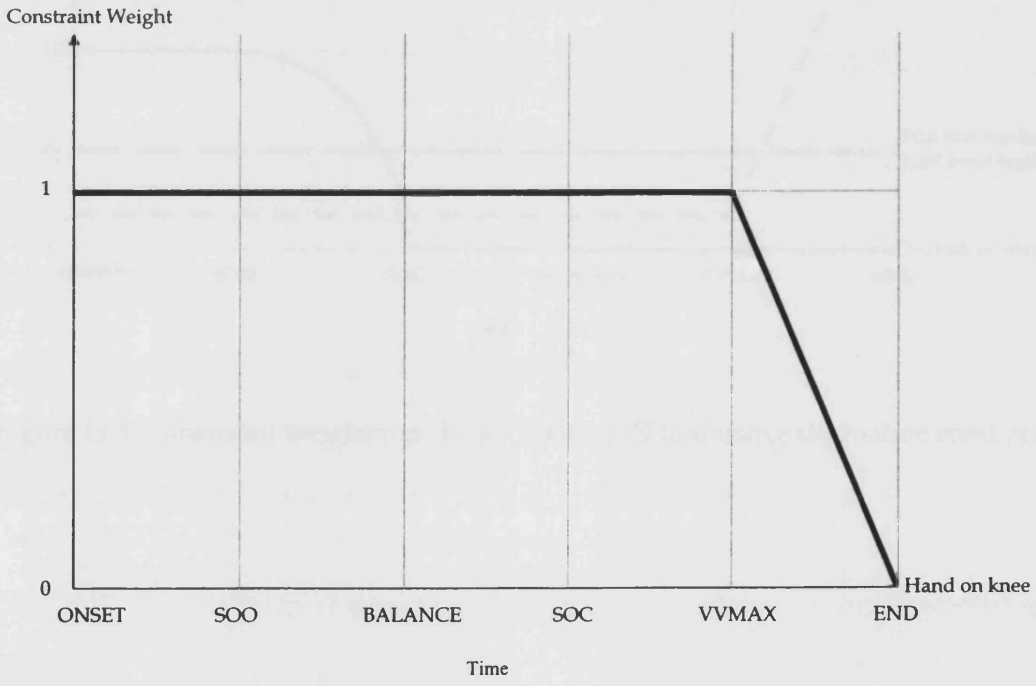

Figure H.2. Hand contact with knee constraint.

Movement *events* were shown to occur in changeable order (Section 7.1.3) and this was reflected in the movement constraints. There were two possible *event* order options that were used, dependent upon the stability strategies employed by the subject (Section 7.1.4). The first of these was demonstrated by Figure H.1. The second option was demonstrated in Figure H.3 and shows the BALANCE occurring after SOC. The constraint sets were adjusted accordingly.

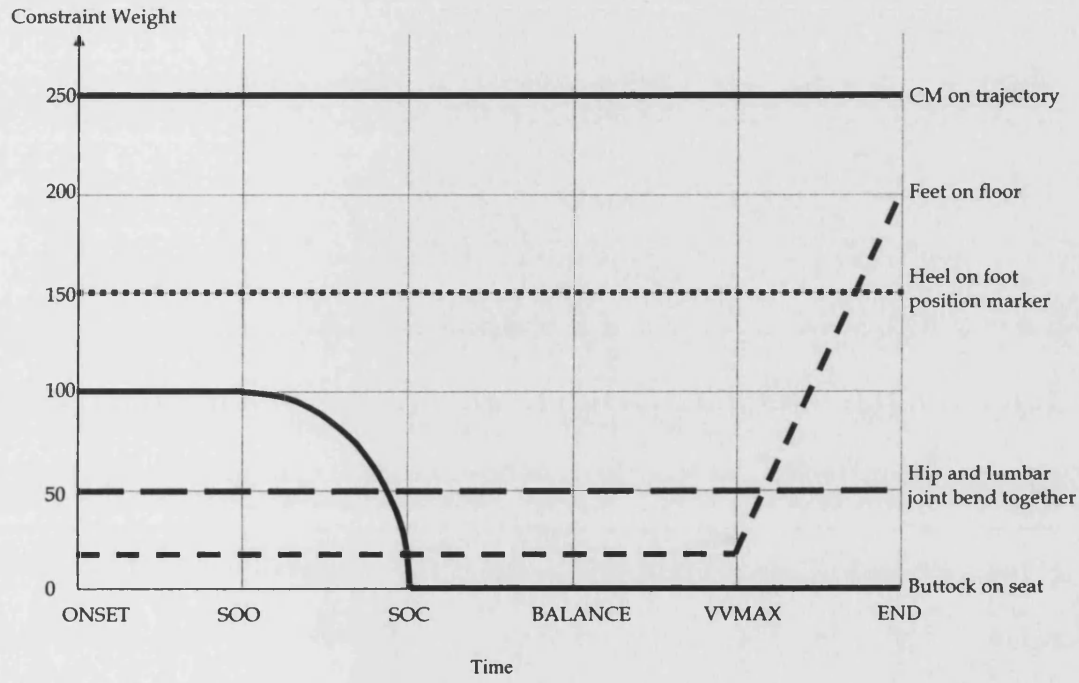

Figure H.3. Constraint weightings throughout a STS trial using alternative *event* order.